A thesis submitted to the National University of Ireland in fulfilment of the requirements for the degree of

Doctor of Philosophy

By

Andreia Ribeiro

Mesenchymal Stromal Cells: their Immunosuppressive Capacity and Protein Production Profile

Immunology and Transplant Biology Group,
Regenerative Medicine Institute,
National Centre for Biomedical Engineering Science,
National University of Ireland, Galway.

Thesis Supervisor: Professor Rhodri Ceredig

August 2016

Table of contents

Acknowledgements

First, to my supervisor Professor Rhodri Ceredig, to whom I am very grateful for give me this opportunity. Thank you for all the support, advice, ideas, encouragement, generosity and for sharing your knowledge. I also would like to thank Professor Matthew Griffin for all the ideas, support and advices.

To my partner in life Tiago, to my sister Lara and my parents Jú and José Carlos, I do not have words to describe my gratitude. I could not done this without your support, understanding and most of all your patience. Thank you all for the encouragement and to make the distance between Ireland and Portugal shorter.

Thank you to all my colleagues in immunology group and Regenerative Medicine Institute (REMEDI) who help me along the way, especially Bairbre McNicholas, Aideen Ryan and Grace O'Malley. A special word of thanks to Joana Cabral for your friendship and for being with me since day one!

I also would like to thank to my friends Diana Gaspar, Diana Pereira and Kieran Fuller for all the help and patience.

Also, to everyone in the DECIDE consortium, I am extremely grateful for the experience, it was a pleasure to meet you all. I would also like to thank the funding bodies that supported this thesis including the Technology Innovation Development (TIDA) project from Science Foundation Ireland and the People Programme (Marie Curie Actions) of the European Union's Seventh Framework Programme FP7/2007-2013 under Research Executive Agency grant agreement No. 315902.

Finally, I want to thank to all who directly or indirectly contributed to the realization of this project, without forgetting all who never said no when I asked for blood!

Abstract

The clinical benefits of mesenchymal stromal cell (MSC) based therapies for immune disorders and degenerative diseases are based on their combined ability to modulate the immune system and to differentiate into different end-stage mature cells. However there is a lack of a potency assay to measure this immunosuppressive property, thereby allowing a comparison of MSC sources, donors and passage number. Another important role of MSC is mediated by the extracellular matrix (ECM) that they produce that can influence the hematopoietic environment. A decellularized MSC-derived ECM scaffold could also be used for tissue engineering and regenerative medicine. For this reason this project was divided into two main parts.

The first part describes the development of a whole blood assay to measure the ability of MSC to suppress the activation of certain immune cells, in this case monocytes, in human whole blood cultures. In the last chapter of this part, the whole blood assay developed was used to assess the immunogenicity of biomaterials and to determine immunological properties, either stimulatory or suppressive, of biological compounds.

A rapid and reliable whole blood flow cytometry-based assay was developed, where different parameters were tested: including the anticoagulants used to collect peripheral blood, the different cell types used to monitor immunosuppression (monocytes and T cells), the different activation stimuli, incubation times, MSC donors, MSC passage number and readouts (production of TNF-α, IFN-γ, MCP-1, IL-6, IL-10 and IL-12). Following optimization, the efficiency of bone marrow MSC (BM-MSC) and adipose derive MSC (ASC) to immunosuppress LPS activated peripheral blood monocytes were compared. In addition, blood samples were obtained from osteoarthritis or rheumatoid arthritis patients. With the whole blood assay, it was also possible to characterize the immunogenic potential of different scaffolds and the immunosuppressive potential of seaweed extracts.

In the second part of this thesis, a comparison was made of two methods for preparing MSC-derived decellularized ECM prepared in either normoxic or hypoxic conditions. The main aim was to compare their composition and biological role on MSC differentiation and stemness properties.

For this work, decellularized ECM derived from a mouse MSC cell line MS5 was obtained either by osmotic shock using a hypotonic solution or by inducing apoptosis with a suicide gene. These matrices produced in normoxia or hypoxia were then characterized and compared by immunocytochemistry (ICC), reverse transcription polymerase chain reaction (RT-PCR) and proteomics. To better understand the role of ECM and hypoxia in MSC fate, Balb/c mouse MSC

were differentiated on top of different ECM and compared to their differentiation on plastic surfaces.

Results obtained showed that different decellularization protocols applied to cells maintained in hypoxia led to different ECM protein composition and different immunogenic potential. Results also suggested that the presence of ECM did not improve MSC differentiation capacity or contribute to their stemness properties. Reasons for these results were proposed.

In conclusion, this thesis brings together different areas of knowledge pertaining to MSC biology; cell biology, immunology, regenerative medicine and bioengineering. A better understanding of MSC biology will ultimately results in an improved therapeutic outcome for the use of MSC in a clinical setting.

List of Figures

List of Tables

Abbreviations

A

Acan	Aggrecan
ADAM	Metalloproteinases with a disintegrin and metalloprotease domain
Adam9	Disintegrin, metalloproteinase
ADAMTS	Metalloproteinase with a thrombospondin motif
AIF	Apoptosis inducing factor
ALS	Amyotrophic lateral sclerosis
AOhw	Absorbance at high wavelength
AOlw	Absorbance at low wavelength
Apaf-1	Apoptotic protease activating factor 1
APC	Allophycocyanin
APCs	Antigen-presenting cells
AR	Reduced alamarBlue
ASC	Adipose derived mesenchymal stromal cells
ATP	Adesonine triphosphate

B

B2M	β-2 microglobulin
BD	Becton dickinson
BM	Bone marrow
BM-MSC	Bone marrow mesenchymal stem/stomal cells
BMP-2	bone morphogenetic protein-2

C

CAMs	Cell adhesion molecules
CCL	Chemokine (C-C motif) ligand
CCMI	Centre for cell manufacturing Ireland
CDC	Centres for disease control and prevention
CLP	Common lymphoid progenitor
CMLP	Common myeloid–lymphoid progenitor
CMP	Common myeloid progenitor
CO_2	Carbon dioxide
Col2	collagen II
Col4a1	Collagen IV
Col6a1	Collagen VI
COX-2	Cyclooxygenase 2
CTLA-4	Cytotoxic T-lymphocyte-associated protein 4
CXCL	C-X-C motif chemokine
cyt-c	Cytochrome c

D

DAMPs	Damage-associated molecular patterns
DC	Dendritic cells
DCTHERA	Dendritic Cells for Novel Immunotherapies
dH_2O	Distilled water
DISC	death inducing signalling complex
DMARDs	Disease-modifying anti-rheumatic drugs
DMSO	Dimethyl sulfoxide
DNA	Deoxyribonucleic acid
DPBS	Dulbecco's Phosphate Buffered Saline

dsRNA	Double-stranded RNA
DTT	Dithiothreitol

E

EDTA	Ethylenediaminetetraacetic acid
EGTA	Ethylene glycol tetra acetic acid
ELISA	Enzyme-linked immunosorbent assay
ELP	Early lymphoid progenitor
EMA	European Medicine Agency
EPO	Erythropoietin
ePTFE	Expanded polytetrafluoroethlyene

F

FACIT	Fibril associated collagens with interrupted triple helices
FADH2	Flavin adenine dinucleotide hydroquinone form
FAO	Food and Agriculture Organization of the United Nations
FBS	Fetal bovine serum
FDA	Food and drug administration
FITC	Fluorescein isothiocyanate
FLSs	Fibroblast-like type B synoviocytes
FSC	Forward scatter

G

G-CSF	Granulocyte colony-stimulating factor
GAGs	Glycosaminoglycans
GAPDH	Glyceraldehyde-3-phosphate dehydrogenase
GM-CSF	Granulocyte-macrophage colony-stimulating factor
GTP	Guanosine triphosphate
GvHD	Graft versus host disease

H

H	Hypoxia
hBM-MSC	Human bone marrow mesenchymal stromal cells
HGF	Hepatic growth factor
HIF	Hypoxia-inducible factor
HLA	Human leukocyte antigen
HLA-DR	Human leukocyte antigen antigen D related
HSC	Hematopoietic stem cells
HSPG2	Heparan sulphate

I

IBD	Inflammatory bowel disease
iCasp9	Inducible caspase 9
ICC	Immunocytochemistry
IDO	Indoleamine 2, 3-dioxygenase
IFN-β	Interferon-beta
IFN-Y	Interferon-gamma
IL	Interleukin
IMS	Industrial methylated spirits
IRF3	Interferon regulatory factor 3
ITAMs	Immunoreceptor tyrosine-based activation motifs
IUIS	International Union of Immunological Societies

L

Lamb2	Laminin
LBP	LPS binding protein
LG	Low glucose
LIF	Leukaemia inhibitory factor
LMPP	Lymphoid-primed multipotent progenitor
LPS	Lipopolysaccharide
LPS^{b}	LPS^{biotin}

M

M-CSF	Macrophage colony-stimulating factor
MAMPs	Microbial–associated molecular patterns
MCP-1	Monocyte chemo-attractant protein 1
MD2	Myeloid differentiation protein 2
mDC	Myeloid DC
MDP	N-acetylmuramyl-L-alanyl-D-isoglutamine or muramyl dipeptide
MFI	Mean Fluorescence Intensity
MHC	Major histocompatibility complex
miRNA	Micro RNA
MIX	1-methyl-3-isobutylxanthine
MM	Multiple myeloma
MMPs	Matrix metalloproteinases
MNC	Mononuclear cells
MPP	Multipotent progenitor
mRNA	Messenger RNA
MS	Multiple sclerosis
MSC	Mesenchymal stem/stromal cells
MDSC	Myeloid derived suppressor cells
MyD88	Myeloid differentiation protein 88

N

N	Normoxia
NADH	Nicotinamide adenine dinucleotide
NF-kB	Nuclear factor kappa B
NO	Nitric oxide
NOD2	Nucleotide-binding oligomerization domain-containing protein 2
NSAIDs	Nonsteroidal anti-inflammatory drugs

O

O_2	Oxigen
OA	Osteoarthritis
OSM	Oncostatin

P

P	Cell culture passage number
P/S	Penicillin/streptomycin
Pam3CSK4	Pam3Cys-Ser-(Lys)4
PAMPs	Pathogen-associated molecular patterns
PBMC	Peripheral blood mononuclear cells
PBS	Phosphate-buffered saline
PCL	Polycaprolactone
PCR	Polymerase chain reaction
pDC	Plasmacytoid DC
PDGF	Platelet-derived growth factor

PDL-1	Programmed death-ligand 1
PE	Phycoerythrin
PerCP Cy5.5	Peridinin chlorophyll protein-cyanine 5.5
PFA	Paraformaldehyde
PGE2	Prostaglandin E2
PHA	Phytohaemagglutinin
PI	Propidium iodite
PK	Plasma kallikrein
PKC	Protein kinase C
PL	Platelet lysate
PLA	Polylatic acid or polylactide
PLGA	Poly(lactide-co-glycolide)
PMA	Phorbol myristate acetate
PolyIC	Polyinosinic-polycytidylic acid
PRP	Platelet-rich plasma
PRRs	Pattern-recognition receptors
PT/PTT test	Prothrombin time and partial thromboplastin time test

R

RA	Rheumatoid arthritis
REMEDI	Regenerative medicine institute
RNA	Ribonucleic acid
RO	Correlation factor
RT-PCR	Real-time polymerase chain reaction

S

SBF	Simulated body fluid
siRNA	Small interfering RNA
SSC	Side scatter

T

TCR	T cell receptor
TERT	Telomerase reverse transcriptase
TGF-β	Transforming growth factor beta
Th	T helper cell
TLR	Toll-like receptors
TNF-α	Tumour necrosis factor alpha
TRAM	Translocating chain-associating membrane protein
Treg	Regulatory T cells
TRIF	TIR domain-containing adaptor inducing interferon-β
TSG6	Tumor necrosis factor-inducible gene 6

U

UCB	Umbilical cord blood
UCM	Umbilical cord matrix

W

WHO	World Health Organization

Chapter 1 | General Introduction

1.1 Haematopoiesis

Tissue stem cells are undifferentiated cells that upon division generate daughter cells one of which remains a stem cell whereas the other become a multi-potent progenitors [1]. The term haematopoiesis describes the self-renewing of process hematopoietic stem cells (HSC) and their differentiation into mature blood cells; it is a process of maintaining blood formation throughout life and occurs in a very unique microenvironment [2]. During embryonic development haematopoiesis begins in the aorta-gonad-mesonephros region and the yolk sac, followed by the placenta, fetal liver, spleen and bone marrow [3]. After birth haematopoiesis occurs mainly in the bone marrow, although in response to haematopoietic stress haematopoiesis can occur in the spleen and liver [3, 4].

Different models have been proposed to explain haematopoiesis, however, Ceredig, Rolink and Brown have proposed a more plastic and different model (**Figure 1.1**). From their point of view there is a continuous relationship between progenitor cells [5].

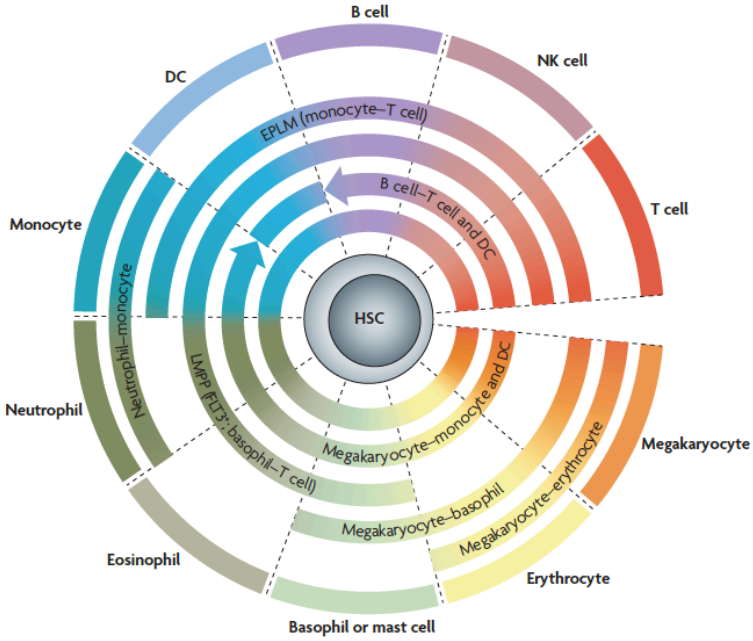

Figure 1.1 - Pairwise relationships model, a revised hematopoietic model [5].

This model suggests that different immune cells can derive from various haematopoietic lineages, from different intermediate progenitors, not in a straight manner. The arcs show the known progenitor cells, and some arcs overlap, indicating that the cells can rise from different progenitors.

From this paper it was created a project that gave rise to the DECIDE consortium. DECIDE aims to understand normal blood cell development and to understand why primate cells fail to differentiate, and blood cell development start with hematopoiesis that occurs in a very specific niche.

1.2 Haematopoietic niche

Tissue-specific stem cells, such as HSC, reside in a very specific and restricted microenvironment, called a niche, where lineage commitment of all blood cells occurs. Therefore, it is important to understand the composition and function of this niche and the effect that has on cells decision.

The maintenance of normal haematopoiesis is a critical process involving interactions between stem cells and the bone marrow microenvironment. Haematopoietic niche play an important role in keeping the self-renewal and multipotency of stem cells [6, 7]. The definition of haematopoietic niche, their components and how they work is a very important matter for the understanding of haematopoietic regulation. This becomes increasingly important in order to improve regeneration following injury or HSC transplantation, as well as to understand how disordered niche function contributes to disease.

HSC migrate and come in contact with diverse niches through the course of their development [8]. The interaction of HSC with these microenvironments regulates their growth and differentiation into more committed lineages [9]. It is presumed that the major haematopoietic niche components are (**Figure 1.2**): 1) specific cell-cell interactions between HSC and other cells, such as mesenchymal stromal cells, osteoblasts, fibroblasts, adipocytes and vascular endothelial cells; 2) soluble or insoluble growth factors, signals released by the cells within the niche; 3) signals presented by the extracellular matrix (ECM) produced by the cells within the niche; and 4) physicochemical factors, such as nutrients and oxygen levels [10, 11].

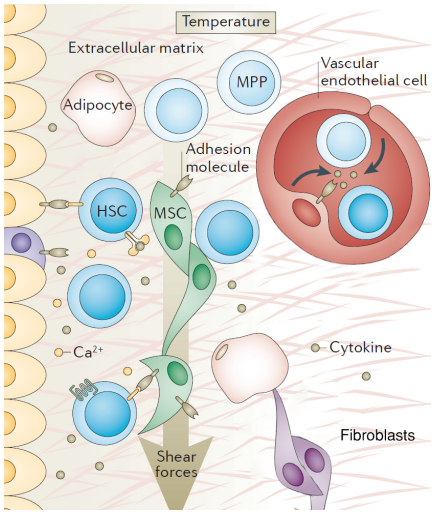

Figure 1.2 - Haematopoietic niche organization and constituents. Figure adapted from [12, 13].

These components not only provide structural, trophic and mechanical support to the haematopoietic microenvironment, but also provide 3D topographical and physiological signals to the cells, having an effect on stem cell functions [3].

1.2.1 Extracellular matrix

The importance of the ECM in the haematopoietic environment is not a recent subject of study. Indeed, in the 80's a few articles were published discussing this topic, suggesting that haematopoietic cell growth factors remain bound to the ECM playing a role in cell differentiation and may regulate haematopoiesis [14]. However, subsequently new approaches have contributed to our knowledge of how stem cells receive information from ECM, and how they respond.

It is known that signals from the ECM can influence cell fate choices, and theoretically all cells in the body are exposed to ECM proteins, even blood cells are exposed to soluble ECM proteins, making ECM a very important structure [15, 16]. ECM components are involved in important events, such as cell adhesion, migration, growth, differentiation and survival [17, 18].

Despite different cells releasing different proteins, the same main molecules constitute the ECM (**Figure 1.3**). The structural support is given by the collagens and elastin. Collagen is the principal biopolymer in the ECM and is a protein with a triple helical structure, where each helix is composed by more than 1000 amino-acids, being glycine the main amino-acid, constituting 33% of the total amino-acids [19]. In humans, so far 28 types of collagen have been identified. The collagens are classified into numerous groups: fibrillar collagens (The most common form), FACIT (Fibril Associated Collagens with Interrupted Triple Helices), FACIT-like collagens, trans-membrane collagens, basement membrane collagens, beaded filament collagens, short chain collagens, as well as some unclassified collagens [20].

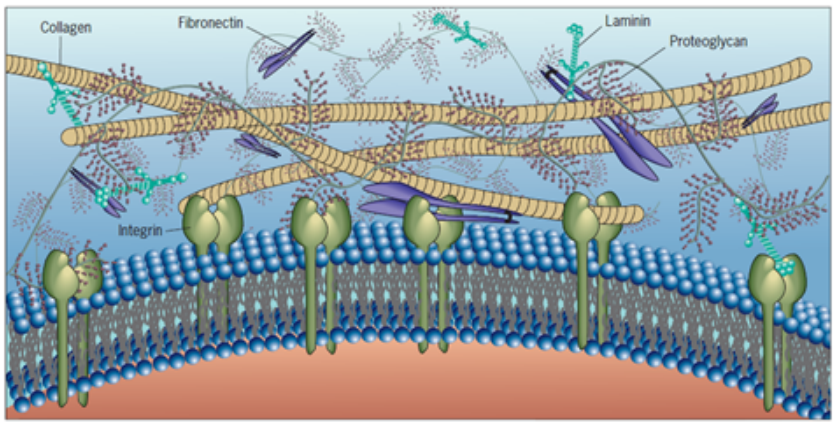

Figure 1.3 - Main ECM component and configuration [21].

Collagens are the most abundant components of the ECM, however elastin is another major component. Elastin, is an insoluble polymer that provides elastic recoil and resilience to a variety of connective tissues. Elastin also plays a role in cell adhesion, cell migration and cell signalling [22].

Fibronectin is a multifunctional glycoprotein that contributes to the adhesion of growth factors, other ECM proteins and cells. Laminin is also a glycoprotein that together with collagen IV is one of the main components of ECM and appears to be associated with cell adhesion, migration and differentiations [14, 23].

Cells bind to ECM using many different cell adhesion molecules (CAMs), and signals from these influences the cells' lineage decisions [24]. CAMs are trans-membrane proteins that make the linkage between cells and the ECM. Cells produce and secrete into the surrounding extracellular space collagens, fibronectin, laminin and other proteins, forming the ECM. These ECM proteins bind to cells mainly through integrins. Integrins are the major category of four classes of CAMs [15, 24]. Many integrins can recognize several ligands, such as fibronectin, laminin, collagen IV, osteopontin, bone sialoprotein, thrombospondin or fibrinogen, and generally, one ligand can be recognized by several integrins [25]. Integrins are composed of two subunits α and β, the combination between them gives them specificity and correspondingly different functions. The extracellular domains of integrins are receptors [24]. These transmembrane glycoproteins are crucially important because they are the main receptor that cells use to attached to ECM molecules, as well as to respond to ECM stimuli by activating intracellular signalling pathways [26]. In general, integrins influence cell-ECM and cell-cell interactions [18]. Integrin can also induce resistance to apoptosis and can contribute to drug resistance, this is especially important in certain diseases [27]. Integrin-ligand interaction also triggers a spectrum of signal transduction pathways, which has effects on cell proliferation, structure, motility and gene transcription [23].

Besides structural proteins and glycoproteins, ECM is also composed of proteoglycans, specialized glycosaminoglycans (GAGs) [14, 23, 28]. Proteoglycans are glycosylated proteins with different functions. For example, aggrecan provides hydration; decorin, may have functions in regulating collagen fibril formation and in modifying the activity of transforming growth factor beta (TGF-β); and perlecan, the major heparan sulfate proteoglycan, may be involved in glomerular filtration [28].

The ECM is a dynamic structure, it is in constant reorganisation with molecules being produced and degraded simultaneously. The degradation of ECM components is function of matrix metalloproteinases (MMPs) [14, 23, 29]. MMPs belong to a group that also includes protein with a disintegrin and metalloprotease domain (ADAM) and with a thrombospondin motif (ADAMTS) [30]. Besides the regulation of ECM homeostasis, MMPs are also involved in the release of bioactive fragments and growth factors, altering ECM structure and modifying cell-ECM interactions [29]. MMPs are also important in several biological processes, such as embryogenesis, angiogenesis, normal tissue remodelling, wound healing, and in diseases such as arthritis, atheroma, tissue ulceration and cancer [31].

Moreover, it has been suggested that haematopoietic growth factors, such as GM-CSF, granulocyte colony-stimulating factor (G-CSF) and erythropoietin (EPO), IL-7, get trapped on ECM, and can have a effect on cells fate [14, 32].

In addition to influencing cell-ECM interactions through ECM composition, haematopoiesis is also mediated by the mechanotransduction properties of ECM. Cells sense the mechanical and physical properties of the ECM, such as topography, having an effect on cell decision [15]. In fact, stem cells also respond to the stiffness and porosity, affecting HSC function [12, 15].

As referred above, ECM components play an important role in cell survival, adhesion, migration, proliferation and differentiation, and the signalling properties of the ECM depend on its organization [33, 34]. Particularly in the haematopoietic niche, where it has been demonstrated that ECM maintain the pluripotency of stem cells and support their differentiation, and specifically collagen I and fibronectin have been shown to affect MSC fate [15, 35, 36]. Ultimately, ECM contributes to the regulation of HSC decisions [15].

New technologies have been used to better understand stem cell interactions with ECM, however several factors have to be considered simultaneously, ECM composition and the mechanical and physical properties [15]. Consequently, the types of cells that produce the ECM, the cell's age and culture conditions, including oxygen concentration, affect the ECM composition and properties [35, 37].

The most common models used to study cell-ECM interactions are the *in vitro* assays. This methodology is a valid option, however it is not the best, since with *in vitro* assays, it is not possible to consider all factors involved. As described above, several factors are involved in cell-ECM interactions that cannot be replicated *in vitro*. For this reason, *in vivo* assays seem to be the best option, especially because strategies can be used involving the knocking out of specific ECM proteins and integrins. However, knocking out ECM proteins would probably have generalized effects on the body, not specifically on hematopoietic environment, but in a general way, leading to several dysfunctions. Consequently, the possible alteration of the stem cells fate could not be related with the absence of the protein itself, but because of the generalized effects. ECM has an important role in haematopoiesis, as well as in several diseases, specially involving cartilage and brain [38, 39].

Cell-ECM interactions are an important research area not just to better understand the role of ECM in haematopoietic environment, but also to comprehend how engineered ECM scaffold can contribute in the regenerative medicine and tissue-engineering field. ECM scaffold has been used to create a more native scaffold constructs that can be implanted *in vivo*, to improve the tissue development process. Several studies have been using engineered ECM

scaffold to support the regeneration of several human tissues and organs for clinical application [40-42].

1.2.2 Hypoxia

In the last years different groups have demonstrated that the physiological environment of haematopoietic niches are under hypoxic conditions (low oxygen concentration) [12, 43].

HSC have been shown to reside either in close association with bone marrow osteoblasts in the endosteum, a more hypoxic niche or in proximity to the vascular niche, where the oxygen concentration is higher (**Figure 1.2**) [44, 45]. The oxygen gradient seems to have an important role in the haematopoietic niche. Hypoxia, together with other factors, has a direct influence on proliferation and differentiation of HSC and MSC, as well as in the maintenance of stemness and multipotency [7, 45]. Several studies show that hypoxia promotes stem cell proliferation and skews them towards specific fates [46]. The balance between hypoxia-stemness-differentiation is not fully understood. Some studies show that hypoxia contributes to keep the "stemness" of stem cells while other studies show that hypoxia is a stimulus for cell differentiation [46, 47]. Despite these facts, some progress has been made and it is now known that some of the effects of hypoxia are directly mediated by the family of transcription factors called hypoxia-inducible factors (HIFs), that directly modify cell differentiation and stemness [46]. HIF proteins are synthesized at a high rate but are immediately degraded under normoxic conditions [48]. It is also known that metabolic activity under hypoxic conditions is regulated by HIFs (HIF-1α and HIF-2α), with HIF-1α being the more important one [6, 12, 49].

Hypoxia has an important role also in the field of cancer, increasing cancer stem cell proliferation and metastasis, as well as contributing to drug resistance [50].

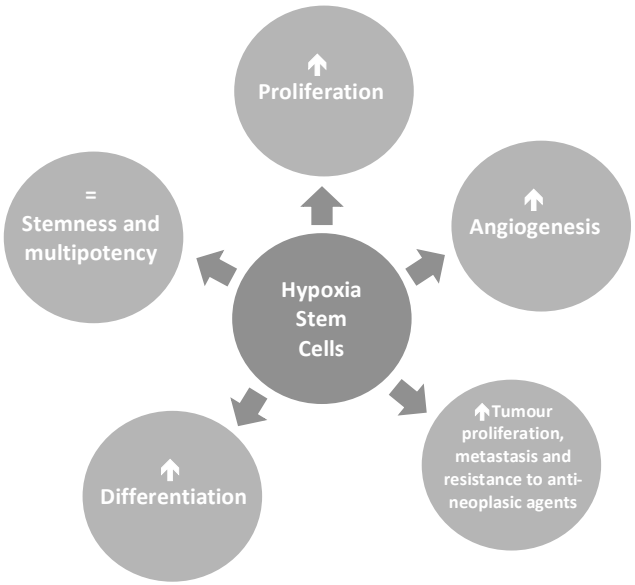

Figure 1.4 - Hypoxia effect on stem cells. Hypoxia promotes proliferation, angiogenesis, tumour growth, metastasis and resistance to antineoplastic drugs. Hypoxia also contributes for maintenance of stemness and multipotency, however studies also show that hypoxia promotes cell differentiation. For these reason is not fully understood how multipotency and differentiation balance works.

Cells obtain energy in the form of ATP (adesonine triphosphate), through the breakdown of carbohydrates (mainly glucose) or fat. Briefly, the process starts with glycolysis (aerobic), where the oxidation of glucose through a series of steps results in the production of pyruvate, and two energetic compounds, ATP and NADH (reduced nicotinamide adenine dinucleotide). Under normoxic conditions, through the Krebs cycle and oxidative phosphorylation, pyruvate is further oxidized generating more ATP. In the mitochondrial matrix, pyruvate is oxidised and NADH, FADH2 (flavin adenine dinucleotide hydroquinone form) and GTP (guanosine triphosphate) are released (Krebs cycle). Then, NADH and FADH2 from glycolysis and Krebs cycle pass through the mitochondria membrane and on the inside of mitochondria these molecules get into a series of redox reactions, where oxygen must be present. This process is designated as oxidative phosphorylation, where at the end of the process, 38 ATP molecules are released. However, in hypoxic conditions, Krebs cycle metabolism and oxidative phosphorylation do not occur and the pyruvate has to be converted into lactic acid and ATP by anaerobic glycolysis. Oxidative phosphorylation generates 38 ATP molecules whereas anaerobic glycolysis generates only 2 [51]. Therefore oxygen concentration regulates ATP production and an adequate balance of oxygen is extremely important to maintain efficient metabolic processes, especially because glucose metabolism is essential for a number of pathophysiological processes [48, 52, 53].

As referred above, in the bone marrow there is an oxygen gradient, where in normoxic conditions the cells obtain energy through oxidative phosphorylation, while in hypoxic conditions the cells obtain energy by anaerobic glycolysis [54]. In normoxic conditions HIF-

responsive genes are repressed, however when oxygen concentration decrease, HIF-responsive genes are rapidly expressed and stabilized, leading to the regulation of hundred of genes that promote an adaptive response. The HIF-regulated pathway regulates the expression of genes related to growth, survival, metabolism and angiogenesis [48]. Hypoxia regulated HIF expression, in turn, regulates HSC cell cycle quiescence, though this regulation has a narrow window, the niches cannot be either too hypoxic or too hyperoxic [12, 49].

The up-regulation of HIF-1α in HSC leads to a shift from mitochondrial oxidative phosphorylation towards anaerobic glycolysis [6]. However, why do cells proliferate more in hypoxia if anaerobic glycolysis is less efficient? The answer is probably because HIF activation also promotes glucose metabolism by aerobic glycolysis and because oxygen is generally not limiting for oxidative phosphorylation until the levels are extremely low [55]. Probably, for this reason, when cells are in hypoxic conditions, they have an advantage of having the energy resultant from oxidative phosphorylation and the associated increased concentrations of macromolecules (nucleotides, amino acids and lipids) necessary for cell division and proliferation by the increase of aerobic glycolysis [55].

In general HIFs are important regulators of homeostasis, consequently when this environment is disturbed HIFs also have a role. During inflammation, immune cells are in a hypoxic environment, therefore the HIF pathway has an important role in the regulation of immunity and inflammation, so HIF dysregulation has an impact on diseases [56]. For this reason the HIF pathway is a possible target for therapeutic strategies [48].

Nevertheless, hypoxia does not only interfere with cell metabolism and stem cell maintenance. Hypoxia also has a role in ECM composition. Distler *et al.* compared the dermal fibroblasts gene expression of several ECM proteins under hypoxic and normoxic conditions, and showed that hypoxia directly contributes to higher release of important ECM proteins [57]. Though, there is not a lot of information regarding the link between hypoxia and ECM, this was the focus of interest in this project.

1.3 Mesenchymal stem/stromal cells

Bone marrow mesenchymal stem/stromal cells (BM-MSC) provide an essential contribution to the haematopoietic niche. These stromal cells together with osteoblasts, fibroblasts, reticular cells, fat cells and endothelial cells contribute to ECM production, releasing different proteins, growth factors and adhesion molecules [4]. Besides a role in ECM production MSC also have other functions during haematopoiesis, MSC contribute to the long-term persistence and differentiation of HSC [58-61].

BM-MSC are currently among the best-studied but most poorly characterized adult stem cells. Despite their important role in haematopoiesis, BM-MSC and MSC from other sources,

are a promising source of cells for tissue engineering and regenerative medicine [62]. MSC are able to differentiate into bone, fat, cartilage and muscle tissue [63]. For this reason, the isolation and manipulation of MSC represents a promising tool for understanding tissue development and regeneration, as well as for studying the engineered repair of tissues and organs.

According with a position paper written by the Mesenchymal and Tissue Stem Cell Committee of the International Society for Cellular Therapy in 2006, cells are characterized as MSC if they fulfil certain minimal criteria. *In vitro* MSC need to have tri-lineage differentiation potency, differentiating into adipocytes, osteocytes and chondrocytes. In standard culture conditions, MSC must be plastic-adherent. Phenotypically, MSC do not express hematopoietic lineage markers CD11b, CD14, CD19, CD34, CD45, CD79α and human leukocyte antigen (HLA)-DR, however they should express CD73, CD90 and CD105 [64]. These criteria were established in an attempt to standardize MSC characterization, since there were already different protocols and different strategies for MSC isolation; and different studies demonstrated different outputs. However, the above characterization is not enough; there is a clear need of an assay to compare MSC.

MSC as a population were already characterized and it was explored whether there were phenotypically distinct subpopulations within BM-MSC [65]. Characterizing BM-MSC directly from fresh samples (without previous culture) allowed an analysis similar to physiological conditions, excluding the phenotypic alterations induced by the factors present in the culture medium and the number of passages. Results suggested that BM-MSC behave as one population, since all the markers were homogeneously expressed [65].

Following cell culture expansion, MSC in general express CD13, CD29, CD44, CD73, CD90, CD105, CD166, and HLA-ABC (human leukocyte antigen), but are negative for CD14, CD19, CD24, CD34, CD36, CD38, CD45, CD49d, CD117, CD133, and HLA-DR. However, there are a significant number of proteins that are not consistently expressed by MSC, such as CD31, CD71, CD80, CD106, CD119, CD130, CD146, CD173, CD271, CD273 or CD274 [65]. Some are not expressed by all the cells comprised in the MSC population, while others display heterogeneous expression, indicating a different quantity of protein per cell within the MSC population [66-70]. Moreover, there are contradictory data concerning the phenotypic characteristics of MSC [66]. Despite these inconsistencies, there is agreement that cultured expanded MSC include phenotypically distinct subpopulations. A recent study compared if single cell-derived clones from human adipose tissue MSC (ASC) had different immune-modulatory properties on T and NK cells, and results indicated that different clones expressed some differently markers [67].

Additionally, some phenotypic differences between MSC from the same source have been associated with different immunosuppressive capacities [67, 68]. Other phenotypic differences are correlated to other MSC features, such as MSC with higher expression of certain markers like CD146, CD271 and HLA-ABC, possess a higher clonogenic potential [66]. It was also reported that a BM-MSC population with tri-lineage capacity present higher expression of CD146, and had higher clonogenic potential and proliferated faster, compared with MSC that just differentiate into one or two lineages [67]. However, contradictory results were also presented, that MSC $CD146^+$ cells proliferate less [66]. This heterogeneity is not just found in human MSC, Claas *et al*. also describe mouse MSC as a heterogeneous population, identifying conditions for the isolation, selection and growth of clonogenic mouse BM-MSC [71].

Previously the importance of ECM growth factors and adhesion molecules in cell adhesion, proliferation, decision and survival was described. Besides their importance in the haematopoietic niche, these molecules are also essential for MSC immunosuppressive activity and for their migratory capacity. This migratory capacity, allows MSC to migrate towards tissues and organs (homing) or immune cells, to interact in close proximity with them. This migratory ability is important for the successful use of MSC in cell-based therapies.

The expression of several adhesion molecules by MSC and their interaction with several types of cells had been studied. For examples, CD29 (integrin β1-subunit) and CD106 (VCAM-1) are important for efficient adhesion of MSC to endothelial cells [70, 72, 73]. CD29 when dimerized with CD49e (integrin α5-subunit) forms a receptor that binds to fibronectin and invasin, promoting MSC-ECM interactions [74]. CD146 (Muc18) plays an important role in cell-to-cell and cell-ECM adhesion and increased expression of this marker on tumour cells is associated with increased cell motility and invasiveness/metastasis capability [75, 76]. The glycoprotein CD90 also regulates cell-to-cell and cell-ECM interactions, being reported to be involved in the MSC adhesion to endothelial cells, migration and tissue regeneration [77, 78]. MSC also express other molecules such as CD271 and CD105. CD271 that regulates nuclear factor kappa B (NF-kB) activation and are also involved in cell apoptosis, tissue regeneration, immune cell activation, proliferation and cell differentiation [79, 80]. CD105 is one of the receptors for TGF-β, involved in the regulation of development, maintenance and proliferation of MSC. It is also known to play an important role in tissue repair and immunosuppression [72].

Some studies show that MSC exposure to inflammatory cytokines increases their expression of immunomodulatory and adhesion molecules, demonstrating that MSC are highly sensitive to their microenvironment [81]. Signalling from their microenvironment allows MSC to rapidly alter their protein expression in order to adapt their functions to the physiologic

needs of the organism. In a pro-inflammatory environment, MSC become polarized towards MSC type 1 (MSC_1), and if the environment is immunosuppressive MSC become polarized towards MSC type 2 (MSC_2). MSC_1 are Toll-like receptors (TLR)-4 primed whereas MSC_2 are TLR-3 primed (**Figure 1.5**). In the end, it is the balance between the cytokines/chemokines released into the microenvironment that will contribute to MSC polarization. Thus, culture conditions can change the phenotype and function of MSC [82].

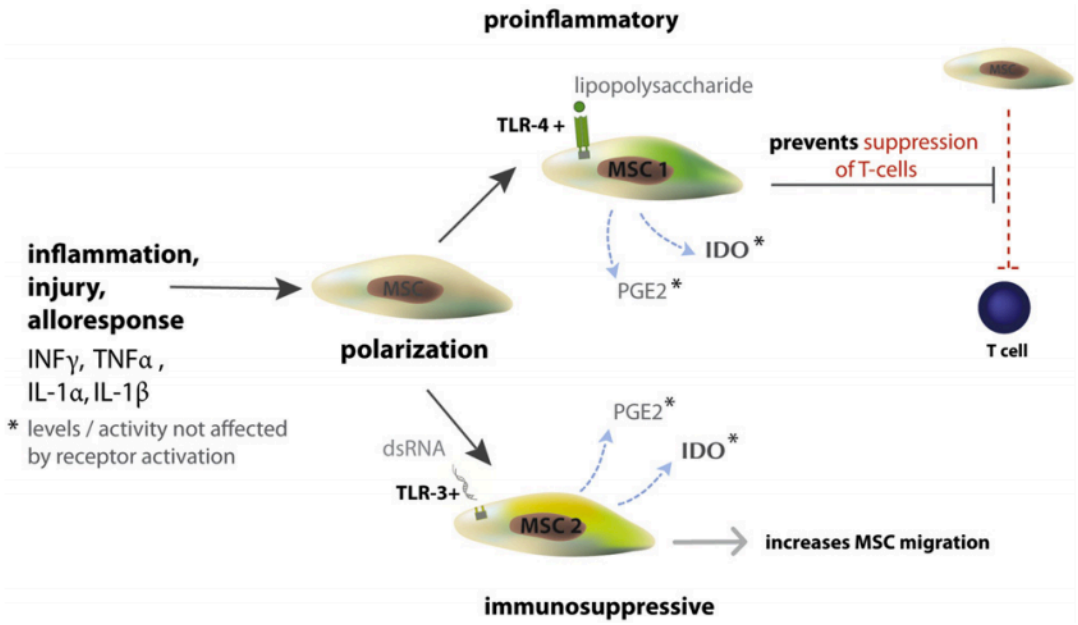

Figure 1.5 - Role of environment in MSC polarization [82].

Several factors influence MSC phenotype and function. The type of culture media, as well as the supplements (platelet lysate, fetal bovine serum) used clearly affect MSC phenotype and genotype [83]. Passage number also affects MSC phenotype; the higher the passage number, the lower is the surface expression of chemokines and adhesion molecules [84, 85]. Other factor is MSC confluence, that also affects gene expression [86].

1.3.1 Different sources of MSC

MSC are a rare population in the bone marrow, being reported to represent between 0.01% and 0.03% of all nucleated bone marrow cells; it is also assumed that this number declines with age, for this reason there was a need to isolate MSC from other tissues [65, 87]. In the adult, MSC can be isolated from adipose tissue (ASC), dental pulp, synovial membrane, lung, skin, menstrual blood and peripheral blood. From fetal tissues, sources include extra-embryonic structures of fetal origin such as umbilical cord blood (UCB), umbilical cord matrix (UCM) or Wharton's Jelly, amniotic fluid, amnion and placenta (the latter contains MSC from fetal and maternal origin) [64, 87]. The use of extra-embryonic fetal MSC not only circumvent ethical issues concerning the use of fetal MSC, because these structures are discarded after

parturition, but also avoids invasive procedures necessary to obtain these cells from adult tissues.

The best source of MSC to be applied in each disease is an important issue; there is evidence that MSC from different sources may have impact on the clinical outcome. In a previous study, human MSC isolated from different tissues, and tested under the same conditions, presented differential immunosuppressive abilities [88].

Despite the common phenotypic features and important functional characteristics shared between MSC from different tissues, it is recognized they display different characteristics which are ultimately reflected in their function, namely in their immune suppressive abilities. Despite the variability in MSC isolated from different tissues, it is also accepted that the culture conditions during cell expansion can influence MSC characteristics and functional behaviour. This is not surprising, given there high sensibility to micro-environmental conditions, and may be one of the features that contributes to their success as therapy. A significant inter-donor variability concerning the immune suppressive ability of MSC has been observed. Taken together, these factors cause difficulties in the comparison of the results in different studies, and raise important issues concerning the optimal protocol to isolate and expand MSC for clinical use. This is demonstrated in studies that compared MSC isolated from different tissues of the same donor, such as UCM-MSC versus UCB-MSC; and MSC derived from dental pulp versus periodontal ligament [89, 90]. For all these reason it is imperative to compare quantitatively MSC sources, cell culture passages (P), batches and donors.

Results from studies that compared human MSC from fetal or adult origin, are contradictory. For example, it was shown that BM-MSC loses their immunosuppressive ability to inhibit T cell proliferation after P_6-P_8, whereas fetal MSC maintained their immunosuppressive capacity for at least 25 passages. This effect was associated with decreased expression of HLA-G by BM-MSC after P_8; this did not happen with fetal derived MSC [91].

In contrast, results from studies comparing adult derived MSC, ASC and BM-MSC are more consistent, indicating that ASC present a higher immunosuppressive capacity. Indeed, in a previous study, it was shown that peripheral blood mononuclear cells (PBMC) stimulated with phytohaemagglutinin (PHA) and co-cultured with ASC or BM-MSC that ASC had a higher immunosuppressive effect on $CD4^+$ and $CD8^+$ T cells and B cells activation and proliferation, as well as $CD56^{dim}$ and $CD56^{bright}$ NK cell activation [88]. It was also shown that ASC had a stronger inhibitory effect on monocyte differentiation into DC and induced a higher secretion of IL-10 by these cells [92]. Also, ASC are more resistant than BM-MSC to Major Histocompatibility Complex (MHC) I specific lysis by $CD8^+$ T cells and to NK cell lytic activity [93, 94].

Finally MSC from different sources cultured in different conditions, present different expansion capabilities and survival capacities, influencing their immune-regulatory capacities. For example, considering molecules directly involved in MSC immunosuppressive functions, it was reported that ASC were shown to produce higher levels of leukaemia inhibitory factor (LIF) and prostaglandin E2 (PGE2), compared to BM-MSC and that ASC have an inferior osteogenic and chondrogenic differentiation potential [95-98]. These differences between MSC have an impact on their function. Also, the expression of chemokines, adhesion and immunosuppressive molecules is variable, thus also influencing MSC immunosuppressive potential. *In vitro* experiments where MSC are subjected to pro-inflammatory cytokines, TLR ligands, among others, can give important indications about how MSC function is conditioned after *in vivo* infusion, under non-homeostatic conditions, such as when tissue damage or infection has occurred.

One detail regarding ASC that has been neglected is the fact that adipose tissue is a very active organ containing many inflammatory cytokines such as IL-6, IL-1 and TNF-α [99]. The question is: are the ASC primed towards MSC_1 (pro-inflammatory) or towards MSC_2 (immunosuppressive), in this inflammatory environment? The adipose tissue microenvironment effect on ASC function remains unknown. In obese individuals it is known that ASC and mononuclear cells interact and it has been shown that the inflamed environment in obesity may stimulate ASC differentiation into adipocytes, which further increase the adipose tissue mass [100, 101]. Finally, in another study from obese patients, it was suggested that ASC together with monocytes and $Th_{17}T$ cells have a role in the pro-inflammatory process [100].

1.3.2 MSC as a therapy

Exists considerable enthusiasm surrounding the therapeutic benefits of MSC. This is because firstly these cells can undergo multi-differentiation, suggesting they can regenerate damaged tissue either by replacing the injured cells or by changing the microenvironment surrounding the degenerating tissues (producing trophic factors or modulating inflammation, allowing a faster and efficient recovery of the damaged cells and tissues). A second MSC property that has been encouraging the use of MSC to treat several diseases is their immunomodulatory capacity. This property is very important in order to control the undesirable or exacerbated immune responses that occur in autoimmune, or inflammatory diseases, like graft rejection and graft versus host disease (GvHD). MSC have the capacity of homing to injured tissue and inflamed sites, undergoing differentiation in a tissue specific manner, contributing to the regulation of immune response and influencing the behaviour of the neighbouring cells.

It has been demonstrated that MSC delivered locally or systemically, as well as within artificial or ECM scaffolds, retain their properties. MSC offer unique advantages as a cell-based therapy. They have been tested in the treatment of a broad spectrum of disorders having a diverse aetiology and pathophysiology, such as myocardial infarction, cerebral vascular accidents, osteogenesis imperfecta, spinal cord injury, wound healing, amyotrophic lateral sclerosis (ALS), multiple sclerosis (MS), myocardial infarction, liver cirrhosis, diabetes mellitus, systemic lupus erythematosus, arthritis, Crohn's disease, acute lung injury and chronic obstructive pulmonary disease, amongst others [102-105].

A wide range of studies has been carried out with MSC in the field of regenerative medicine and tissue engineering. Remarkable results have been achieved using MSC based therapies in tissue regeneration, where MSC release growth factors contributing to tissue regeneration, and decrease scar formation. Although it is important to conduct more clinical trials in different disorders, and some fundamental questions need to be answered before MSC therapies enter routine clinical practice. One concern is the long-term safety of MSC-based therapy, including the potential risk of malignant transformation or ectopic tissue formation. Although malignant transformation of MSC has not yet been described following injection *in vivo*, some studies suggest that MSC may favour the survival and metastatic potential of pre-existing tumours [106-108]. In a mouse model of myocardial infarction, MSC may also contribution to intramyocardial calcification [109].

An important factor in the outcome of MSC therapy is the duration of the treatment, Lucchini *et al.* suggest that even the same patient may respond differently to MSC infusion at different time points of their clinical history, and the phase II clinical trial study of MultiStem cell therapy for treatment of ischemic stroke confirmed this idea [110, 111].

Another question is whether autologous or allogeneic MSC should be used. Theoretically, autologous MSC do not trigger the donor-specific immune responses that are typically associated with allo-transplants. MHC-mismatched MSC are able to immunosuppress T cells. For these reasons, MSC have been considered as "immune privileged" cells being a good off-the-shelf product for cell-therapies [105, 112]. However, recent studies show that MSC may not actually be immune privileged. There is an increasing body of evidence showing that allogeneic MSC trigger both T and B cell responses [113]. However, whether rejection of donor MSC influences the efficacy of allogeneic MSC is not known.

There is no clinical advantage of using autologous versus allogeneic MSC. However, it is important to consider that, as referred above, culture-expanded MSC consist of a heterogeneous population expressing different phenotypes and functional properties [105]. It is also worth mentioning that an autologous MSC transplant may not be a good option in an already sick patient. For example, in a case of GvHD, patient using the patient's own BM-MSC

would not be beneficial, because a malignant cell may be present [114]. In fact, MSC isolated from myelodysplasic patients had the same genetic alterations, while MSC isolated from individuals with other diseases did not show genetic alterations [115]. It is also important to point out that MSC are a rare population in the bone marrow, for this reason and in situations of acute organ failure, autologous MSC are not an option and where a ready-to-use source of allogeneic MSC would be more advantageous.

Another possibility in using MSC as a cell therapy is that MSC can be manipulated in culture to obtain phenotypes that more effectively treat one disease over another [105]. Other issues that need considering are the cell preparation techniques, the route of administration, the optimal timing of administration, the cell dose and the number of infusions needed for successful outcome. Further investigation will be needed to determine the optimal protocol for each disorder that can benefit from MSC-based therapy.

1.3.3 MSC Immunosuppressive capacity

In the last decade, several studies have emerged demonstrating that autologous and allogeneic culture-expanded MSC from different sources possess immunomodulatory properties [1–3]. However not all the studies are in agreement. This is not surprising, because MSC are highly sensitive to microenvironment and there are technical differences between studies (MSC source, MSC expansion conditions, cells ratio, types of cell present in the co-culture, different stimulus, among others).

MSC immunosuppressive mechanism is complex and despite several groups trying to complete the story, it is still not fully understood. It is known that to inhibit an immune response, MSC rely on soluble mediators and/or cell-to-cell contact. Studies demonstrate that MSC immunosuppressive capacity was not dependent on cell contact, but was increased by close proximity to the target cell [105]. MSC immunosuppression mechanism differs between immune cell types. However, in general, human MSC release PGE2, hepatic growth factor (HGF), or indoleamine-2,3-dioxygenase (IDO), and these molecules have been demonstrated to modulate the immune response. Other molecules may be also involved, such as TGF-β, human HLA-antigen G (HLA-G), IL-6, IL-10, HGF, IL-1RA, IL-6 and tumour necrosis factor-inducible gene 6 protein (TSG6) (**Figure 1.6**) [112, 116]. English, in a review, explains very well the MSC immunomodulation mechanism and the effect of some of this soluble factors and MSC-cell contact-dependent pathways [117].

However, MSC from different species may employ different immunosuppressive molecules, as is the case with nitric oxide (NO) produced by mouse MSC and which seems to be an important immune suppressive factor employed by mouse MSC, but not by human MSC. Likewise, there is evidence that in man, distinct immunomodulatory factors may have a

different importance for the immune-regulatory function of MSC from different sources. This occurs because there are important differences in the expression levels of immunomodulatory molecules between MSC derived from different tissues.

MSC immunomodulate innate and adaptative responses using different factores/mechanisms, that is dependent on the environment (proinflammatori/TLR4 or immunosuppressive/TLR3). Blanc and Davies, summarized very nicely in **Figure 1.6** the factors involved in MSC modulation with different immune cells [118].

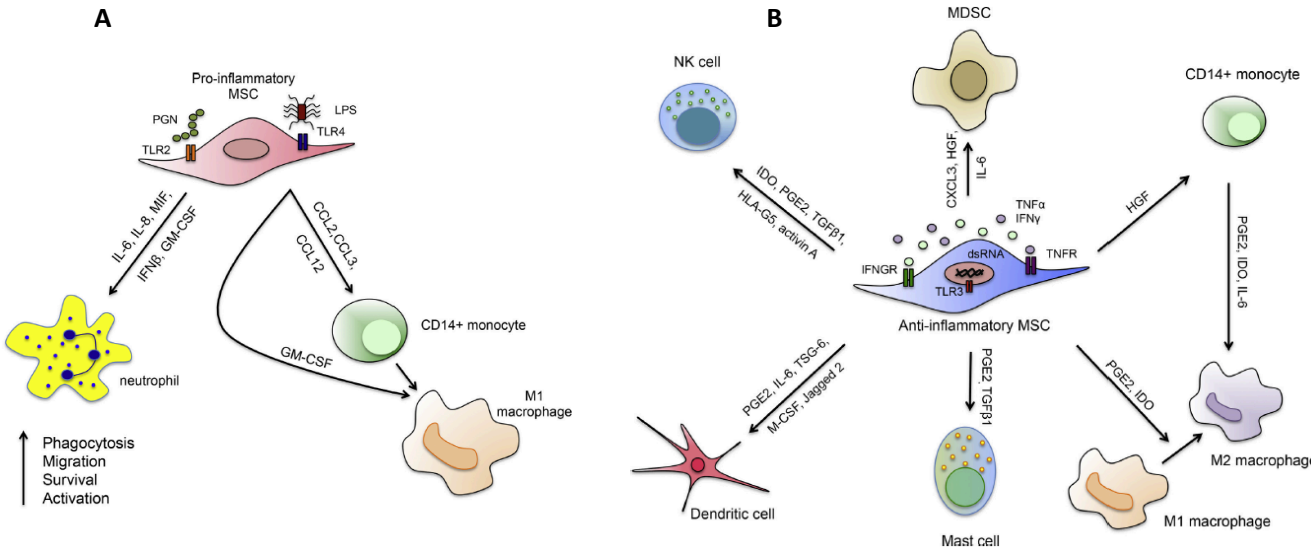

Figure 1.6 - MSC immunosuppressive mediators and targets. **A** pro-inflammatory MSC interaction with Neutrophils, monocytes and macrophages. **B** anti-inflammatory MSC interaction with Myeloid-derived suppressor cells (MDSC), monocytes, macrophages, mast cells, dendritic cells and NK cells [118].

Recently a new field has emerged that focuses on the paracrine effects of MSC. Components such as vesicles released by cells, have been receiving increased attention as immunosuppressive cell-free factors, especially those mediated by the release of exosomes by MSC. This is a possible strategy for the treatment of conditions where it is not possible to deliver MSC or the homing of the cells is not fast enough, such as in the case of cerebral vascular accidents. Exosomes are a subpopulation of small extracellular vesicles; are lipid bilayer enclosed membrane vesicles [119]. These small particles (30-100 nm) contain proteins, lipids, messenger RNA (mRNA) and microRNA (miRNA) that can be transferred between cells, playing an important role in intercellular communication [120]. MicroRNA constitute a major regulatory gene family. They regulate the translation of many genes affecting protein production of recipient cells [121]. MicroRNA are likely to be involved in several biological processes, since they affect the translation of mRNA and gene regulation [120]. The human genome may encode over 1 000 miRNA that target approximately 60% of mammalian genes [122].

Different cells release exosomes with different content, even the same cell produces exosomes with different composition, depending on the microenvironment [119]. Exosomes have been implicated in many aspects of immune regulation such as the differentiation of monocytes into dendritic cells or the stimulation of T cell proliferation (**Figure 1.7**) [123-126]. It has been suggested that exosomes released by MSC have a possible immunomodulatory capacity [127, 128]. However, disease cells also release exosomes, for example, in Parkinson and Alzheimer patients it was reported that neurons from these patients release exosomes that could contribute to the dissemination of the diseases [128].

Nevertheless exosomes not only provide biologically active molecules, they can also be used as a vehicle for drug delivery [129].

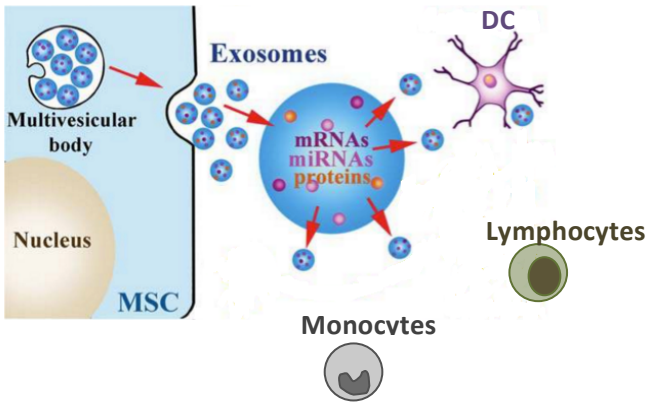

Figure 1.7 - MSC exosomes release to the microenvironment. Figure adapted from [130].

Recently, it was shown that the immunosuppressive activity of so-called regulatory T cells (Treg) on naïve T cell activation was mediated by the transfer of small interfering RNA (siRNA) contained in Treg-derived exosomes [131]. Using a similar protocol, we investigated whether MSC-mediated immunosuppression was mediated by a similar mechanism.

1.4 Monocytes

Monocytes, macrophages, and dendritic cells (DC), and their respective committed progenitors constitute one lineage, often called the myeloid lineage, of bone marrow hematopoietic cells [132, 133]. Together, these cells play important roles in the maintenance of tissue integrity during development and its restoration after injury, as well as the initiation and resolution of innate and adaptive immunity [132].

Monocytes are a subset of leukocytes that represent between 5 to 10% of peripheral blood leukocytes. These cells originate from a myeloid precursor in the bone marrow that with the aid of growth factors such as granulocyte-macrophage colony stimulating factor (GM-CSF) and macrophage colony-stimulating factor (M-CSF), begin their differentiation in the bone

marrow (BM) with the formation of monoblasts followed by promonocytes and monocytes [134]. From the BM monocytes circulate into the bloodstream and migrate into various tissues. In the different tissues, monocytes can further differentiate into mature myeloid effector cells including macrophages and dendritic cells [133]. Pulmonary alveolar macrophages, hepatic Kupffer cells, pleural and peritoneal macrophages, osteoclasts, Langerhans and interdigitating dendritic cells in various tissues, and perhaps microglial cells in the central nervous system are all examples of cells of the myeloid lineage [133, 135, 136]. However not all tissue-resident macrophages derive from peripheral blood monocytes, a significant number of tissue macrophages have a independent embryonic origin, but can be replaced by monocytes [137].

When inflammation occurs due to tissue damage or infection there is activation of resident macrophages, with a corresponding increase in the production of cytokines, chemokines, and other inflammatory molecules and the recruitment of circulating monocytes [138, 139]. Monocytes are implicated in host antimicrobial defence because of macrophages phagocytic activity and are the first cells being recruited to sites of inflammation. Monocytes produce anti-inflammatory, as well as pro-inflammatory cytokines, helping in the recruitment of other cells to sites of inflammation. However, monocytes are also associated with increasing pathogenicity, such as atherosclerosis, or can inhibit tumour-specific immune defence mechanisms [140].

Monocytes have critical roles in innate and adaptive immunity during infection and sterile inflammation, and respond rapidly to activation signals via an array of pattern recognition receptors [139, 141, 142]. Monocytes coordinate the interaction of T and B cells during antigen presentation. Monocytes also have an immune-regulatory function being involved in suppression of lymphocyte proliferation and inhibition of lymphokine production.

Within 24 hours of its production, the mature monocyte, in the G1 phase of cell cycle, is released from the bone marrow and enters the peripheral circulation. The half-life of bloodstream monocyte is relatively short, of the order of 3 days, fostering the concept that circulating monocytes may continuously repopulate tissue populations to maintain homeostasis and, during inflammation, fulfil critical roles in innate and adaptive immunity [142]. Following migration, monocytes increase cell size and acquired the cytological appearance of a tissue macrophage.

During inflammation, monocytes produce several key pro-inflammatory mediators including tumour necrosis factor alpha (TNF-α), interleukin (IL)-12, IL-6 and monocyte chemo-attractant protein 1 (MCP1; also known as CCL2) [142, 143]. TNF-α is involved in the pathogenesis of several diseases such as arthritis, sepsis, acute tissue ischemia, inflammatory bowel disease and GvHD. MSC administration could be used to decrease the severity of inflammation [144-147].

Currently, human peripheral blood monocytes are subdivided into three subpopulations according to CD14 and CD16 expression. Thus, three subpopulations of monocytes are defined: $CD14^{++}CD16^{-}$ so-called "classical", $CD14^{++}CD16^{+}$ "intermediate" and $CD14^{+}CD16^{++}$ "non-classical" monocytes [148]. This nomenclature was adopted by a group of experts from the World Health Organization (WHO), International Union of Immunological Societies (IUIS), Dendritic Cells for Novel Immunotherapies (DCTHERA), European Network of Excellence, and from the European Macrophage and Dendritic Cell Society. This agreement is especially important for DC sub-populations, where different groups define DC and monocyte subsets differently, leading to confusing results. In this way, there are three subpopulations of monocytes (classical, intermediate and non-classical) and three subpopulations of DC: two types of myeloid DC (mDC) and one type of plasmacytoid DC (pDC) [148]. In healthy human subjects, classical monocytes represent the majority of the peripheral blood monocytes, compromising around 85% of total monocytes, intermediates are 5% and non-classical 10% [149]. The non-classical monocyte is the subpopulation that creates most confusion regarding their nature; there is still not a consensus about that subject.

Besides CD14 and CD16 expression, peripheral blood monocyte and DC subsets can be distinguished by their expression of CD45, CD33, HLA-DR and IREM-2, as well as by their side scatter (SSC) and forward scatter (FSC) properties. Human and mouse monocyte subsets are defined differently, but their clear identification allows a more concordant investigation to determine their functional roles during homeostasis and inflammation.

Different monocyte subsets have different phenotypes, morphology and specific functions [150]. As explained in the following Chapter, the classical monocytes was the subset of most interest.

It has been demonstrated by deep genetic and proteomic analyses that monocytes subsets are functionally distinct. Zhao *et al.* and Zawada *et al.* revealed new functional differences between monocyte subpopulations, distinguished by different markers. Zhao *et al.* looked into gene expression of proteins and mRNA while Zawada *et al* analysed transcriptomes using high-throughput sequencing. These differences may reflect the fact that different monocyte subsets regulate innate and adaptive immune responses differently [151, 152]. Another study shows that classical and non-classical monocytes have the same common myeloid precursor with non-classical monocytes having a more macrophage and DC like transcriptional profile, suggesting that these monocytes are in a more advanced stage of differentiation [153]. One interesting feature of non-classical monocytes is that these cells can present antigens to B cells leading to antibody production in a T cell independent way [154].

As referred above, an important role of monocytes in the immune response, is the production of cytokines. Monocytes have the ability to produce IL-1β, IL-6, IL-12, IL-8, TNF-α

and interferon-gamma (IFN-γ) in response to lipopolysaccharide (LPS), however the percentage of monocytes subpopulation producing cytokines is different. Classical monocytes produce more cytokine than non-classical monocytes [150].

1.5 T cells

T cells are thymus-derived lymphocytes that express CD3 and comprise several subpopulations, however the main ones are defined by the expression of $CD4^+$ (T helper) and $CD8^+$ (T cytotoxic). T helper cells play a central role in immune protection. $CD4^+$ cells interact with B cells helping them to make antibodies. They also induce macrophages to develop enhanced microbicidal activity. $CD4^+$ T cells are also involved in neutrophil, eosinophil, and basophil recruitment to sites of infection and inflammation. These cells also help in the orchestration of immune responses through their production of cytokines and chemokines [155]. $CD4^+$ T cells following activation undergo clonal expansion and differentiation into distinct effector phenotypes: Th_1, Th_2, and Th_{17}, and memory $CD4^+$ T cells. $CD8^+$ T cytotoxic cells rapidly kill target cells either by the secretion of lytic granules or by ligation of death receptors. Lytic granules are secretory vesicles containing the pore-forming proteins perforin and granzymes [156]. Treg cells ($CD4^+CD25^+$) play an important role in the maintenance of self-tolerance, preventing autoimmune and inflammatory diseases [157]. It is the balance between the recruitment and activation of T and B cells, as well as Treg that leads to a critical control of the quality and importance of adaptive immune responses [158].

T cells are important cells of acquired immunity, with distinct effector functions, having a central role in cell-mediated immunity. Following T cell activation and depending on the micro environmental conditions, T cells will secrete cytokines, and the molecules produced will determine the recruitment and activity of other immune cells [159].

1.6 Monocytes and MSC

The effects of MSC on monocytes have been recently a focus of interest of some groups. It has been shown that MSC support monocyte survival through physical contacts, as well as an inhibitory effect on monocyte differentiation into DC [160-162].

Figure 1.8 represents a scheme for the interactions between MSC and monocytes. The figure shows that in an anti-inflammatory situation (**A**) MSC secrete IL-6, IDO and PGE2 which polarizes monocytes toward M2 macrophages. These cells will then produce more IL-6 and IL-10, contributing to a more anti-inflammatory environment. This polarization is initiated by and dependent on cell-cell contact. The polarizing effect of MSC on macrophages is related to their ability to favour the emergence of so-called regulatory T cells (Treg). Besides IL-6 and PGE2, MSC also produce TGF-β, and soluble HLA-G while the macrophages contribute with CCL18.

In the absence of IL-6, MSC polarize monocytes toward M1 macrophages (**Figure 1.8 B**). When the monocytes are becoming pro-inflammatory macrophages, they release IFN-γ and IL-1, and express CD40L. The M1 macrophages also release IFN-γ and TNF-α, and start expressing CD86, a co-stimulatory molecule that promote T cell activation. The increase concentration of molecules such as IFN-γ and TNF-α lead to an anti-inflammatory pathway, described previously. The balance between these two pathways is very important for host defence and inflammation, preventing excessive tissue damage [117, 163].

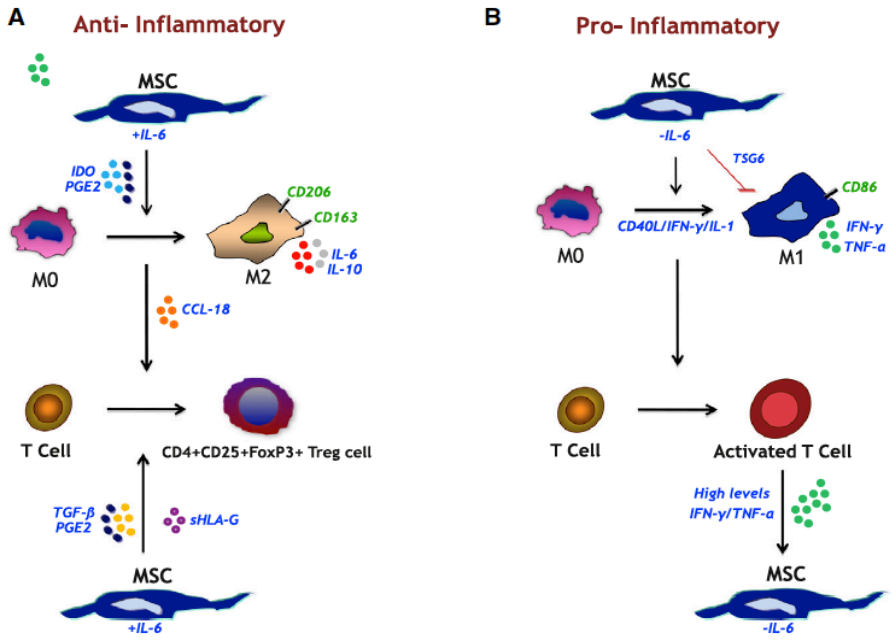

Figure 1.8 - MSC-monocyte interaction. **A** monocytes are polarized by MSC toward anti-inflammatory macrophages M2. In **B** monocytes are polarized toward pro-inflammatory M1 [163].

1.7 T cells and MSC

As discussed above, MSC have an effect on T cell proliferation and differentiation. These studies have been carried out independently by different groups using different activation methods or different sources of MSC.

1.8 Monocytes and T cell activation

To study monocytes and T cell activation, there are several methods that can be used *in vitro*. For monocytes, the majority of activation methods involve stimulation of their TLR, whereas for T cells, T cell receptor (TCR) activation is one of the methods. Nevertheless, for both cell types, there are other activation methods not involving TLR or TCR activation.

TLR are largely divided into two subgroups depending on their cellular localization and respective pathogen-associated molecular pattern (PAMPs) ligands. One group is composed of TLR1, TLR2, TLR4, TLR5, TLR6 and TLR11, that are expressed on cell surfaces and recognize mainly microbial membrane components such as lipids, lipoproteins and proteins. The other group is composed of TLR3, TLR7, TLR8 and TLR9, that are expressed exclusively in intracellular vesicles such as the endoplasmic reticulum, endosomes, lysosomes and endolysosomes, where they recognize microbial nucleic acids.

LPS is a polysaccharide anchored to Lipid A found in the membrane of Gram-negative bacteria. Lipid A, also known as endotoxin, it is responsible for the immune-stimulatory activity of LPS. Via their TLR4 molecules, LPS is commonly used to activate monocytes *in vitro*.

According to current models, Lipid A is delivered to the CD14 molecule by the LPS binding protein (LBP). Then the LPS is translocated to the myeloid differentiation protein 2 (MD2) and there is a formation of TLR4–MD2 complex. After that, TLR4 forms dimers and a signal enters the cell. Following dimerization, two distinct signalling pathways are initiated, the first myeloid differentiation protein 88 (MyD88)-dependent, leading to the production of pro-inflammatory cytokines, and the second TIR domain-containing adaptor inducing interferon-β (TRIF)-dependent (or MyD88-independent) pathway, a less inflammatory pathway (**Figure 1.9**). In the MyD88-dependent pathway, a signalling cascade is initiated leading to the activation of NF-κB. NF-kB is translocated into the nucleus and there induces the transcription of pro-inflammatory cytokines genes such as those encoding TNF-α, IL-6 and IL-12. The MyD88-dependent response is used by every TLR except TLR3. TRIF-dependent pathway occurs after internalization of the endosome with TLR4–MD2 complex. Translocating chain-associating membrane protein (TRAM) and TRIF recruitment triggers a transduction signal that leads to the activation of interferon regulatory factor 3 (IRF3) and late-phase NF-κB. The TRIF-dependent pathway is characterized by the production of interferon-β (IFN-β), G-CSF, MCP1, chemokine (C-C motif) ligand 5 (CCL5) and C-X-C motif chemokine 10 (CXCL10).

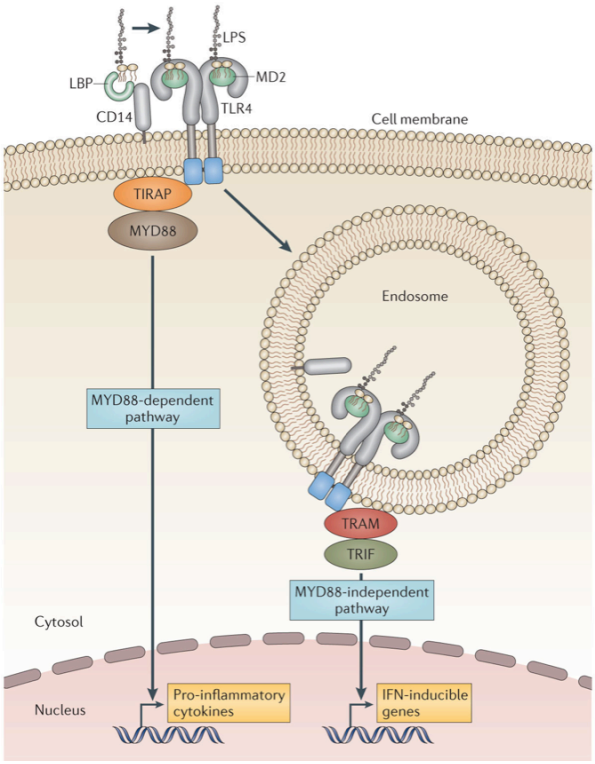

Figure 1.9 - TLR4 activation, MyD88-independent and TRIF-dependent pathways [164].

Pam3Cys-Ser-(Lys)4 (Pam3CSK4) is a TLR2/TLR1 agonist, a synthetic analogue of bacterial lipoproteins, with three lipid chains (triacylated). TLR2 agonists induce mainly the production of inflammatory cytokines. TLR2 is involved in the recognition of a wide range of PAMPs. In general TLR2 forms heterodimers with TLR1 or TLR6. TLR2/TLR1 heterodimer recognizes triacylated lipopeptides from Gram-negative bacteria and mycoplasma. Pam3CSK4 interact with TLR2 with two lipid chains, whereas the third chain binds the hydrophobic channel of TLR1, creating a TLR2/TLR1-ligand complex [165]. Following TLR2/TLR1-ligand complex formation, the MyD88-dependent pathway is initiated and the activation proceeds as described previously (**Figure 1.10**).

Polyinosinic-polycytidylic acid (PolyIC) is a TLR3 ligand, and is a synthetic analogue of double-stranded RNA (dsRNA). PolyIC mimics a viral infection and induces antiviral immune responses by promoting the production of both type I interferon and inflammatory cytokines, suggesting that TLR3 has an essential role in preventing virus infection [165]. TLR3 is expressed exclusively in intracellular vesicles such as the endoplasmic reticulum, endosomes, lysosomes and endolysosomes, where it recognizes microbial nucleic acids. TLR3 activates the TRIF-dependent pathway and activates NF-κB and IRF3.

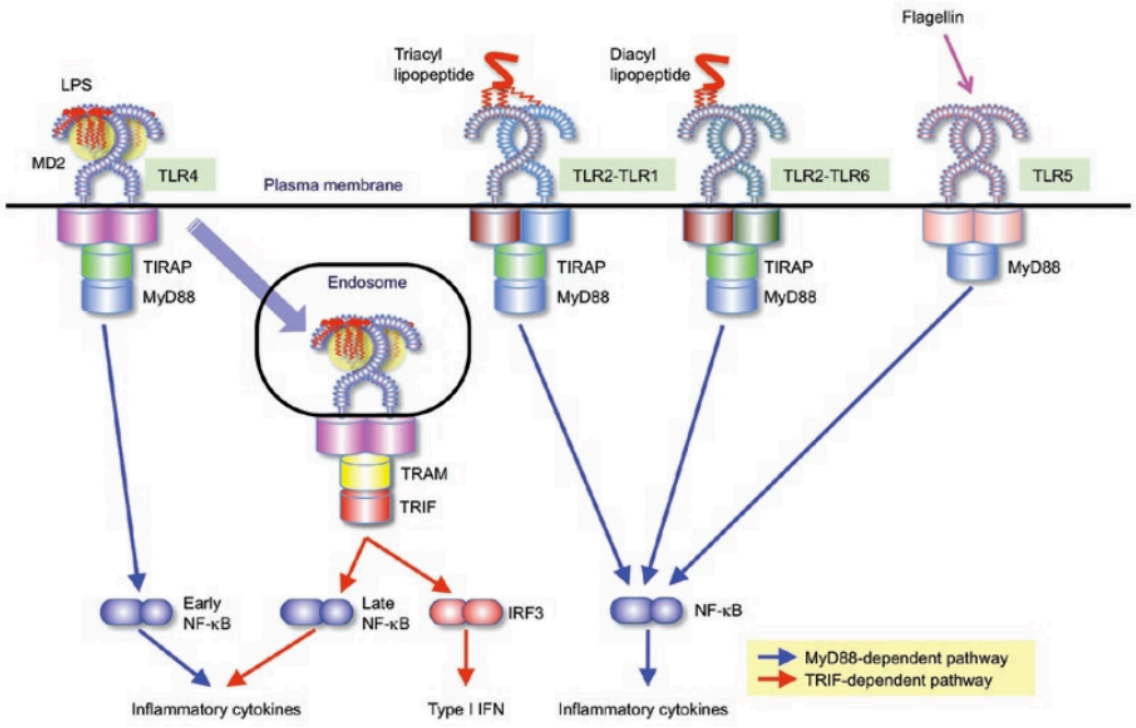

Figure 1.10 - PAMPs recognition by cell surface TLR [165].

N-acetylmuramyl-L-alanyl-D-isoglutamine or muramyl dipeptide (MDP) is a neurotrophic and immunomodulatory factor. MDP is the minimal bioactive peptidoglycan motif common to all bacteria, the essential structure required for adjuvant activity in vaccines. MDP has been shown to be recognized by the intracellular receptor nucleotide-binding oligomerization domain-containing protein 2 (NOD2), but not TLR2, nor TLR2/TLR1 or TLR2/TLR6 associations [166, 167]. PAMPs can also be recognised by cytosolic pattern-recognition receptors (PRRs). Among the PRRs, NOD2 recognize the degradation products of bacterial cell wall components, and NLRP3 responds to various stimuli to form the inflammasome complex, which promotes the release of IL-1β and IL-18 via caspase-1.

Phorbol myristate acetate (PMA) is a potent nanomolar activator of protein kinase C (PKC). PKC is a family of kinase enzymes evolved in the regulation of other proteins. These enzymes have an important function in several signal transduction cascades. PKC are activated by increasing concentrations of calcium or diacylglycerol. Schultz *et al.* showed that PMA induced activation of the $p38^{RK}$ cascade, downstream of PKC [168]. PMA is used to activate different types of cells, as well as to differentiate monocytes into macrophages. PMA with a calcium ionophore, ionomycin, mimic early signal transduction pathways and lead to T cell activation, proliferation and cytokine production [169].

Phytohaemagglutinin (PHA) is a lectin found in plants. Lectins are proteins that recognize and bind to specific carbohydrate targets, each lectin recognize a specific sugar group [170].

TCR T cell activation requires the presence of an antigen that is normally presented to them in the form of a peptide bound to a molecule of the MHC on the surface of so-called antigen-presenting cells (APCs). T cells do not respond to antigens in solution. The T cell receptor is composed of a series of associated proteins including the heterodimeric T cell receptor and its associated signalling molecules collectively called CD3. Following TCR and antigen binding (antigen presentation) a subsequent downstream activation occurs. This activation leads to the rearrangement and clustering of receptors in the surface of lymphocytes. The clustering is very important to bring all signalling receptors close enough to propagate the activation signal. Therefore, PHA binds to carbohydrate components of the TCR complex and mediates receptor clustering with consequent activation [170].

T-cell activation and initiation of effector functions (e.g., cytokine production, proliferation, cytotoxicity of target cells or stimulation of antibody production by B cells) is a very complex process. In a simplistic manner TCR activation needs two signals: signal one is the binding of TCR to a MHC molecule carrying a peptide antigen. The second is provided by the binding of the co-stimulatory receptor CD28 on T cells to proteins in the surface of the APCs, such as B7-2 or B7-1.

Currently, exists a variety of models to explain T cell activation, the interactions between TCR and peptide-MHC complexes and TCR intracellular signalling. Once a T cell has been appropriately activated it alters its cell surface expression of a variety of proteins. Activated T cells change their cell surface glycosylation profile and activation markers that include CD69, CD71 and CD25, and HLA-DR. CD152 (cytotoxic T-lymphocyte-associated protein 4/CTLA-4) expression is also up-regulated on activated T cells, which in turn outcompetes CD28 for binding to the B7 proteins. At this stage the cells have a checkpoint to prevent over activation.

The TCR consists of a variable TCRαβ heterodimer that binds to ligands. All CD3 complex subunits contain immune-receptor tyrosine-based activation motifs (ITAMs) in their cytoplasmic domains. TCRαβ binds complexes of peptide and MHC molecules on the surface of APCs or target cells, which results in biochemical changes in the cytoplasmic portions of the CD3 complex.

In vitro, there are several methods to activate T cells, some of them were previously described, however the most physiologic method is probably that using CD3/CD28 commercial beads (**Figure 1.11**).

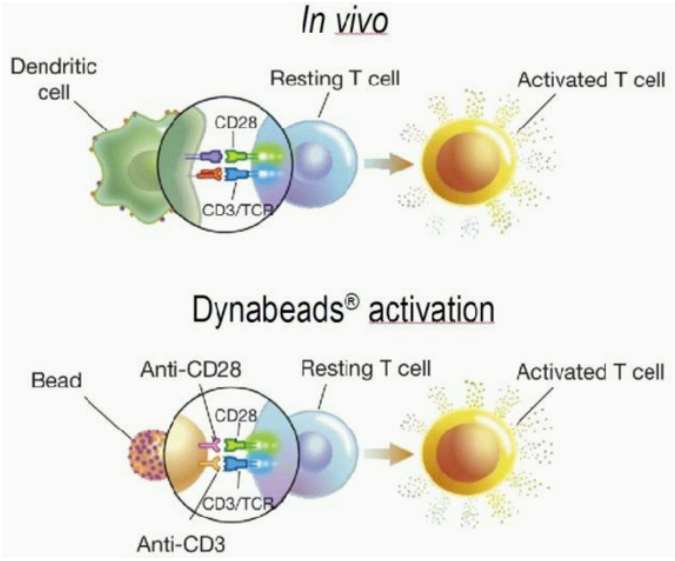

Figure 1.11 - *In vitro* T cell activation with CD3/CD28 beads. The beads mimic *in vivo* T cell activation from APC (above) by using the two activation signals CD3 and CD28, bound to a 3D bead similar in size to the APC (below).

1.9 Overall objectives

The first part of this project was to develop a whole blood assay to screen for the potency of human MSC to suppress innate immune responses (Chapter 2). Another aim was to compare the potency of MSC isolated from bone marrow and adipose tissue using blood samples collected from healthy, osteoarthritis and rheumatoid arthritis individuals (Chapter 3, first part), this aim was reached using the whole blood assay. In the second part of Chapter 3, the assay was used to investigate the effect of synthetic and biological scaffolds on monocyte activation, as well as for the screening of the immunosuppressive capacity of several seaweed extracts on monocytes. In Chapter 3, the main aim was to show the applications of the whole blood assay developed in the previous chapter. Chapters 2 and 3 are then discussed in Chapter 4.

In Chapter 5, the nature and quality of ECM produced by MSC is investigated. For this, a cloned mouse bone marrow MSC line was used and two methods for the isolation of ECM compared. Particular attention was made to the effect of hypoxia on ECM composition. Experiments were also done to investigate the biological function of ECM prepared under different conditions. Results of this work are presented in Chapter 5, followed by Chapter 6 entitled Future Perspectives.

Chapter 2 | Development of a flow cytometry-based potency assay to measure the *in vitro* immunomodulatory properties of human Mesenchymal Stromal Cells

2.1 Introduction

In the last decade, several studies have emerged demonstrating that autologous and allogeneic culture-expanded BM-MSC possesses immunomodulatory properties [112, 171, 172]. It has been convincingly shown that such immunomodulatory properties of MSC play specific roles in the maintenance of peripheral transplantation tolerance, autoimmunity, tumour evasion, as well as feto-maternal tolerance [172]. The anti-inflammatory activities of both, autologous and allogeneic MSC, are being exploited clinically with administration of MSC now being used to treat or prevent a range of immune/inflammatory diseases such as GvHD, inflammatory bowel disease (IBD), diabetes mellitus, MS, myocardial infarction among others [143, 173, 174]. Furthermore, the immunomodulatory activities of MSC *in vitro* have been measured on different immunological cell types, including T cells, B cells, NK cells and monocytes [88, 175-178].

2.1.1 MSC commercial value and potency assays

Currently, there are at least 572 on-going clinical trials worldwide which aim to exploit the anti-inflammatory and immunomodulatory properties of MSC (www.clinicaltrials.gov). Global commercialization activities in the stem cells market have increased dramatically during the past decade with the establishment of several heavily capitalized companies focusing on MSC manufacturing and cryopreservation [112]. In the United States, stem cell and tissue engineering market had a commercial growth of 3 fold between 2011 and 2015. The number of companies selling products or offering services has increased over 2 fold, generating a remarkable 3.5 billion dollars in profits, and employing almost 14,000 employees. The stem cell and tissue engineering industry has stabilized and is on a path pointing toward continued success [179]. As more individual MSC sources and products are developed and trialled as clinical products, and as the regulatory framework for clinical trials of stem cell products continues to evolve, there will be a clear need to confirm and compare the potency of the immunomodulatory/anti-inflammatory effects of each product for optimal treatment of disease [180-182].

Although these effects are linked to their therapeutic benefit in diverse diseases, a reliable, quantitative assay of the immunomodulatory potency of individual human MSC preparations is lacking. There are some assays available, however they have several limitations, the most common being the duration of the assay. Also, some of the assays use ELISA (enzyme-linked immunosorbent assay) as readout, this means it is not possible to identify which cells produce the cytokines or to quantify the number that are activated; also it takes longer to have results.

As example of potency assays, Jiao *et al*. in 2011, developed a potency assay in models of inflammatory organ failure, where MSC conditioned medium or lysate were cultured for 16-18 hours with PBMC. The readout of this assay is just IL-10 measurement by ELISA [181]. In 2015, Ketterl *et al*. developed an assay where they could observe donor variation. However the MSC culture with PBMC took at least 4 days in culture and the readout was just T cell proliferation by flow cytometry [178, 183].

For this reasons the main aims of this study was to develop an optimised rapid turnaround, flow cytometry-based whole-blood assay to monitor MSC potency.

2.1.2 Coagulation and anticoagulants

When peripheral venous blood samples are collected during a project, it is necessary to use an anticoagulant. In this chapter there was a need to look into the differences between anticoagulants.

Coagulation is a process that combines the activities of cellular fragments (platelets) as well as proteins (coagulation factors). First, platelets that are fragments of megakaryocytes, form a platelet plug at the site of injury; this is called primary haemostasis. Then, secondary haemostasis occurs in which plasma components or coagulation factors, initiate a coagulation cascade, that leads to the polymerization of fibrin strengthening the platelet plug.

Two pathways can initiate the coagulation cascade: so-called extrinsic and intrinsic pathways. Both pathways converge to a common final pathway (**Figure 2.1**) [184]. The extrinsic pathway is initiated when factor VII is activated by thromboplastin. Active factor VII will then activate factor X in the final common pathway. The intrinsic pathway starts with plasma kallikrein (PK) activating factor XII, XI and IX, in cascade. Factor IX in the presence of calcium and factor VIII activates factor X, initiating the common final pathway. Active factor X is responsible for the transformation of prothrombin into thrombin. Thrombin converts fibrinogen into fibrin monomer, but also activates factor XIII leading to fibrin polymerization. Calcium ions are essential component of the coagulation cascade and its removal inhibits and stops a series of events, in both intrinsic and extrinsic pathways.

Clinically and in haematological tests, different anticoagulants are used for different purposes. Tubes containing the divalent cation chelator EDTA (ethylenediaminetetraacetic acid) are the most used in haematological procedures because EDTA does not distort blood cells. EDTA inhibits coagulation by removing calcium from the blood. This anticoagulant has been used to prevent clotting in blood specimens since the early 1950s.

Studies have demonstrated that the white blood cell count remained stable in blood collected in EDTA for at least 3 days when stored at room temperature [185, 186]. Neutrophils and monocytes appeared to be the cells most sensitive to storage in EDTA, whereas

lymphocytes were the most stable [187]. Chelation therapy using EDTA is the medically accepted treatment for lead poisoning and heavy metal toxicity.

Citrate ($C_6H_7O_7$) is a small negatively charged molecule. Sodium citrate is an anticoagulant commonly used in blood transfusion services for stored blood products and also as an extracorporeal anticoagulant for coagulation studies. Citrate is a calcium-depleting agent that prevents activation of platelets and coagulation. The majority of the studies that used this anticoagulant pretend to assess platelet-monocyte or platelet-polymorphonuclear leukocyte complexes in peripheral blood. Citrate is also used in leukapheresis techniques and plasma exchange.

Heparin is used for collection of heparinized plasma or whole blood for chemistry and special chemistry testing, since it has minimal chelating properties, minimal effects on water shifts, and relatively low cation concentration. Heparin is the only anticoagulant that should be used in a blood collection for the determination of pH, blood gases, electrolytes and ionized calcium. Heparin should not be used for coagulation or haematology testing. Heparin ($C_{12}H_{19}NO_{20}S_3$) is a very negatively-charged molecule that has a very strong electrostatic interaction with thrombin. Antithrombin is a glycoproteins that inactivates several enzymes in the coagulation system. Antithrombin III activity increases in the presence of heparin. Heparin binds to Antithrombin III forming a complex. This complex leads to the inactivation of factor X and inhibition of the common coagulation pathway, preventing thrombin activation, which in turn prevents the formation of fibrin from fibrinogen.

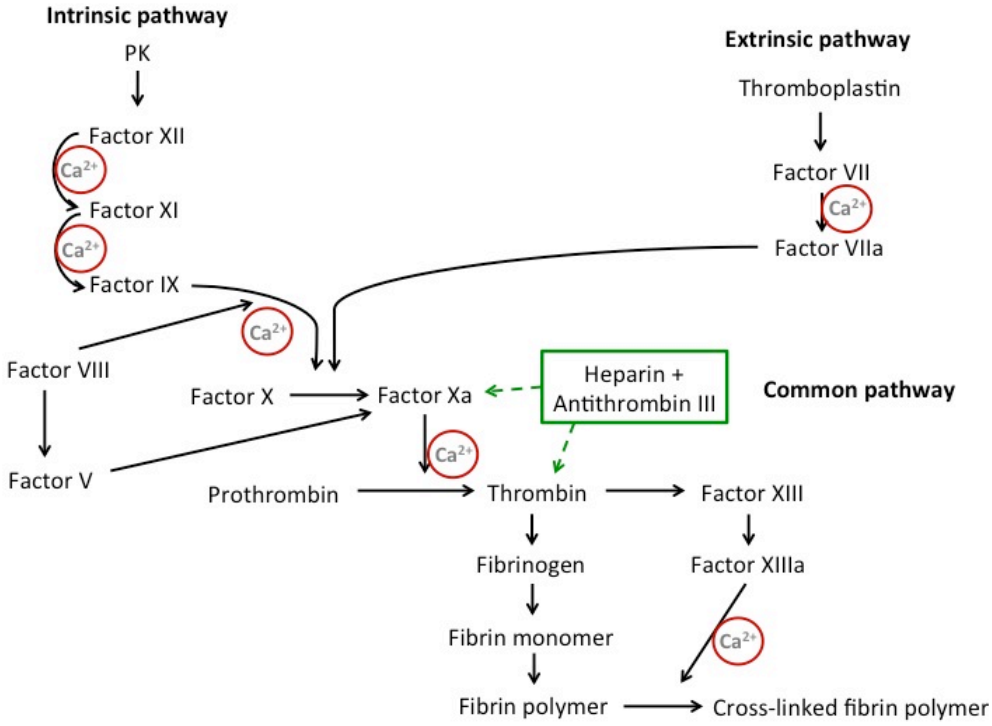

Figure 2.1 - Coagulation cascade. Red circles are where EDTA and citrate avoid coagulation while green arrows is where heparin works.

2.1.3 Objectives

In this study the development of a flow cytometry-based whole blood assay to screen for potency of human bone marrow-derived MSC to suppress innate immune responses is described. A key goal was to develop an assay methodology with potential to be rapidly and practically employed in cell manufacturing facilities to allow optimal selection of MSC donors or at point of care to facilitate “personalized” matching of a cell product to each patient. It was intended to develop a rapid, reliable, quantifiable and commercial assay to assess the immunomodulatory properties of allogeneic hBM-MSC.

Flow cytometric methods give rapid, quantitative and qualitative results. With flow cytometry, it is possible to detect both cell surface molecules, characteristic of cell populations, as well as their content of cytokines and chemokines simultaneously, thereby allowing the identification of cells that express that cytokine and chemokine. In order to more closely approach physiological conditions and to simplify and speed up the assay, it was decided to use a whole blood assay. Investigations were carried out to determine whether the ability of MSC to suppress the activation of monocytes and T cells depended upon the tissue source, donor, passage number as well as source of responder blood cells.

Summary of aims:

- To develop a flow cytometry-based whole blood assay to screen the potency of hBM-MSC
- To study possible mechanism by which MSC inhibit monocyte activation
- Another point of interest was whether MSC immunosuppression was contact dependent or mediated by soluble factors.

2.2 Methods

Details regarding reagents, solutions, antibodies and material are described in Annexes F to J.

2.2.1 Monocytes

2.2.1.1 Optimization of monocyte activation to use in a 4 colour flow cytometer

Peripheral blood from a total 10 healthy adult volunteers ranging in age from 24-64 years was collected into heparin, K_2EDTA and citrate BD Vacutainer tubes, according to the protocol approved by the ethics committee of the National University of Ireland in Galway. Once collected, blood was used within three hours. Heparinised blood was also tested several days after collection, stored at room temperature. In deep round bottom 96 well plates was added RPMI 1640 medium, Brefeldin A, ultrapure LPS-EB and blood at concentrations indicated in the results. Other stimuli of TLR and PKC, such as Pam3CSK4, PolyIC, MDP and PMA were also tested. The plates were sealed and incubated for different lengths of time (4, 6, 8 and 24 hours) at 37°C in a humidified incubator containing 5% CO_2 in air. Then, cells were surface stained for 10 minutes at room temperature in the dark with the following monoclonal antibodies (all titrated before): CD16 FITC, CD45 PerCP Cy5.5 and CD14 APC. Following surface staining, cells were fixed using reagent 1 (formaldehyde) from Beckman Coulter IntraPrep Kit. The cells were incubated again for 10 minutes at room temperature in the dark. Then, cells were washed with 1 mL 1X PBS and centrifuged at 250 g for 5 minutes at room temperature and the supernatant discarded. Then, cells were permeabilized using reagent 2 (saponine) from Beckman Coulter IntraPrep Kit. Cells were stained intra-cytoplasmically with PE labelled monoclonal anti-TNF-α antibody. In some experiments, cytokines and chemokines were also stained with PE-labelled anti-IL-10, anti-IL-12/IL-23 p40 and anti-CCL2 (MCP-1). In other experiments CD16 FITC was stained intra-cytoplasmically, as well. Subsequently, samples were washed, resuspended in FACS buffer and acquired by the BD Accuri C6 (Becton Dickinson) 4 colour flow cytometer. Data were analysed with the following flow cytometry softwares: BD CSample Analysis software (Becton Dickinson), FlowJo version 10 (Tree star) or Infinicyt version 1.7 (Cytognos). As outlined in results, experiments were designed to determine the optimal conditions of anticoagulants, Brefeldin A dose, LPS dose, incubation time and blood dilution to use in the immunosuppressive assay.

2.2.1.2 Analysis of LPS surface binding and calcium chelation

To study if the monocyte subpopulations were binding differently to LPS, heparinized PBMC isolated by Ficoll density gradient centrifugation, were resuspended in DPBS (Dulbecco's

phosphate buffered saline) without $CaCl_2$ and $MgCl_2$. Then, monocytes were stimulated at room temperature for 30 minutes with or without 1 μg/mL biotinylated LPS (LPS^{biotin}) and 0.6 μg/mL Brefeldin A. Ultrapure LPS-EB was biotin labelled using Biotin amidocaproate N-Hydroxysuccinimide ester, according to the protocol described by Brunialti *et al*. 2002 [188]. After activation, PBMC were washed twice using DPBS, incubated with CD16 FITC, CD45 PerCP Cy5.5 and CD14 APC for 10 minutes at room temperature and light protected. After washing twice, monocyte binding to LPS^{biotin} was revealed by adding streptavidin PE for 10 minutes at the same conditions describe previously. Then, an additional wash was made and the cells were finally resuspended in DPBS for acquisition on BD Accuri C6. Cell populations were identified by applying multiple gates, based on CD16, CD45, CD14 and FSC/SSC profile, using Infinicyt version 1.7 software.

To determine the effect of calcium chelation, heparinized blood diluted 2 fold was cultured for 4 hours at 37°C with 0.6 μg/mL Brefeldin A, with or without addition of 1 ng/mL of LPS and in the presence or absence of 2mM of the calcium-specific chelator ethylene glycol tetra acetic acid (EGTA). Following activation, cells were stained, fixed and permeabilized as described above. In other experiments, PBMC ($2x10^4$ monocytes) were resuspended in DPBS and stimulated with or without 1 μg/mL LPS^{biotin} in the presence or absence of 2 mM EGTA and cultured at room temperature for 30 minutes with 0.6 μg/mL Brefeldin A. After activation, PBMC were washed twice using DPBS, incubated with CD45 PerCP Cy5.5, and CD14 APC for 10 minutes at room temperature and light protected. Following two new washes, PBMC binding to LPS^{biotin} was revealed by adding streptavidin PE in the same conditions describe above. Following a new wash, cells were resuspended in DPBS for acquisition on BD Accuri C6.

To determine LPS binding to monocytes and MSC, PBMC ($1x10^4$ monocytes) were stimulated with or without 1 μg/mL LPS^{biotin} in the presence or absence of $3x10^5$ hBM-MSC (P_5-P_7) and cultured for 1 hours at 37°C with 0.6 μg/mL Brefeldin A. Following activation cells were stained, washed and resuspended as described above. Samples were acquired, once again on BD Accuri C6.

2.2.1.3 Isolation and expansion of hBM MSC

Bone marrow (BM) aspirates were obtained from the iliac crest of healthy donors between the ages of 19 and 24. From each donor, a trained physician collected 30 mL of BM aspirate into sodium heparin tubes under sterile conditions in a clinical procedure room at Galway University Hospital. Enrolment of healthy adult volunteers and collection of bone marrow samples for the purpose of generating culture-expanded MSC was approved by the Research Ethics Committee of Galway University Hospitals.

The bone marrow aspirate was diluted with DPBS and filtered through 70-100 μm cell strainer. Mononuclear cells (MNC) were isolated from BM aspirates by Ficoll density gradient centrifugation. Viable cell numbers in MSC suspensions were calculated using Trypan blue exclusion. The first plating was at a cell density of $5x10^4$ cells/cm^2 in cell culture flasks with complete medium, namely MEM alpha with Glutamax supplemented with 10% (v/v) Fetal Bovine Serum (FBS) and 1% (v/v) Penicillin/Streptomycin (P/S), for 4 days at 37°C in a humidified incubator containing 5% CO_2 in air. After 4 days, non-adherent cells were gently removed with DPBS and fresh complete medium added. When cells reached 80-90% confluence in P_0 or P_1, MSC were detached using 0.25% Trypsin-EDTA and the trypsin inactivated by adding 10X volume of complete medium. Detached cells were then centrifuged (250 g for 5 minutes at room temperature) and counted.

MSC were cryopreserved at $1x10^6$ cell/mL with freezing medium: FBS containing 10% (v/v) dimethyl sulfoxide (DMSO). MSC were thawed, washed extensively and seeded at a density of $5x10^3$ cells/cm^2 into cell culture flasks with complete medium and culture as before. The medium was renewed every 2 days until the cells reached 80-90% confluence. For passaging, MSC were detached, centrifuged (250 g for 5 minutes at room temperature), counted and seeded again at $3x10^3$ cells/cm^2. To use the cells for co-culture with peripheral blood monocytes, MSC were kept in culture until they reached 90-100% confluence and then detached and counted.

2.2.1.4 Immunophenotyping

The immunophenotypic characterization of hBM-MSC was performed on the day used for co-culture. Using the human MSC analysis kit from BD Stemflow™, $2x10^5$ cells were stained according to the manufacturer's protocol with antibodies against CD44, CD73, CD90, CD105, CD11b, CD19, CD34, CD45, HLA-DR and propidium iodide (PI). The samples were acquired in the BD Accuri C6 flow cytometer and analysed with Infinicyt version 1.7.

2.2.1.5 Optimised immunosuppressive assay protocol

This assay is divided in 2 parts. Firstly, MSC were co-cultured with peripheral blood and then monocytes stained intra-cytoplasmically for TNF-α or IL-12 expression, using the same protocol as described above. To prepare the co-culture, peripheral blood cells collected as described above were diluted 10X with RPMI 1640 medium. The blood was cultured with 0.6 μg/mL Brefeldin A, with or without Ultrapure LPS-EB at 1 ng/mL. hBM-MSC at passages P_2-P_7 were added to the culture in different numbers of viable cells ($2.5x10^3$, $5x10^3$, $1x10^4$, $2.5x10^4$, $5x10^4$, $1x10^5$, $2x10^5$, $4x10^5$, $5x10^5$ cells/well) and incubated for 6 or 24 hours at 37°C. For flow cytometry experiments, the viability of monocytes and MSC was determined by PI exclusion.

As positive controls for the inhibition of monocyte activation by LPS, in the same conditions describe above, either 10 ng/mL of dexamethasone or varying numbers of immortalized hBM-MSC (TERT cells, provided by Professor Tim O'Brien [189]) were added to cultures containing blood cells. Different concentrations of Dexamethasone and TERT cells were tested. As negative controls, equivalent numbers of either Multiple myeloma (MM) or Jurkat T cell lines were added. Graded numbers of these cells were also tested. To evaluate the potency of different hBM-MSC on monocytes, $4x10^5$ MSC preparations from different donors, at different passage number were simultaneously tested on four blood donors.

2.2.1.6 Monocyte count

In the monocyte immunosuppressive assay a fixed volume (50 μL) of heparinized peripheral blood was used per sample/test. To reach the final dilution of 10 fold the final volume per test is 500 μL.

To quantify the number of monocyte in each blood donor, 50 μL of peripheral blood was stained with CD45 PerCP Cy5.5 and CD14 APC for 10 minutes at room temperature, in the dark. Afterwards, erythrocytes were killed using 1X BD FACS Lysing Solution for 10 minutes in the same conditions. Following staining, samples were washed twice and resuspended in 200 μL of FACS buffer and 100 μL of cell suspension was acquired on BD Accuri C6. Monocyte counts were calculated with BD CSample Analysis software. The BD Accuri C6 cytometer allows to acquire a certain volume, for example 100 μL, and to determine the number of gated $CD14^+$ monocytes per acquired volume. Therefore, the number of monocytes per μL of blood can be calculated.

2.2.1.7 Cell contact-dependence of Immunosuppression

To determine if hBM-MSC immunosuppression was contact dependent, 24 flat bottom plates with 0.4 μm transwell inserts instead of using 96 round bottom plates was used. For these, $3x10^5$ MSC where placed in the bottom chamber with 50 μL heparinised blood (diluted 10X), 1 ng/mL LPS and 0.6 μg/mL Brefeldin A in the top chamber. Culture was incubated for 6 hours at 37°C. Three separate experiments were carried out using 7 different healthy blood donors and 2 MSC donors P_2-P_5 (n=10). To determine if supernatants from MSC had immunosuppressive activity, 3 different MSC preparations were seeded in 6 well plates ($4x10^5$ MSC/well) for 4 hours at 37°C in the presence or absence of 1 ng/mL LPS. Then, in 96 well plates, 10X diluted bloods were incubated with ($4x10^5$ MSC/well) or MSC supernatants and incubated for 6 hours at 37°C, again in presence or absence of 1 ng/mL LPS.

2.2.1.8 siRNA Transfection

To assess if vesicles/exosomes were responsible for the immunosuppression, hBM-MSC were transfected with 25 nM of siRNA transfection indicator SiGlo Red with DharmaFECT transfection reagents, according to manufacturer's instructions. This allowed the tracking of siRNA delivered via MSC-derived exosomes to monocytes. Following transfection, $3x10^5$ $siRNA^+MSC$ (P_5-P_8) from each of 3 different donors, were co-cultured with PBMC ($1x10^4$ monocytes) from 4 healthy blood donors, in the presence or absence of 1 ng/mL LPS, 0.6 μg/mL Brefeldin A for 6 hours at 37°C. Supernatant of transfected MSC ($siRNA^+$ supernatant) were also added to PBMC cultures. Supernatants were collected after $3x10^5$ MSC were 48 hours in culture. Some supernatants were filtered through PES-membrane with 0.2 μm pore size.

The medium used for these experiments was supplemented with 10% bovine FBS rendered exosome free by ultracentrifugation at 4°C for 18 hours at 100,000g.

2.2.1.9 Statistical analysis

Results are expressed as average and standard deviation of percentage of TNF-α or IL-12 production by monocytes. To determine the statistical significance of the differences observed between different conditions, unpaired multiple t-tests correct for multiple comparisons using the Holm-Sidak method were performed, using GraphPad Prism software (version 6). Statistically significance differences were considered * when P-value was lower than 0.05, ** when P-value was lower than 0.01, *** when P-value was lower than 0.001 and **** when P-value was lower than 0.0001.

2.2.2 Lymphocytes

2.2.2.1 Immunosuppressive assay with T cells

2.2.2.1.1 T cell activation with PMA and PHA

Peripheral blood from 9 healthy adult volunteers ranging in age from 24-65 years was collected into sodium heparin BD Vacutainer tubes, according to the protocol approved by the ethics committee of the National University of Ireland in Galway. Once collected, blood was used within three days, being kept at room temperature.

As described previously this assay is divided in two parts. First, in this T cell assay peripheral blood diluted 10X with RPMI, was co-cultured with different numbers of TERT cells (P_{43}-P_{44}) ($2.5x10^3$, $5x10^3$, $1x10^4$, $2.5x10^4$, $5x10^4$, $1x10^5$, $2x10^5$, $4x10^5$, $5x10^5$ cells/well) and incubated in deep round bottom 96 well plates with 0.6 μg/mL Brefeldin A, and in presence or

absence of either 5 ng/mL of PMA and 0.5 μg/mL Ionomycin or 20 μg/mL of PHA. The plates were sealed and incubated for different lengths of time, depending on the experiment, at 37°C in a humidified incubator containing 5% CO_2 in air.

In the second part of the assay, cells were surface stained for 10 minutes at room temperature in the dark with the following monoclonal antibodies: CD3 FITC, CD8α PE Cy7 and CD4 APC. Following washing, fixation and permeabilization using the IntraPrep Kit from Beckman Coulter, cells were stained intra-cytoplasmically with PE labelled monoclonal anti-TNF-α antibody or anti-IFN-γ antibody. Subsequently, samples were washed, resuspended in FACS buffer and acquired by the BD Accuri C6 4 colour flow cytometer. Data were analysed with BD CSample Analysis software (Becton Dickinson) or FlowJo version 10 (Tree star).

2.2.2.1.1.1 Activation markers after T cell activation with PMA

Preliminary experiments were carried out in order to see if simultaneous detection of cell surface activation markers CD69 and CD25 could be undertaken at the same time as intracellular expression of cytokines. Thus, heparinised blood was diluted 10X with RPMI and activated with 5 ng/mL PMA plus 0.5 μg/mL Ionomycin, in the presence or absence of 0.6 μg/mL Brefeldin A, and was incubated for 6 and 24 hours at 37°C. Then, T cells were surface stained for 10 minutes at room temperature, in the dark, with CD3 FITC, CD8 APC and CD69 PE Cy7 or CD25 PerCP Cy5.5. Following washing, samples with Brefeldin A present were fixed and permeabilized using the IntraPrep Kit from Beckman Coulter. Cells were stained intra-cytoplasmically with anti-IFN-γ PE. Subsequently, samples were washed, resuspended in FACS buffer and acquired on BD Accuri C6.

However, when the culture occurred in absence of Brefeldin A, T cells were just stained in the surface as described above. Following staining with antibodies, erythrocytes were killed using 1X BD FACS Lysing Solution for 10 minutes at room temperature, in the dark. Afterwards, samples were washed twice and resuspended in FACS buffer and acquired on BD Accuri C6.

Data were analysed with Infinicyt version 1.7 software.

2.2.2.1.2 T cell activation with CD3/CD28 beads

In other set of experiments T cells from heparinized blood or PBMC were activated with Dynabeads® Human T-Activator CD3/CD28 in the presence of complete RPMI 1640 medium (supplemented with 10% FBS and 1% P/S) and 0.6 μg/mL Brefeldin A for 6, 24 and 48 hours at 37°C. $CD3^+$ cells from PBMC were cultured with different ratios of beads; T cells:beads - 10:1 ($5x10^5$: $5x10^4$), 5:1 ($25x10^4$: $5x10^4$), 1:1 ($5x10^4$: $5x10^4$), 1:5 ($5x10^4$: $25x10^4$) and 1:10 ($5x10^4$:$5x10^5$).

As mentioned above this protocol is composed by two parts, and following cell activation/incubation the samples were stained intra-cytoplasmically and acquired as described previously. Results were analysed using Infinicyt version 1.7.

2.2.2.1.3 T cells co-cultured with MSC

Following the optimization of T cells activation with beads, $5x10^4$ $CD3^+$ cells were activated with $5x10^4$ CD3/CD28 beads (in a 1:1 ratio) and co-cultured with $5x10^5$ TERT cells (P_{43}-P_{44}) in a 1:10 ratio, in presence of complete RPMI 1640 medium and 0.6 μg/mL Brefeldin A for 24 hours at 37°C. Samples were stained, acquired and analysed as described previously.

2.2.2.2 Statistical analysis

Results are expressed as average and standard deviation of percentage of TNF-α or IFN-γ production by T cells. To determine the statistical significance of the differences observed between different conditions, unpaired multiple t-tests correct for multiple comparisons using the Holm-Sidak method were performed, using GraphPad Prism software. Statistically significance differences were considered * when P-value was lower than 0.05, ** when P-value was lower than 0.01, *** when P-value was lower than 0.001 and **** when P-value was lower than 0.0001.

2.3 Results

2.3.1 Monocytes

2.3.1.1 Optimization of monocyte activation

In peripheral blood, it is possible to distinguish three (**Figure 2.2**) or four subsets of monocytes, as described in the introduction, however in preliminary experiments it was observed that upon *in vitro* culture and particularly after LPS activation, CD16 expression was down-regulated (**Figure 2.3**), making it impossible to identify non-classical and intermediate subpopulations of monocytes.

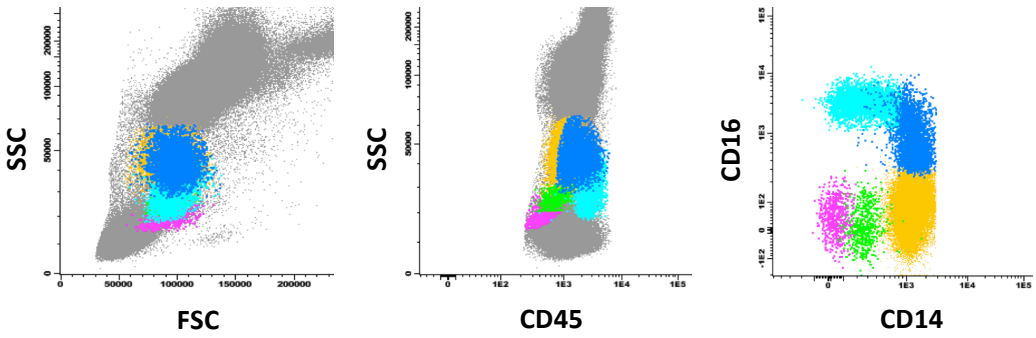

Figure 2.2 - Gate strategy used to identify monocytes subpopulations according to CD14 and CD16 expression. Different colours represent different cell populations: **plasmacytoid dendritic cells**, **myeloid dendritic cell**, **classical monocytes** ($CD14^{++}CD16^{-}$), **intermediate monocytes** ($CD14^{+}CD16^{+/++}$), **non-classical monocytes** ($CD14^{+}CD16^{++}$).

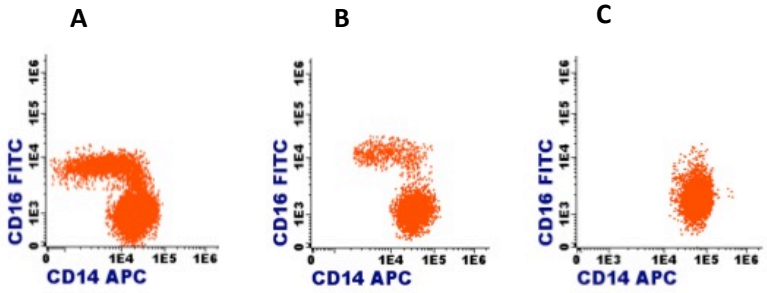

Figure 2.3 - Down-regulation of CD16 expression in monocytes. Hepatized peripheral blood was diluted 10X and cultured with 0.6 μg/mL Brefeldin A for 0 h (**A**), 4 h without LPS (**B**) and 4 h with 2 ng/mL LPS (**C**). The figure is a representative result of one experiment from three.

CD16 down-regulation is not dependent on the anticoagulant used to collect blood or blood dilution factor, the same down-regulation of CD16 was observed in blood collected in heparin and EDTA, and blood not diluted or diluted 5X and 10X. However, CD16 down-regulation is dependent on culture duration time, as the longer the incubation time, the lower CD16 expression. This effect was not seen after 30 minutes but it was observed after 2 hours incubation. One possible explanation for the disappearance of CD16 was that, especially after

activation, non-classical monocytes internalized CD16. However, this does not seem to be the case, as shown in **Figure 2.4**, where after 4 hours is not possible to see intracellular expression of CD16. These results could indicate that possibly there were no intracellular CD16 receptors.

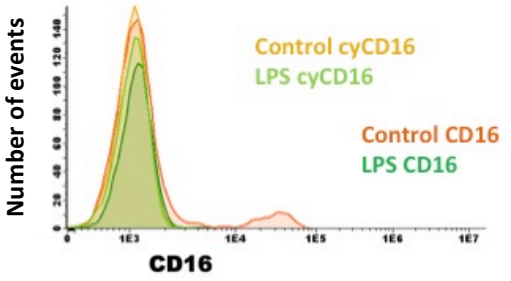

Figure 2.4 - CD16 staining and CD16 intra-cytoplasmically staining (cyCD16) in heparinized peripheral blood diluted 10X and culture with 0.6 μg/mL Brefeldin A and 2 ng/mL LPS for 4 h. Control conditions do not have LPS present. The figure is a representative result of one experiment from two.

Another important question was related to whether LPS could bind to monocyte subsets. To see if classical and non-classical monocytes bind LPS differently, biotin-labelled LPS (LPS^{biotin}) was prepared, and any bound LPS revealed with streptavidin PE. The biotinylated LPS prepared was as biologically active as the unlabelled material. Following incubation of PBMC with 1 μg/mL LPS^{biotin} (optimized concentration) it was possible to see (**Figure 2.5**) that all monocyte subsets bound LPS. In this experiment, dendritic cells in the lower left of the CD14/CD16 cytogram, did not stain with LPS^{biotin}. In addition, LPS^{biotin} staining intensity of monocytes is proportional to cell size. Non-classical monocytes are smaller and express less LPS^{biotin}, classical monocytes had higher ratio compared with non-classical monocytes (**Table 2.1**).

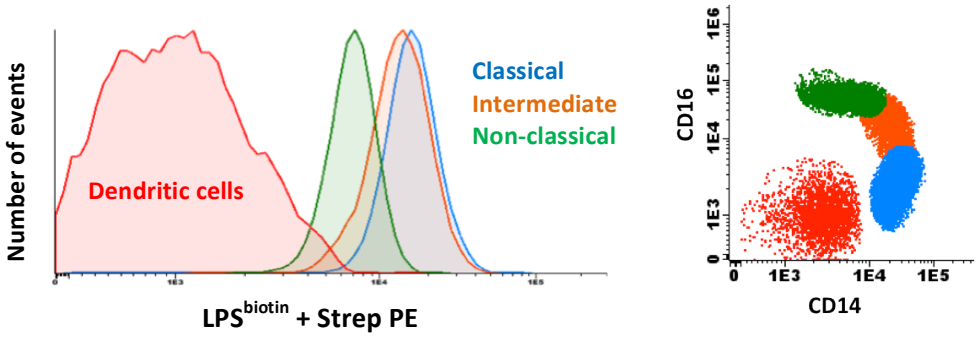

Figure 2.5 - LPS^{biotin} binding to different cells revealed by streptavidin PE. The figure is a representative result of heparinized PBMC incubated with 1 μg/mL LPS^{biotin} for 30 minutes at room temperature in presence of 0.6 μg/mL Brefeldin A.

Table 2.1 - Ration between mean fluorescence intensity (MFI) of LPS^{biotin} + Streptavidin PE with FSC.

Monocytes	MFI PE	FSC	Ratio
Classical	16620	2827828	**0.006**
Intermediate	13665	2909780	**0.005**
Non-classical	7136	2795103	**0.003**

Because of this CD16 down-regulation, in all future experiments, monocyte subsets are all included by the term "monocytes". The gate strategy used for a majority of the experiments is described in **Figure 2.6**. Monocytes are identified according with CD45 and CD14 expression and by their distinct light scatter profile (panel A and B). Gated monocytes were then analysed for intra-cytoplasmic TNF-α and IL-12 with a clear LPS dose-dependent increase in the proportion staining positively at concentrations between 0 and 20 ng/mL LPS (panel C).

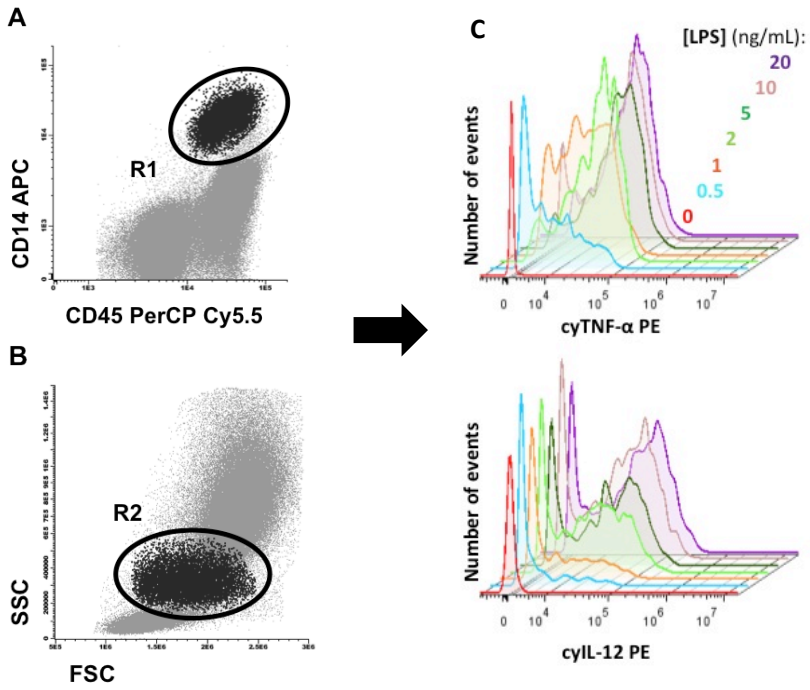

Figure 2.6 - Gating strategy used to identify monocytes and their intracytoplasmic TNF-α and IL-12 expression. **A** shows the gating strategy used to identify monocytes by $CD14^+$ and $CD45^+$ expression (black dots), and **B** shows monocyte identification by SSC and FSC among total cells (black dots) after $CD14^+CD45^+$ gating. **C** are histograms of LPS dose titration versus intracytoplasmic TNF-α or IL-12 staining. The figure is a representative result of heparinized blood diluted 10X and incubated for 6h in presence of 0.6 μg/mL Brefeldin A.

In order to optimize the assay, variations of multiple parameters were investigated to determine optimal efficiency and sensitivity. To optimize intra-cytoplasmic accumulation of cytokines and chemokines, Brefeldin A was added to the cultures. Results indicated that concentrations from 0.6 to 3.1 μg/mL of Brefeldin A did not significantly alter the proportion of

monocyte expressing TNF-α and their staining intensity was indistinguishable (**Figure 2.7**). Therefore, the lowest concentration of Brefeldin A, 0.6 μg/mL, was used for all subsequent experiments. It should be noted that monocyte viability, determined by Propidium Iodide exclusion, was not compromised during the assay.

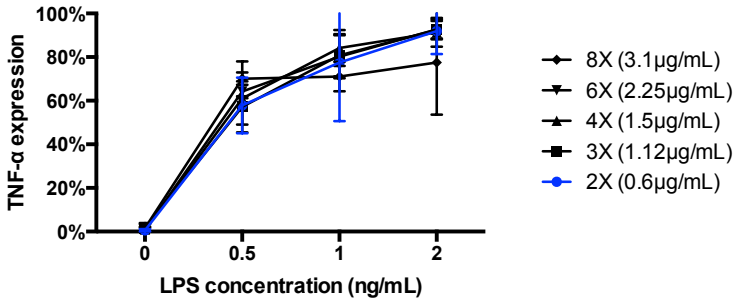

Figure 2.7 – Brefeldin A titration. Monocyte %TNF-α expression following 4 h activation with different LPS concentration and in presence of different Brefeldin A concentrations (n=2).

Afterwards, peripheral blood was collected in three different anticoagulants, namely heparin, K_2EDTA and citrate. Percentage TNF-α^+ monocytes were quantified following 6 hours stimulation with or without LPS.

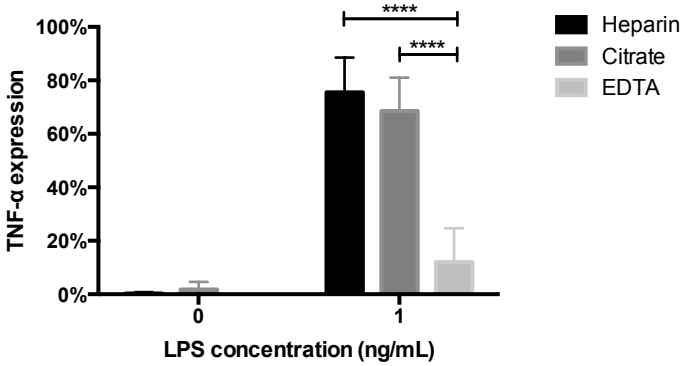

Figure 2.8 - Differences between anticoagulants in monocyte activation. Monocytes TNF-α expression from blood collected in the indicated anticoagulant. Whole blood was diluted 5X in RPMI and activated or not with 1 ng/mL LPS for 6 h (n=4). Unpaired multiple t-tests * P<0.05, ** P<0.01, *** P<0.001 and **** P<0.0001.

As shown in **Figure 2.8**, there was a strikingly lower TNF-α expression when blood was collected in EDTA. EDTA is a divalent cation chelator binding Ca^{2+}, Mg^{2+} and Zn^{2+} and to determine whether Ca^{2+} was involved in LPS-mediated monocyte activation, the calcium-specific chelator EGTA was used as anticoagulant. As shown in **Figure 2.9**, where heparinized whole blood was diluted and activated with 1 ng/ml LPS, TNF-α was readily detectable in heparin (panel A), while there was no TNF-α staining in cells cultured in the presence of 2 mM EGTA (panel B). To investigate whether Ca^{2+} was involved in LPS binding to monocytes, PBMC were incubated with 1 μg/mL biotin-labelled LPS (LPS^{biotin}) and the LPS binding revealed with Streptavidin PE. As shown in panels C and D, EGTA did not affect the binding of LPS to

monocytes. In addition, LPS did not bind to gated lymphocytes in the same PBMC preparation (panel E), thus LPS binding was specific to monocytes.

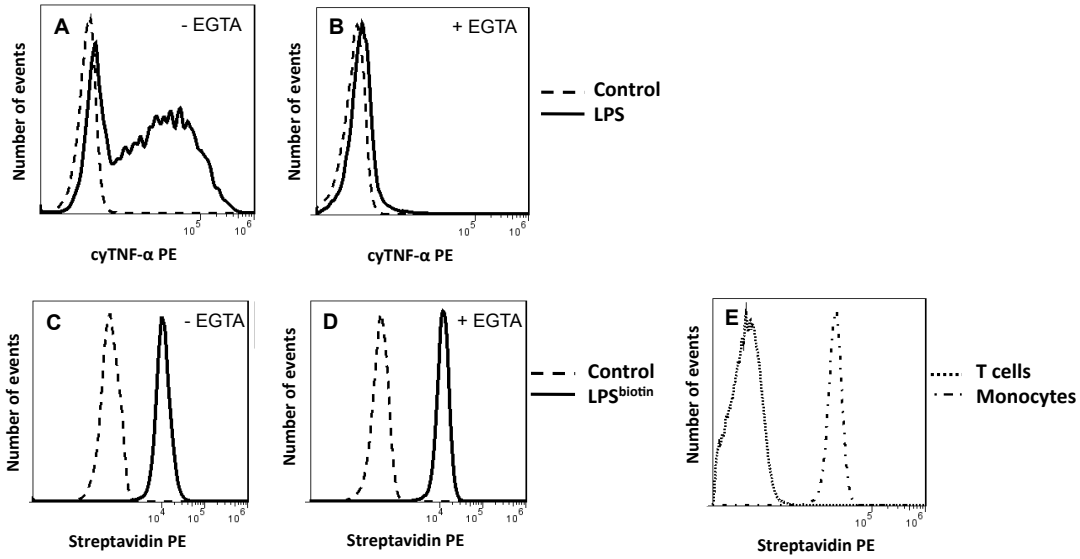

Figure 2.9 - Role of calcium in monocyte activation. Histograms in the top show TNF-α expression by monocytes in heparinized blood stimulated with 1 ng/mL LPS in absence (**A**) or presence (**B**) of 2 mM EGTA. Blood was diluted 2X in RPMI and incubated for 4 h at 37°C. In the bottom histograms monocytes (PBMC) were stained for 30 minutes, at room temperature, with 1 µg/mL biotin-labelled LPS revealed by streptavidin PE. Histograms show the binding in the absence (**C**) and presence (**D** and **E**) of 2 mM EGTA. **E** shows LPS binding to monocytes but not to T cells. This figure is a representative result of one experiment from four.

Dilution of whole blood with RPMI prior to addition of LPS was found to significantly enhance the sensitivity of the assay as reflected in the proportion of monocytes staining positively for TNF-α for a given concentration of LPS (**Figure 2.10**). When blood collected in heparin, sodium or EDTA was diluted with RPMI 5X, and activated with different LPS concentrations, the % TNF-α^+ monocytes were higher in heparin and citrate, compared with EDTA (panel A). However, when blood was diluted 10X, optimal stimulation was achieved in the three anticoagulants (panel B).

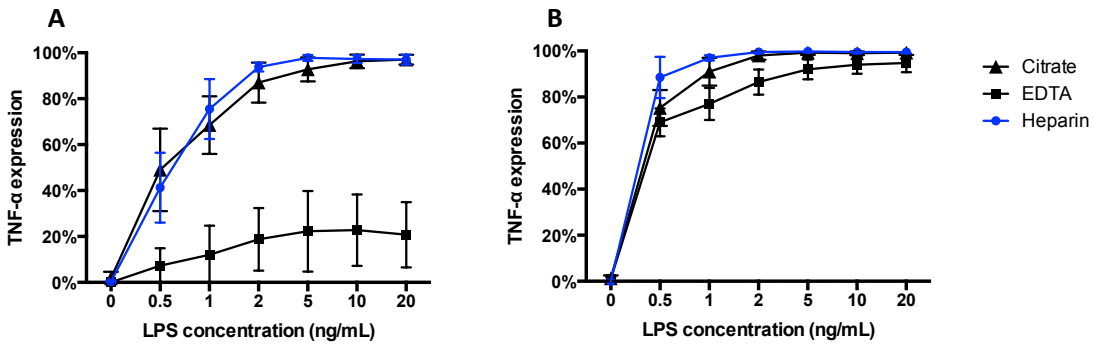

Figure 2.10 - Effect of blood dilution and anticoagulant on monocytes TNF-α expression. Monocytes TNF-α expression from blood collected in indicated anticoagulant and diluted 5X (**A**) or 10X (**B**) and stimulated with different LPS concentrations for 6 h (n=3).

The stimulus used to activate monocytes was LPS (or endotoxin), because it is one of the most potent pathogen-associated stimuli for monocytes and mediates its effect via binding to LPS receptor complex consisting of TLR4 and its co-associated proteins CD14 and LBP. However, other TLR and PKC activation stimuli, including Pam3CSK4, PolyIC, MDP and PMA were tested in blood collected in heparin and EDTA tubes. The majority of the stimuli were capable of inducing TNF-α expression in monocytes from heparinized bloods, but not in blood collected in EDTA (**Figure 2.11**).

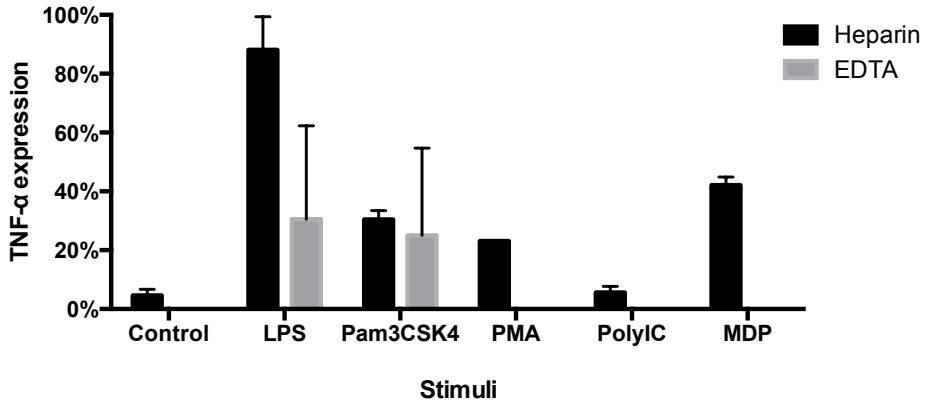

Figure 2.11 - Monocyte activation using different stimuli, blood was collected in heparin and EDTA. Blood was diluted 10X and activated with 1 ng/mL LPS, 10 ng/mL Pam3CSK4, 10 ng/mL PMA, 10 ng/mL PolyIC or 10 ng/mL MDP, within 6 h incubation. Control samples did not have any stimuli (n=2).

Based on the combined results to this point and on the previously unappreciated calcium dependency of LPS-stimulated TNF-α production, heparin was used preferentially as anticoagulant. Following selection of the best anticoagulant, other conditions were screened in order to design an assay such that the inhibition of optimally-stimulated monocytes would be observed. Simultaneously titrations of LPS concentration, blood dilution factor and incubation time were performed. Results are represented in **Figure 2.12**, where panel A, B, C and D represent %TNF-α+ monocytes after 4, 6, 8 and 24 hours of activation, respectively. Screening these conditions would give results regarding maximum stimulation but still near the exponential part of the titration curve. According to these criteria and the results presented in **Figure 2.12** the LPS concentration was fixed at 1 ng/mL and whole blood diluted 10 fold (10X) in RPMI. The optimum time for the incubation was determined to be 4-6 hours (**Figure 2.13**).

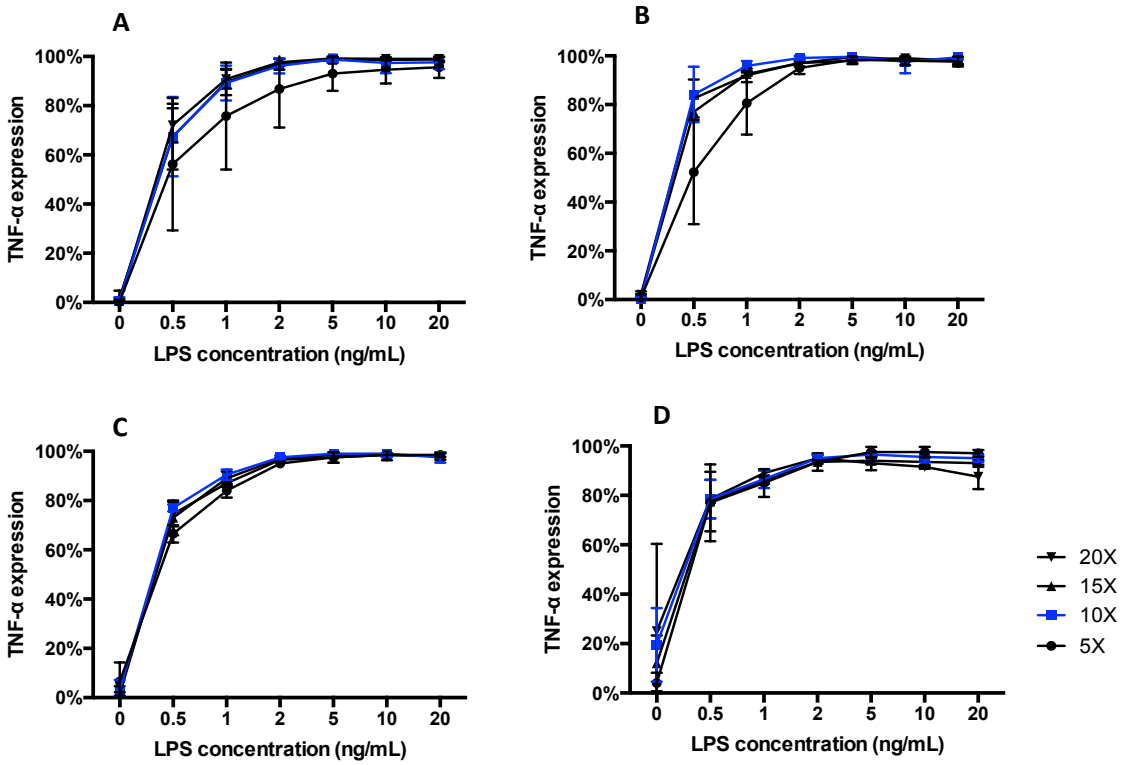

Figure 2.12 - Effect of blood dilution, LPS concentration and incubation time on monocytes TNF-α expression. Heparinized blood was diluted 5, 10, 15 and 20 fold in RPMI and activated with different LPS concentrations for (**A**) 4 h, (**B**) 6 h, (**C**) 8 h and (**D**) 24 h (n=4).

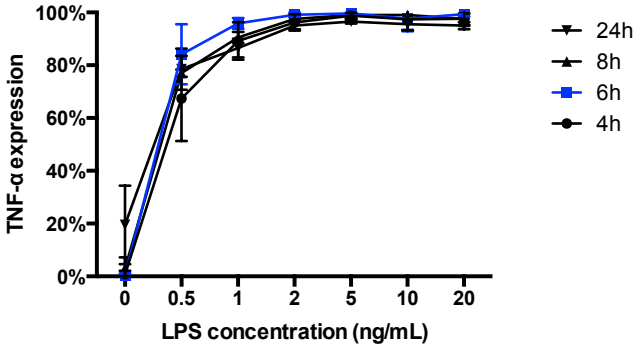

Figure 2.13 - Comparison between incubation times on monocytes TNF-α expression. Heparined blood was diluted 10X and activated with different LPS concentrations for 4, 6, 8 and 24 h (n=4).

As an alternative to TNF-α expression, IL-10, IL-12 and MCP-1 were assayed (**Figure 2.14**). However, after 8 hours activation, it was not possible to observe IL-10 (panel A) or MCP-1 (panel C) expression, though it was possible to see IL-12 expression (panel B). After 24 hour activation it was still not possible to observe IL-10 expression, whereas MCP-1 expression was not consistent and with low expression (**Figure 2.15**). On the other hand IL-12 expression was slightly increased after 24 hours, when compared with 8 hours (**Figure 2.16**). When IL-12 expression was compared in different blood dilutions (**Figure 2.17**), the least efficient was 5X while other blood dilutions were not very different. According to these results, and considering

also TNF-α results, it was decided just to look into IL-12 expression in heparinised blood diluted 10X and activated with 1 ng/mL LPS for a optimum incubation time of 24 hours.

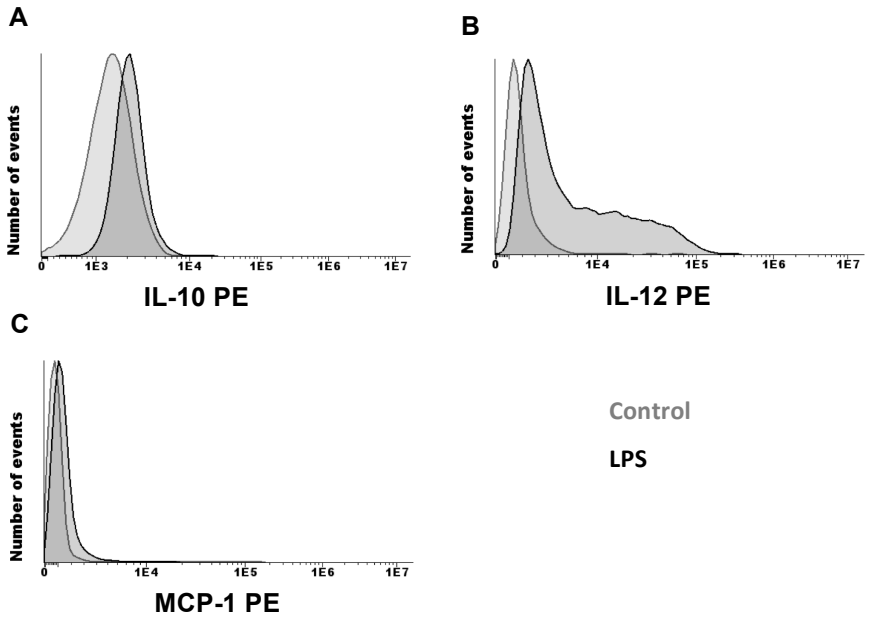

Figure 2.14 - Different interleukins and chemokine expression by monocytes. Histogram **A** and **C** show no IL-10 and MCP-1 expression, respectively. Histogram **B** shows some IL-12 expression. Heparinized blood was diluted 10X and activated with 1 ng/mL LPS for 8 h. Control samples contained no LPS. This figure is a representative result of one experiment from two.

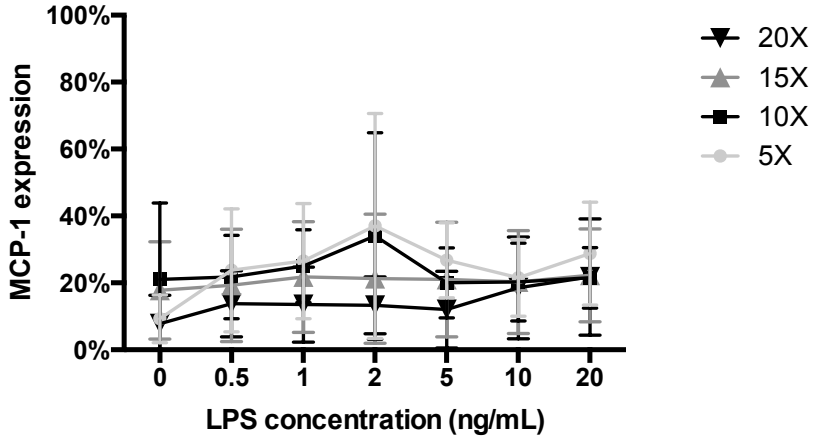

Figure 2.15 - MCP-1 expression by monocytes following 24 h incubation. Heparinized blood was diluted 5, 10, 15 and 20 fold in RPMI and activated with different LPS concentrations (n=4).

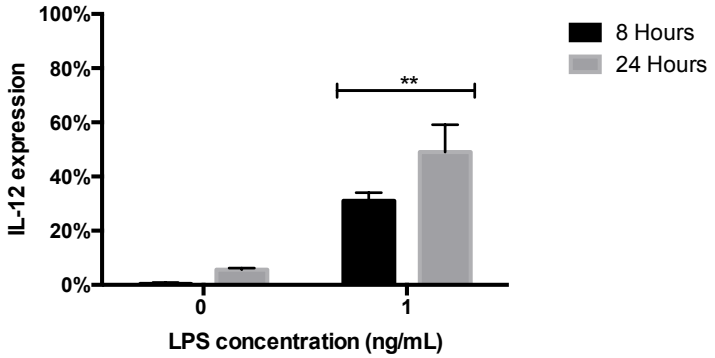

Figure 2.16 - Comparison between incubation times on monocytes IL-12 expression. Heparinized blood was diluted 5X and activated with 1 ng/mL LPS for 8 and 24 h (n=3). Unpaired multiple t-tests * P<0.05, ** P<0.01, *** P<0.001 and **** P<0.0001.

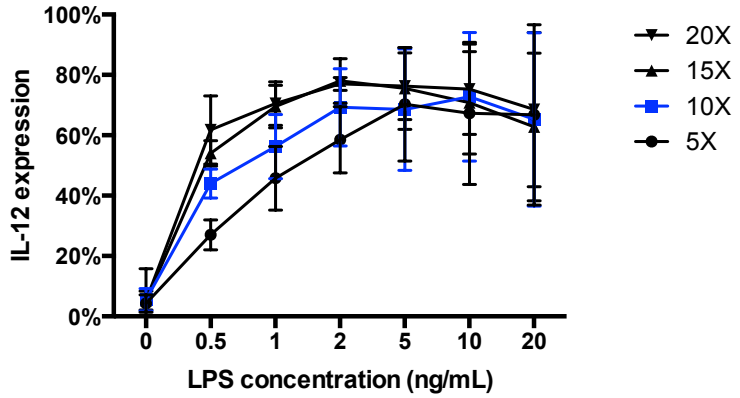

Figure 2.17 - Effect of blood dilution on monocytes IL-12 expression. Heparinized blood was diluted 5, 10, 15 and 20 fold in RPMI and activated with different LPS concentrations for 24 h (n=4).

Other important aspect of this assay was whether monocytes stored for several days would still be viable and be able to produce cytokines, especially if samples needed to go to a different laboratory to be tested. Thus peripheral blood was collected in heparinized tubes and stored at room temperature for 3 days prior to being used for the assay. As shown in **Figure 2.18**, it is possible to observe TNF-α expression in LPS activated monocytes 3 days after blood collection, however it is not possible to look into IL-12 expression (not shown). In addition there was no spontaneous activation of monocytes.

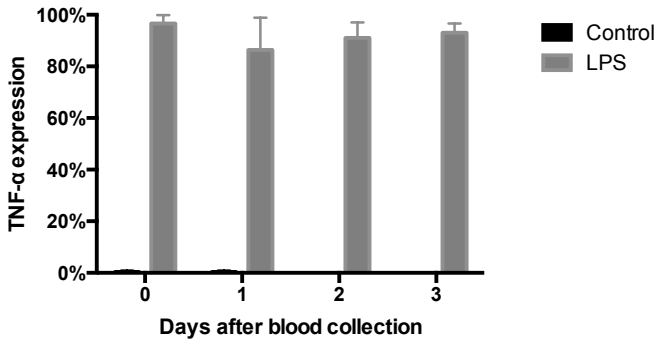

Figure 2.18 - Monocytes TNF-α expression after 3 days blood collection. Heparinized blood was collected and stored at room temperature for 0, 1, 2 and 3 days. Following storage, whole blood was diluted 10X and activated with 1 ng/mL LPS for 6 h. Control samples contained no LPS (n=3).

2.3.1.2 BM-MSC immunophenotyping

The human BM-MSC preparations used in the assays were characterized for positive expression of CD73, CD90, CD105 and CD44 and for lack of expression of CD19, CD34, CD45 and HLA-DR, on gated viable cells (**Figure 2.19**).

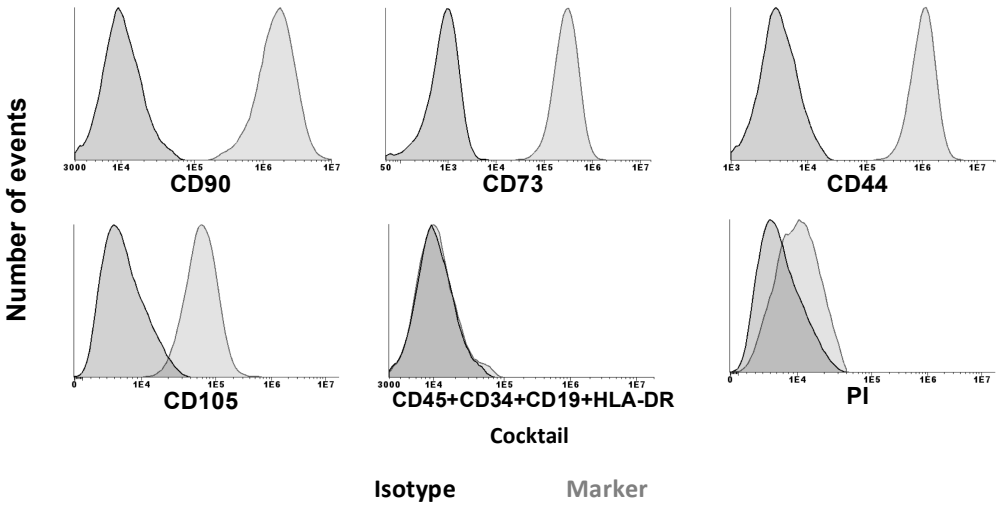

Figure 2.19 - Human BM-MSC immunophenotyping. Representation of one hBM-MSC donor labelled with the indicated monoclonal antibodies (grey line) and corresponding isotype control (black line).

2.3.1.3 Immunosuppressive assay

Having optimised the various parameters for the assay, experiments were conducted to see whether hBM-MSC would inhibit monocyte activation. The results suggested that allogeneic hBM-MSC have an immunosuppressive effect on LPS activated monocytes from peripheral blood. **Figure 2.20** shows that in the presence of MSC, there was reduced monocyte TNF-α expression after 6 hours co-culture. Addition of graded numbers of MSC resulted in a dose-dependent reduction in monocyte %TNF-α expression. Titration experiments indicated that inhibition of monocyte TNF-α production became statically significant between $1x10^4$ and $5x10^5$ MSC per sample. This inhibition increase progressively with higher number of MSC.

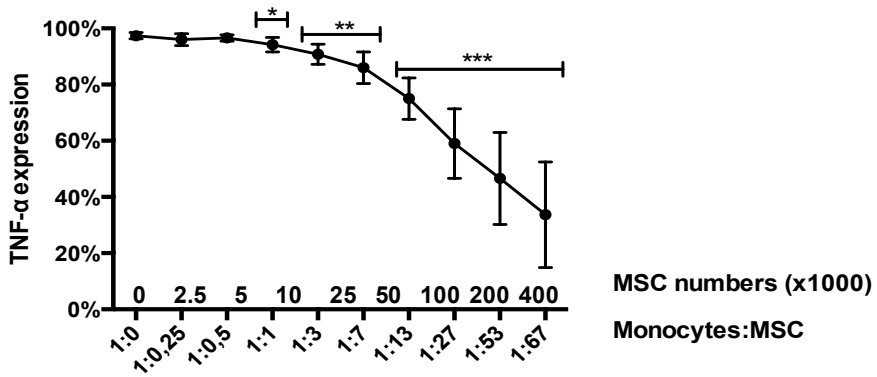

Figure 2.20 - Inhibition of monocyte TNF-α expression by hBM-MSC. Results of immunosuppression involving 3 different MSC preparations (P_3-P_7) and 5 different blood donors. Heparinized blood was diluted 10X and monocytes were stimulated for 6 h with 1 ng/mL LPS. The *x* axis shows the number of MSC added per well which contained a fixed volume of blood (50 μL) and an average ration between monocytes and MSC (n=5). All the statistic differences are compared with control (0 MSC). Unpaired multiple t-tests * P<0.05, ** P<0.01, *** P<0.001 and **** P<0.0001.

In these experiments, a fixed volume of blood, 50 μL, containing a certain number of monocytes was added to each well. From ten different donors, the average number of monocytes in 50 μl was 7,500 cells and differences between donors was <10%. To each well was then added a variable number of MSC so that the corresponding ratio of monocytes to MSC corresponded to the number of MSC added as indicated in **Figure 2.20**. Setting up the experiment this way was rapid and simple.

It was decided to investigate if pre-activated monocytes were still susceptible to being inhibited by added MSC. Thus, as shown in **Figure 2.21**, monocytes that had been pre-activated by LPS for 1 hour prior to MSC addition were still susceptible to inhibition of TNF-α production at between 4 and $5x10^5$ MSC per sample.

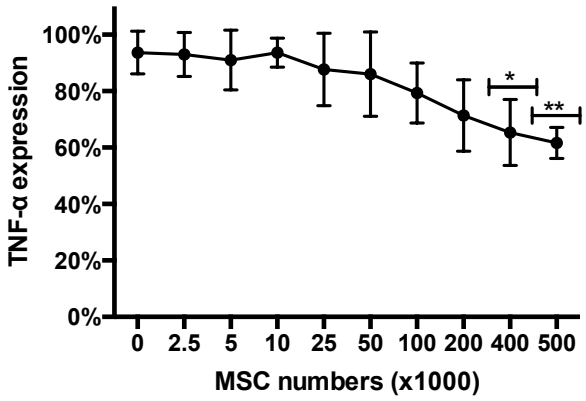

Figure 2.21 - Human BM-MSC reduce TNF-α expression of pre-activated monocyte. Immunosuppression results involving 2 different MSC preparations (P_4-P_6) and 3 different blood donors. Heparinized blood was diluted 10X and monocytes were pre-stimulated for 1 h with 1 ng/mL LPS before being culture for 6 h with different numbers of MSC. The *x* axis shows the number of MSC added per well which contained a fixed volume of blood (50 μL) (n=3). All the statistic differences are compared with control (0 MSC). Unpaired multiple t-tests * P<0.05, ** P<0.01, *** P<0.001 and **** P<0.0001.

Figure 2.22 shows that the presence of MSC also reduced monocyte IL-12 expression after 24 hours co-culture. Sequential numbers, 0 to $2x10^5$ cells, of hBM-MSC resulted in a dose-dependent reduction in monocyte IL-12 expression. Although the % IL-12-expressing cells is lower than for TNF-α expression and large standard deviations of the values were obtained, the inhibition of monocyte IL-12 production is not statically significant.

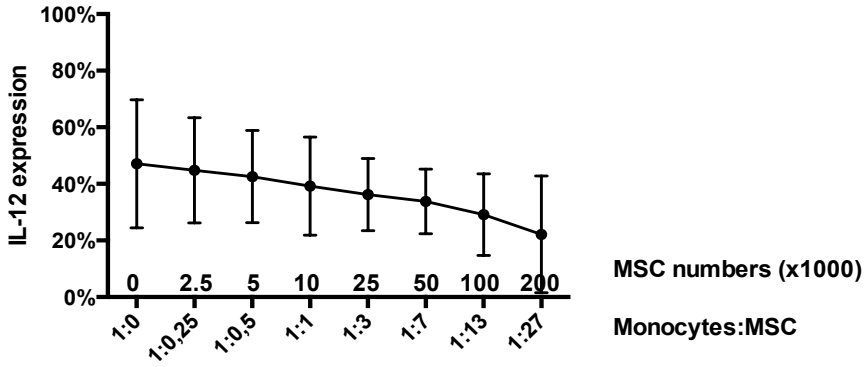

Figure 2.22 - Inhibition of monocyte IL-12 expression by hBM-MSC. Results of immunosuppression involving 4 different MSC preparations (P_3-P_6) and 7 different blood donors. Heparinized blood was diluted 10X and monocytes were stimulated for 24 h with 1 ng/mL LPS (n=9). The *x* axis shows the number of MSC added per well which contained a fixed volume of blood (50μL) and an average ration between monocytes and MSC.

Control experiments where monocytes and allogeneic hBM-MSC were co-cultured in the absence of LPS stimulation did not result in any TNF-α expression by monocytes (blue box **Figure 2.23**). Taken together, this indicates that i) allogeneic MSC themselves do not activate monocytes, ii) that LPS stimulation is necessary for monocyte activation and iii) the inhibition is MSC-specific.

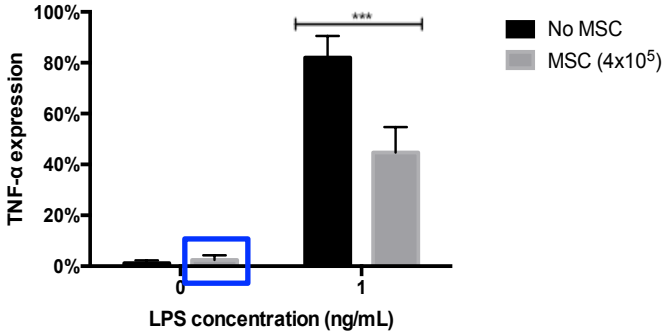

Figure 2.23 - Human BM-MSC do not have an "immunogenic" effect on unstimulated monocytes. Monocytes do not express TNF-α in presence of $4x10^5$ hBM-MSC (P_3-P_7) and absence of LPS (blue box). Heparinized blood was diluted 10X and monocytes were stimulated for 6 h with 1 ng/mL LPS (n=9). Statistic differences are compared with no MSC. Unpaired multiple t-tests * P<0.05, ** P<0.01, *** P<0.001 and **** P<0.0001.

2.3.1.3.1 Positive controls

In order to validate the *in vitro* monocyte immunosuppressive assay two additional positive and negative controls were included in all experiments.

Positive controls were used to ensure that monocyte TNF-α production could be reduced. First graded concentrations of the corticosteroid dexamethasone were tested. As shown in **Figure 2.24**, a dose-dependent reduction of monocytes TNF-α expression was observed and was maximal at 10 ng/mL dexamethasone, the chosen concentration subsequently used as a positive control in experiments involving hBM-MSC.

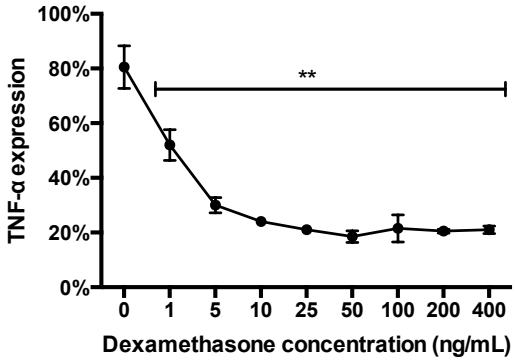

Figure 2.24 - Dexamethasone as positive control for inhibition of monocyte TNF-α expression. The indicated concentrations of dexamethasone were culture for 6 h with 10X diluted heparinized blood activated with 1 ng/mL LPS (n=2). All the concentrations when compared with control (0 ng/mL) are statistically significant. Unpaired multiple t-tests * P<0.05, ** P<0.01, *** P<0.001 and **** P<0.0001.

As an additional positive control, immortalized hBM-MSC, TERT cells, were included into the whole blood culture. TERT cells are capable of reducing TNF-α expression of activated monocytes without producing any effect on unstimulated monocytes (**Figure 2.25**, blue box).

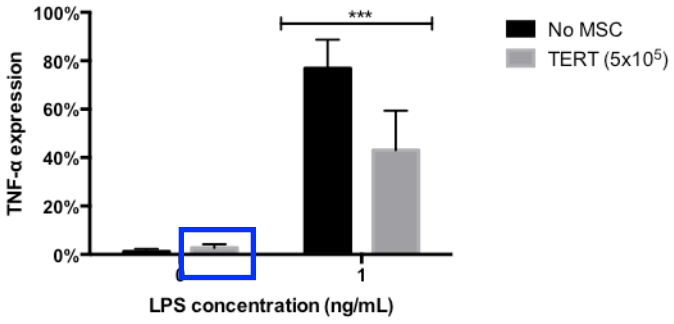

Figure 2.25 - TERT cells as positive control for inhibition of monocyte TNF-α expression. Heparinized blood was diluted 10X and monocytes were stimulated or not with 1 ng/mL LPS in presence or absence of $5x10^5$ TERT cells (P_{22}-P_{24}) (n=6). Blue box shows that TERT cells in culture do not activate unstimulated monocytes. * P<0.05, ** P<0.01, *** P<0.001 and **** P<0.0001.

2.3.1.3.2 Negative controls

In contrast, **Figure 2.26** shows that addition of human Multiple Myeloma (MM) and Jurkat cell lines, at different concentrations, did not result in inhibition of monocyte TNF-α production (panel A) and had no effect on monocytes (panels B and C, blue boxes).

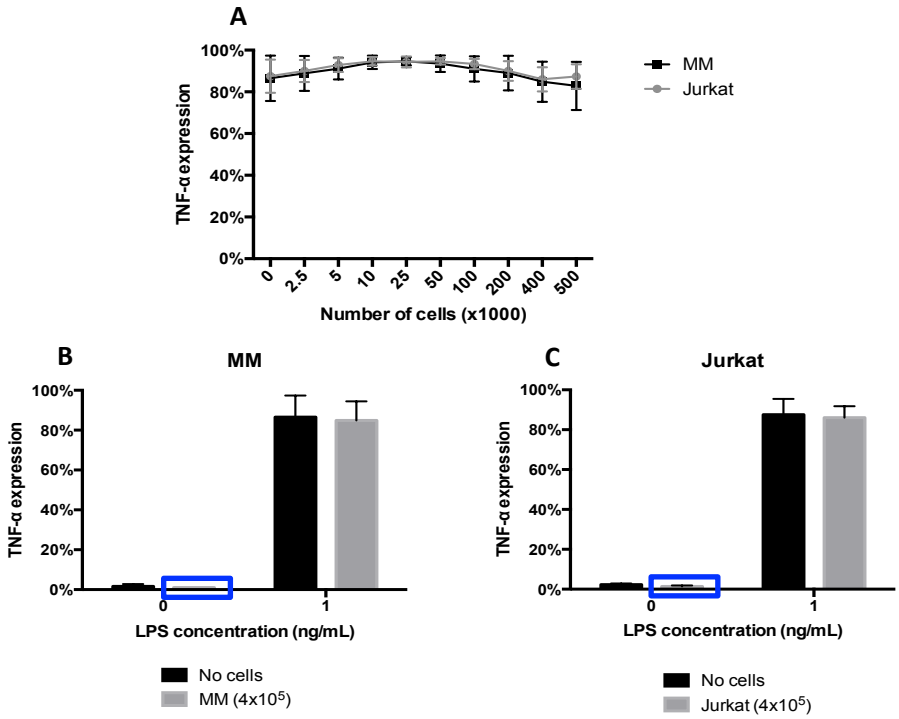

Figure 2.26 - MM and Jurkat cell lines as negative control for inhibition of monocyte TNF-α expression. Heparinized blood was diluted 10X and monocytes were stimulated for 6 h with 1 ng/mL LPS (n=6). In **A** *x* axis shows the number of cells added per well. **B** and **C** show that $4x10^5$ MM (P_{31}) and Jurkat (P_{57}), respectively, do not activate unstimulated monocytes.

2.3.1.4 Mechanism of action of MSC

2.3.1.4.1 MSC and LPS^{biotin}

Given that hBM-MSC inhibited monocyte activation in a dose-dependent manner, it was wished to investigate their mechanism of action, and one possibility was that MSC in the whole blood culture would remove sufficient LPS so that monocyte activation would not occur. Therefore, it was used biotinylated LPS to stain PBMC and MSC cultured separately and together. (**Figure 2.27**). As shown in panel A, LPS bound to monocytes in PBMC preparations (solid line) however there was a slight reduction in LPS binding to monocytes in the presence of MSC (dotted line). In panel B is shown that LPS did not bind to MSC (solid line) even in the presence of PBMC (dotted line). Thus, sequestration of LPS by added MSC was not the cause of reduced monocyte activation.

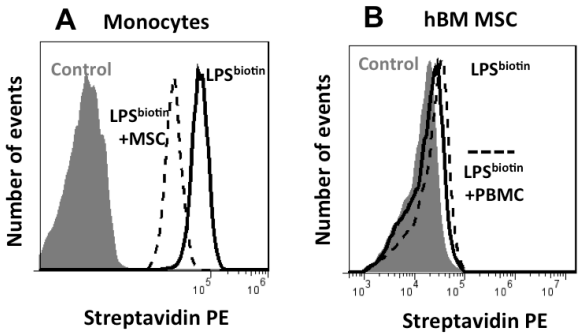

Figure 2.27 - Biotinilated LPS bind to monocytes but not to MSC. **A** show LPS^{biotin} binding to monocytes alone (solid line), while dotted line show LPS^{biotin} binding of monocytes co-cultured with MSC (P_5-P_7). **B** show that LPS^{biotin} does not bind to MSC alone (solid line), as well as in presence of PBMC (dotted line). $1x10^4$ monocytes were cultured with $3x10^5$ MSC and 1 μg/mL LPS^{biotin} for 1 h. The figure is a representative result of one experiment from two.

2.3.1.4.2 Immunosuppression by contact or soluble factors

Other factor of interests was if MSC immunosuppression was contact dependent or mediated by soluble factors.

In these experiments, transwell cultures are frequently used in which cells are cultured in flat bottom plates with porous filter inserts, allowing soluble factor to pass through but does not allow cell contact. Carrying out these experiments, it was noted that despite MSC being capable of inhibiting monocyte activation in round bottom well plates, no such inhibition was seen when similar cell densities were cultured in flat bottom plates (**Figure 2.28**). Even when whole blood monocytes are activated in round bottom and flat bottom plates, they behave differently (LPS condition – black and grey bar). In the presence of MSC, TNF-α production by activated monocytes decreased more in 96 well plates compared with 24 well plates. Other interesting result was that independently of whether MSC and monocytes were in contact, "interaction", or physically separated by the transwell, there was no reduction of monocyte TNF-α production, within 6 hours incubation. Thus, changing the geography of how the assay occurs, changes monocyte activation and the MSC immunosuppression effect.

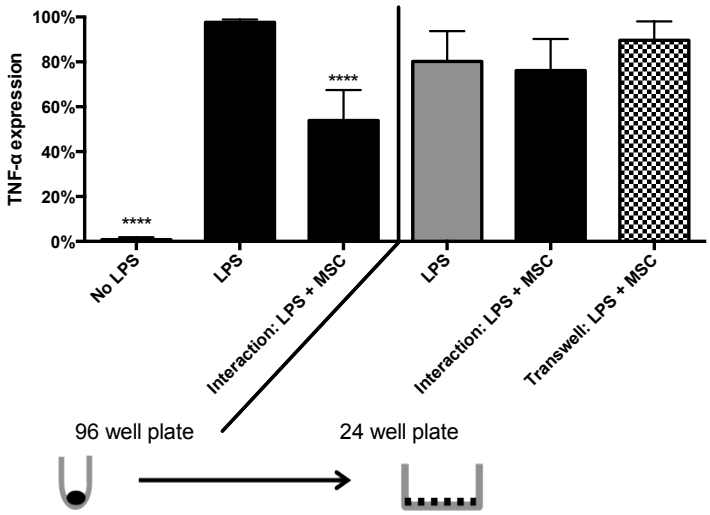

Figure 2.28 - Monocytes need to be in contact with MSC to occur immunosuppression in a 6h co-culture system. Results show the differences between performing the whole blood assay in a 24 flat bottom plate instead a 96 round bottom plate. This figure shows %TNF-α expression produce by monocytes from 7 blood donors in the presence of 2 MSC donors (P_2-P_5) (n=10). Heparinized blood was diluted 10X and activated for 6 h with 1 ng/mL LPS. Statistic differences are compared with LPS. Unpaired multiple t-tests * P<0.05, ** P<0.01, *** P<0.001 and **** P<0.0001.

However, when the assay occurs in presence of hBM-MSC supernatants, in 96 round bottom culture plates, the supernatants are as potent as MSC at inhibiting monocyte activation, following 6 hours culture (**Figure 2.9**). It should be noted that supernatants were collected after MSC had been in culture for 4 hours, after culturing MSC in the absence or presence of 1 ng/mL LPS ("primed" MSC supernatant) before being added to whole blood culture. The same inhibitory effect occurred when the assay was performed in the presence of both supernatants harvested from MSC, monocyte TNF-α production was reduced.

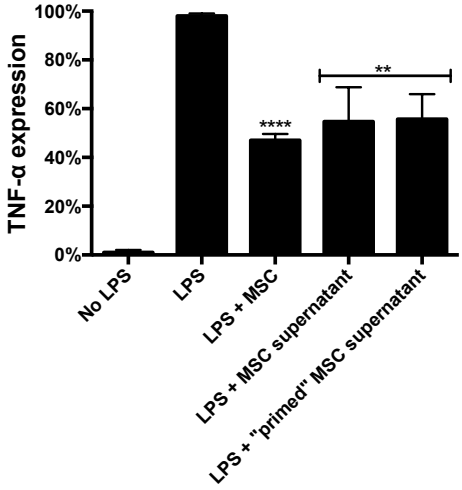

Figure 2.29 - Soluble factors release by MSC are able to immunosuppress monocyte activation. Whole blood from 3 donors were diluted 10X and activated for 6 h with 1 ng/mL LPS and cultures in presence of 3 MSC donors P_4-P_6 or their supernatants (n=3). MSC supernatant indicates that the supernatant were collected from cultured MSC in absence of LPS while LPS-activated MSC supernatants are identified as "primed" MSC supernatant. All the statistic differences are compared with LPS. Unpaired multiple t-tests * P<0.05, ** P<0.01, *** P<0.001 and **** P<0.0001.

2.3.1.4.3 siRNA – MSC exosomes

Whereas the transwell experiments did not give a clear answer regarding the need for contact between monocytes and MSC, and the supernatant results were interesting, it was decided to investigate whether vesicles/exosomes released by MSC had immunosuppressive activity. **Figure 2.30 A** shows that MSC were efficiently (>96%) transfected/labelled with siRNA PE. Panel **B** shows the gate strategy used to identify monocytes ($CD14^+$) and T cells ($CD3^+$). It is possible to observe that T cells when cultured with labelled MSC do not uptake the labelled exosomes (panel **C**), whereas some monocytes uptake the exosomes in the absence (panel **D**) or presence of LPS (panel **E**). When TNF-α expression by monocytes was determined, labelled MSC ($siRNA^+$ MSC) (panel **H**) were as efficient as unlabelled MSC ($siRNA^-$ MSC).

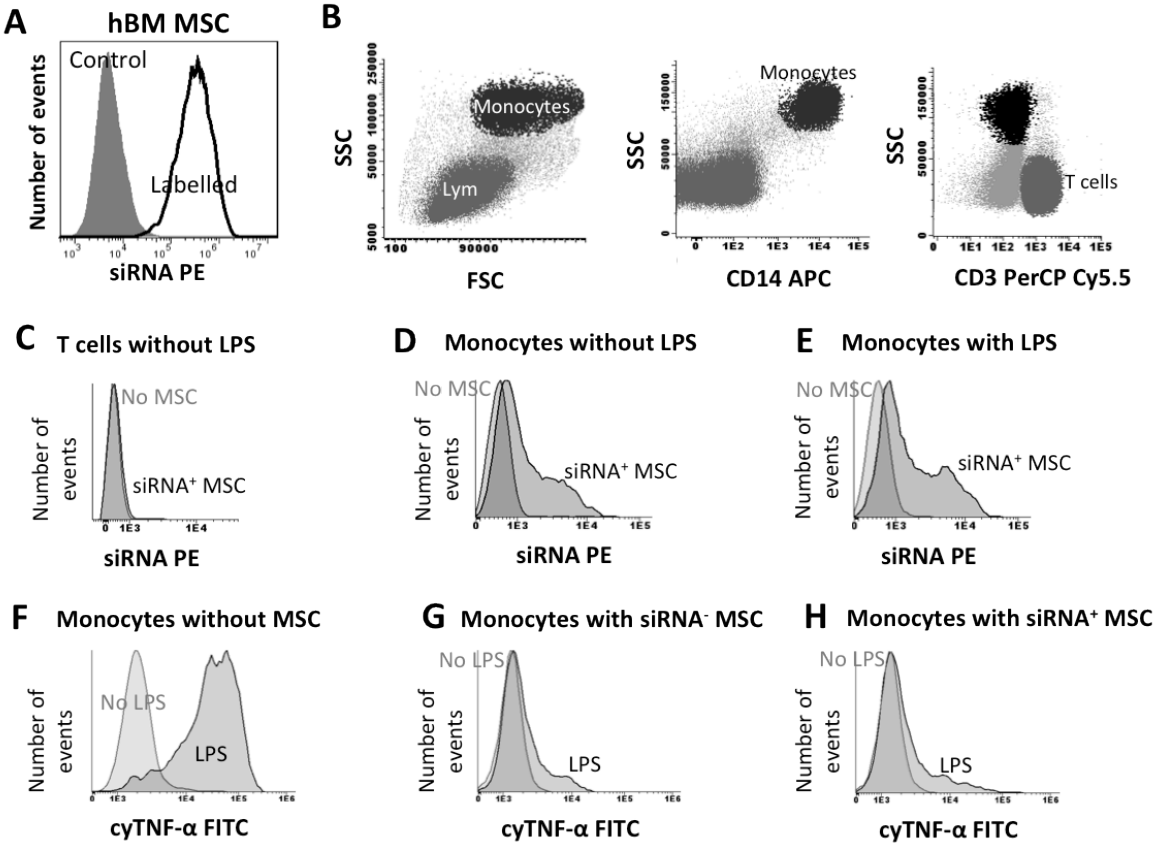

Figure 2.30 - Transfected hBM-MSC transfer siRNA specifically to monocytes. **A** shows that MSC were efficiently transfected with siRNA PE ($siRNA^+$ MSC). **B** shows the gate strategy used. Monocytes were identify by SSC and FSC among total cells (black dots) after $CD14^+$ gating, as well as $CD45^+$ (not shown). T cells were identify by SSC and FSC among total cells (dark grey dots) after $CD3^+$ gating, as well as $CD45^+$. **C** shows that T cells do not uptake siRNA PE in culture with $siRNA^+$ MSC, without LPS present, while **D** and **E** show that monocytes uptake siRNA PE from $siRNA^+$ MSC, in absence and presence of LPS, respectively. **F** shows the negative (no LPS) and positive control (LPS) for monocyte activation by expressing TNF-α. **G** and **H** show that $siRNA^+$ MSC cells are as efficient as not transfected MSC ($siRNA^-$ MSC) regarding to immunosuppression. $3x10^5$ of each $siRNA^+$ MSC donor (P_5 – P_8) were co-cultured with $1x10^4$ monocytes (PBMC) for 6 h with 1 ng/mL of LPS in round bottom plates. The figure is a representative result of one experiment from four.

Figure 2.31 is another way of representing the results presented in **Figure 2.30 F**, **G** and **H**. Despite previous results shown that a direct interaction was necessary between monocytes and MSC, it was investigated if material was being transferred from MSC to monocytes. With this aim it was decided to add siRNA^{+} MSC supernatants to LPS stimulated and unstimulated monocytes. However, in these circumstances, transfer of labelled material was not seen. On the other hand, TNF-α expression was reduced when monocytes were cultured with siRNA MSC supernatants. At the same time, it was verified that after filtration through 0.2 μm filters, the supernatant was less efficient at reducing TNF-α expression (**Figure 2.31**).

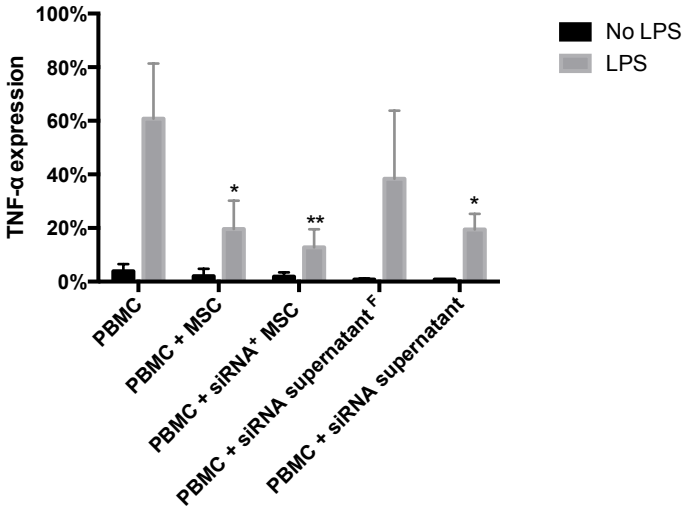

F Filtered by 0.2μm

Figure 2.31 - Soluble factors release by siRNA^{+}MSC (siRNA supernatant) are able to immunosuppress monocyte activation. TNF-α production by LPS activated monocytes is reduced in presence of siRNA^{+}MSC and siRNA supernatants. When the siRNA supernatant is filtered by 0.2 μm pore monocyte TNF-α production increase. 3x10^{5} of each siRNA^{+} MSC donor (P_5-P_8) were co-cultured with 1x10^{4} monocytes (PBMC) for 6 h with 1 ng/mL of LPS in round bottom plates (n=3). Supernatants were collected after 3x10^{5} MSC were 48 h in culture. All the statistic differences are compared with PBMC LPS. Unpaired multiple t-tests * P<0.05, ** P<0.01, *** P<0.001 and **** P<0.0001.

2.3.2 Lymphocytes

Regarding T cells in the immunosuppressive assay, results suggested different interactions, mechanisms and kinetics compared with monocytes. Once it was obtained a good positive control for MSC immunosuppression in the monocyte assay using the TERT cells, it was decided to use the same cells to develop and optimize a rapid T cell assay.

2.3.2.1 PMA activation

Three methods were tested to activate T cells. First, the immunosuppressive effect of TERT cells on PMA activated $CD3^+$ cells (after PMA and Ionomycin titration) was tested. T cells from peripheral blood were activated with PMA and Ionomycin and were co-cultured with TERT cells. **Figure 2.32 A** and **B** show that there was no reduction of TNF-α or IFN-γ expression by T cells in the presence of TERT cells. Additionally a graded number of TERT cells were included but no difference between ratios (panel C and D) were noted. Results also show that TERT cells alone do not have an stimulatory effect on T cells (blue boxes).

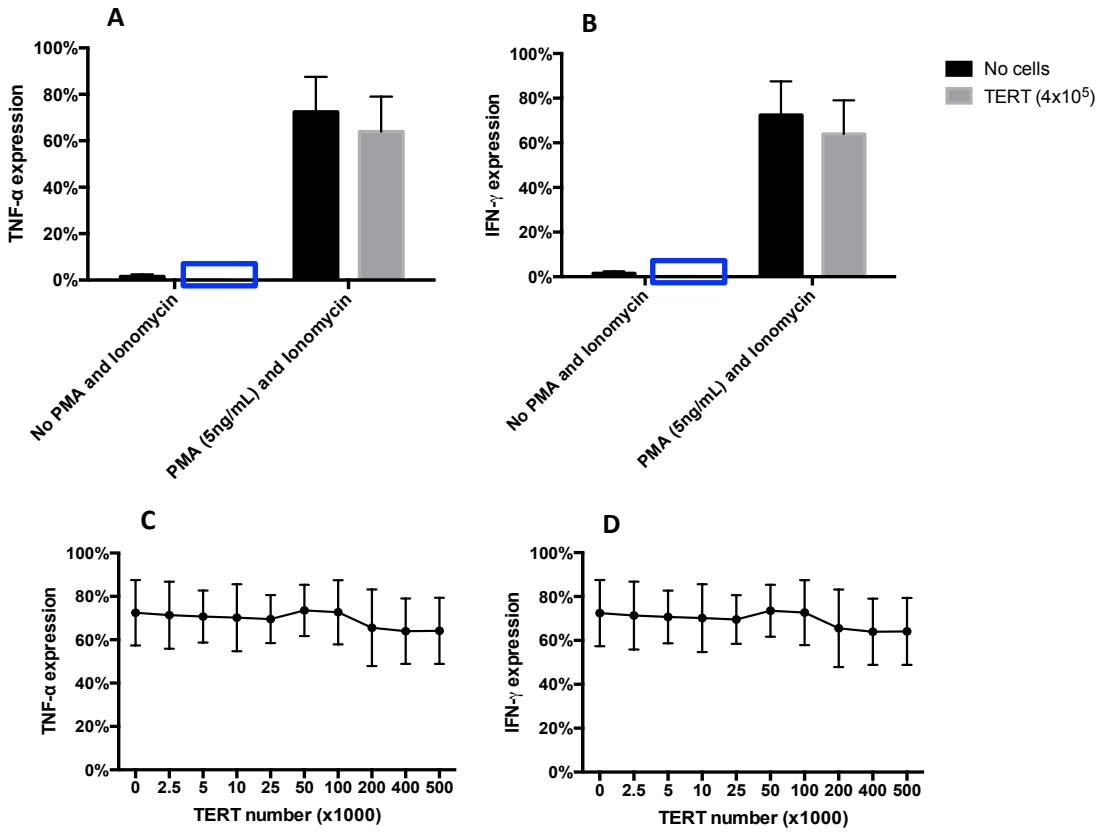

Figure 2.32 - TERT cells do not immunosuppress T cells activated with PMA. $4x10^5$ TERT cells (P_{43}-P_{44}) do not reduce TNF-α (**A**) and IFN-γ (**B**) expression on $CD3^+$ cells. Unstimulated T cells in presence of TERT cells do not express TNF-α and IFN-γ (blue box). **C** and **D** show that TERT cells at different concentrations cultured with a fixed volume of blood (50 μL) did not reduce TNF-α and IFN-γ expression, respectively. Heparinized blood was diluted 10X and T cells were stimulated with 5 ng/mL PMA and 0.5 μg/mL Ionomycin, in presence of 0.6 μg/mL Brefeldin A for 6 h (n=5).

2.3.2.1.1 T cell activation markers

One of the initial aims of this project was to look into T cell activation markers, like CD69 and CD25, following T cell activation and co-culture with MSC. However, even without having the T cell immunosuppressive assay working properly, interesting results were found. After T cell activation with PMA and Ionomycin for 24 hours it was observed that in the presence of Brefeldin A it was not possible to see CD69 or CD25 expression (**Figure 2.33**). In the absence of Brefeldin A CD69 and CD25 were detected on activated T cells. Indeed, as expected, CD69 but not CD25 was observed on T cells after 6 hours incubation (data not shown). Differences in kinetics between CD69 and CD25 expression are shown for $CD8^+$ (panel A) and $CD8^-$ cells ($CD4^+$) (panel B).

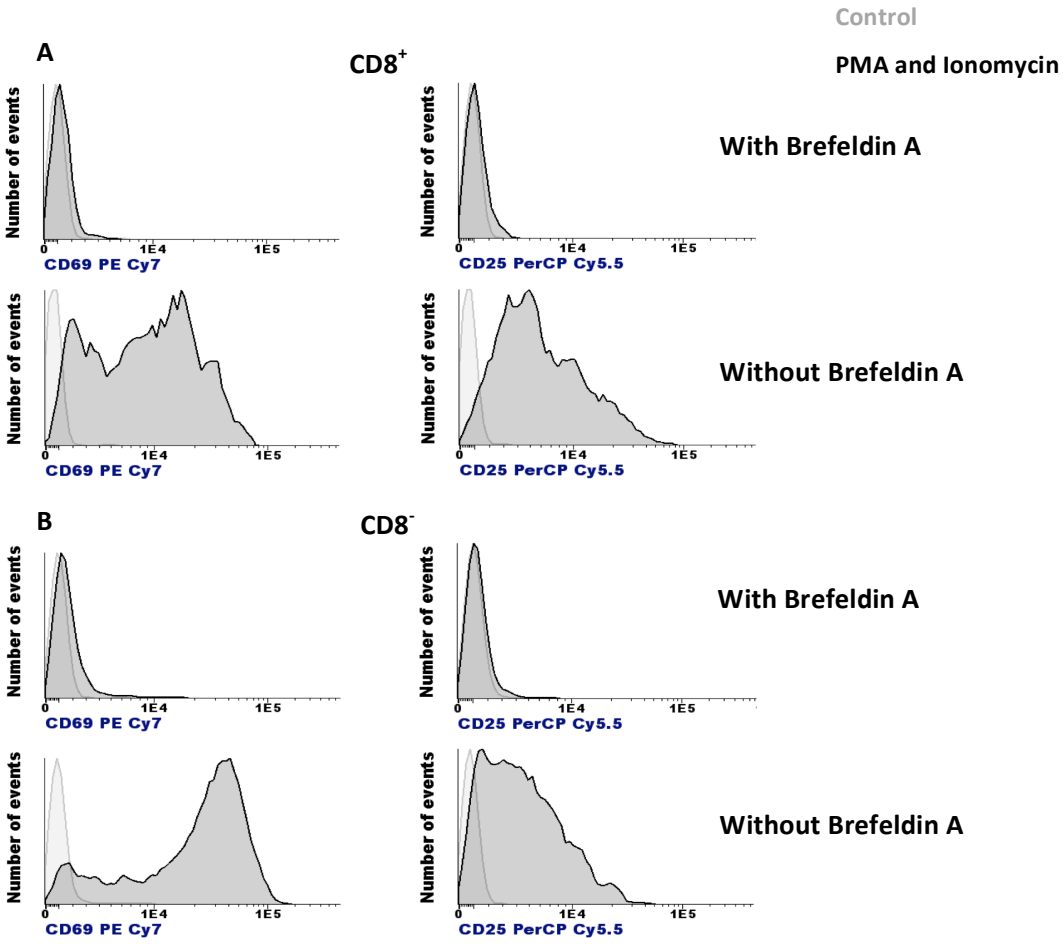

Figure 2.33 - CD69 and CD25 expression by $CD8^+$ and $CD8^-$ T cells after activation. Heparinized blood was diluted 10X and T cells were stimulated with 5 ng/mL PMA and 0.5 μg/mL Ionomycin for 24 h, in presence or absence of 0.6 μg/mL Brefeldin. Histograms on the left represent CD69 expression and histograms on the right CD25 expression. **A** and **B** represent $CD8^+$ and $CD8^-$ cells, respectively, from the same sample. The figure is a representative result of one experiment from three.

2.3.2.2 PHA activation

The second stimulus tested for T cell activation was the lectin PHA. In this case, peripheral blood was incubated for 6 and 24 hours with PHA (**Figure 2.34**). However, that period of time was not enough to see significant TNF-α production by T cells.

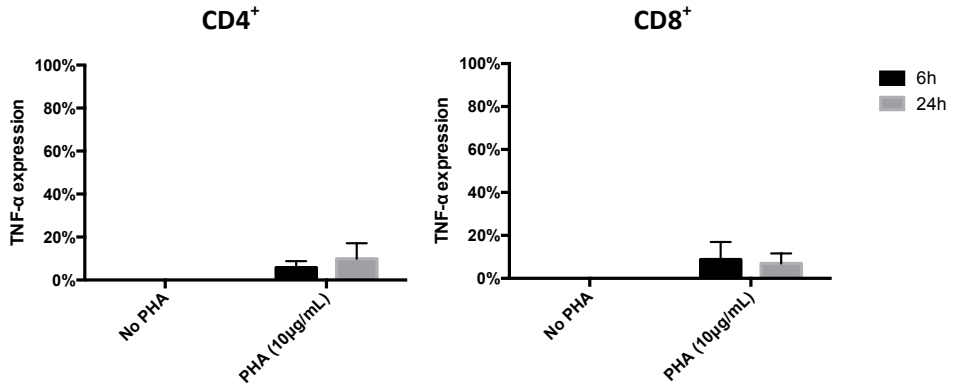

Figure 2.34 - T cells activation with PHA for 6 and 24 h. TNF-α expression by $CD4^+$ and $CD8^+$ cells. Heparinized blood was diluted 10X and T cells were stimulated with 10 µg/mL PHA in presence of 0.6 µg/mL Brefeldin A, for 6 and 24 h (n=4).

2.3.2.3 CD3/CD28 activation beads

The last T cell activation method tested was the commercial CD3/CD28 bead kit. However, it transpired that it was not possible to activate T cells in whole blood with beads. Different ratios of T cells and beads were tested, for different time points and it was not possible to have TNF-α expression. On the other had, the kit could be used to activate T cells in PBMC. At different bead to cell ratios, it was possible to have an increase TNF-α expression by T cells (**Figure 2.35** A), in a dose dependent manner. The increase of TNF-α expression was also time dependent. Comparing $CD4^+$ (panel B) with $CD8^+$ (panel C) cells, $CD4^+$ cells reach maximum TNF-α expression after 24 hours whereas for $CD8^+$ this is reached after 6 hour. Panel D shows that IFN-γ expression by $CD3^+$ cells is not very high using the kit.

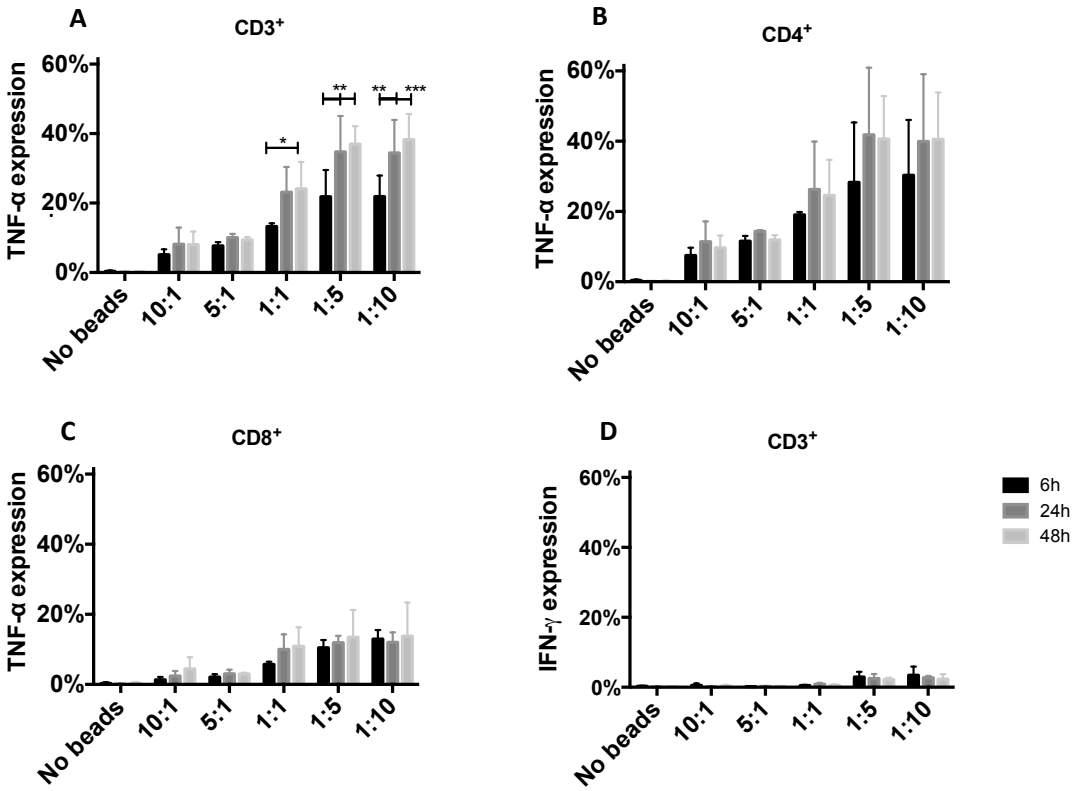

Figure 2.35 - T cells activation with CD3/CD28 beads for 6, 24 and 48 h. **A**, **B** and **C** show TNF-α expression by $CD3^+$, $CD4^+$ and $CD8^+$ cells, respectively, while **D** show IFN-γ expression by $CD3^+$. Different ratios of $CD3^+$ (PBMC) were stimulated with different concentrations of beads, in presence of 0.6 μg/mL Brefeldin A (n=3). Comparison between "No beads" and 1:1, 1:5 and 1:10 ratios gives static significance in A, B and C. Static significance between time points, ANOVA * P<0.05, ** P<0.01, *** P<0.001 and **** P<0.0001. No static significance was found between time points on $CD8^+$ and $CD4^+$.

Following optimization of T cell activation with CD3/CD28 beads, PBMC were activated with beads at 1:1 ration and co-cultured with TERT cells for 24 hours. **Figure 2.36** shows that TERT cells do not have an immunosuppressive effect on T cells. There was no reduction in TNF-α expression by T cells in the presence of TERT cells.

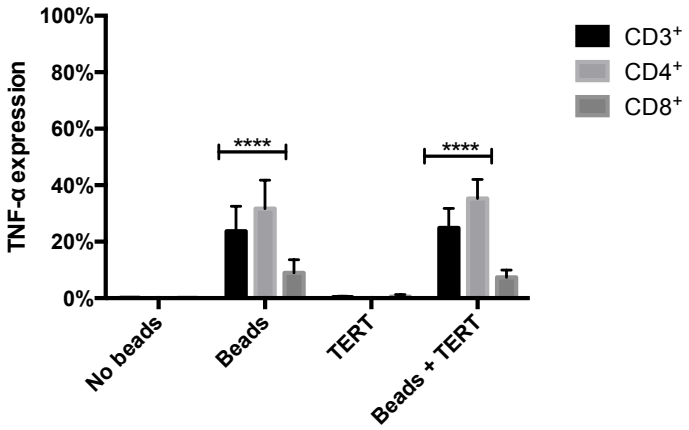

Figure 2.36 - TERT cells do not immunosuppress T cells activated with CD3/CD28 beads. PBMC were stimulated with CD3/CD28 beads at 1:1 ratio ($5x10^4$ $CD3^+$:beads), in presence of $5x10^5$ TERT cells (1:10) (P_{43}-P_{44}) and 0.6 μg/mL Brefeldin A, for 24 h (n=3). Statistic significance compared to "No beads". ANOVA * P<0.05, ** P<0.01, *** P<0.001 and **** P<0.0001.

2.4 Discussion

2.4.1 Monocytes

2.4.1.1 Optimization of monocyte activation

The results presented in this chapter concern the optimization of different conditions to activate monocytes and to find the best co-culture system to reveal the inhibitory effects of hBM-MSC on this activation. The final results indicated a fast, reliable and quantifiable assay to measure MSC immunosuppressive capacity was developed.

Monocytes were used as the target population because they are known to respond rapidly to activation by pathogen-associated and damage-associated molecular patterns (PAMPs and DAMPs respectively). Currently, three monocyte subsets are defined, namely so-called classical ($CD14^{++}CD16^{-}$) non-classical ($CD14^{+}CD16^{++}$) and intermediate ($CD14^{+}CD16^{+/++}$) monocytes. However, in the beginning of this project one limitation was found, namely that individual monocyte subpopulations could not be analysed, since CD16 expression was down-regulated *in vitro*. In retrospect a substitute marker such as CD38, CD33, HLA-DR or IREM-2 differentially expressed by monocyte subpopulations could be used [190]. This would also address the issue of whether the absence of $CD16^{+}$ cells was the result the their disappearance as the result of some differential toxicity effect of LPS or simply the modulation of CD16 expression following monocyte activation, the latter possibility would probably be the more likely. LPS was found to bind equally to monocyte subpopulations (**Figure 2.5**). In addition, this work highlights one limitation of the assay as set up in that only four fluorescent markers were being analysed. It would be easier to analyse monocyte subpopulations with additional markers.

TNF-α was chosen as the main readout of this assay because the kinetics of production following activation is extremely rapid [191]. In addition, TNF-α is an important cytokine that is involved in the regulation of a wide spectrum of biological processes and regulates the immune response by activating cell proliferation, receptor expression, and migration. In addition, TNF-α has been shown to regulate the production of other cytokines [143]. In the context of the therapeutic use of MSC, important immunosuppressive activities of MSC are mediated via the TNFa/TNFaR pathway [144-146]. This emphasizes the potential of MSC to modulate inflammatory lesions such as GvHD and inflammatory bowel diseases.

However, other possible readouts of this assay were also tested, such as IL-10, IL-12 and MCP-1. IL-10 is an anti-inflammatory cytokine that is involved in multiple effects in immuno-regulation and inflammation. IL-10 is involved on progression of immunological and inflammatory responses because of its capacity to down-regulate MHC class II expression [175,

192]. As is often the case with IL-10, this could not be detected using intracytoplasmic staining and flow cytometry. Probably because TNF-α and IL-10 have different kinetics, TNF-α expression is up-regulated faster than IL-10. IL-10 is known to inhibit the production of pro-inflammatory cytokines such as TNF-α, however if TNF-α is produced first it is not possible to be inhibited by IL-10 [193].

Monocyte chemoattractant protein 1 (MCP-1 or CCL2) is an important chemokine responsible for the initiation, regulation and mobilization of monocytes to inflammatory sites [194]. MCP-1 is associated with obesity and diabetes conditions that are associated with accelerated rates of atherosclerosis. MCP-1 attracts monocytes to the active sites of inflammation in the vascular subendothelial area, initiating migration of monocytes into the arterial wall to form excessive macrophage-derived foam cells [195]. MSC are envisioned as a therapeutic tool not only for cardiovascular diseases but also to treat limb ischemia in diabetic patients [196]. Expression of MCP-1 by activated monocytes was highly variable and for this reason MCP-1 was not considered as a readout in this study.

Another cytokine that was considered for the measurement of MSC immunosuppression was IL-12, more specifically IL-12/IL-23 p40. IL-12p40 with two polypeptides generates the heterodimeric cytokines IL-12 and IL-23. They play critical and distinct roles in host defence and can be rapidly secreted in response to inflammatory signals [197]. IL-12, when compared with TNF-α has a slower kinetic of up-regulation and monocytes take longer to produce this cytokine.

As already mentioned, several parameters in the immunosuppressive assay were considered and optimized. The first reagent being titrated was Brefeldin A, also called “Golgi-block”. Brefeldin A inhibits protein transport from the endoplasmic reticulum to the Golgi apparatus, allowing the accumulation of proteins intra-cytoplasmically, thereby facilitating their detection. Brefeldin A does not interfere with monocyte activation or with their immunosuppressive properties. However, with the T cell assay, it was not possible to detect cytokine production and the activation markers CD69 and CD25, simultaneously. Brefeldin A blocks the IFN-γ secretion but also blocks the glycosylation of CD69 and CD25 receptors, not allowing them to be expressed on the cell surface.

One of the most critical parameters identified during the development phase, was the type of anticoagulant in which blood was collected. Three anticoagulants, heparin, sodium citrate and potassium EDTA, were tested. As has been previously reported, the selection of anticoagulant may significantly impact the accuracy of whole blood-based diagnostic tests for hematologic disease, since different anticoagulants have varying effects on blood cells for immunophenotying, morphology or other parameters [198]. Indeed, in a recent publication by Duffy *et al*. in which multiple stimuli were used in a human whole blood assay to standardize

stimulation systems and define boundaries of a healthy human immune response, the same three anticoagulants used here were also tested [199]. Duffy *et al.* also found that activation by a multiplicity of stimuli, including bacterial, viral, cytokine, TCR and microbial–associated molecular patterns (MAMPs) were optimally achieved when blood was collected in heparinized tubes. However, these authors made no further comments on this finding.

Heparin inhibits coagulation by preventing thrombin activation, heparin forms a complex with antithrombin III, limiting antithrombin III availability. Citrate and EDTA are calcium chelators. Results show that monocytes from blood collected in EDTA tubes expressed significantly less TNF-α, when compared with heparin and citrate. The difference between EDTA and citrate can be explained because citrate binds to calcium ions, whereas EDTA chelates also other divalent cations such as Zn^{2+} and Mg^{2+}. Bournazos *et al.* show that in blood samples, citrate is a less efficient calcium chelator compared with EDTA [200]. Then, to determine if calcium plays a role in LPS binding to monocytes, a selective chelator of calcium, namely EGTA, together with LPS^{biotin} was used. Results showed that LPS binding to monocytes did not require calcium.

Other interesting results obtained with the different anticoagulants was that of blood dilution. Monocytes could be efficiently activated at higher dilutions, when collected in the three anticoagulants. The most likely explanation for this is calcium availability. Dilution of blood in RPMI medium, in which the calcium nitrate concentration is 100 mg/L, will saturate the calcium chelating activity of the added anticoagulants and therefore at 5X dilution, monocyte activation is achieved in citrate but not in EDTA. At a 10X dilution, the initially superior chelating capacity of available EDTA is also compromised and the free calcium concentration becomes sufficient to activate monocytes.

When other activation stimuli (Pam3CSK4, PMA, PolyIC or MDP) that are not TLR4 specific, were tested in blood with heparin or EDTA, the majority of the ligands activated heparinized monocytes but not in EDTA, showing that the need of calcium for monocyte activation is not TLR4 specific.

Pam3CSK4 is a TLR2/TLR1 agonist, PolyIC is a TLR3, and MDP activates the intracellular receptor NOD2. The difference between stimuli is not clear, though there are two possible explanations: 1) monocytes have more TLR4 receptors that the others, and 2) TLR4 is more efficient. Regarding to point 1, there are not a lot of studies that quantify different TLR in monocytes, two of the studies shown by Western blot that monocytes have present in an ascending order, TLR3, TLR1/6, TLR2 and TLR4 [201, 202]. However when quantified by flow cytometry one study showed more TLR2 and another study more TLR4 receptors [202, 203]. Considering the second point, there are no studies comparing the efficiency between TLR in monocytes, however there is one study showing that TLR4 is a more efficient regulator of

neutrophils survival, compared with TLR2 [204]. Interestingly, one other study shows that monocyte-derived DC stimulated with LPS, Pam3CSK4 and PolyIC (10 fold more concentrated as well) led to the same mRNA IL-12 expression [205]. So, probably TLR4 activation is more efficient than the other.

Taken together, these results indicate that extracellular calcium is not involved in LPS binding but plays a critical role in monocyte activation by TLRs ligands. Indeed, a recent publication by Rossol *et al*. shows that, via a G-protein coupled calcium receptor, extracellular calcium has a role as a danger signal activating inflammasomes in monocytes and macrophages [206].

Another question was how long could blood be stored prior to being used in the assay. This is important especially if samples have to be transported from on location to another for testing. Results show that even after collection in heparin and storage for 3 days at room temperature, monocytes were not spontaneously activated and still responded to LPS stimulation.

2.4.1.2 Immunosuppressive assay

All MSC used in the assay were characterized phenotypically and for their differentiation capacities into adipocytes, osteocytes and chondrocytes (not shown). When activated monocytes were co-cultured with allogeneic hBM-MSC, results suggested that it was possible to measure MSC immunosuppressive capacity even using pre-activated monocytes. Results also showed some variations in the ability of monocytes from different blood donors to be inhibited by the same added MSC, however this recipient variability has not been previously reported.

In this immunosuppressive assay it was possible to observe MSC immunosuppressive effect on monocytes looking into two cytokines. Both, TNF-α and IL-12, show the same reduction in expression in a MSC dose dependent fashion. However, there is a limitation on IL-12 results, the highest number of MSC tested was $2x10^5$ cells with 20-30% reduction compared to control. Higher number of MSC should be tested to observe if IL-12 immunosuppression would be more than 30%.

2.4.1.3 Mechanism of action of MSC

MSC express TLRs suggesting a role in modulating early immune responses [118]. The innate immune response is often initiated by recognition of microbial PAMPs such as LPS, viral dsRNA) or prokaryotic DNA motifs such as CpG [118].

In this assay, since whole blood, LPS and MSC were cultured all at the same time, there was the possibility that in the presence of MSC, monocytes were not expressing the cytokines

because LPS was being bound by the added MSC and was not available to bind to monocytes. To eliminate this possibility, results show that at 1 μg/mL LPS (higher concentration that the one used in the assay, necessary to reveal staining by flow cytometry), LPS bound to monocytes and not to MSC.

Release of soluble immune-regulatory factors by MSC such as IDO, HGF, TGF-β, IL-10, PGE2 and HLA have been implicated in their ability to inhibit of T cell proliferation [112, 116]. Nonetheless, how MSC inhibit monocyte activation is currently unknown. It has been demonstrated, however, that monocyte removal from PBMC co-cultures with MSC reduces the suppressive effect [207]. Luk *et al*., using heat-inactivated MSC saw that these cells do not suppress T cell proliferation and B cell formation, however they modulate monocyte function. Their work suggests that the immunomodulatory effect of MSC does not depend on their secretome or active crosstalk with immune cells, but monocyte recognition of MSC [208].

To try to understand if monocytes and MSC need to be in contact for immunosuppression to occur, or if soluble factors are the main players in the immunosuppression, experiments using transwells were executed. These experiments involved a change in the configuration of the culture system, and finally the results were not enlightening. Culture well geometry is known to affect cellular interactions and these results would indicate a similar phenomenon for the inhibition of monocyte activation by MSC. Changing the geography of how the assay occurs changes the output.

Nevertheless, when the assay was performed in the normal round bottom plates and MSC supernatants were added, there was an immunosuppressive effect by MSC secretome.

As already mentioned, limited work has been done to understand the relation between MSC and myeloid cells, although is known that MSC soluble factors play an important role in their interactions. CXCL3, a chemokine secreted by MSC, is directly involved in myeloid cell differentiation and function [209].

In this study, instead of investigating a possible soluble factor, such as HGF, it was decided to look into vesicles/exosomes released by MSC, since exosomes produced by MSC have been show to be immunologic active [127, 131]. Exosomes allow the transfer of proteins and RNA, being a method of transport of different molecules [123, 210]. To study the effect of MSC exosomes on monocytes the same strategy published by Okoye *et al.,* it was used. In this approach, supposedly MSC exosomes were labelled. Results show that when in contact, MSC transfer material (siRNA PE) to monocytes. However, when monocytes are cultured with supernatants, it was not possible to see siRNA PE in monocytes. However, it was possible to see immunosuppression in both conditions, cell contact or with secretome. Other interesting fact was that when the supernatants were filtered, the immunosuppression was lower. One

important limitation of this part of the work was that it was not possible to characterize the exosomes.

Zhang *et al.* have shown that MSC exosomes activate monocytes through TLR signalling (MYD88-dependent pathway), leading to M2-like macrophage phenotype, producing anti-inflammatory cytokines; in turn, inducing Treg cell expansion [127]. The approach of Zhang *et al.* shows that monocytes play an important role in the immunosuppressive activity of MSC. However, they did not explain the mechanism of interaction behind exosomes and monocytes, they just explained that LPS induces a pro-inflammatory response from monocytes, while exosomes induced an attenuated pro-inflammatory cytokine response but a much enhanced anti-inflammatory response [127]. There are not many studies explaining exosomes-cell interactions. For example, Lai *et al.* have shown that 20S proteasome is an exosome protein that possibly could synergize with other exosome components contributing to the therapeutic efficacy in ameliorating myocardial ischemia/reperfusion injury [211]. However, further investigation need to be done to better understand how MSC exosomes and monocytes interact. The exosome field is a new and exciting area that can contribute to the knowledge of how cells interact. In general, more studies need to be done to understand how MSC interact with monocytes and how immunosuppression occurs.

2.4.2 Lymphocytes

Lymphocyte immunosuppression by MSC has been extensively investigated. However, the main objective of the study reported herein was to develop a rapid assay to measure the MSC immunosuppressive capacity on lymphocytes. In most studies, such assay is performed by culturing MSC with lymphocytes (PBMC) for several days prior to readout. In order to activate lymphocytes polyclonally and very rapidly, it was used the combination of PMA, that activates lymphocytes directly through PKC, and ionomycin, a calcium ionophore allowing calcium ion entry and release from intracellular stores. However, following such activation, the results were very disappointing, TERT cells were not able to immunosuppress T cell activation. There are three possible explanations for these results. First the culture time was not long enough for complete T activation; the kinetics of T cell activation is slower than monocytes. A second possibility is that TERT cells are not as efficient as primary MSC in inhibiting T cell activation. This does not seem likely, but it is possible; however, there was no time to test this hypothesis. The third explanation is that PMA is a very strong stimulus, even at the lowest concentration tested. It was also used PHA to stimulate T cells, however, even after 24 hours, this was not long enough to activate T cells. Finally, a more physiologic activation method was tested, namely CD3/CD28 beads. Once again the results were very discouraging. First, the beads were not able to activate T cells in whole blood suspension and there are not studies showing the

opposite. The problem it was not that the stimuli was not strong enough, 10 beads for 1 T cells, seems a concentration high enough, however in a whole blood culture system there are not just MNC, there are other cells, cytokines, plasma, platelets, etc, that can interferer with T cell activation. This is an interesting point to show that is important to consider the all environment when *in vitro* observations are made. Second, in 24 h TERT cells did not immunosuppress T cells, in MNC cultures activated by CD3/CD28 beads.

2.4.3 MSC immunogenicity

One of the great advantages of the use of MSC in cell therapy is their low immunogenicity [212]. This characteristic enables the use of allogeneic MSC for cell therapy with a low risk of immune recognition and rejection by the recipient, increasing their window of action inside the host. In humans, the expression of low surface levels of MHC-I molecules contributes to MSC hypo-immunogenicity and protects them from NK cell-mediated lysis. The absence of MHC-II and co-stimulatory molecules, such as CD40, CD80, and CD86, prevents MSC recognition by $CD4^+$ T cells [68]. Under the influence of IFN-γ, the expression of MHC-I and MHC-II is up-regulated and, in the presence of an inflammatory environment, the expression of CD40 is induced in MSC as well [68]. In these circumstances, there are studies reporting that MSC still do not elicit an immune response due to the absence of other co-stimulatory molecules and of proteins with a strong inhibitory effect over T cells, many of which are up-regulated under inflammatory conditions [68]. Other studies describe that IFN-γ enables human BM-MSC to become non-professional antigen-presenting cells [213]. In addition, MSC are protected from damage by complement because they express factor H and other complement control proteins [214, 215]. However, these concepts of low immunogenicity and inability to mediate T cell activation are being challenged by an increasing number of studies showing that MSC can, indeed, be recognized and destroyed by the specific arm of the recipient's immune system.

Even though monocytes do not have anti-MHC receptors, they were not activated in the presence of MHC allogeneic MSC. In addition, it was shown (**Figure 2.32**) that BM-MSC and immortalized BM-MSC (TERT) were also not immunogenic. It would be also interesting to study if there is any difference between using frozen or cultured MSC. This is especially relevant in the case of trauma situations, where time is precious. There are some preliminary results indicating that there is no impact on the outcome. One study shows no changes in CFU-f numbers when compared fresh and cryopreserved MSC [216]. Nevertheless further studies need to be done.

2.4.4 Conclusion

In conclusion, this chapter describes the development of a rapid, reliable and quantifiable assay to measure the MSC immunosuppressive capacity on monocytes. Unfortunately it was not possible to simultaneously deliver a rapid T cell immunosuppressive assay. Once developed, it is also important to mention that the monocyte assay could be used to study the immunosuppressive effects of chemical or biological compounds (e.g. drugs or seaweed extracts) or solid materials (e.g. scaffolds in tissue engineering). Results of these studies will be presented further in Chapter 3. Lastly, the assay is also being used in the context of a project investigating monocyte biology in IBD patients

Chapter 3 | Applications of the whole blood assay

This chapter is composed of two parts. In the first part the whole blood potency assay was used to measure the potency of different MSC preparations from different sources on blood cells from different donors. The second part shows the versatility of the whole blood assay, i) measuring the effect of biomaterials used to create scaffolds on monocytes and lymphocytes and ii) the effect of biologic compounds (seaweed extracts) on monocyte activation.

3.1 Validation of a potency assay for measuring *in vitro* immunomodulatory properties of human Mesenchymal Stromal Cells in Osteoarthritis and Rheumatoid Arthritis

3.1.1 Introduction

Arthritis, rheumatism and back/spine problems are leading causes of disability worldwide. According with CDC (Centers for Disease Control and Prevention), between 2010 and 2012 around 23% (52.5 million) of adults in the United States were diagnosed with arthritis, being more prevalent in women (23.9%) than in men (18.6%). It is estimated that by 2030, 25% of Americans (67 million) will be diagnosed with arthritis. This is due to the combined effects of an ageing population and current trends in obesity. Almost 43% of the 52.5 million adults had reported arthritis-attributable activity limitations, and 31% of these individuals are limited in work due to arthritis [217].

Arthritis is characterized by swelling, pain, stiffness and decreased range of motion in joints, known as synovial joints. There are more than 100 different types of arthritis and related conditions, however these can be categorized into: degenerative (osteoarthritis is the most common type of arthritis), inflammatory (rheumatoid arthritis), infectious (when a bacterium, virus or fungus can get into the joint and trigger inflammation) and metabolic (when uric acid levels are high and it can become chronic) [218]. Inflammation occurs in the majority of arthritis conditions. The main differences between osteoarthritis and rheumatoid arthritis are briefly described in **Figure 3.1**.

Synovial joints are complex structures composed of articular cartilage, synovial membrane, also designated as synovium, subchondral bone, ligaments, menisci and articular capsule [219]. Together, these tissues give each synovial joint its unique shape, organization and biomechanical function [220]. Healthy articular cartilage provides a smooth surface with very low friction allowing for smooth joint movement. Articular cartilage is a very complex tissue and is organized into distinct areas [221, 222].

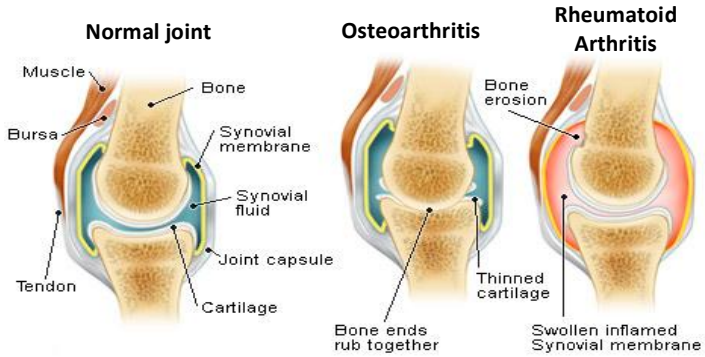

Figure 3.1 - Schematic representation of normal and arthritic joints. The two main types of arthritis are osteoarthritis which is break-down of cartilage by wear and tear usually brought around by excessive use or damage to the joint and rheumatoid arthritis which is an autoimmune disease where the synovium is attacked by the body's own cells [223].

Cartilage is an avascular connective tissue, this means that cartilage does not possess regenerative capacity and that nutrients and oxygen supply to the subchondral bone and synovium the is made by chondrocytes [224]. During skeletal development, chondrocytes arises by differentiation from MSC and they are responsible for producing a very large amount of ECM composed mainly of collagens and proteoglycans. These proteins determine the biomechanical properties of the cartilaginous tissue [225, 226]. In healthy tissue, chondrocytes maintain the ECM components under normal, low-turnover conditions in which the glycosaminoglycans, proteoglycans and other non-collagen molecules can be replaced [221].

The synovial joints are surrounded by synovium, a specialized mesenchymal tissue that holds the synovial fluid in place when the joints are under pressure. The physical constituents of synovial fluid is a big subject of study, since it acts as a biochemical pool to which the nutrients are transferred into the cartilage and undesirable substances are removed through the sub-synovium back into the blood. Oxygen and nutrients move from the blood through the synovial fluid into the cartilage while waste coming from the cartilage moves in the opposite direction into the blood [227, 228].

Synovitis is the occurrence of inflammation in the synovial joints, more specifically in the synovial membrane. Synovitis occurs in arthritis as well as in other conditions such as meniscal injury, lupus and gout [221]. Usually this inflammation is followed by swelling, due to accumulation of synovial fluid, and it is thought to result from cartilage debris and catabolic mediators entering the synovial cavity [229].

3.1.1.1 Osteoarthritis

Osteoarthritis (OA) is the most common form of arthritis, affecting more than 27 million people in the United States and 70 million in Europe [230, 231]. Although the exact cause of

OA is unknown, some factors play an important role. In the general population diagnosed with OA, between 39% to 65% of cases, can be attributed to genetic predisposition [232]. OA is one of several chronic conditions that are becoming more prevalent with ageing of the population, and women over 50 years of age are more affected than men [222, 230]. Obesity, trauma and abnormal joint shape/alignment also influence disease progression [230, 233, 234]. The knee, hip, and hand are the areas most affected by this disease [230, 231].

OA is a progressive disease characterized by structural and functional changes in the affected joints causing pain. The pain is associated with systemic high levels of C-reactive protein, reflecting synovitis, while swelling and deformation is correlated with collagen degradation [221, 225]. The disease progression causes disability and loss of independence. OA confers a huge burden to the individuals in the day-to-day life and economically [222, 235].

The disease occurs when the joint cavity is reduced and there is a degeneration of articular cartilage and ultimately the bones rub together and cause more damage and pain. In advanced OA patients, it can also cause meniscal and ligamentous lesions, atrophy in the surrounding muscle and limb deformity [226, 236-238]. The cartilage degradation occurs because of the presence of matrix-degrading enzymes, MMPs and ADAMTS, produced by chondrocytes [224]. OA pathophysiology is characterised by the failure to repair the damaged cartilage due to biomechanical and biochemical changes in the joint [222].

Over 50% patients with OA in the knee present with synovitis, and the prevalence increases with OA progression [239-241]. Inflammation is a feature in OA however, it is controversial why the synovium becomes inflamed; there are some theories. The most accepted theory is that once the cartilage is degraded, it comes into contact with synovial cells. These cells are activated and produce inflammatory mediators that are then released into the synovial fluid [221, 242]. A more recent hypothesis involves synovial tissue as a primary trigger of inflammation. Many immune cells have been described as having a role in the inflammatory process in OA. Geven *et al.* showed that locally induced OA, leads to a clear skewing towards a pro-inflammatory monocyte subset, in the bone marrow, indicating that locally induced OA may also be systemically regulated [243]. In another study where synovial macrophages were depleted reduced MMP-mediated cartilage damage and decreased osteophyte formation was reported [221, 244].

Currently there is no cure for OA. The treatment of this disease is focused mostly on pain relief rather than modifying the disease process. The treatment includes pharmacological agents with potential ‘‘chondroprotective’’ properties, such as nonsteroidal anti-inflammatory drugs (NSAIDs), diet supplements with glucosamine, chondroitin sulphate, vitamins C, D, and E, platelet-rich plasma (PRP), polyunsaturated fatty acids; S-adenosylmethionine;

methylsulfonylmethane and intra-articular injections of hyaluronic acid [245]. A very important part of treatment is physiotherapy, as well as, non-pharmacological treatments including patient education, body weight reduction and use of orthopedic equipment facilitating motility [222]. In some cases, patients are submitted to surgical procedures to restore the integrity and function of a joint by arthroplasty or joint replacement. Clinicians recognise that the diagnosis of OA is established late in the disease process, maybe too late to expect improvements following treatment [222].

3.1.1.2 Rheumatoid Arthritis

Rheumatoid arthritis (RA) is a chronic, destructive, autoimmune inflammatory polyarthritis (affects several joints) disease that confers a considerable burden for patients, and their families [246, 247]. Rheumatoid arthritis, by contrast with OA, mainly affects young people and is a fast-developing, generalized inflammatory disease driven by autoimmune processes. Interestingly, the prevalence of RA is much lower than OA, although until now the field of RA has attracted more scientific attention than OA [242]. RA affects approximately 0.4-1.3% of the population in Northern European and North American [248]. Several incidence and prevalence studies suggest a significant variation of the disease occurrence between different populations [248]. RA is considered to be a multifactorial disease. The disease results from the interaction of genetic, environmental factors and autoimmunity, which triggers its occurrence and expression [249]. There is evidence that genetic predisposition increases the risk of RA [249]. However there are other risk factors such as gender, age, smoking, infectious agents, hormonal, dietary, socioeconomic, and ethnic origin, and disease occurrence and severity are related with these risk factors [248, 249].

According to the CDC there are at least three possible disease courses, conferred by disease severity: monocyclic, polycyclic and progressive. Monocyclic patients just have one episode whereas in the progressive case, there is an increase in severity for a long period of time.

In RA there is a loss of immunological self-tolerance causing the activation of immune cells to attack joint components and subsequent initiate chronic inflammation [250]. The synovial membrane inflammation occurs via infiltration of immune cells (T and B cells, dendritic cells and macrophages) and inflammatory cells (osteoclast and fibroblast), followed by synoviocyte proliferation. This disease causes chronic synovitis. Ultimately, the synovial membrane becomes hyperplastic. As disease progresses, synovial tissue becomes invasive destroying articular cartilage and bone [251, 252].

Several immune cells are involved in RA pathology; antigen presenting cells, such dendritic cells and B cells, activate T cells in the synovium. Activated T cells stimulate B cells and macrophages by soluble factors or by cell contact, leading to increased production of pro-inflammatory mediators such as TNF-α, IL-1β, IL-6 and IL-15 [252, 253].

The RA therapeutic approaches, either as monotherapy or combined therapies, are: NSAIDs, steroids, disease-modifying anti-rheumatic drugs (DMARDs) or immunotherapy, targeting T and B cells, as well as, cytokines including TNFα, IL-1β, IL-6 and IL-15 [252, 253]. However, many of these treatments have potentially serious side effects. These drugs tend to relieve pain and reduce inflammation and some of them can slow disease progression preventing joint and organ damage. If medications fail to prevent or slow joint damage, surgery to repair damaged joints is the final option [254, 255].

There is no cure for rheumatoid arthritis, for this reason early diagnosis and immediate, effective therapy are crucial to prevent joint deterioration, long-term disability and unfavourable disease outcome [254]. One other disease that is associated with poor RA outcomes is depression. Depression is highly prevalent in RA patient with no effective treatment. Optimal care of RA patients, as well as in other inflammatory diseases may include detection and management of depression [256].

An important factor in the RA outcome is the very narrow "window of opportunity" that occurs to achieve remission, RA patients need to be treated within 3 to 6 months following diagnosis [257].

3.1.1.3 ADIPOA2

ADIPOA is a pan-European clinical study with the aim of investigating the safety and efficacy of infusion of autologous ASC in the knee of OA patients. To reach this stage, three pre-clinical models, mouse, rabbit and goat, were used to investigate the modulatory effect of ASC in OA.

Overall, results of ADIPOA showed that ASC reduced inflammation in the synovium and helped prevent thickening of the synovial layer and joint destruction. Results also suggested that an inflammatory environment was necessary to activate the immunosuppressive effects of ASC. These pre-clinical results led to the next phase where 18 patients with OA received an intra-articular dose of autologous ASC into the knee. The success of these results led the ADIPOA2.

ADIPOA2 is an on-going two-year phase IIb trial that involves several groups and is a blinded trial, where three different ASC doses are being tested in a single intra-articular injection. Since the monocyte potency assay was successfully validated, this is now being used

in ADIPOA2. By doing this, it will be possible to correlate *in vitro* potency results with clinical outcome. However, one possible limitation is that for the above results, allogeneic MSC from healthy donors were used whereas in the ADIPOA2 trial, autologous ASC will be used. This might mean that autologous ASC may be less efficient, since the proliferative, chondrogenic and adipogenic capacities of MSC obtained from OA patients are reportedly reduced [258].

3.1.2 Objectives

The main aim of this chapter was to validate the optimised rapid turnaround, flow cytometry-based whole-blood assay to monitor MSC potency developed in the previous chapter. One of the aims was to assess and compare the immunosuppressive potency of BM-MSC and ASC on blood cells from healthy controls, osteoarthritis and rheumatoid arthritis patients. In particular, TNF-α and IL-6 expression by LPS-activated monocytes was determined. The hypothesis being tested was that using such an *in vitro* test, it might be possible to predict, prior to clinical use, if MSC from a particular source would have the capacity to inhibit the activation of recipient patients' monocytes and thereby indirectly predict their anti-inflammatory activity. As part of these studies, the issue of whether the immuneregulatory activity of MSC altered with increasing passage number.

Summary of aims:

- To validate the monocyte whole blood assay with Osteoarthritis and Rheumatoid Arthritis patient samples;
- To compare immunosuppressive capacity of ASC and BM-MSC;
- To study MSC donor variability and blood donor (monocyte) variability.

3.1.3 Methods

Details regarding reagents, solutions, antibodies and material are described in Annexes F to J.

3.1.3.1 Isolation and expansion of MSC

Bone marrow MSCs were isolated and expanded according with protocol describe in the method section 2.2.1.3 of chapter 2.

Adipose derived stromal cells were obtained by liposuction from three healthy donors. Enrolment of healthy adult volunteers and collection of lipoaspirate samples for the purpose of generating culture-expanded ASC was approved by the Research Ethics Committee of Galway University Hospitals.

The ASC were isolated at CCMI (Centre for Cell Manufacturing Ireland). Briefly, the lipoaspirate was diluted with DPBS and centrifuged, the upper oil phase and lower phase containing erythrocytes were removed. The remaining adipose tissue was digested with collagenase and filtered through 100 μm cell strainer. A sample was removed for counting, viable cells were calculated using Trypan blue exclusion, following acetic acid lysis. Cells were plated at a density of $5.1x10^6$ per cell culture stack with complete medium, namely MEM Alpha with Glutamax supplemented with 5% (v/v) pooled human platelet lysate (PL) and 1% (v/v) P/S, for few days at 37°C in a humidified incubator containing 5% CO_2 in air. After a few days, non-adherent cells were gently removed with DPBS and fresh complete medium added. When cells reached 80-90% confluence in P_0, ASC were detached using 0.25% Trypsin-EDTA, and the trypsin inactivated by adding 10X volume of complete medium. Detached cells were then centrifuged (250 g for 5 minutes at room temperature) and counted.

ASC were cryopreserved at $1x10^6$ cell/mL with freezing medium and thawed when necessary. ASC were washed extensively with DBPS and complete medium and seeded at a density of $5x10^3$ cells/cm^2 into cell culture flasks with complete medium and culture as before. The medium was renewed every two days until the cells reached 80-90% confluence. For passaging, ASC were detached, centrifuged (250 g for 5 minutes at room temperature), counted and seeded again at $3x10^3$cells/cm^2. To use in the whole blood assay, ASC were kept in culture until they reached 90-100% confluence and then detached and counted.

3.1.3.2 Immunophenotyping

The immunophenotypic characterization of hBM-MSC was performed as in Chapter 2 using the human MSC analysis kit. On the other hand, ASC immunophenotyping was made with individual antibodies all in PE. ASC were trypsinized, neutralized and counted, $2x10^5$ cells

were placed in cytometer tubes and stained with CD73, CD90, CD105, CD3, CD14, CD19, CD34, CD45, HLA-DR, PI and appropriated isotype controls, for 10 minutes at room temperature, in the dark. Following staining, ASC were washed twice and resuspended in 200 μL of FACS buffer. The cell suspensions were acquired and $1x10^5$ ASC were recorded using BD Accuri C6. Phenotypic characterization was made using BD CSample Analysis software.

3.1.3.3 Blood samples collection

Peripheral blood from 12 healthy adult volunteers ranging in age from 24-64 years was collected into BD Vacutainer sodium heparin tubes, according to the protocol approved by the ethics committee of the National University of Ireland in Galway. Once collected, blood was used within three days being kept at room temperature.

Peripheral blood from a total of 4 OA patients and 5 RA patients were collected in a room at Galway University Hospital, into BD Vacutainer sodium heparin tubes. Enrolment of volunteer patients and collection of peripheral blood was approved by the Research Ethics Committee of Galway University Hospitals. OA patients were ranging in age from 59-84 years, while RA patients were between 30-62 years old, and three females in each group. Once collected, blood was transported to the bioscience building and used within a day.

3.1.3.4 Whole blood assay – monocyte co-culture with MSC/ASC

As described in previous chapter this assay is divided in two parts. First, BM-MSC and ASC are trypsinized, neutralized and counted. Cell suspensions at $5x10^5$ cells/test in 50 μL of appropriate complete medium were prepared. In sterile cytometer tubes was added 0.6 μg/mL Brefeldin A, 1ng/mL ultrapure LPS-EB, heparinised blood diluted 10 fold in RPMI 1640 medium and $5x10^5$ BM-MSC, ASC or TERT (positive control). The tubes were sealed with parafilm and incubated for 6 or 24 hours at 37°C in a humidified incubator containing 5% CO_2 in air. The second part of the assay is the staining. Cells were surface stained for 10 minutes at room temperature in the dark with CD45 V500 and CD14 APC. Following surface staining cells were fixed using reagent 1 from Beckman Coulter IntraPrep Kit. The cells were incubated again for 10 minutes at room temperature in the dark. Then, cells were washed and permeabilized using reagent 2 from Beckman Coulter IntraPrep Kit. Cells were stained intra-cytoplasmically with anti-IL-6 FITC and anti-TNF-α PE. In same cases after 24 hours incubation the cells were stained intra-cytoplasmically with anti-IL-12/IL-23 p40 PE. Following other 10 minutes incubation at room temperature in the dark samples were washed twice, resuspended in FACS buffer and acquired by the BD Canto II (Becton Dickinson) 8 colour flow cytometer. Data were

analysed with flow cytometry softwares: FlowJo version 10 (Tree star) or Infinicyt version 1.7 (Cytognos).

This part of the project it was performed by Aoife Dunne, a Master student under supervision of Professor Marry Murphy (REMEDI).

3.1.3.5 Monocyte count

Monocytes from healthy and patients sample were counted after whole blood assay preparation. To quantify the number of monocyte in each blood sample, 50 μL of peripheral blood was stained with CD14 APC for 10 minutes at room temperature, in the dark. Afterwards, erythrocytes were lysed using 1X BD FACS Lysing Solution for 10 minutes in the same conditions. Following staining, samples were washed twice and resuspended in 200 μL of FACS buffer and 100 μL of cell suspension was acquired on BD Accuri C6. Monocyte counts were calculated with BD CSample Analysis software. BD Accuri C6 cytometer has a unique characteristic, allows to acquire a define volume of cell suspension. For this reason is possible to know how many cells there are per μL.

3.1.3.6 Statistical analysis

Results are expressed as average and standard deviation of percentage of TNF-α, IL-6 or IL-12 production by monocytes. To determine the statistical significance of the differences observed between different conditions, two-way ANOVA (95% confidence intervals), multiple comparisons were performed, or using unpaired multiple t-tests correct for multiple comparisons using the Holm-Sidak method. GraphPad Prism software was used. Statistically significance differences were considered * when P-value was lower than 0.05, ** when P-value was lower than 0.01, *** when P-value was lower than 0.001 and **** when P-value was lower than 0.0001.

3.1.4 Results

3.1.4.1 ASC immunophenotyping

The human ASC preparations were characterized for lack of expression of CD3, CD14, CD19, CD34, CD45 and HLA-DR and for positive expression of CD73, CD90 and CD105, on gated viable cells.

The ASC were also differentiated into adipocytes, osteocytes and chondrocytes, to prove they were MSC. However, the differentiation assays were not performed during this project.

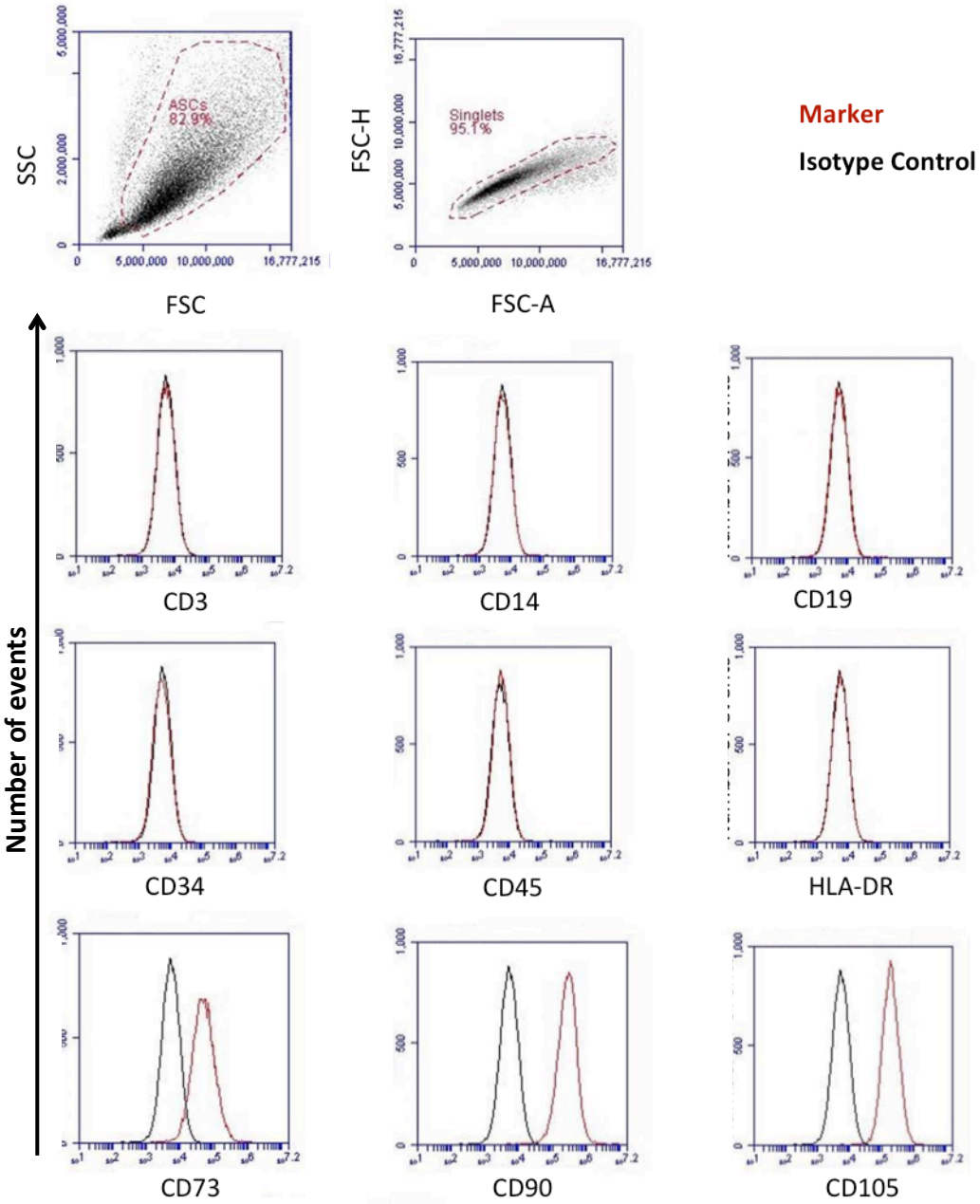

Figure 3.2 - Human ASC immunophenotyping. Representation of one ASC donor labelled with the indicated monoclonal antibodies (red line) and corresponding isotype control (black line).

3.1.4.2 Whole blood monocyte assay validation with patient samples

The gating strategy used to identify monocytes is described in **Figure 3.3**. Monocytes were identify according with CD45 and CD14 expression and by their distinct light scatter profile (panel A and B). Gated monocytes were then analysed for intra-cytoplasmic TNF-α and IL-12 expression.

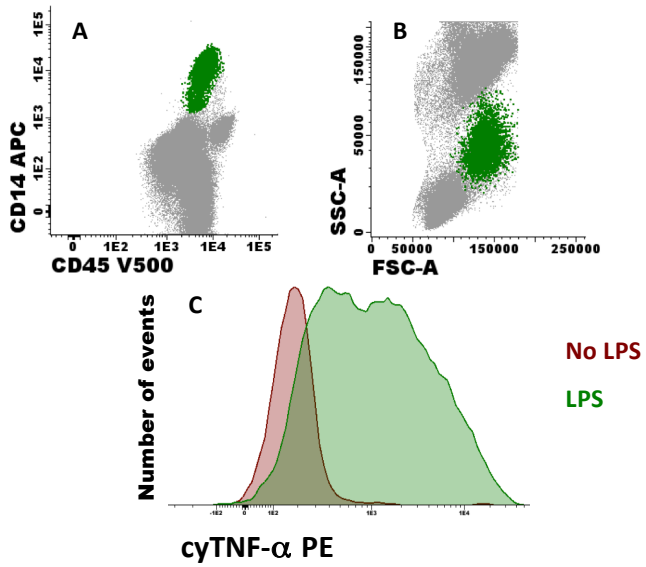

Figure 3.3 - Gating strategy used to identify monocytes and their intracytoplasmic TNF-α expression. **A** Monocytes were identified by $CD14^+$ and $CD45^+$ expression (green dots), and **B** by SSC and FSC among total cells (grey dots) after $CD14^+CD45^+$ gating. **C** Histogram of intracytoplasmic TNF-α staining in presence and absence of LPS. The figure is a representative result of heparinized blood diluted 10X and incubated for 6 h in presence of 1 ng/mL LPS.

In the previous chapter it was shown that BM-MSC and TERT cells did not stimulate monocytes directly, designated as "immunogenic" effect. The results in **Figure 3.4** show that ASC also do not stimulate monocytes directly, in absence of LPS.

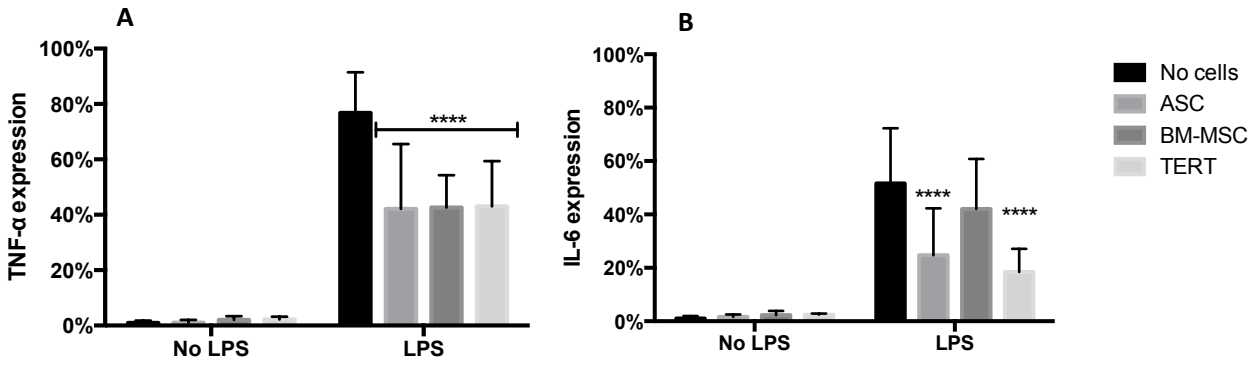

Figure 3.4 - Human ASC, BM-MSC and TERT cells do not have an "immunogenic" effect on unstimulated monocytes. Monocytes do not express TNF-α (**A**) and IL-6 (**B**) in presence of $5x10^5$ cells and absence of LPS. Healthy heparinized blood was diluted 10X in RPMI and monocytes were stimulated for 6 h with 1 ng/mL LPS. ASC (P_1-P_4) n=12; BM-MSC (P_1-P_6) n=11 and TERT (P_{44}-P_{45}) n=6. Statistic significance when compared to "No cells". Two-way-ANOVA * P<0.05, ** P<0.01, *** P<0.001 and **** P<0.0001.

When the whole blood assay was performed with blood samples from OA patients, a generally higher expression of TNF-α and IL-6 by monocytes was observed compared with healthy samples (**Figure 3.5**). In addition, in the presence of ASC, the percentage of monocytes that expressed TNF-α and IL-6 was significantly reduced in healthy and OA samples, when compared with LPS without MSC. The same effect was seen in the presence of BM-MSC and TERT.

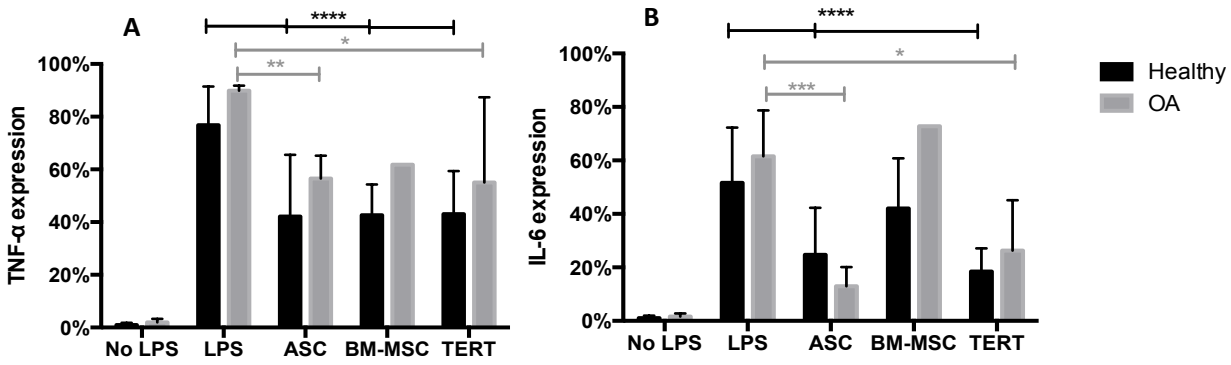

Figure 3.5 - Human ASC, BM-MSC and TERT cells are able to reduce %TNF-α (**A**) and %IL-6 (**B**) produced by monocytes. Blood samples from healthy (n=15) and OA (n=4) individuals were diluted 10X with RPMI and monocytes were stimulated for 6 h with 1 ng/mL LPS. In presence of $5x10^5$ cells: ASC (P_1-P_4) n=12|4 (healthy|OA); BM-MSC (P_1-P_6) n=11|1 and TERT (P_{44}-P_{45}) n=6|2. Two-way-ANOVA * P<0.05, ** P<0.01, *** P<0.001 and **** P<0.0001.

When the whole blood assay was performed with blood samples from RA patients, similar results were observed (**Figure 3.6**). In the presence of ASC, the percentage of monocytes expressing TNF-α and IL-6 was significantly reduced in healthy and RA samples, when compared with LPS without ASC. With RA samples, it was not possible to test BM-MSC and TERT cells since there were not enough numbers of cells in the moment that the samples arrived.

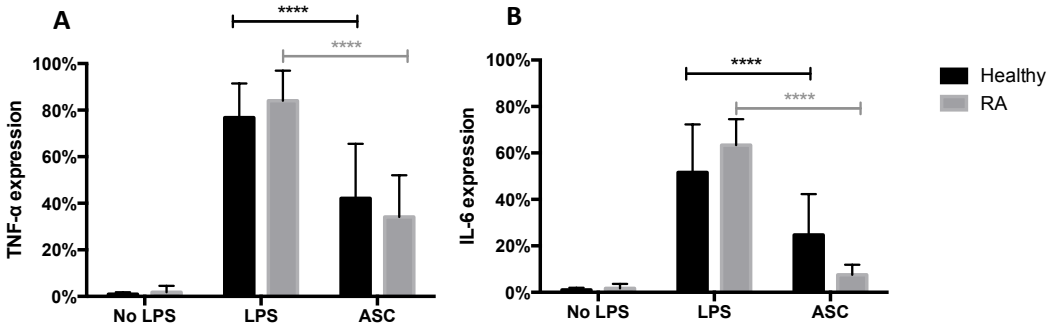

Figure 3.6 - Human ASC are able to reduce %TNF-α (**A**) and %IL-6 (**B**) produced by monocytes. Blood samples from healthy (n=15) and RA (n=5) individuals were diluted 10X with RPMI and monocytes were stimulated for 6 h with 1 ng/mL LPS, in presence of $5x10^5$ ASC (P_1-P_4) n=12|5 (healthy|RA). Two-way-ANOVA * P<0.05, ** P<0.01, *** P<0.001 and **** P<0.0001.

Figure 3.7 shows the differences between healthy, OA and RA samples. The percentages of monocytes in the three groups, in the presence of LPS and ASC, that express TNF-α and IL-6 were lower, compared with culture without ASC present.

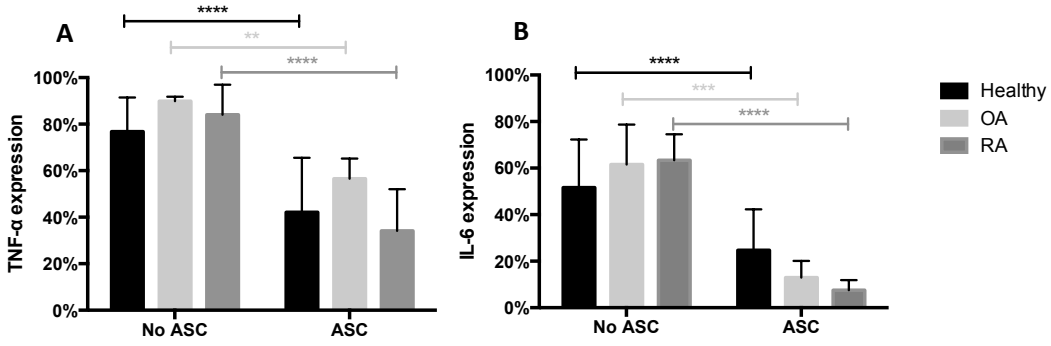

Figure 3.7 - Differences between healthy, OA and RA samples in presence of ASC. %TNF-α and %IL-6 produced by monocytes in the three groups. Blood samples were diluted 10X with RPMI and monocytes were stimulated for 6 h with 1 ng/mL LPS, in presence of $5x10^5$ ASC (P_1-P_4) n=12|4|5 (healthy|OA|RA). Two-way-ANOVA * P<0.05, ** P<0.01, *** P<0.001 and **** P<0.0001.

3.1.4.3 Donor variation and passage number

To observe if there was any difference between ASC donors, blood from one healthy volunteer was simultaneously cultured in the presence of three ASC preparations, and no difference was found.

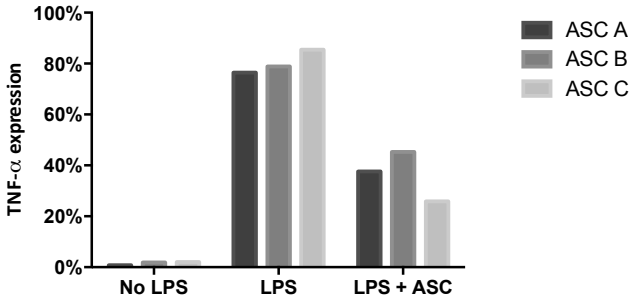

Figure 3.8 - Differences between ASC donors. Percentage of TNF-α expression by monocytes in presence of three different ASC preparations. Blood from one healthy donor was diluted 10X with RPMI and monocytes were stimulated for 6 h with 1 ng/mL LPS, in presence of $5x10^5$ ASC A (P_2), ASC B (P_1) or ASC C (P_3), n=1.

The potency of different BM-MSC preparations was compared simultaneously on monocytes from different blood donors. MSC derived from three different BM donors at three different passage numbers were assayed in blood samples from four individual volunteers (**Figure 3.9**).

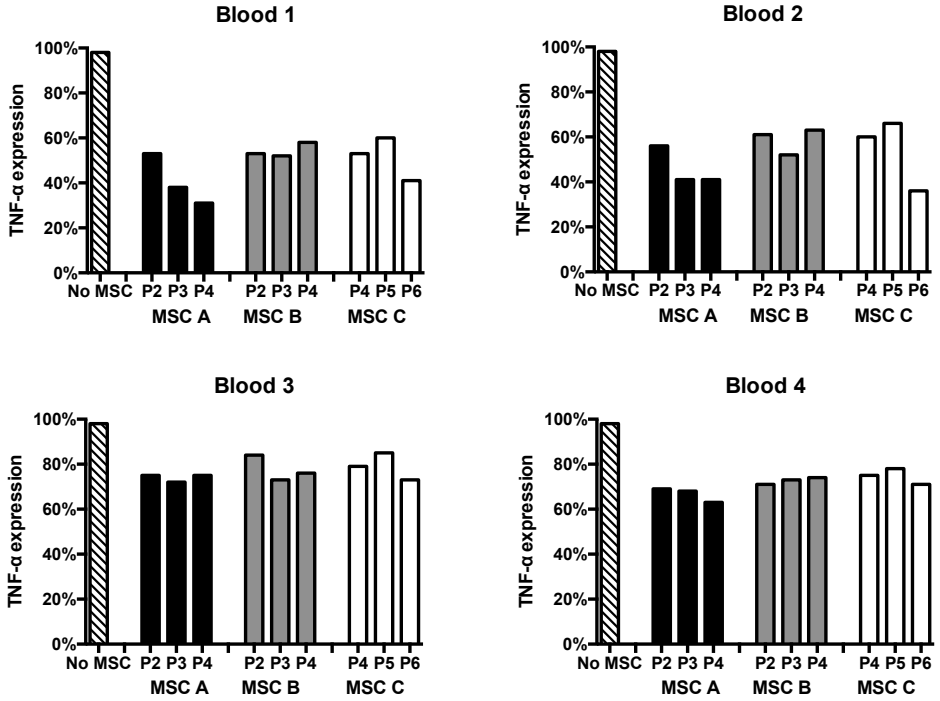

Figure 3.9 - Differences between passage number and hBM-MSC donor in different blood donors. Graphs show TNF-α expression of 4 blood donors, in presence of 3 different MSC preparations at 3 different passage numbers. Heparinized blood was diluted 10X and activated for 6 h with 1 ng/mL LPS and co-cultured with $4x10^5$ MSC. No statistically differences were found; n=1.

Results indicate comparable suppressive potency of all three MSC cultures with variability across passage number. Of note, the suppression patterns observed for the three MSC cultures and their different passage numbers were very similar for all blood donors, except blood 1 MSC A, where results suggest that the higher the passage number, the lower the %TF-α^+ monocytes, indicating a higher immunosuppressive capacity.

Regarding IL-12 expression, the results suggest that passage number have an effect. However, is not possible to say if the difference is regarding MSC donor or passage number. **Figure 3.10** shows that MSC E at P_6 have no immunosuppressive effect, when compared with MSC D in P_3.

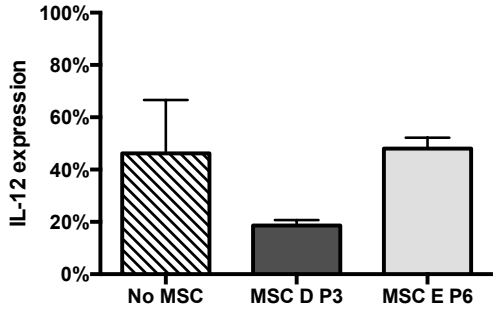

Figure 3.10 - Differences between passage number and hBM-MSC donor in different blood donors. IL-12 expression of 3 blood donors, in presence of 2 different MSC preparations at different passage numbers. Heparinized blood was diluted 10X and activated for 24 h with 1 ng/mL LPS and co-cultured with $1x10^6$ MSC (n=3). No statistically differences were found.

When suppressive potencies of MSC from three BM donors, all in P_4 (**Figure 3.11**) were averaged (panel A) from previous results for four separate blood samples (panel B), a greater inhibition of monocyte %TNF-α^+ was seen for one MSC (MSC A) when compared to the other two MSC (MSC B and C).

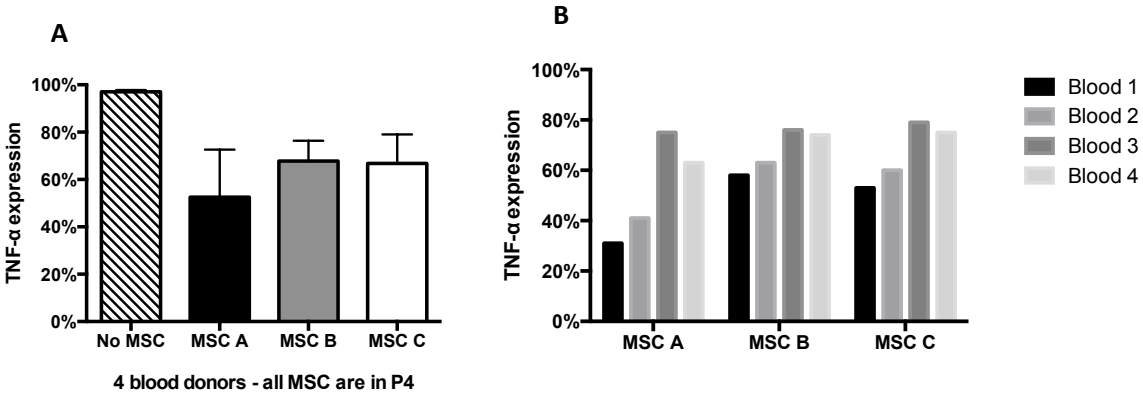

Figure 3.11 - Differences between hBM-MSC donor and blood donors. TNF-α expression of 4 blood donors, in average (**A**) and individually (**B**), in presence of 3 different MSC preparations all at P_4. Heparinized blood was diluted 10X and activated for 6 h with 1 ng/mL LPS and co-cultured with $4x10^5$ MSC. No statistically differences were found.

3.1.5 Discussion

Stem/stromal cell therapy prospective to treat a range of diseases and injuries have been reported in the last decade, and their potential applications to treat OA and RA have been considered in several studies.

3.1.5.1 Osteoarthritis and MSC

Despite the efforts to develop a treatment that prevents cartilage matrix breakdown or cartilage restoration, there is no effective treatment for OA. MSC are known for their anti-inflammatory and immune-modulatory properties and since inflammation is a very important aspect of OA, several methods of using MSC have been tested in the last decade. The traditional method of marrow stimulation, which provide access to the bone blood supply by penetrating the subchondral bone to provide MSC within the fibrin clot, have demonstrated mixed and poor long-term results. However, autologous chondrocyte implantation offers a better outcome; the limitation of this process is the low availability of healthy chondrocytes [259, 260]. The next logical step would be to exploit the ability of MSC to differentiate into the chondrogenic lineage. Besides reducing inflammation, MSC could also improve function and regeneration. Several MSC cell-based therapies have already shown encouraging results to treat OA [260, 261]. In contrast to mature chondrocytes, which have to be surgically harvested from a limited supply of healthy articular cartilage, MSC can be harvested from multiple tissues, *in vitro* cultured expanded and maintaining multi-lineage potential [260].

Several studies were successful at differentiating MSC into chondrocytes. However, there is a need to develop effective methods of maintaining the cartilage phenotype of differentiated MSC without hypertrophy, ossification or fibrinogenesis. Also required is a delivery system for MSC into the lesion, without compromising MSC chondrogenic differentiation or the integrity of the repaired tissue. For this reason, it may be easier to deliver MSC directly into the joints. In a rabbit model, intra-articular delivery of ASC attenuated osteoarthritis progression [262]. In other animal models, ASC were also able to promote cartilage and meniscal repair and attenuate synovial inflammation, inhibiting OA progression [258, 262, 263]. However, in humans there is not enough data proving that MSC are beneficial for OA treatment. There are some case reports, pilot studies and some clinical trials. In January 2016, according with National Library of Medicine ClinicalTrials.gov website, there are 54 clinical trials involving OA patients that are or will be treated with MSC (alone or with anti-inflammatory drugs). The majority of these studies involve the use of autologous, culture-expanded BM-MSC, however ASC and MSC from umbilical tissue are also used in 11 and 9 cases, respectively.

In one pilot study, patients exhibited rapid and progressive improvement of *algofunctional indices* (a term used to describe the index of severity for OA) that approached 65% to 78% by 1 year, with improvement of cartilage quality in 11 of the 12 patients [261]. The same group in 2015 finished two clinical trials using allogeneic and autologous MSC to treat OA patients. Results from the allogeneic trial show the same results as that of the pilot study. A group of 15 patients were treated with intra-articular injection of allogeneic BM-MSC while the control group of 15 patients received intra-articular hyaluronic acid. One year later, patients treated with MSC presented a significant improvement in algofunctional indices compared with the control group. Also observed was a significant decrease in poor cartilage areas, with cartilage quality improvements in MSC treated patients [264]. A different group showed that intra-articular injection of ASC into osteoarthritic knees improved function and reduced pain without causing adverse effects. A reduction in cartilage defects by regeneration of hyaline-like articular cartilage was also observed [263].

Intra-articular injection of MSC seems to be an efficient OA treatment, since they have anti-inflammatory, immunomodulatory and regenerative properties. However there is still a long way to find a cure for OA. Probably new efforts to prevent the development and progression of OA might include strategies that slow the progression of chondrocyte senescence or slowing ECM degradation. Using MSC directly or taking advantage of their paracrine effect, non-cellular therapy using MSC-conditioned media could be proposed.

3.1.5.2 Rheumatoid Arthritis and MSC

Currently there are RA treatments that can slow disease progression and prevent irreversible joint damage. RA patients can live comfortable and productive lives on medical therapy. However, no therapy is curative and the drugs are expensive and produce side effects, for this reason more affordable and successful therapies are needed.

In the last two decades several achievements were made to better understand the inflammatory, immune and tissue remodelling mechanisms in RA. With clear evidence that MSC are able to differentiate into cartilage similar to that in joint tissues, stem cell-based therapy has receiving extraordinary attention, raising an opportunity for therapeutic interventions via targeting intrinsic repair mechanisms [251].

Under physiological conditions, MSC in the joint are believed to contribute to the maintenance and repair of joint tissues. In addition, since MSC have the capacity to suppress effector cells and inflammatory responses, they can interact with immune cells and play an active role in reduction of inflammation. However, in RA, the repair function of MSC seems to be blocked by the inflammatory milieu, and it is important to realise that MSC and FLSs are

part of synovial membrane stroma. Since FLSs have an essential role in RA, it is important to consider MSC-FLSs interactions. MSC could perpetuate arthritis and progression of joint damage [251].

Gonzalez-Rey *et al* shows that human ASC are key regulators of immune tolerance, with a capacity to suppress T cell and inflammatory responses and to induce the generation/activation of antigen-specific regulatory T cells, in RA patients [250]. Another study suggested that UCX® cells (human umbilical cord tissue-derived mesenchymal stromal cells) may be an effective and promising new approach for treating both local and systemic manifestations of inflammatory arthritis [265]. Although, Papadopoulou *et al.* work shows that, *in vitro*, MSC inhibit FLSs but, *in vivo*, they are ineffective, unless MSC administration occurs before disease onset or inflammation being reduced [266].

It is imperative to better understand the relationship between MSC and other cells, especially FLSs, in RA patients, particularly if MSC will be considered as a treatment. It is generally agreed that MSC have immunosuppressive and immune-regulatory properties, however it is also known that they support unwanted growth in tumours and FLSs in RA. MSC can have beneficial or detrimental effects, depending on the situation [251].

3.1.5.3 Differences between MSC

Human ASC and BM-MSC present the same immunophenotype and both had tri-lineage potential (not performed during this project). It is known there are some differences between ASC and BM-MSC [267, 268]. For example, ASC have a poor chondrogenic and osteogenic differentiation capacity [98]. Also, other studies suggest that BM-MSC may be more effective for bone tissue replacement and septic shock, while ASC treatment is a more efficient cell therapy in immunomodulatory diseases [267, 269]. Nevertheless, both MSC and ASC have been proved to have immunosuppressive capacity [270, 271]. Then, since during joint destruction, it is known that pro-inflammatory cytokines (TNFα, IL-1β, IL-6, IL-15 and IL-17) and tissue-destructive enzymes are involved, MSC therapy seems a plausible option [252]. In OA, MSC are a possible treatment because of their chondrogenic capacity and longevity, and their anti-inflammatory capacity is an asset whereas in RA, it is their anti-inflammatory and immunomodulatory capacity that is important.

In this study, results show that ASC and BM-MSC are both able to immunosuppress monocyte TNF-α and IL-6 production in healthy individual (**Figure 3.4**), as well as in OA patients (**Figure 3.5**). In the presence of ASC and BM-MSC, the proportion of monocytes that express TNF-α is not very different. However, IL-6 expression was higher in presence of BM-MSC, when compared to ASC and TERT. Whether these results reflect differences in MSC

efficiency is an open question. However it does not seem to be source related, since TERT cells are from BM and had the same IL-6 expression than ASC.

Other interesting results is, in presence of ASC the three groups had more or less the same percentage of monocytes expressing TNF-α, while the healthy group had the higher percentage of monocytes expressing IL-6. Probably because LPS stimulated monocytes from patient samples take more time to produce IL-6.

Regarding MSC isolated from different donors, results obtaind (**Figure 3.8** and **Figure 3.9**) showed that BM-MSC and ASC do not present huge donor variability. Siegel *et al.* demonstrated that part of this donor-to-donor phenotypic variability among human BM-MSC was associated with donor age and gender [66]. Importantly, the inter-individual heterogeneity underlines the utility of MSC potency tests prior to their clinical application. Regarding the donor's age, it was found that younger and older donors possess MSC with different phenotypes, and younger donors form more colony-forming units-fibroblast (CFU-F) than older donors. However, the proliferation capacity of BM-MSC (and the cell size) were not correlated to donor age [66]. Different expression of these proteins may imply important differences in the immunosuppressive potential of MSC arising from different donors. A significant variability in the amounts of PGE2 secreted from human BM-MSC arising from different donors was also described [177]. It was also shown that BM-MSC isolated from different donors display distinct immunosuppressive potential over T cell proliferation and IFN-γ production. Interestingly, the immunosuppressive potential was correlated with IDO mRNA and protein expression levels [66, 272]. The donor variability is also visible in the ability of BM-MSC to support neural growth *in vivo*, which is associated with the different amounts of cytokines and growth factors that BM-MSC isolated from different donors produced and their potential to form CFU-F [66, 273]. Interestingly, donor variability was also visible in gender; BM-MSC from female donors have higher potential to form CFU-F than men [66]. In this study it was not possible to ascertain if gender or donor age influence the immunosuppressive capacity of MSC, however the potency of MSC from different passage numbers was investigated. Some reports say that MSC change their potency with passage number and in higher passages MSC are less efficient, less immunosuppressive [274, 275]. However, the results in this study were not conclusive. In general and as shown in **Figure 3.9**, no significant difference in the immunosuppressive potency of MSC from different donors in 3 consecutive passages was noted. However, **Figure 3.10** shows that two MSC donors in different passages have different immunosuppressive capacity, though further studies need to be done to assess if the results were a reflection of donor variability or passage number.

An interesting result was that MSC from a particular donor had different effects on blood taken from different donors (**Figure 3.11 B**). Taken together, these results suggest that particular combinations of MSC and donor blood will behave differently in these assay conditions.

In this study despite the low number of samples used, the results also show that using patient samples it is possible to quantify immunosuppression of pro-inflammatory cytokines, in the presence of MSC. The possibility of having off-the-shelf MSC to treat OA and RA it would allow a simple intervention, contributing to pain relief and decrease of inflammation. Besides MSC direct use to treat OA, other possible strategic can be also used, such as MSC condition medium where several soluble factors and exosomes have anti-inflammatory effect, or the use of scaffold with MSC ECM.

3.2 Immune responses to materials - Biocompatibility *in vitro* assay to assess biomaterials and natural compounds

3.2.1 Introduction

As referred in the beginning of the chapter, in this second part is shown the versatility of the whole blood assay. Different materials were tested using the whole blood assay, for this reason this chapter is further divided in two parts: biomaterials (scaffolds) and natural compounds (seaweed extracts).

3.2.1.1 Biomaterials

Regeneration of tissues and organs is one of the great challenges of clinical medicine, and science is constantly seeking better methods for tissue repair and replacement.

Tissue engineering has been an important and prominent tool in regenerative medicine. However the application of tissue engineering technologies in the clinical field has been rather restricted, since the number of biomaterials approved for human use is limited. In the last decade numerous excellent biomaterials have been developed, the problem is that translation into clinical practice has been slow [276].

Scaffolds represent important components for tissue engineering. Usually made of polymeric biomaterials, scaffolds provide a structural support for cell attachment, acting as a template for subsequent tissue development [277]. *In vitro* or *in vivo,* scaffolds provide mechanical support and shape to seed cells that proliferate and differentiate, creating new tissues or improving regeneration of the existing ones [276, 277]. In tissue engineering, a scaffold can be considered a substitute for ECM [278]. For these reasons, numerous efforts have been made to improve scaffolds, making them more similar to native ECM. However that is a huge task. ECM is a dynamic matrix that is constantly changing in composition and structure as tissues develop, remodel, repair and age [276].

Different scaffolds are composed of different biomaterials, such as poly-ε-caprolactone (PCL), polylatic acid or polylactide (PLA) and poly(lactide-co-glycolide) (PLGA) [279]. Natural biological polymers such as alginate, chitosan, collagen, laminin, elastin and fibronectin can also be used in combination with synthetic polymers to be more similar to native ECM [276]. These biomaterials are used due to their easy fabrication, suitable mechanical properties (polymers with a range of strengths and porosities can be made), tractable degradation kinetics and reasonable biodegradability [280]. Scaffolds of these synthetic and natural polymers have been extensively used to tissue engineer blood vessel, skin, cartilage and bone [276, 281].

However all biomaterials used in humans, medical devices or prostheses lead to a series of tissue responses when they are implanted, as well as by their presence in living tissue [279, 282]. Medical devices should not significant harm the patient or user, however some biomaterials create better environments for the cells than other materials, which is why it is important to evaluate the material's biocompatibility. Biocompatibility is the assessment of biological responses to the implantation and presence of scaffolds or medical devices. Biocompatibility tests pretend to predict whether a biomaterial, medical device or prosthesis presents potential harm to the patient or user, evaluating conditions that simulate clinical use [282].

Currently, biomaterials are tested firstly using *in vitro* assays for cytotoxicity, haemolysis, complement activation, PT/PTT testing and Ames test for mutagenicity and carcinogenicity, because these are fast and cheap tests. Only those biomaterials that had successful results in *in vitro* assays will be tested *in vivo*. Tests in animals provide a better pre-clinical condition, where toxicity, irritation, sensitization, implantation among others are tested. However, animal studies are time consuming and expensive. Cell cycle analysis, alkaline phosphatase assay and Alizarin red S staining are *in vitro* tests made to observe the effect of scaffolds, where the readout is cell cycle analysis and proliferation, as well as the measurement of calcium deposition [279]. The apatite-forming ability measured by simulated body fluid (SBF) test has been used as a predictor for *in vivo* bioactivity, however researchers have argued in favour and against this supposition [283]. Zadpoor *et al*. showned that the SBF immersion test has been quite successful in predicting the relative performance of biomaterials *in vivo*. However it is necessary to have two or more material to have a comparison, the results are expressed as relative performance of biomaterials and not their absolute performance [283].

The implementation of biomaterials/medical devices is a stressful event, where tissues or organs can be damaged. The injury and the perturbation of homeostatic mechanisms prime an immune response leading to the wound healing process. This response is dependent on multiple factors including the extent of injury, blood-material interactions, the loss of basement membrane structures, provisional matrix formation, the extent or degree of cellular necrosis and the extent of the inflammatory response. Ultimately, these events, may affect granulation tissue formation, foreign body reaction and the development of fibrosis and fibrous capsule [282, 284] (**Figure 3.12**).

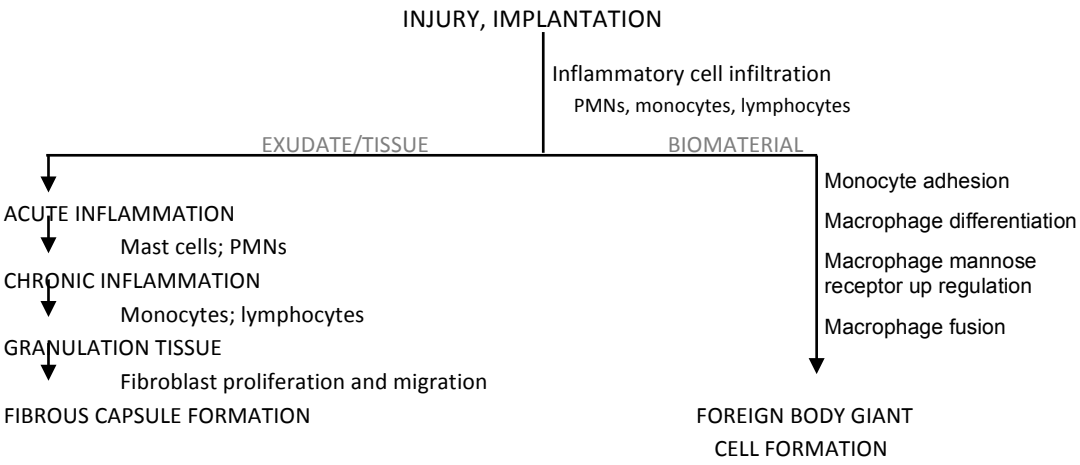

Figure 3.12 - Sequence of events following an implant of biomaterials/medical devices and following an injury [284].

The first event, after implementation/injury is blood-material interaction. Platelets and clot release chemoattractants like: platelet factor 4 (CXCL4), platelet-derived growth factor (PDGF), TGF-β, leukotriene (LTB4) and IL- 1 [284, 285]. When the macrophages assemble to the implant site, they adhere and release more chemoattractive factors: PDGF, TNF-α, IL-6, G-CSF, GM-CSF, MCP-1, among others; recruiting monocytes from the blood stream to the implant site, in the tissue, they can differentiate into macrophages and DCs [284, 286].

Development of provisional matrix at the implant site is also one of the early events happening after implementation of biomaterials/medical devices and blood-material interactions [282]. Provisional matrix consists of fibrin, produced by activation of coagulation and thrombosis systems, and inflammatory products, released by the complement system, activated platelets, inflammatory cells and endothelial cells [287]. Components within or released from the provisional matrix, initiate the resolution, reorganization, and repair processes leading to the recruitment of immune cells and fibroblasts. Activation of platelets and macrophages leads to the release of several chemotactic factors, contributing to the recruitment of monocyte and lymphocyte, and also their activation generates additional chemotactic factors, recruiting fibroblasts and other immune cells, initiating the healing process [282]. Monocyte and macrophage activation, followed by proliferation of fibroblasts and vascular endothelial cells to the implant site, leads to the formation of granulation tissue and wound healing, the hallmark of healing inflammation. In general, the wound healing response is dependent on the extent or degree of injury or defect created by the implantation procedure[282].

Regardless of the tissue or organ into which a biomaterial is implanted, there is an initial inflammatory response, a healing inflammation. When inflammation occurs but no cellular necrosis or loss of basement membrane structures has occurred, the wound healing occurs

normally. However, when necrosis occurs, inflammation increases [282]. Inflammation may be acute or chronic, depending on the nature of the stimulus and the effectiveness of the initial reaction in eliminating the stimulus or the damaged tissue. Acute inflammation is rapid and with short duration (hours or few days) whereas chronic inflammation may follow acute inflammation or may be the only inflammatory response seen in certain cases, such as in viral infections and hypersensitivity reactions, particularly if the cause of inflammation is persistent. Chronic inflammation takes a longer duration and is associated with the presence of lymphocytes and macrophages, proliferation of blood vessels, fibrosis and tissue destruction.

An inflammatory response is characterized by changes in the vascular flow. During acute inflammation anaphylatoxins, small immune-mediating molecules released at the inflammation site, stimulate mast cells to release histamine, serotonin and prostaglandins, which cause vasodilation, vascular tissues become more permeable, allowing fluid, proteins and different blood cells to migrate into affected tissue through the capillary wall (diapedesis) into the inflammation site [288]. In the site of inflammation plasma and immune cells get in contact with biomaterials, and although the injury initiates the inflammatory response, this can increase, and biomaterial degradation can occur. During inflammation, plasma, blood cells and injured tissue release important chemical mediators, like vasoactive agents, plasma proteases, lysosomal proteases, oxygen-derived free radicals, platelets activating factors, cytokines and growth factors, having an important role in biomaterials degradation [282]. Typically neutrophils are the first to be recruited during acute inflammation and are capable of eliminating pathogens by multiple mechanisms. Following neutrophils, monocytes are rapidly recruited to sites of injury and their migration may continue for days to weeks, depending on the injury and implanted biomaterial [286]. Neutrophils, macrophages and monocytes phagocyte microorganisms and foreign materials. Phagocytosis is a three-step process: recognition and attachment, engulfment and killing or degradation [289]. Regarding biomaterials, engulfment and degradation may or may not occur, depending on the properties of the biomaterial. Although, in general the biomaterials are not phagocytosed by neutrophils or macrophages because of the size disproportion, some events in phagocytosis can occur [282]. Phagocytosis is initiated by the ligation of cell-surface receptors that either directly bind to the particle or to opsonins that are deposited on the particle surface [290]. IgG and the complement-activated fragment C3b are the two major opsonins. Both of these plasma-derived proteins are known to adsorb biomaterials and both neutrophils and macrophages have corresponding cell membrane receptors for these opsonization proteins [291]. Since the biomaterials are bigger than the cells, the biomaterial can not be phagocytosed, however the cells can release enzymes by direct extrusion or exocytosis to the extracellular space, that can

lead to biomaterial degradation [282]. The amount of enzyme released during this process depends on the size of the polymer particle, suggesting that the specific mode of cell activation in the inflammatory response is dependent on the size of the implant. Other important factor is the fact that if the biomaterial is in a phagocytosable form (powder or particulate) can aggravate the degree of inflammatory response [282].

Persistent inflammatory stimuli lead to chronic inflammation. The physical and chemical properties of the biomaterials can lead to chronic inflammation, as well as the biomaterial implantation. However, little is known regarding to the role of lymphocytes and plasma cells during that event, cell-mediated immunity to synthetic biomaterials implantation is still an area where information is sparse.

When chronic inflammation does not occur, the natural end-stage of inflammatory responses and wound healing after implantation of medical devices, is the foreign body reaction composed by macrophages and foreign body giant cells [284]. Biomaterial surface adherent monocyte-derived macrophages fuse to form foreign body giant cells (**Figure 3.13**). IL-4 and IL-13 were found to up-regulate mannose receptors leading to the fusion of monocyte derived macrophages, however the exact molecular mechanisms that lead to macrophage fusion have not been fully elucidated [292].

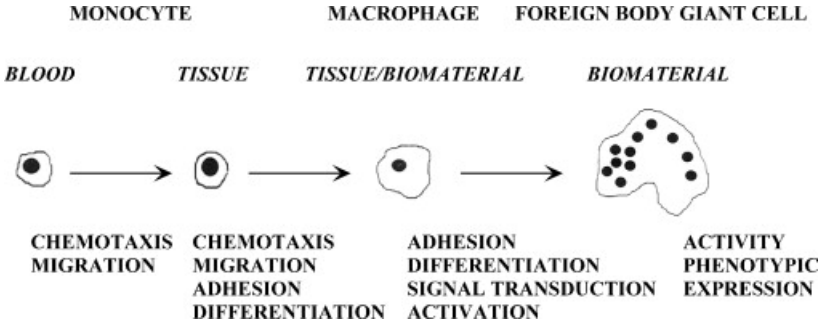

Figure 3.13 - Transition of blood stream monocytes to the implant site and macrophage differentiation and fusion into foreign body giant cells [284].

Adherent macrophages and foreign body giant cells in the foreign body reaction are now known to lead to degradation of biomaterials with subsequent clinical device failure. It is known that biomaterial surfaces in a privileged microenvironment for degradative agents, such macrophages phagolysosomes, making this materials susceptibility to biodegradation [284].

That is why the next phase in tissue engineering is the development of smart biomaterials and nanotechnology. Smart biomaterials will increase cell attachment, growth and differentiation, as well as reduce inflammation [276, 293]. This new and smart scaffolds can release several molecules, including drugs, that will bring multiple advantages, such as reducing inflammation [294]. Other emerging field in tissue engineering is nanomaterials

smaller than 100 nm that facilitate cellular uptake, delivering drugs, cells or cellular products [293].

3.2.1.2 Natural compounds

Seaweeds are marine macroalgae that generally live attached to rocks or other hard subtract in coastal areas. They are simple plant-like organisms that are organize in three types: green (around 1 500 species), brown (about 1 800 species) and red (around 6 200 species) [295, 296].

Green seaweeds (*Chlorophyta*) are green due to presence of chlorophyll *a* and *b*. These seaweeds normally live in freshwater and marine habitats, however some species also grow in soil, trees or rocks. The most commercial green seaweeds are *Dunaliella salina*, *Caulerpa* and *Chlorella* [296].

Brown seaweeds (*Phaeophyceae*) are the second most abundant group of seaweeds and the most used in clinical studies [297]. These seaweeds are mostly found in cold marine environment and normally they are large algae. The total commercial value of brown algae worldwide is about 300 million dollars [296].

Red seaweeds (*Rhodophyta*) are the biggest group of seaweeds. These algae are red because of the presence of phycoerythrin and phycocyanin pigments. The vast majority of these alga are marine and can be found in depths up to 40 or 250 meters. A very important group of red seaweeds is *Corallina*, the popular Nori (*Porphyra* species) and *Kappaphycus* and *Betaphycus* [296].

Currently there are 42 countries in the world with reports of commercial seaweed activity, being led by China followed by North Korea, South Korea, Japan, Philippines, Chile, Norway, Indonesia, USA and India. Around 90% seaweed production comes from culture practices and the most cultivated seaweed, with 60% of the total cultured production, is *Laminaria japonica*, however the most valuable is the algae Nori, used as food in Japan, China and Pacific [298, 299].

According to FAO (Food and Agriculture Organization of the United Nations) statistics, global production of seaweed increased from less than 4 million wet tonnes in 1980 to almost 20 million wet tonnes in 2010 [300]. Seaweeds have been used by humans in agriculture, as food and as compounds in medicine and cosmetic for several decades [297, 301].

An epidemiological study in 2007, showed that rich seaweed diets in Japan were associated with lower all-cause mortality and lower mortality from lung cancer, and pancreatic cancer in men and cerebrovascular disease in women [301]. In the Western diet, the direct

consumption of seaweeds is not common, though alga compounds can be consumed by ingestion of natural supplements.

Seaweeds have natural bioactive components include polyphenols, polysaccharides, polyunsaturated fatty acids, peptides, polyunsaturated fatty acids, pigments, plant growth hormones among other, and these active compounds lead to several biological effects [297, 302]. Seaweeds are rich in sulfated polysaccharides that have anticoagulant and antithrombotic action. Other important effect is the anti-proliferative and antitumor activity, since seaweeds contain fucoidans, a sulfated polysaccharide. Teruya *et al.* showed that sulfated fucoidan has anti-proliferative properties [303]. While, Heneji *et al.* reported that fucoidan extracted from *Cladosiphon okamuranus* induces apoptosis of human primary adult T cell leukemia, indicating that fucoidan can be a potential therapeutic agent for patients with T cell leukemia [304]. Another study shows that fucose extracted from *Ecklonia cava* has antiproliferative effects on human promyelocytic leukemia, human leukemic monocyte lymphoma, murine colon carcinoma and mouse melanoma [305]. Seaweed extracts also have immunomodulatory properties, some studies show that oligosaccharides have a variety of effects on the immune system, inhibiting cancer metastasis, complement activation, antitumor activity and probably are effective candidates for tumour immunotherapy [306]. Fucoidan also has immunomodulatory effects on dendritic cells, fucoidan has immunestimulatory and maturation effect on bone marrow derived dendritic cells [307]. Another important property is the anti-inflammatory activity of seaweed extracts. Kang *et al.* used LPS stimulated monocytic mouse cell line RAW 264.7 to observe the anti-inflammatory property of purified polysaccharides from brown seaweed [308].

As described previously in the first part of this chapter, there are several drugs available to reduce inflammation, however they provoke undesirable side effects, such as gastrointestinal irritation. For this reason the rheumatic and arthritic patients combine these drugs with natural compounds or even search for alternative and more natural anti-inflammatory medicines and drugs [309]. Moreover, the medicines are expensive and are an unbearable cost to several patient families worldwide. Natural compounds from several plants and seaweeds have proven pharmacological activity [308, 309]. For these reasons seaweed extracts are very important compounds to be considered as therapy in several clinical conditions.

The majority of the studies that looked into the beneficial properties of seaweed extracts, used time consuming and not efficient methods. These studies include culture of seaweed extracts with cell lines and the results obtained were readouts of Western blots, ELISA, proliferation and viability assays, etc. Therefore, clinical research needs a fast assay that

can measure the seaweed extracts' properties on human primary cells. There is a need of efficient analytical tools that can measure the seaweed extract properties, yet there are significant technical challenges to overcome. The technique must be able to quantify effects of seaweed extracts, or even to be able to characterize microalgae in size and lipid content, with the challenge of chlorophyll autofluorescence [310]. Sample analysis must attain high throughput without sacrificing data quality and flow cytometry assays can give powerful and quantitative results. For this reason the whole blood assay applied to seaweed extract to measure their effects seems a fast, efficient and quantifiable method.

3.2.2 Objectives

The main aim of this chapter was to test if the rapid and quantifiable flow cytometry-based whole-blood assay can be used to assess the properties of materials.

Scaffolds composed of ECM are rapidly degraded and are associated with constructive tissue remodelling and minimal fibrosis [311]. For this reason the first aim was to test if the whole blood assay can be used to assess the biocompatibility of PCL scaffold in the presence or absence of different ECM. In addition, the test was used to see if the biocompatibility of the different biomaterials used in scaffolds could be compared.

The second aim was to test if the whole blood assay was able to measure the immunosuppressive capacities of seaweed extracts, natural compounds.

Summary of aims:

- To test if the whole blood assay could be used to assess the biocompatibility of scaffold, with and without ECM;
- To test if the whole blood assay could be used to measure the immunosuppressive capacities of natural compounds.

3.2.3 Methods

Details regarding reagents, solutions, antibodies and material are describe in Annexes F to J.

3.2.3.1 Biomaterials

3.2.3.1.1 Scaffold and ECM

In 24 well plate the scaffold (PCL) was placed and fixed with a silicon O-ring. The material was endotoxin free. In a hood the wells with material were sterilized for 24 hours with 70% ethanol at 4°C, washed repeatedly with sterile DPBS and was left overnight in UV light. Then the wells were coated with 500 μL of 0.1% gelatine and left overnight at room temperature. Gelatine was removed and dried for 1 hour at 37°C. Three different ECM were prepared: 1) by cloned mouse mesenchymal stromal cell line - mMSC (MS5); 2) using neonatal human foreskin fibroblasts in P_{20} – hFB and 3) using a human BM-MSC immortalize cells in P_3 transduce with a iCasp9 vector - hMSC (methodology explained further in chapter 5) provided by Professor Ivan Martin. After a few days following thawing, cells were trypsinized, neutralized, counted and $5x10^5$ hFB and mMSC were seeded per well, while were seeded $6x10^4$ hMSC per well. Following 3 days in culture at 37°C in a humidified incubator containing 5% CO_2 and 21% O_2 in air, cells were treated with 10 μg/mL of Mitomycin C for 3 hours at 37°C. Then, cells were washed twice with DPBS and fresh complete medium was placed in the wells. The cells were kept in culture for more 4 days, after that hFB and mMSC were lysed with a Tris/EDTA buffer overnight at 4°C while it was induced apoptosis in hMSC with 1 nM B/B homodimerizer overnight at 37°. Cell debris were washed with DPBS and ECM with and without PCL were kept with DPBS at 4°C until assay was performed. **Figure 3.14** describes the plate design.

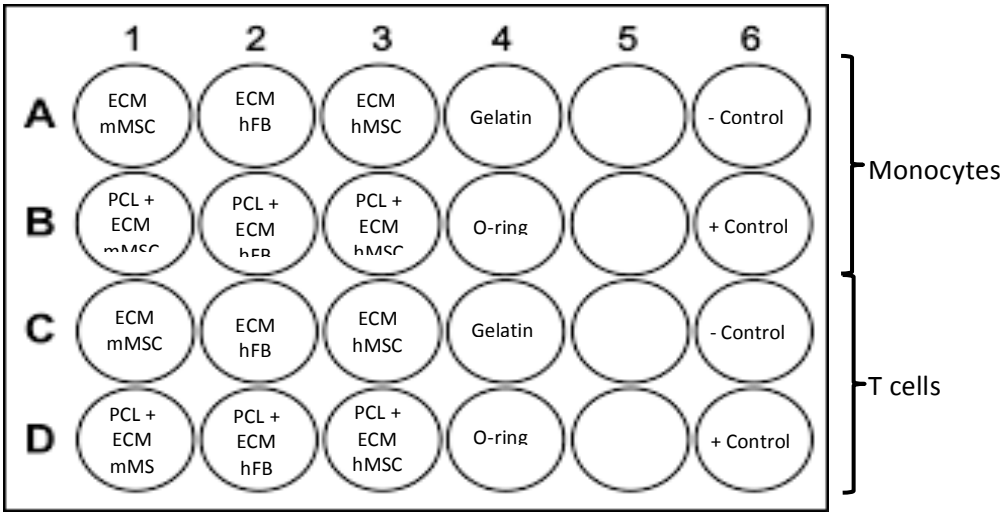

Figure 3.14 - Plate design for each blood donor.

3.2.3.1.2 Scaffold with or without ECM and whole blood assay

Following plate preparation with scaffold and different ECM, peripheral blood from 4 healthy adult volunteers ranging in age from 26-65 years was collected into BD Vacutainer sodium heparin tubes, according to the protocol approved by the ethics committee of the National University of Ireland in Galway. Once collected, blood was used within few hours being kept at room temperature.

For each blood sample, in a Falcon tube, was added RPMI, 0.6 μg/mL Brefeldin A and whole blood at 10 fold dilution. The preparation was mixed and 2 mL was placed into each well, except the "+ Controls". To the monocyte "+ Control" was also added 1 ng/mL of ultrapure LPS-EB, while to the T cell "+ Control" was added 1 μg/mL of Ionomycin and 10 ng/mL of PMA. An average of 30 000 monocytes, 100 μL of peripheral blood, was added to each well. The plates were covered and placed in the incubator at 37°C in a humidified incubator containing 5% CO_2 and 21% O_2 in air for 6 hours. After incubation the samples were transferred to a 96 deep well plate to perform cell staining to identify monocytes and T cells. To the monocytes wells was added CD45 PerCp Cy5.5 and CD14 APC, while in the T cells wells was added CD3 FITC, CD8α PE Cy7 and CD4 APC. Cells were incubated for 10 minutes at room temperature in the dark. Following surface staining cells were fixed using reagent 1 from Beckman Coulter IntraPrep Kit. The cells were incubated again for 10 minutes at room temperature in the dark. Then, cells were washed and permeabilized using reagent 2 from Beckman Coulter IntraPrep Kit. Cells were stained intra-cytoplasmically with anti-TNF-α PE. Following another 10 minutes incubation at room temperature in the dark samples were washed twice, resuspended in FACS buffer and acquired by the BD Accuri C6 (Becton Dickinson) 4 colour flow cytometer. Data were analysed with flow cytometry software BD CSample Analysis software (Becton Dickinson).

3.2.3.1.3 Scaffolds and whole blood assay

In this experiment four biomaterials were tested and compared: elesctrospun PCL (Polycaprolactone espun with an average fibre diameter 2-3 μm in NFB; NUIGalway by Kieran Fuller), expanded polytetrafluoroethlyene (ePTFE) (from Proxy Biomedical), polypropylene (PP) (from Ethicon) and BioWed (from Zeus). The material was endotoxin free. In a hood the material was cut small pieces (1 x 1 cm) and were sterilized for 24 hours with 70% ethanol at 4°C, washed repeatedly with sterile DPBS and was left overnight in UV light.

Peripheral blood from 2 healthy adult volunteers ranging in age from 26-31 years was collected as described above. In sterile cytometer tubes was added RPMI, 0.6 μg/mL Brefeldin A and whole blood at 10 fold dilution, were added in average $3x10^4$ monocytes to each tube.

Different scaffold were placed in suspension into each tube. To the negative control no scaffold was added and to the monocyte positive control 1 ng/mL of ultrapure LPS-EB, while to the T cell positive control was added 1 μg/mL of Ionomycin and 10 ng/mL of PMA. Tubes were sealed with parafilm and incubated for 6 hours at 37°C in a humidified incubator containing 5% CO_2 and 21% O_2 in air. After incubation the samples were stained, acquired and analysed as describe above.

3.2.3.2 Natural compounds

3.2.3.2.1 Seaweed extracts

In total, 12 seaweed extracts were tested, 6 were from green algae (seaweed A-F) and 6 from brown (seaweed G-L). The species were not scientifically identified. The marine compounds were obtained and processed by the Chemistry Department of NUIG and provided to REMEDI in powder with a known weight.

To the partition for natural extracts was used the Kupchan method. Briefly, the samples were added into a separation funnel containing Hexane and 10% H_2O in Methanol (1:1) and shaken for 3 minutes. The Hexane phase was drained into a 0.5 L round bottom flask. This step was repeated twice. Hexane phases were then mix and evaporated on the Heldolp rotary evaporators. Afterwards, the percentage of H_2O was increased up to 35%, with Chloroform (1:1) and the funnel was shaken for 3 minutes. This step was also repeated twice. Chloroform phases were mix and evaporated, so as the aqueous phase.

All extracted were resuspended in DMSO (100%) to achieve 10 mg/mL. The samples were then diluted to 500 μg/mL using DPBS, giving a concentration of 5% DMSO. To each assay/well as added 50 μL of each seaweed extract in a final volume of 500 μL, meaning that the final concentration of each extract was 50 μg/mL, giving a final concentration of 0.5 % DMSO.

3.2.3.2.2 Monocyte whole blood assay with seaweed extracts

Peripheral blood from 2 healthy adult volunteers ranging in age from 27-50 years was collected as described above. In 96 deep well plate was added RPMI, 0.6 μg/mL Brefeldin A, heparinized whole blood at 10 fold dilution and 50 μg/mL seaweed extracts to the control samples. To the test samples was also added 2ng/mL of ultrapure LPS-EB. An average of $7.5x10^3$ monocytes were added to each well. The plates were sealed and placed in the incubator at 37°C in a humidified incubator containing 5% CO_2 and 21% O_2 in air for 8 hours. Following incubation the cells were stained as described above.

This part of the project it was performed by Alexandra Buchholz, a Master student, under supervision of Professor Deniz Tasdemir (Chemistry Department) and Professor Thomas Ritter (REMEDI).

3.2.3.3 Statistical analysis

Results are expressed as average and standard deviation of percentage of monocytes or T cells that produced TNF-α. To determine the statistical significance of the differences observed between different conditions, two-way ANOVA (95% confidence intervals), multiple comparisons were performed, using GraphPad Prism software. Statistically significance differences were considered * when P-value was lower than 0.05, ** when P-value was lower than 0.01, *** when P-value was lower than 0.001 and **** when P-value was lower than 0.0001.

3.2.4 Results

3.2.4.1 Biomaterials

3.2.4.1.1 Scaffold with or without ECM and whole blood assay

The biocompatibility of PCL in the presence or absence of different ECM were analysed by observing the intracellular expression of the pro-inflammatory cytokine TNF-α, produced by monocytes and T cells. Monocytes in the presence of PCL alone were not very activated, less than 15% of monocytes expressed TNF-α (**Figure 3.15**). Observing the three ECM, the human Fibroblasts ECM is the least inflammatory, however in the presence of PCL, there were some samples where the percentage of monocytes expressing TNF-α increased considerably. This effect was more evident in the presence of ECM prepared with the human MSC cell line.

In this experiment, two additional controls were added: gelatine and O-ring. These controls were used because ECM is prepared on top of gelatine and the PCL was fixed with an O-ring. It is clear that the gelatine alone had an effect on monocytes, the percentage of monocytes that express TNF-α was significantly higher than the negative controls. While in the presence of the O-ring alone, TNF-α expression was similar to that of PCL alone.

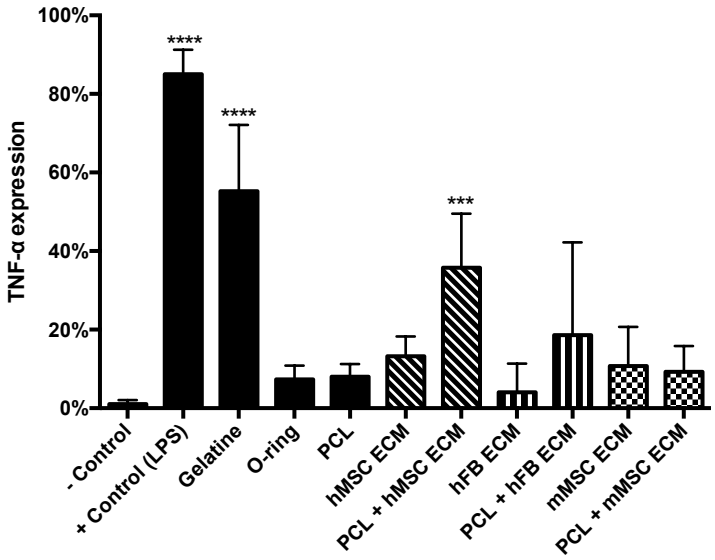

Figure 3.15 - Monocyte TNF-α expression in presence of PCL with or without different ECM. The graph shows the percentage of monocytes that express TNF-α after 6 h in culture in presence or absence of PCL with or without ECM produced by human MSC cell line, human Fibroblasts or a mouse MSC cell line (n=4). All the conditions were tested in absence of LPS except the "+ Control". All the statistic differences are compared with "- Control". Two-way ANOVA * P<0.05, ** P<0.01, *** P<0.001 and **** P<0.0001.

Figure 3.16 shows the same experiment described above however, the readout was TNF-α expression by $CD4^+$ and $CD8^+$ T cells. In this case no T cells expressed TNF-α after 6

hours in culture with PCL in presence or absence of different ECM. The positive controls showed that both T cells subpopulations were potentially responsive.

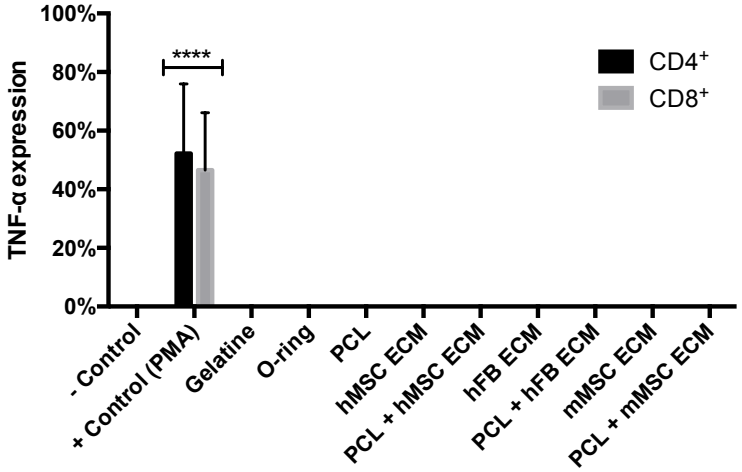

Figure 3.16 - $CD4^+$ and $CD8^+$ T cells TNF-α expression in presence of PCL with or without different ECM. The graph shows the percentage of T cells that express TNF-α after 6 h in culture in presence or absence of PCL with or without ECM produced by human MSC cell line, human fibroblasts or a mouse MSC cell line (n=4). All the conditions were tested in absence of PMA except the "+ Control". All the statistic differences are compared with "- Control". Two-way ANOVA * P<0.05, ** P<0.01, *** P<0.001 and **** P<0.0001.

3.2.4.1.2 Scaffolds and whole blood assay

Regarding the effect of four different scaffolds on monocytes, the results are very clear, PCL ePTFE and BioWed led to less than 5% of monocytes expressing TNF-α, whereas addition of PP induced 15% more monocytes to express TNF-α (**Figure 3.17**). In this experiment one additional control was added, namely "film". The film is the solvent casted PCL. It is important to note that these results were the reflection of the effect of different scaffolds suspended in the whole blood culture.

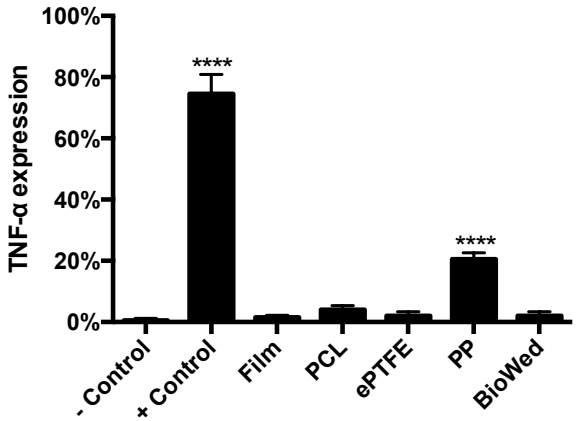

Figure 3.17 - Monocyte TNF-α expression in presence of different scaffolds. The graph shows the percentage of monocytes that express TNF-α after 6 h in culture in presence PCL, ePTFE, PP and BioWed (n=2). All the statistic differences are compared with "- Control". Two-way ANOVA * P<0.05, ** P<0.01, *** P<0.001 and **** P<0.0001.

Regarding the T cell response to the presence of these biomaterials, the results were also very clear. There were no $CD4^+$ and $CD8^+$ T cells expressing TNF-α after 6 hours in culture with different scaffold (data not shown).

3.2.4.2 Seaweed extracts

Regarding the immunosuppressive capacity of seaweed extracts, there were differences in the compounds extracted from green and brown algae, as well as differences between different green and brown extracts. **Figure 3.18** shows that different green seaweed extracts led to different results. In the control samples, where monocytes were cultured in the presence of seaweed extracts A, D, E and F, without LPS, the producing TNF-α was seen, particularly with seaweed extract D. In the test samples, where LPS was added, addition of seaweed extracts resulted in reduced TNF-α production with extracts E and F being the most effective.

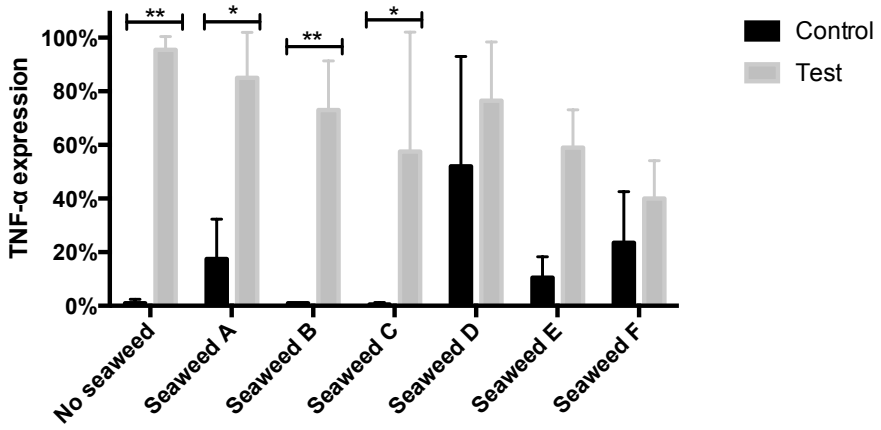

Figure 3.18 - Percentage of monocytes that express TNF-α in presence of different compounds extracted from green seaweeds. Controls samples do not have LPS present while test samples have 2 ng/mL LPS. Whole blood was cultured for 8 h in presence of six green seaweed species (n=2). All the statistic differences reflect the comparison between control and test. Two-way ANOVA * P<0.05, ** P<0.01, *** P<0.001 and **** P<0.0001.

Brown seaweed extracts seem to be more efficient at reducing TNF-α expression and generating less undesirable effects on monocytes (**Figure 3.19**).

Comparing test conditions seaweed I, K and L were significantly more immunosuppressive than the other extracts. Seaweed J was the one that lead to more activated monocytes in absence of LPS.

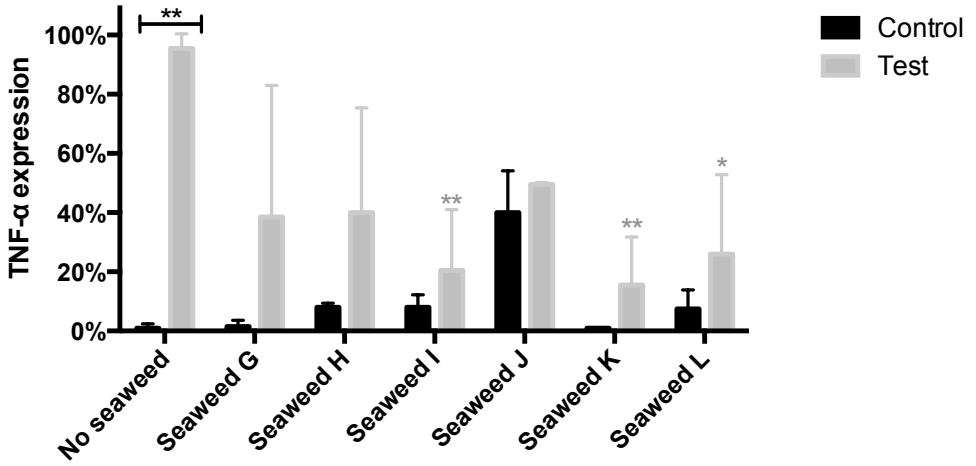

Figure 3.19 - Percentage of monocytes that express TNF-α in presence of different compounds extracted from brown seaweeds. Controls samples do not have LPS present while test samples have 2 ng/mL LPS. Whole blood was cultured for 8 h in presence of six brown seaweed species (n=2). The statistic differences in black reflect the comparison between control and test using the same compound, while grey reflects the statistic differences between seaweed tests with no seaweed test. Two-way ANOVA * P<0.05, ** P<0.01, *** P<0.001 and **** P<0.0001.

3.2.5 Discussion

3.2.5.1 Biomaterials

Scaffolds can be composed of several biomaterials, either as one synthetic polymer alone or as combinations of synthetic and natural polymers, and there are several *in vitro* tests to evaluate their biocompatibility. However the readout of these assays is not good enough from an immunologic point of view, since only cell lines were used. Cell lines are not as sensitive as primary cells; a study were THP-1 cells were compared with peripheral blood monocytes shown exactly that monocytes need less stimuli [312]. Also cell/death and proliferation assays are not enough. For these reasons it is important to have a rapid and quantifiable way of measuring the inflammatory potential of biomaterials on immune cells. This fact is even more import for biotechnology companies, where they want to know in a fast and efficient way if the materials they are producing is good enough to pass to the next stage of production.

The results presented above are very clear; 6 hours is enough to observe the biomaterial effect on monocytes but not on T cells. A possible future experiment it would be to incubate the biomaterials for a longer period of time and observe the percentage of T cells expressing TNF-α, to better understand if T cells need more time or if no TNF-α is expressed at all. Probably, even if the T cells were incubated for a longer period of time, they would not express TNF-α, since T cells need specific receptor recognition to be activated.

PCL did not seem to be a potent activator of monocytes, however in the presence of hMSC ECM and hFB ECM, a higher percentage of monocytes were expressing TNF-α. Possibly, there is an additive effect of having PCL together with ECM, while these two components alone did not have any stimulatory activity.

Gelatine from bovine skin was added to all wells in order to help attachment of ECM proteins. The gelatine control cultured activated about 60 % of the monocytes, but this effect was reduced when ECM was present in the well, presumably because the gelatine was masked by the added ECM. One possible explanation was that the gelatine preparations contained endotoxins.

Finally it was not clear if TNF-α expression by monocytes in the PCL conditions was due to the O-ring present. In cultures containing the O-ring alone, around 5% of monocytes expressed TNF-α. For this reason subsequent experiments were designed to have the scaffolds in suspension.

In the following experiment the aim was to compare different biomaterials in suspension in peripheral blood. Once again, after 6 hours, T cells did not express TNF-α while

monocyte assay worked very well. First of all is possible to observe that PCL in suspension led to a lower percentage of monocytes expressing TNF-α (< 5%) when compared with PCL fix to the well with O-ring (around 10%). These results can be explained by the possible contamination of the O-ring with endotoxin, probably the O-ring was not efficiently sterilized.

PCL is a biodegradable polymer proposed to be used in multiple applications: as drug delivery carriers, scaffolds for growing fibroblasts and osteoblasts and grafts for skin tissue [279].

ePTFE is a versatile polymer known for its strength, chemical inertness, biocompatibility among other characteristics. This polymer is used in cardiac patching and to create blood vessels [313, 314].

Polypropylene (PP) is commonly used in medicine in sutures, and it has been also used in hernias and pelvic organ prolapse repair to protect the body from new hernias in the same location [315]. However, Food and Drug Administration (FDA) released a communication warning about the use of PP mesh kits in pelvic organ prolapse interventions informing that this material leads to tissue erosion [316].

BioWed is composed of PTFE and actually there are no biological data, however animal tests and clinical trials are being conducted by the company, which is currently working on this material for a specific cardiac related application.

Using the whole blood assay it is possible to compare the above biomaterials. Anderson *et al*. also develop a human monocyte culture system [317]. However, this assay has several limitations comparing with the whole blood assay. First of all, a whole blood assay is more relevant physiologically, since different interactions between the different blood cells (platelets, MNC, neutrophils and eosinophils) and the molecules they produce is being measured. In the study of Anderson *et al.* only the presence of monocytes and lymphocytes (MNC) are being considered [282]. Second, it takes between 3 to 10 days to culture the monocytes with biomaterials. Third, the readout is cytokine production measured by ELISA, so they cannot determine how much each responding cell produces. Nevertheless, a very positive point is that they are able to measure 77 cytokines/chemokine, while possible some of them are not detectable by flow cytometry for technical reasons.

Therefore, the whole blood assay can be used in combination with other tests to assess the biocompatibility of biomaterials. One other test that could be made is monocyte phagocytosis assay using flow cytometry, especially to study the biocompatibility of nanoparticles that is becoming an area of increasing importance.

3.2.5.2 Seaweed extracts

Extracts from natural marine compounds have been shown to have a range of immune-modulating, anti-proliferative, antitumor, antipyretic, analgesic and anti-inflammatory effects [297, 301, 318].

The immunosuppressive and anti-inflammatory properties of seaweed extracts collected from green and brown algae were assessed, and differences between the two groups were found.

Brown seaweed extracts seem to present better immunosuppressive capacity. In general more species led to a reduction of monocytes that express TNF-α, when compared with green seaweed extract. Also brown seaweed extracts are less stimulatory to monocytes.

There are more clinical proven studies using seaweed extracts collected from brown algae [302, 319]. Also, it is known that the composition of extracts strongly depends on the raw material (geographical location of harvested algae and algal species) as well as on the extraction method [302].

Overall, results show that seaweed extract B and K are probably the best compounds, since they did not activate monocytes alone but nevertheless reduced TNF-α expression by activated monocytes. However, it is important that more experiments should be done to confirm these preliminary results.

Another limitation of these experiments was that the compounds were not totally dissolved in DMSO as there was still a residue present in the preparations. Therefore, the actual concentrations of product could not be accurately determined. Finally, the seaweed extracts used contained chlorophyll pigments that have significant autofluorescent properties that make compensation adjustments to the flow cytometer very difficult.

Chapter 4 | Overall Discussion – whole blood assay

4.1 Overall discussion

A potency assay is designed to generate data indicating whether a product will be potent or not [320, 321]. Such assays have been used for decades in the pharmaceutical industry. However, it is not easy to develop a potency assay when cell-based therapies are concerned, since each cellular therapy product has individual characteristics and developing a potency assay for each product is a very time consuming and expensive task.

There are two main agencies that regulate cellular and gene therapy product: the US FDA and the European Medicine Agency (EMA). Potency, according to the FDA is the therapeutic activity of a drug. For the EMA, potency is the "quantitative measure of biological activity based on the attribute of the product, which is linked to the relevant biological properties" [322]. The potency assays should prove that a product has individual biologic activity.

It is known that MSC, MSC products, scaffolds and natural compounds bring beneficial properties to different patients with different conditions. Nevertheless there is a transversal problem. How to test the potency of these products?

Chapter 2 described a method whereby the immunosuppressive potency of BM-MSC could be measured in a dose dependent manner. This was dependent on being able to observe the reduction of intracellular expression of the anti-inflammatory cytokine TNF-α in LPS activated monocytes upon addition of BM-MSC. For this, a whole blood assay was developed where different cell types, in this case monocytes or T cells, could be identified by surface marker analysis and expression of cytokine determined by simultaneous intra-cytoplasmic stating for the corresponding protein. Chapter 3 validated the monocyte whole blood assay, proving that MSC derived from bone marrow or adipose tissue could immunosuppress LPS activated monocytes from OA and RA patients. With these two chapters it was possible to conclude that a rapid, reliable and quantifiable assay to measure MSC potency had been developed. In the second part of Chapter 3 was shown two possible additional uses of the whole blood assay, demonstrating that it was possible to i) quantify the response of monocytes or lymphocytes to a scaffold made from synthetic or natural polymers and ii) to screen different natural compounds (seaweed extracts) for immune-suppressive activities.

It goes without saying that the isolation, manufacture and characterization of cell-based products should be standardized. However, more important than that, is the need to develop a robust, reproducible and economic potency assay that can measure the efficiency/potency of each cell-based product before its administration to patients [178, 183, 322].

In vitro studies rely on the possibility to manipulate the variables in order to better understand the function and mechanisms of MSC. MSC co-cultured with purified immune cells

is usually used to determine if the MSC have a direct or paracrine effects on other cells. Neutralization of specific molecules is a simple and good methodology to better understand the contribution of distinct molecules. However, these assays cannot mimic all the complexity that occurs *in vivo*, especially because MSC are sensitive to the microenvironment. MSC are influenced by the presence of other cells, by the presence of cytokines, and by PAMP. The environment from where the MSC were isolated is especially important. In general, most clinical studies have used autologous MSC infusion and in cases where the MSC come from diseased patients, they may already be primed towards a pro-inflammatory MSC_1 type. For this reason it is important to test in a whole blood assay if the MSC have the immunosuppressive capacity on the patient's own blood.

During this study it was also possible to determine if healthy MSC used were polarized towards pro-inflammatory (MSC_1, TLR4-primed) or immunosuppressive (MSC_2), using the whole blood assay [82]. Results showed that MSC did not detectably bind to LPS (**Figure 2.27**) and were not spontaneously expressing TNF-α, demonstrating that the MSC were type 2, immunosuppressive (Annex A).

Economically speaking, the whole blood assay is not expensive. Each whole blood test to assess MSC potency costs around €100, while to assess biomaterials and natural compounds it costs around €40 per test.

The whole blood assay was also tested using a Perkin-Elmer JANUS automated workstation. However, because of the necessity of providing additional consumables, carrying out the assay in this way was more expensive and more time consuming than performing it manually. However, it could be shown that the assay could be performed semi-automatically.

An important feature of potency assays is controls and controlled conditions. For the whole blood assay, flow cytometry was chosen for the readout, because it is a fast, powerful and effective method, allowing the measurement of several cellular properties in a quantifiable way. In the majority of the experiment an Accuri C6 four colour flow cytometer equipped with a 96 well plate reader was used because it is a fast, reliable cytometer with little use of consumables. However, if equipped with a plate reader, analysis could also be performed on a BD Canto II, a commonly used cytometer in the clinic, and where standard quality control can be applied. Additionally, it is possible to measure different cytokines and chemokines simultaneously using the flow cytometry based whole blood assay. Besides, all products used in the whole blood assay are commercially available and are used for clinical proposes, therefore they are well characterized.

Another important control was the use of a "universal MSC cell ruler", concept defined by Dr. Mahendra Rao from the National Institutes of Health (USA), at the MSC 2013

conference, where standardization and nomenclature of MSC were debated [322, 323]. Two negative (MM and Jurkat cell lines) and two positive controls (Dexamethasone and TERT cells) were used for the whole blood assay. Multiple myeloma (MM) and Jurkat T cell are two human cell lines that do not have immunosuppressive capacity. MM cell line arose from malignant plasma cells whereas Jurkat is a cell line that arose from leukaemia T cell. Dexamethasone is a synthetic corticosteroid used to reduce inflammation, by preventing the release of pro-inflammatory cytokines. TERT is a telomerase reverse transcriptase (TERT) immortalized cell line that arose from human BM-MSC that gives constant immunosuppressive results. TERT cells are a strong possibility to be a "universal MSC cell ruler". These controls can be included even in assays to measure the immunosuppressive capacity of synthetic and natural compounds that present immunosuppressive properties.

Different patients react differently to cell-based therapies or even need different numbers of cells [324, 325]. Each individual has a different optimal dosing. Vaes *et al*. observed that the dose-response is not consistent [325]. With the whole blood assay it is possible to calculate if a patient will need more or less than the optimized dose.

A significant part of developing the potency assay was to investigate the mechanism whereby MSC inhibited LPS activated monocytes. However, the MSC-immune cell relationship is a very complex interaction that is still not fully characterized, making it harder to identify the exact mechanism of immunosuppression [322]. Ultimately, it is probably the combination of MSC-immune cell interactions and MSC paracrine factors that leads to the immunosuppressive effect [112]. Moreover, it is not just one soluble immune-regulatory factor that contributes to these effects, probably it is the combination of several molecules (PGE2, IDO, HGF, exosomes, etc).

Several attempts have been made to develop a potency assay to measure the immunomodulatory properties of MSC. However the majority of the studies use PBMC cultures instead of peripheral whole blood. This is an important fact since whole blood is a more realistic and physiologic culture method, comparing with PBMC. As has been previously discussed, in the whole blood assay, the interaction between many different blood cell types (platelets, MNC, neutrophils and eosinophils) and the molecules produced by them is being measured. In contrast, in assays involving PBMC only monocytes and lymphocytes (MNC) are present, the other cell types having been separated and discarded.

In this project it was also possible to observe that monocytes and T cells have different responses to MSC. It is well known that MSC can immunosuppress T cells in the classic mixed lymphocyte reaction assay, where the culture takes long periods of time (more than 24 hours).

Although in Chapter 2 it was demonstrated that T cells can be activated, but 24 hours co-culture is not enough to observe the MSC immunosuppressive effect.

Nonetheless, one group used a different approach, instead of developing a test to characterize the potency of stem cells, they create a MultiStem® product. MultiStem is a stem cell product derived from mononuclear bone marrow that are depleted of $CD45^+$/glycophorin-A^+ cells, which has proven benefits in treating several conditions. The product has completed Phase I trial to treat acute myocardial infarction and GvHD and is in Phase II clinical studies for the treatment of ischemic stroke and ulcerative colitis [325].

4.2 Conclusion

In conclusion, a rapid, reliable and quantifiable assay to determinate the effects of MSC on LPS activated monocytes was developed. This assay can also be used to screen synthetic and natural compounds. Such an assay contributes to personalized medicine.

Chapter 5 | Comparison of two ECM preparation methods and their effect on Mesenchymal Stromal Cell differentiation

5.1 Introduction

5.1.1 ECM and the haematopoietic niche

The haematopoietic niche is a unique microenvironment that regulates the self-renewal and differentiation of HSC, giving rise to blood cells. During haematopoiesis, different cells, especially HSC, receive signals such as cytokines and growth factors from other cells (mesenchymal stromal cells, osteoblasts, fibroblasts, adipocytes, vascular endothelial cells) and from the extracellular matrices that they produce, especially that from stromal cells [11, 63, 326, 327]. Defining niche components and how they regulate haematopoiesis offers the possibility to better understand regeneration following injury or HSC transplantation [328]. ECM in addition to maintaining the structural integrity of tissues, also has physiologic functions, such as passing nutrients to the cells, acting as a reservoir of mediators and intervening in cellular functions through interaction with cell surface receptors [63]. For this reason the ECM, in a disordered niche, contributes to diseases and can influence the efficiency of therapy [328, 329]. It is also known that MSC play a role in haematopoiesis and that ECM has an effect on MSC and HSC. Moreover, although there is increasing evidence regarding the role of growth factors and cytokines as inducers and mediators of stem cell differentiation, little is known regarding the influence of ECM on cell differentiation [63]. Therefore, it is important to clarify the role of ECM in stem cell differentiation or in maintaining their stem cell capacity.

The ECM is a complex structure composed of different types of proteins, polysaccharides, growth factors and cell adhesion molecules [11, 330]. ECM acts as a medium of extracellular communication through CAMs [331]. ECM also has an important role in cell adhesion, survival and proliferation, not only because of integrins but because it gives a stable support for cells. ECM produced *in vitro* mimics the tethering of growth factors of a substrate, which can enhance cell viability [330]. Adhesion of stem cells to matrices, or other cells, is essential for their survival. Thus most cells (mature blood cells being one exception) need to be attached because, in general, they do not survive in suspension. For this reason cells have to be cultured on top of materials, such as Matrigel or in 3D systems, that improve their proliferation and survival [330].

Integrins are the major family of ECM receptors that allows the transit of information between matrices and cells, thereby playing an important role in regulation of cell adhesion, survival, proliferation, differentiation and matrix remodelling [63]. Several studies suggest that integrins have the capacity to regulate *in vitro* osteogenic differentiation [332].

ECM provides mechanical support and is a biochemical barrier. ECM is mainly composed of structural proteins such as collagens, elastin, glycoproteins such as fibronectin and the

basement membrane constituent laminins. These components contribute to the organization and mechanical support of the matrix and also help in cell attachment. ECM is also composed of proteoglycans, specialized glycoproteins that carry GAGs, important in cell signalling due to their localization on the cell membrane and in the ECM. ECMs also have MMPs, which hydrolyse ECM components; these proteinases play a central role in many biological processes, such as embryogenesis, normal tissue remodelling, wound healing and others processes [11, 33, 333].

Another important factor that has to be taking into account in the haematopoietic niche is the gradient of oxygen concentration. Oxygen is an important biochemical signalling molecule and plays a key role in regulating a broad range of cellular events in normal and pathological conditions [334]. It has been suggested that the haematopoietic niche is hypoxic, and hypoxia seems to maintain stem cell characteristic for longer and increases cell proliferation and colony forming potential. Hypoxia also promotes a more homogeneous population believed to be the true stem cells [18].

It is not easy to recreate the haematopoietic niche *in vitro*; several factors and different cells are involved. In the last years, several groups have been using decellularized matrices to recreate a more genuine haematopoietic environment. To consider the presence of ECM is a more physiological method to study the haematopoietic niche, and it is important to understand how HSC and MSC are promoted to differentiate or not in the presence of ECM. Also, it is clinically relevant to understand the interaction between MSC and matrices, since the study of ECM and MSC interactions is a growing research area in tissue engineering and regenerative medicine [330, 332].

5.1.2 ECM scaffolds

ECM scaffolds have been suggested to be used for tissue regeneration, for bone replacement, or to treat injury and trauma resulting from accidents or diseases. Several publications have demonstrated the potential of ECM scaffolds in clinical applications as an immune-compatible and off-the-shelf alternative to living grafts for tissue and organ repair [335-337]. However, there are several factors to consider. First, different cells produce different matrices with different compositions; ECM composition is cell/tissue-specific [11]. Second, there are several different methods of preparing ECM, in combination or not with scaffolds; and third there are different decellularization methods.

In this project the ECM used was produced by MSC, since MSC and their matrix have an important role in the HSC niche. Obviously, MSC are also good candidates to create tissue engineered ECM scaffolds because of their multiple lineage potential, including osteogenic, adipogenic and chondrogenic. The different MSC differentiation methods are well identified *in*

vitro. The soluble factors involved in the regulation of the differentiation processes are known [62]. In adipogenic differentiation: 1-methyl-3-isobutylxanthine (MIX), dexamethasone, insulin and indomethacin play a key role. While in osteogenesis the differentiation is promoted by bone morphogenetic protein-2 (BMP-2), TGF-β, ascorbic acid, β-glycerophosphate, as well as dexamethasone [62]. For clinical applications, it is more relevant to investigate osteogenic regulation and differentiation of MSC rather than adipogenesis, especially in presence of scaffolds. Recent studies have demonstrated that scaffolds made of biomaterials or ECM scaffolds have a synergistic effect enhancing osteogenic differentiation of MSC, contributing for bone tissue engineering applications [338, 339]. The ideal tissue engineered scaffold would support cell attachment and osteogenic differentiation as well as subsequent bone matrix deposition and formation [338].

Some studies suggest that ECM preserves stem cell characteristics and that stem cells cultured in spheroid systems increased the expression of stemness genes (Oct4, Sox2 and Nanog) [33, 340]. Nonetheless, little is known regarding ECM-MSC interactions.

As described above, one important step for the production of ECM *in vitro* is the decellularization methods used. Decellularization is the process of killing and eliminating the cells that produce the ECM, and all the decellularization methods rely on cell lysis [341]. Cell lysis results in the release of the cell content into the matrix, which can possibly get trapped there, increasing the immunogenicity of the material [342]. The common decellularization methods are: acids and bases, hypertonic and hypotonic solutions, detergents, enzymes and physical methods. Each method has limitations [343]. Acids and bases, detergents and enzymes can damage ECM structure and components, especially collagens, GAGs and growth factors. Hypertonic and hypotonic solutions do not efficiently remove all cellular residues. The most common physical method is repeated ECM freezing and thawing, leading to the formation of ice crystals that damage ECM structure [11, 341]. In general, to increase the efficiency of decellularization, the ECM can be subjected to several decellularization methods, leading to the degradation of some of its components and ultrastructure [343]. For these reasons Bourgine *et al.* 2013 presented an alternative method of decellularization, namely that induced by apoptosis [341]. Instead of cell lysis, cell apoptosis would have more advantages, since apoptosis is a natural cell death process. This new and different approach will supposedly reduce ECM degradation and immunogenicity, since during apoptosis the cellular components are kept within the cell membrane and in the apoptotic bodies. Also, during apoptosis, cytomorphological changes occur that lead to the loss of cell contact with ECM, meaning that there will be less cellular components attached to the ECM. The maintenance of ECM integrity

after decellularization is important, especially to create a more reproducible, predictable and effective clinically-useable ECM [341].

5.1.2.1 Apoptosis

Programmed cell death, often called apoptosis, is an important process that is regulated by multiple signalling pathways that have an effect on chemotaxis, phagocytosis, regeneration and immunogenic processes [344]. Cells die naturally by necrosis or apoptosis, and recently the cancer field has been using programmed cell death pathways as a treatment. In addition, it is also possible to use apoptosis in the tissue-engineering field [345, 346].

Several factors lead to necrosis that can be induced by TNF and is negatively regulated by caspases. Necrosis involves the loss of cell membrane integrity, leading to a leakage of cellular components and inducing inflammation [347, 348].

Apoptosis is a form of programmed cell death that is determined genetically. Typically, apoptosis occurs during tissue and organ development but may also act as a homeostatic mechanism or as a defence mechanism in immune reactions as a means of eliminating infected cells. Although, there is a wide range of stimuli and conditions, both physiological and pathological, that can trigger apoptosis, not all cells necessarily die in response to the same stimulus [349].

There are two apoptotic pathways: intrinsic and extrinsic, differing in their initial activation (**Figure 5.1**). The intrinsic pathway or "mitochondrial pathway" is initiated by the release of apoptogenic factors such as cytochrome c (cyt-c), apoptosis inducing factor (AIF), among others, from the mitochondrial intermembrane space. Stress stimuli trigger mitochondria permeabilization that results in the release of these molecules into the cytosol. These molecules together with the apoptotic protease activating factor 1 (Apaf-1) and caspase-9 form the complex apoptosome. The formation of this complex activates caspase-9, which activates the effector caspases-3, 6, and 7 [341, 350]. In contrast, the extrinsic pathway or receptor pathway is triggered by external signals that bind to specific cell surface death receptors of the tumour necrosis factor receptor superfamily. Such binding results in the formation of a death inducing signalling complex (DISC), leading to caspase-8 dimerization, which can disseminate the apoptotic signal by direct cleavage of downstream effector caspases (3, 6 and 7), the same involved in the intrinsic apoptotic pathway [341, 350].

Following activation of the effector caspases and the fact that caspases can activate each other by cleavage at identical sequences, this results in amplification of caspase activity through a protease cascade [351]. Caspases cleave a number of different substrates in the cytoplasm or nucleus leading to many of the morphologic features of apoptotic cell death.

Different endonucleases and proteases lead to DNA fragmentation and nuclear protein and cytoskeletal degradation [341, 350]. These results lead to structural changes in the cells, including chromatin and cytosol condensation and finally small apoptotic bodies are formed allowing their phagocytosis by immune cells [341, 349, 352].

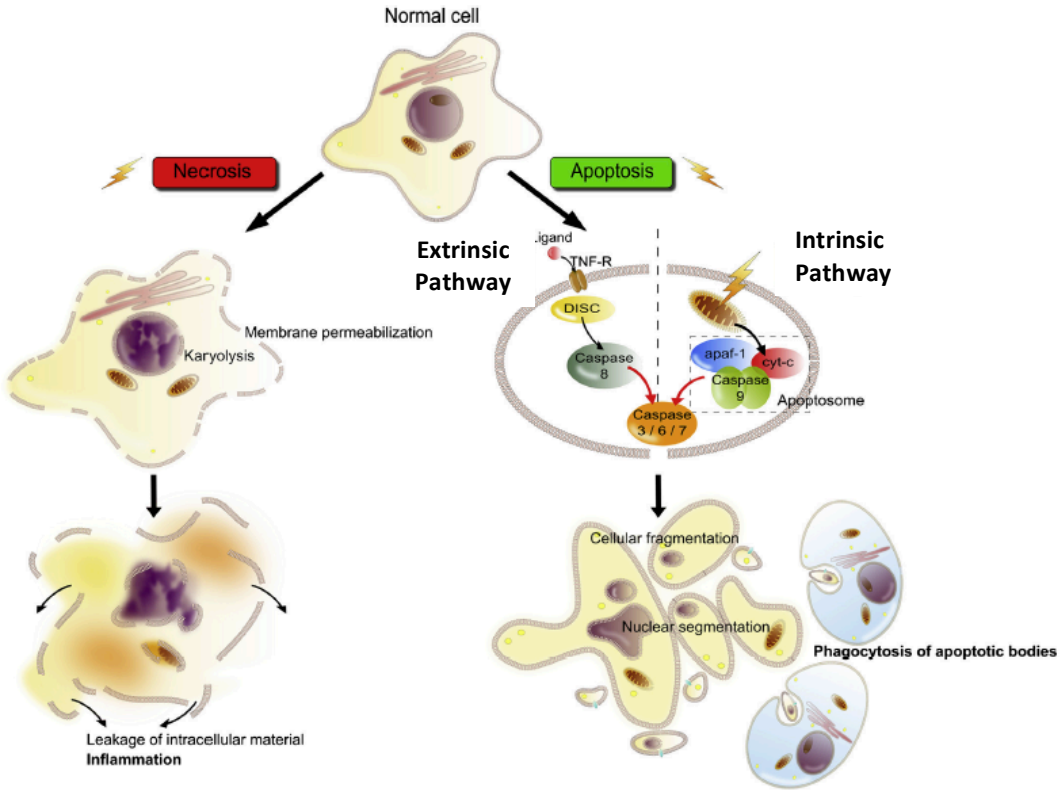

Figure 5.1 - Cell death by necrosis or apoptosis, and intrinsic and extrinsic apoptotic pathways. Necrosis leads to inflammation by the leakage of intracellular material, while apoptosis lead to the formation of apoptotic bodies that are phagocytized [341].

Several mechanisms have been identified for the induction of apoptosis. These mechanisms differ according with activation pathway, and this induction can be physical, biological or chemical.

Some factors, such as CO_2/O_2 concentration, nitric oxide, pH or temperature, can lead to the perturbation of the mitochondria, designated as lethal-environment-conditioning method, that can induce apoptosis [341]. A different approach is to directly activate members of the TNF receptor family, activating the extrinsic apoptotic pathway, designated as “kiss-of-death” [353]. A third mechanism is engineered apoptosis, using chemical inducers to trigger apoptosis, to produce decellularized ECM [341].

A critical step in the induction of apoptosis is the activation of the apoptotic initiator caspase 9. In a normal physiological condition, caspase 9 is found as an inactive monomer but its activation can be induced by dimerization [354]. This dimerization occurs when the

apoptosome is formed [355]. Activation of caspase-9 leads to activation of caspase-3, subsequently activating the downstream caspase cascade causing apoptosis [345].

The apoptotic process is a sequence of events during which phosphorylation and dimerization of specific molecules have an important role [341]. It is not possible to induce apoptosis by simply overexpressing or silencing key genes. Consequently, one option was to modify caspase 9 into an inducible caspase 9 suicide gene system (iCasp9), by which it would be possible to activate caspase 9 dimerization by a chemical inducer [346].

Cell dimerization and activation can be induced by a specific dimerizer ligand. In the case of the inducible caspase 9, it is necessary to use a B/B homodimerizer ligand because the iCasp9 has a DmrB domain. This means that iCasp9 has a drug-binding domain that can be dimerized by administration of a B/B homodimerizer, leading to an activated form of the molecule, which then initiates a signalling cascade leading to apoptosis of transduced cells (**Figure 5.2**) [346]. The B/B homodimerizer (AP20187) is a synthetic, cell-permeable ligand that has no immunosuppressive activity and is non-toxic to the cells [356].

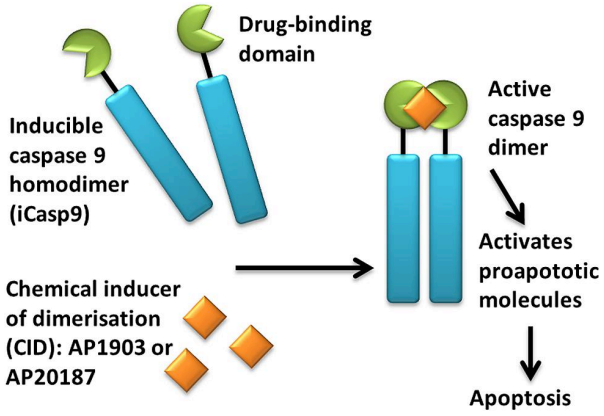

Figure 5.2 - iCasp9 dimerization by a chemical inducer [346].

To reach the objectives of this chapter, ECM produced by MS5 was used. MS5 is a cloned mouse stromal cell line established by Itoh *et al.* in 1989 [357]. To establish MS5 cells, bone marrow from C3H/HeN mice was subject to irradiation and the adherent surviving cells following a long-term culture were designated MS5. ECM produced by MS5 has been used in several studies and, in one of them, MS5 ECM prepared in normoxia was shown to be good for expanding human HSC and committed progenitors while MS5 ECM prepared in hypoxia was better for primitive progenitors [45].

5.1.3 Objectives

The first aim of this chapter was to compare two methods for the preparation of decellularized ECM; ECM decellularized with a hypotonic lysis solution versus ECM prepared by apoptosis using a Caspase 9 dimerization approach. The hypothesis was that ECM prepared with an engineered approach, the suicide gene, would be less immunogenic, therefore a better ECM than the method using hypotonic solutions.

The second aim was to study the effect of hypoxia on ECM composition, to compare the quality and quantity of ECM produced by MSC produced in normoxic and hypoxic conditions. To better understand the role of hypoxia in ECM composition and influence on MSC differentiation and stemness. For this reason the biological role of matrices prepared with different methods and under normoxic and hypoxic conditions, on MSC, more specifically Balb/c mouse BM-MSC, was studied. For this aim, the hypothesis was that ECM prepared in hypoxia would better at preserving stem cell properties during MSC culture. To study the matrices' biological role the differentiation capacity and stem cell characteristics of MSC were evaluated.

In general, the objective was to improve the knowledge regarding the biological organization of ECM and ECM-MSC interactions, contributing with information regarding the haematopoietic niche and tissue engineering ECM scaffolds, for clinical applications.

Summary of aims:

- To compare two methods to prepare decellularized ECM;
- To study the effect of hypoxia on ECM composition, especially the proteomic profile;
- To study if ECM with different compositions have a different role on MSC differentiation capacity and stemness.

5.2 Methods

Details regarding reagents, solutions, antibodies, primers, material and equipment are described in Annexes F to J.

5.2.1 MS5 extracellular matrix production

The matrix produced using this method was designated as "ECM". A pre-selected clone of MS5 cells was used to produce MS5 ECM (P_2-P_5). The cells were thawed and cultured under standard conditions with complete DMEM low glucose (LG) supplemented with 10% FBS and 1% P/S, in the presence of 21% O_2 (normoxia) or 5% O_2 (hypoxia). When the cells reached approximately 80% confluence, they were trypsinized, neutralized and counted.

The volume of solutions and number of cells used were correlated with the number of wells per plate or flask, and are described in **Table 5.1**. The numbers were not extrapolated according to cm^2, since a larger area needed more cells. In general, ECM prepared in chambers was used for ECM characterization, in plates for differentiation assays and in flasks for proteomic analysis.

First, in a sterile environment, the wells were coated with 0.1% gelatine from bovine skin and left for 2 hours. Then the gelatine was aspirated and plates or flasks were dried in the incubator at 37°C for 1 hour. MS5 cell suspensions were prepared and cells were seeded on top of the gelatine. The cells were cultured for 3 days at 37°C in a humidified incubator containing 5% CO_2 and 21% O_2 (Normoxia, ECM N) or 5% O_2 (Hypoxia, ECM H) in air. After 3 days, MS5 cells reached confluence and were treated with 10 µg/mL of Mitomycin C for 3 hours at 37°C in normoxia or hypoxia, to stop cell proliferation. Then cells were washed twice with DPBS and fresh complete medium was added. MS5 were left for 4 more days in culture, without changing medium, allowing protein deposition, in normoxic or hypoxic conditions. Following MS5 ECM production, cells were lysed by osmotic shock with Tris/EDTA (10 mM / 1 mM) hypotonic lysis buffer overnight at 4°C. On the following morning, cell debris was washed with DPBS four times. ECM were kept covered with DPBS with 1% P/S at 4°C in sterile conditions, and used within one month [358].

Table 5.1 - Number of MS5 and 0.1% gelatine, complete medium, Mitomycin C solution and Tris/EDTA lysis buffer volumes used per well or flask.

	Number of MS5	Gelatine	Medium	Medium + Mitomycin C	Lysis buffer
Per well - chamber	$3x10^4$	0.3 mL	0.8 mL	0.25 mL	0.5 mL
Per well - 48 well plate	$3x10^4$	0.5 mL	1 mL	0.25 mL	0.5 mL
Per well - 12 well plate	$1.5x10^5$	1 mL	2 mL	1 mL	1 mL
Per T_{75} flask	$2.5x10^5$	10 mL	15 mL	7 mL	7 mL

5.2.2 MS5 transduction with inducible caspase 9

To create ECM from MS5 cells using the suicide gene strategy, it was necessary to transduce the MS5 cell line with an inducible caspase 9. This procedure was accomplished in the Institute for Surgical Research, Basel University, Switzerland, in the laboratory of Professor Ivan Martin.

The mouse stromal cell line MS5 was thawed and cultured under standard normoxic conditions with DMEM LG supplemented with 10% FBS and 1% P/S, for a week. The transduction was performed using a retroviral vector prepared in advance. Briefly, the retrovirus was produced after transfecting the phoenix ECO human cell line with an inducible caspase 9 gene coupled to the human CD19 (iCasp9-ΔCD19) vector (**Figure 5.3**). The virus was collected every 12 hours, passed through a 0.45 μm filter and conserved at -80°C [359].

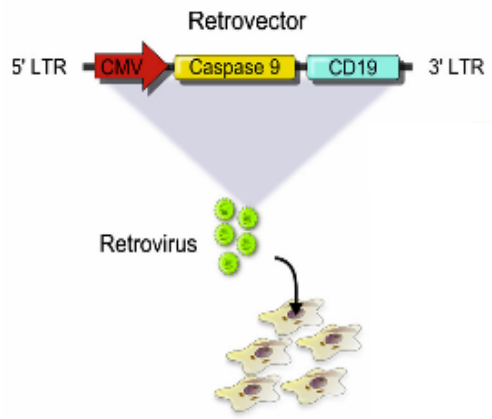

Figure 5.3 - Retrovector carrying the modified caspase 9 and CD19. Retrovirus was produced and transduced into MSC [341].

In small petri dishes $5x10^4$ MS5 cells were seeded and left in a humidified incubator containing 5% CO_2 and 21% O_2 at 37°C until the following day. Then cells were checked for confluence, which was should be between 40-60%. The medium was removed and 8 μg/mL polybrene diluted in DMEM LG supplemented with 10% FBS, was added to the cells and incubated for 1 hour at 37°C. One hour later, the medium was removed and polybrene and virus were added to the cells in the same conditions. The tissue culture dishes were wrapped in parafilm and centrifuged at 1 036 g for 30 minutes at room temperature. Following centrifugation the medium was removed and fresh culture medium was added. Cells were incubated for 5 more hours in a humidified incubator at 37°C in normoxic conditions. The process was repeated one more time and finally fresh medium was added to the cells and left until they reached confluence. These transduced cells were designated as MS5 iDS cells, indicating that it is possible to induce apoptosis in them. Then, these cells were trypsinized, neutralized, counted, re-plated and characterized.

5.2.3 Characterization of MS5 iDS cells

To know the efficiency of transduction, an aliquot of MS5 iDS cells were labelled with CD19 APC for 10 minutes in the dark at room temperature and washed twice with FACS buffer. The cells were resuspended and analysed using the 4-colour flow cytometer BD Accuri C6 (Becton Dickinson) and data analysed using Infinicyt version 1.7 software (Cytognos).

To ensure that 100% of the MS5 iDS cells were iCasp9^{+}, a selection of MS5 iDS clone (CD19^{+}) was made by limiting dilution and single cell sorting. Using a 96 plate format, 3 cells per well were sorted using the BD FACS Aria II (Becton Dickinson), this number of cells was chosen based on the plating efficiency of sorted MS5 cells. Several successful colonies were later picked and re-plated in flasks to achieve the enough number of cells needed for ECM preparation. They were verified for homogeneous and stable CD19 expression.

To confirm that MS5 iDS cells keep the same phenotype, MS5 and MS5 iDS cells were stained with antibodies to CD11b, CD31, CD34, CD45, HLA-DR, CD29, CD44, CD49e, CD90, CD105 and Sca1 and respective isotype controls. Following 10 minutes incubation, the cells were washed twice and resuspended in FACS buffer. Cells were acquired using the BD Accuri C6 flow cytometer and analysed with Infinicyt software.

To demonstrate MS5 iDS cell death following induced apoptosis with B/B homodimerizer treatment was indeed apoptosis, a simple PI and annexin V staining was performed. MS5 iDS cells after 2 days in culture in normoxia were treated, or not, with 1 nM B/B homodimerizer overnight at 37°C. Following treatment the cells were trypsinized, neutralized and collected into cytometer tubes. Medium was removed and the cells were resuspended in 1X annexin binding buffer. Annexin V FITC was added and incubated for 10 minutes in the dark at room temperature. PI was also added and incubated for 1 minute just before the samples were acquired by the BD Accuri C6 flow cytometer. Results were analysed using Infinicyt software.

5.2.4 MS5 iDS extracellular matrix production

The ECM produced by MS5 iDS cells with a suicide gene was designated “ECM iDS”.

Following characterization, a clone of MS5 iDS cells (P_5-P_7) was used to produce ECM iDS. The MS5 iDS cells were thawed and cultured under standard conditions in normoxia and hypoxia. When the cells reached around 80% confluence, they were trypsinized, neutralized and counted. The volumes and number of cells used were exactly the same as used to prepare ECM and described in **Table 5.2**.

As described above the wells or flasks were pre-coated with 0.1% gelatine from bovine skin and MS5 iDS cell suspensions were prepared and cells were seeded on top of gelatine. The

cells were cultured for 3 days at 37°C in a humidified incubator containing 5% CO_2 and 21% O_2 (ECM iDS N) or 5% O_2 (ECM iDS H) in air. After 3 days, the culture medium was changed and the cells were left in culture for further 4 days, in normoxic or hypoxic conditions. Following ECM deposition by MS5 iDS cells, cell death was induced by adding 1 nM B/B homodimerizer overnight at 37°C. The next day, cell debris was washed away using 4 washes with DPBS. This protocol was adapted from [359]. ECM iDS was kept covered in DPBS with 1% P/S at 4°C in sterile conditions, and used within one month [358].

Table 5.2 - Number of MS5 iDS and 0.1% gelatine, complete medium and B/B homodimerizer volumes used per well or flask.

	Number of MS5 iDS	Gelatine	Medium	B/B homodimerizer
Per well - chamber	$3x10^4$	0.3 mL	0.8 mL	0.5 mL
Per well - 48 well plate	$3x10^4$	0.5 mL	1 mL	0.5 mL
Per well - 12 well plate	$1.5x10^5$	1 mL	2 mL	1 mL
Per T_{75} flask	$2.5x10^5$	10 mL	15 mL	7 mL

5.2.5 Matrices characterization and comparison

5.2.5.1 ECM - Live/Dead viability assay

To prove cell death following overnight lysis treatment, a live/dead viability assay was performed on the ECM prepared according to the method described above in normoxia and hypoxia. Some live MS5 cells were also seeded as positive control. DPBS and medium were removed from ECM and MS5 cells, and 2 μM calcein AM and 4 μM ethidium homodimer solution were added to each sample. The dyes were incubated for 10 minutes at room temperature and then washed twice with 1X PBS to remove excess dyes. Pictures of live and dead cells were taken using the Olympus IX71 inverted fluorescent microscope.

5.2.5.2 ECM - AlamarBlue assay

With the aim of proving that ECM did not have metabolic activity, an alamarBlue assay was performed. ECM was prepared according to the method described above in normoxic and hypoxic conditions. Some MS5 live cells were also seeded as positive control.

ECM and MS5 cells were removed from the fridge or incubator 1 hour before the assay in order to reach room temperature. DPBS and medium were removed from ECM and MS5 cells, and 200 μL (in 48 well plate) of 10% alamarBlue solution were added into each sample. The samples were incubated for 3 hours at 37°C in a humidified incubator containing 5% CO_2 and 21% O_2 in air. Following incubation, 100 μL of these solutions were transferred into a 96

flat bottom well plate and the absorbance was measured at 550 nm (low) and 595 nm (high) wavelength using the Varioskan Flash (Thermo Scientific) microplate reader.

To calculate the metabolic activity of the samples, the following calculations were made using Excel. First it was calculated the average absorbance (A) value measured at low and high wavelengths. Then the PBS absorbance value was subtracted to the absorbance of 10% AlamarBlue at low (AO_{lw}) and high (AO_{hw}) wavelengths. The correlation factor (RO) was found by dividing the AO_{lw} by AO_{hw} ($RO = AO_{lw} / AO_{hw}$). To calculate the percentage of reduced AlamarBlue (AR) the following formula was used: $AR = A_{lw} – (A_{hw} \times RO) \times 100$.

5.2.5.3 ECM iDS apoptosis

Following ECM production it was important to prove that the ECM did not interfere with the apoptotic process. For this reason MS5-ECM iDS cells, prepared according to ECM protocols described above, and MS5 iDS cells just cultured for 2 days (without ECM present), in normoxia and hypoxia, were treated with B/B homodimerizer for 4 hours, 8 hours or overnight. After apoptosis induction, cells were trypsinized, neutralized and collected in cytometer tubes. Medium was removed and the cells were resuspended in 1X annexin binding buffer. Annexin V FITC was added and incubated for 10 minutes in the dark at room temperature. PI was also added and incubated for 1 minute just before the samples being acquired in the flow cytometer BD Accuri C6. Data was analysed using BD CSample Analysis software (Becton Dickinson).

5.2.5.4 ECM and ECM iDS immunocytochemistry

To demonstrate that the matrices produced contained the common ECM proteins, immunocytochemistry (ICC) staining was performed on ECM and ECM iDS prepared in 1 μm ibiTreat chambers in normoxia and hypoxia, according to the protocol described above.

All samples were incubated for 30 minutes at room temperature with blocking buffer (4% FBS in 1X PBS). Blocking buffer was removed and each well of each condition was stained with antibodies to collagen IV, collagen VI, fibronectin, laminin, heparin sulphate and thrombospondin, and incubated at room temperature for 1 hour on a shaker (slow rotation). The samples were then washed twice with DPBS and the corresponding secondary antibody was added and incubated for 30 minutes at 4°C on shaker (slow rotation). Samples were washed again twice with DPBS and DAPI was added. After a 10 minute incubation in the dark at room temperature, DAPI was removed and samples were covered with water and kept at 4°C in the dark until the next day. Pictures were taken using an Olympus IX81 confocal microscope equipped with XYZ camera.

5.2.5.5 MS5 and MS5 iDS expression of ECM related genes

With the aim of correlating ECM proteins present in the matrices with gene expression, as well as to observe if hypoxia increased the expression of these genes, RNA from MS5 and MS5 iDS cells cultured in normoxia and hypoxia was extracted.

MS5 P_2 and MS5 iDS P_5 cells were cultured under normoxic and hypoxic conditions following thawing, then were trypsinized, counted and $1x10^6$ cells were seeded in T_{175} culture flasks. The MS5 iDS P_6 were further cultured in normoxia and hypoxia for 3 days. Then, RNA was isolated from samples using High Pure RNA Isolation kit from Roche. Manufacture's instructions were followed and RNA samples were stored at -80°C. RNA quality and quantity was investigated using NanoDrop 2000 spectrophotometer (Thermo Scientific). Only high quality RNA was used for cDNA synthesis, samples with ratios of absorbance at 260nm and 280nm (260/280) between 2.0 and 2.1. Reverse transcription polymerase chain reaction (PCR) of samples was accomplished using High Capacity cDNA Reverse Transcription kit (Applied Biosystems) according to the manufacture's instructions using random primers. The amplification occurred in Veriti Gradient thermal cycle (Applied Biosystems), under the following conditions: 10 minutes at 25°C, 120 minutes at 37°C and 5 minutes at 85°C. Afterwards, real time PCR (RT-PCR) was performed using LightCycler SYBR Green I Master kit (Roche) with LightCycler 480 II Real Time PCR 384 wells system (Roche), each sample was in triplicate. The following primers were used: Col4α1 (collagen IV), Col6α1 (collagen VI), fibronectin, HSPG2 (heparan sulphate), Lamb2 (laminin), integrin β1, Acan (aggrecan), Adam9 (disintegrin, metalloproteinase) and Col2 (collagen II) (Annex G). The reference genes used were β-2 microglobulin (B2M) and glyceraldehyde-3-phosphate dehydrogenase (GAPDH), however for results analysis just B2M was used. Primers are commercially available in OriGene. Final concentration of all primers was 0.5 μM and RT-PCR conditions were: 5 minutes at 95°C, 45 cycles at 95°C for 10 seconds, 60°C for 30 seconds and 72°C for 20 seconds. In all RT-PCR the melt curve was evaluated for 5 seconds at 95°C, 1 minute at 65°C and finalizing at 97°C.

5.2.5.6 MS5 and MS5 iDS cells proliferation rate

To observe if MS5 iDS cells following transduction had the same proliferation rate, as well as to observe if normoxia or hypoxia interfered with proliferation rate, MS5 and MS5 iDS cells were seeded at high confluence and the cells were counted. Cells were seeded at the same densities that were seeded to produce ECM and ECM iDS. The cells were thawed and cultured under normoxic and hypoxic conditions, then were trypsinized, neutralized and counted using the cytometer Accuri C6. In 48 well plates $3x10^4$ MS5 (P_3-P_4) and MS5 iDS (P_5-P_7)

cells were seeded in triplicate in pre-coated gelatine or directly in the wells and cultured for 72 hours, once again, in normoxic and hypoxic conditions. After 3 days, the cells were trypsinized with 50 μL of 0.25% Trypsin-EDTA and neutralized and resuspended in 450 μL of medium. A total of 200 μL of cell suspension was removed and placed in a 96-well round bottom plate. Samples were incubated for a few minutes with PI and 100 μL of cell suspension were acquired using the flow cytometer Accuri C6. Results were analysed with BD CSample Analysis software.

5.2.5.7 ECM and ECM iDS proteomic characterization

To characterize more extensively the composition of ECM's, proteomic analyses were carried out on ECM and ECM iDS prepared in normoxia and hypoxia, according to the protocols described above. These matrices were prepared in T_{75} flasks and submitted to an extra decellularization step, with 10 mM dithiothreitol (DTT) and 5 M guanidine hydrochloride solution for 1 hour at 4°C on an orbital shaker. Matrices were collected by scraping the matrix from the flasks and transferred to tubes that were then centrifuged for 20 minutes at 4 000 g to precipitate the insoluble material. The samples were stored at -80°C straight away and subsequently sent on dry ice to the Proteomic facility at Bristol University, UK. In the proteomic facility the samples were run in a gel to separate the proteins, then the gel/proteins were cut into small pieces and submitted to an enzymatic digestion, to cleave proteins into peptides. The peptides were then analysed by mass spectrometry and the results were compared with a library that gave the identification of the peptides. All the peptides were identified with at least 95% confidence. The results were expressed as peptide spectrum match (PSM). Then, just the proteins with a PSM>2.5 were considered. The results were analysed by Panther and Gorilla softwares, to study gene ontology, and DAVID functional annotation to observe certain pathways. All softwares are available online. Normoxia and hypoxia files were also merged and normalized to observe the fold changes.

Mass spectrometry results were then analysed by a company, SEQOME Limited.

5.2.6 Biologic role of matrices

5.2.6.1 Release of inflammatory cytokines and DAMPs

Apoptosis is a stressful cellular event and for this reason it was decided to investigate if MS5 iDS cells released any DAMPs or inflammatory cytokines after apoptosis. Thus, supernatants from ECM iDS N and ECM iDS H were collected and analysed by ELISA. Simultaneously the supernatants from ECM N and ECM H were collected to compare both ECM preparation methods.

Firstly, matrices prepared in 48 well plates were made according with protocols describe above. Following cell debris washes 500 μL of 1X PBS was added to each well and was left for 10 days at 4°C in sterile conditions. After 10 days, supernatants were collated and 3 ready-to-go ELISA kits were used to detect TNF-α, IFN-γ and HSP70 (a DAMP). All protocols were followed according to the manufacturer's instructions. Absorbance was measured in triplicated using the Varioskan Flash microplate reader and all results were processed in Excel.

5.2.6.2 Induction of inflammation

Since the presence of inflammatory cytokines and DAMPs in the supernatants was not an indication that they could initiate an inflammatory response on cells, different cells were cultured on top of the matrices. ECM (N and H) and ECM iDS (N and H) were prepared in 48 well plates according to the protocols described above.

For these experiments, cell lines representative of macrophages (Raw 264.7) or monocytes (J774A.1), T cells or MSC were cultured on top of ECM prepared from MS5 or MS5 iDS cells under normoxic or hypoxic conditions. Raw 264.7 and J774A.1 cells were thawed and cultured in normoxic conditions one week before the assay with appropriate culture media. T cells were collected from the spleen and subcutaneous lymph nodes of 5 to 12 week old C57BL/6.FoxP3.EGFP transgenic mice. These mixed CD4 and CD8 T cells were acquired by cell sorting in the context of other project and the remaining cells were used in this assay. The MSC used were harvested from Balb/c mouse BM, described bellow.

On top of 3 wells of each ECM N, ECM H ECM iDS N and ECM iDS H, $2x10^5$ cells of each type were seeded. Cells were also added to normal plastic wells, as negative controls. For positive controls Raw 264.7 (P_9-P_{11}) and J774A.1 (P_{10}-P_{11}) were activated with 100 ng/mL of ultrapure LPS-EB with complete DMEM HG medium, while Balb/c MSC (P_7-P_{10}) were activated with 500 units/mL of IFN-γ diluted in complete MEMα medium, and T cells were activated with Dynabeads® Mouse T-Activator CD3/CD28 in the presence of complete RPMI 1640 medium (1 bead: 2 T cells). All samples were incubated for 24 hours in the presence of 0.6 μg/mL of Brefeldin A, at 37°C in a humidified incubator containing 5% CO_2 and 21% O_2.

Following incubation, all samples were trypsinized, neutralized and transferred into cytometer tubes. Samples were centrifuged for 5 minutes at 250 g and the supernatants were discarded. Cells were fixed with 1% PFA (paraformaldehyde) for 10 minutes at room temperature. Following washing with FACS buffer, cells were permeabilized with 0.5% saponin. Cells were stained intra-cytoplasmically with anti-TNF-α PE antibody and after 10 minutes incubation at room temperature in the dark, the samples were washed twice. Subsequently, samples were resuspended in FACS buffer and acquired on Accuri C6 cytometer. Results were

analysed using BD CSample Analysis software and were presented by percentage of cells that express TNF-α.

5.2.6.3 Balb/c mice BM-MSC

To better understand the ECM biologic role on MSC, MSC harvested from bone marrow of Balb/c mice were cultured on top of ECM. Balb/c MSC were obtained from another research group in REMEDI. Briefly, the femurs and tibiae of 8-14 week old Balb/c mice were removed and the bones were cut to expose the marrow and cells were flushed out with culture medium using a 35 gauge needle. Clumps were removed by filtering through a 70 μm mesh filter. Cells were then centrifuged and resuspended. The cells were cultured at 37°C in a humidified incubator containing 5% CO_2 and 21% O_2, and non-adherent cells were removed 24 hours later. This process was repeated until cells reached confluence. At this point cells were trypsinized, neutralized and counted. An aliquot of the cells was cryopreserved and the remaining cells were re-plated for later characterization.

Balb/c cells were already in P_7 when they were given to this project. The cells were thawed and cultured with complete culture medium in normoxic conditions for a week before being cultured on top of matrices and characterized.

Using a panel of 11 antibodies Balb/c MSC were characterized by a standard surface staining protocol. FITC labelled CD45, CD49e and Sca-1 antibodies were used. PE labelled CD11b, CD44, CD73, CD90.2, and CD105, and APC labelled CD29, CD34 and MHC II antibodies were also used to characterize Balb/c cells. The cells were incubated for 10 minutes in the dark with the above antibodies and then washed twice with FACS buffer. Next, Balb/c MSC were resuspended in FACS buffer and acquired by the BD Accuri C6 flow cytometer. Data were analysed using the flow cytometry software BD CSample Analysis.

5.2.6.4 Mouse BM-MSC adipogenic and osteogenic differentiation on top of matrices

To compare the biological role of both ECM preparations and to better understand if ECM or hypoxia have an effect on MSC differentiation; Balb/c mouse BM-MSC cells were cultured on top of ECM (N and H), ECM iDS (N and H) or plastic (N and H), and adipogenic and osteogenic differentiation assays were performed.

The matrices were produced in 48 well culture plates and Balb/c MSC were thawed and cultured with complete medium in normoxia for one week before the assay. On top of these ECM, ECM iDS or just on top of plastic, $3x10^4$ Balb/c (P_9-P_{12}) MSC cells were seeded per well. The following day, for adipogenic differentiation, cells were exposed for 3 days to adipogenic induction medium (Annex E) and 1 day to adipogenic maintenance medium, completing one

cycle. Three cycles were completed before lipid quantification and 2 cycles for gene expression analysis. For osteogenic differentiation Balb/c MSC were cultured in osteogenic differentiation medium (Annex E) and the medium was changed every 2 days. Cells were differentiated under normoxic and hypoxic conditions. Balb/c MSC in normoxia or hypoxia that were not subjected to osteogenic or adipogenic differentiation, served as controls.

5.2.6.4.1 Lipid quantification

Following adipogenic differentiation, lipids were stained and quantified by Oil red O. Medium was removed, cells washed twice with 1X PBS and fixed for 30 minutes at room temperature with 10% neutral buffered formalin. Cells were rinsed with distilled water and stained for 5 minutes with previously diluted and filtered Oil red O. Then, the stain was discarded and the excess removed with 60% isopropanol. Cells were rinsed once again with running tap water. Pictures of lipid drops were taken using the Olympus IX71 inverted fluorescent microscope.

Lipid quantification was obtained by colorimetric measure of Oil red O staining. Oil red O was extracted by adding 200 μL of 99% isopropanol to the samples and left for 1 hour at room temperature on the shaker (fast rotation). Following several pipettings 150 μL of extracted stain were transferred to a 96 well plate and the absorbance measured at 520 nm wavelength using Varioskan Flash microplate reader.

5.2.6.4.2 Calcium quantification

Following osteogenic differentiation, calcium deposits were formed and identified by Alizarin red S staining, and calcium quantified using a StanBio kit. Medium was removed, cells washed twice with DPBS and fixed with ice cold 95% methanol for 10 minutes at room temperature. Cells were washed twice with distilled water and stained for 5 minutes with previously filtered 2% Alizarin red S solution. Excess stain was removed quickly with distilled water. Pictures of calcium deposits were taken using the Olympus IX71 inverted fluorescent microscope.

For calcium quantification, medium was removed, cells washed twice with DPBS and 200 μL of 0.5 M HCl was added to each sample/well. Plated were placed on shaker (fast mode) for 1 hour at room temperature. Balb/c and ECM were scraped and transferred into Eppendorf tubes. A further 200 μL of 0.5 M HCl was used to remove the remaining cells/ECM. Samples were shaken overnight in the cold room. The following day, the calcium was quantified using the StanBio calcium liquicolor kit according to the manufacturer's instructions. Absorbance

was measured at 595 nm wavelength using Varioskan Flash microplate reader and results were processed in Excel.

5.2.6.5 Confirmation of MSC differentiation by RT-PCR

To confirm that the differentiated Balb/c MSC were expressing the appropriated adipogenic or osteogenic genes, after 2 and 4 differentiation cycles, respectively, RNA extraction was completed. However, the experiment design was singly different from the differentiation protocol, since it was technically challenging and expensive to have exactly the same conditions used in the differentiation assay. For PCR experiments it was just considered differentiation occurred in normoxic conditions. The matrices were prepared as normally, in normoxia and hypoxia, however all Balb/c were cultured and differentiated under normoxic conditions. Following cell culture, RNA was extracted from samples and RT-PCR for different genes of interest were performed.

Balb/c cells were thawed and cultured in normoxic conditions one week before the assays. Matrices were produced in T_{75} tissue culture flasks according with protocols described above, under normoxic and hypoxic conditions. On top of these matrices or just on top of plastic of T_{75} flasks, $1x10^6$ Balb/c (P_{10}-P_{12}) were seeded. Following differentiation, medium was removed and cells washed with DPBS. Subsequently 10 mL of DPBS was added and ECM/Balb/c were scraped and transferred to falcon tubes. The samples were centrifuged for 5 minutes at 250 g and supernatant discarded. RNA was isolated from samples using High Pure RNA Isolation kit from Roche as described above. The following primers were used in samples that were under adipogenic differentiation; c/EBPβ and aP2. While primers BMP2, RUNX2, Osterix and Osteopontin were used in samples cultured with osteogenic medium. These genes were also analysed in control samples, were Balb/c were cultured with normal medium for the duration of differentiation processes. The reference genes used were B2M and GAPDH, however for results analysis propose just B2M was used. Primers were design and tested in the house by a previous member of the immunology group. Final concentration of all primers was 0.5 μM and PCR conditions were: 5 minutes at 95°C, 45 cycles at 95°C for 10 seconds, 60°C for 30 seconds and 72°C for 20 seconds. In all PCR the melt curve was evaluated for 5 seconds at 95°C, 1 minute at 65°C and finalizing at 97°C.

5.2.6.6 Effect of matrices and hypoxia on MSC stemness

Furthermore, to better understand if the matrices had any effect on stemness properties of MSC, Balb/c MSC were cultured under normoxic conditions in the presence of ECM (N and H), ECM iDS (N and H) and plastic with adipogenic, osteogenic and normal medium

for a week. To study the kinetics of stem cell genes expression, Balb/c MSC were also cultured in the presence of matrices and plastic under normoxic conditions with normal medium for 3 and 7 days.

Additionally, oxygen concentration was also considered on stem cell genes expression. Balb/c MSC in plastic and in the presence of matrices, were cultured in normoxic and hypoxic conditions for 3 days, and stem cell and HIF genes were relatively quantified.

Balb/c cells were thawed and cultured with complete MEMα medium in normoxic or hypoxic conditions one week before the assay. Matrices were produced in T_{75} tissue culture flasks according with protocols described above, under normoxic and hypoxic conditions. On top of these matrices or just on top of plastic of T_{75} flasks, $1x10^6$ Balb/c (P_{10}-P_{12}) were seeded. Cells were cultured under normoxic or hypoxic conditions for 3 or 7 days at 37°C in a humidified incubator containing 5% CO_2. Then, medium was removed and the cells were washed with DPBS. Subsequently 10 mL of DPBS was added and ECM/Balb/c were scraped and transferred to falcon tubes. The samples were centrifuged for 5 minutes at 250 g. Supernatants were discarded and RNA was isolated from samples using High Pure RNA Isolation kit from Roche as describe above. Afterwards, real time PCR was performed using LightCycler SYBR Green I Master kit with LightCycler 480 II Real Time PCR 384 wells system. Stem cell genes (Sox2, Nanog and Oct4) and HIFs (HIF-1α and HIF-2α) expression were relatively quantified (Annex G). The reference gene used was B2M. Final concentration of all primers was 0.5 μM and the PCR conditions are described above.

5.2.7 Statistical analysis

To determine statistical significance of differences observed between each condition, two-way-ANOVA tests were performed, using GraphPad Prism software. Statistically significance differences were considered * when P-value was lower than 0.05, ** when P-value was lower than 0.01, *** when P-value was lower than 0.001 and **** when P-value was lower than 0.0001.

5.3 Results

5.3.1 Characterization of MS5 iDS cells

Following MS5 transduction, it was important to characterize the MS5 iDS cells, in order to show that the phenotype did not change and that it was possible to induce apoptosis in the cells.

To demonstrate that MS5 cells were efficiently transduced, MS5 iDS cells were stained for CD19 expression using an anti-human CD19 MAb. Normally, MSC do not express CD19, but the iCasp9 vector used in these experiments was coupled with the cDNA encoding the human CD19 molecule. Therefore, if CD19 were expressed on the surface of transduced MS5 cells, this would indicate successful stable incorporation of the vector containing the suicide gene. **Figure 5.4** indeed shows that, MS5 iDS cells were $CD19^+$ while normal MS5 cells were negative, indicating that MS5 iDS cells had iCasp9 inserted.

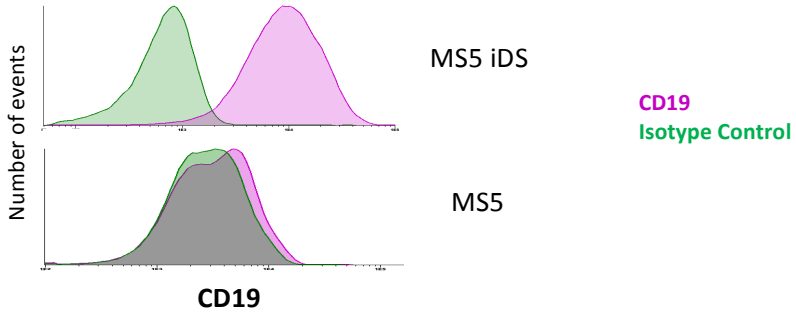

Figure 5.4- Expression of human CD19 by MS5 iDS cells. MS5 cells that express CD19 (top histogram), compared with isotype control, indicates that MS5 iDS cells were transduced efficiently with iCasp9.

Meanwhile, following transduction, 90% of the MS5 cells were positive for CD19, and to obtain 100% MS5 $CD19^+$, cell sorting was performed. Following sorting, single colonies were picked and expanded and designated as MS5 iDS cells and were then immunophenotyped. MS5 iDS cell retained their original MSC phenotype; they did not expressed CD11b, CD31, CD34, CD45 or HLA-DR, but were positive for CD29, CD44, CD49e, CD90, CD105 and Sca1 (**Figure 5.5**). Thus, MS5 containing the iCasp9 vector did not change their phenotype.

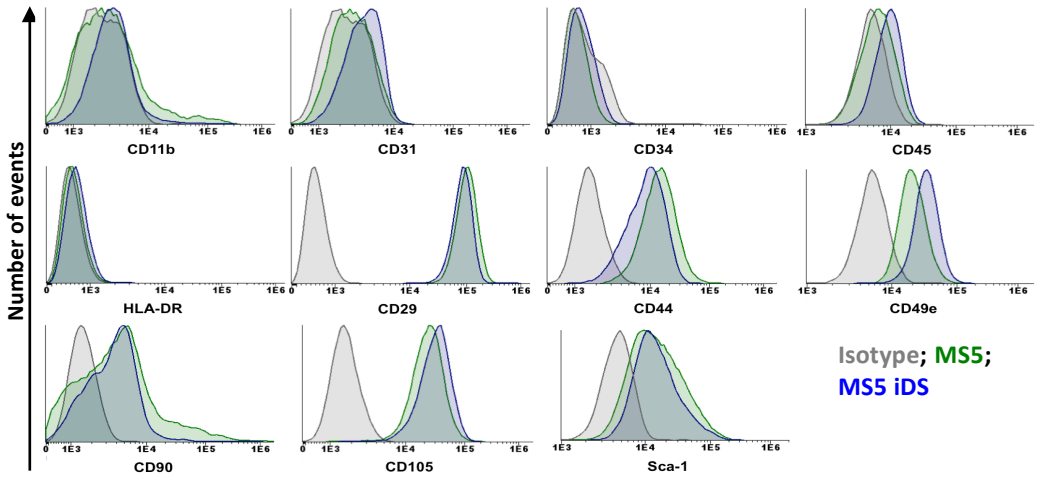

Figure 5.5 - The histograms show MS5 and MS5 iDS cells immunophenotyping. Isotype control in grey, MS5 cells in green and MS5 iDS in blue. Both cells do not express CD11b, CD31, CD34, CD45 and HLA-DR. They do express CD29, CD44, CD49e, CD105 and Sca-1. Regarding to CD90 not all the cell express this marker.

Propidium iodide is a DNA intercalating agent and a fluorescent molecule used for identifying dead and dying cells. Entry of PI into the cytoplasm of cells indicates the inability of dying cells to exclude this dye from their cytoplasm. Eventually in dead cells, the dye enters the nucleus where it binds DNA. Annexin V binds to phosphatidyl serine that is normally present on the inner cytoplasmic side of the cell's lipid membrane bilayer but appears on the outside of early apoptotic cells. According to combined PI and annexin V staining, it is possible to distinguish 3 populations (**Figure 5.6**): viable/live, early apoptotic and in late apoptosis/necrotic.

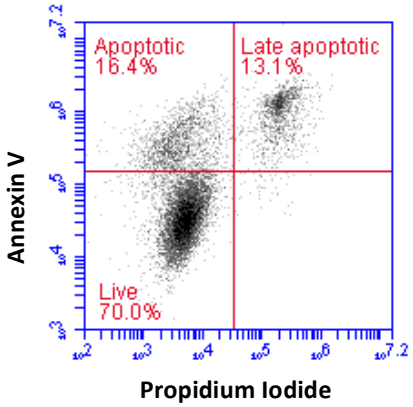

Figure 5.6 – Exemple of Annexin V and PI staining, definition of 3 populations used in Figure 5.10.

To prove that B/B homodimerization was able to induce apoptosis in MS5 iDS cells, **Figure 5.7** shows that, following overnight treatment with 1 nM B/B homodimerizer, the majority of MS5 iDS cells were PI^+ or dead. This indicates that the iCasp9 vector was active in these cells and that apoptosis could be induced.

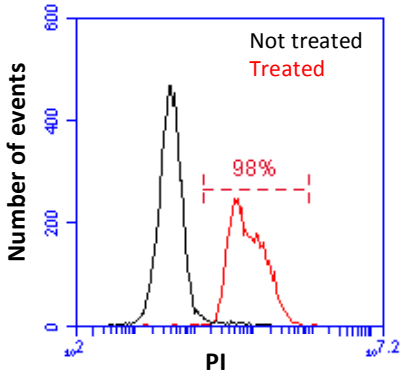

Figure 5.7 - MS5 iDS cell PI staining following overnight treatment with 1 nM B/B homodimerizer.

5.3.2 Characterization and comparison of ECM

First of all, it was important to make sure that both methods used to produce ECM were equally efficient at producing material that was devoid of dead cells and cellular debris.

5.3.2.1 ECM

To demonstrate that ECM generated in normoxia or hypoxia was devoid of viable cells and that the matrices did not have metabolic activity, a Live/Dead viability assay and AlamarBlue assay were carried out.

Live cells can be distinguished by the presence of intracellular esterase activity, determined by the enzymatic conversion of the virtually non-fluorescent cell-permeant calcein AM stain to fluorescent calcein. The polyanionic calcein dye is well retained within live cells, producing an intense uniform green fluorescence in live cells. In contrast, dead cells can be identified using ethidium homodimer staining. This material enters into cells with damaged membranes, binds DNA and produces a bright red fluorescence in dead cells.

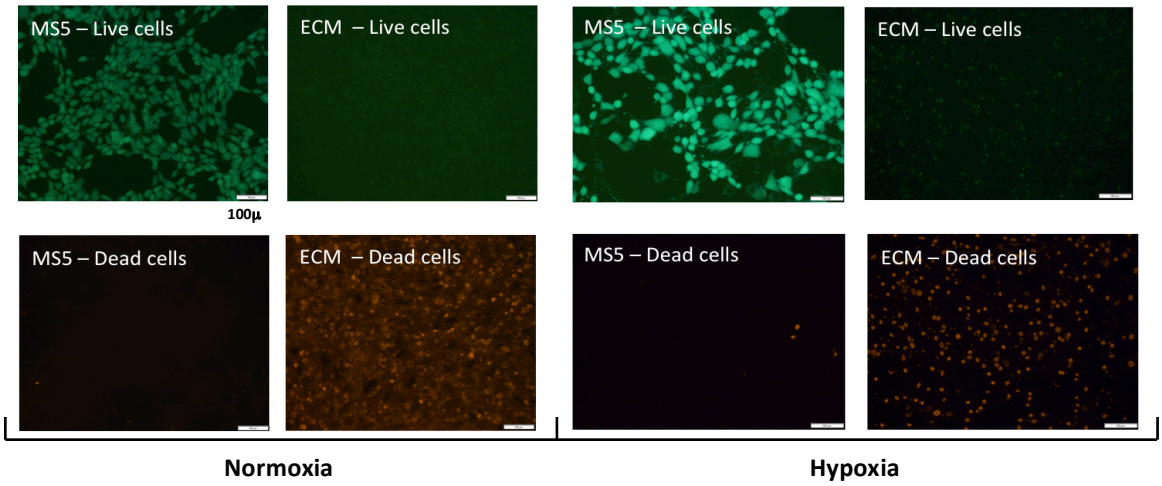

Figure 5.8 - Live/Dead assay. Representative pictures of MS5 and ECM in normoxia, left side, and MS5 and ECM in hypoxic conditions, on the right. On top calcein stain live cells; in green, and in the bottom ethidium homodimer stain dead cells, in red.

Figure 5.8 shows that in live cells (upper panels), MS5 cultured in normoxia or hypoxia had green calcein fluorescence but no red ethidium fluorescence, indicating that the controls were alive whereas ECM N and H samples did not have green fluorescence but instead were red (lower panels). This shows that ECM preparations harvested from MS5 cultured overnight with a hypotonic solution did not contain residual viable cells.

To measure the metabolic activity of the matrices, the AlamarBlue assay was performed. This assay is based on the ability of metabolically active cells to convert the reagent into a fluorescent and colorimetric indicator. Damaged and non-viable cells have lower innate metabolic activity, and generate a proportionally lower signal. The results are presented according to the percentage of reduced AlamarBlue.

The graph from **Figure 5.9** shows that ECM N and ECM H had a lower percentage of reduced AlamarBlue, when compared with respective MS5 cells. As expected, these results indicate that live cells, MS5 N and MS5 H, had high metabolic activity whereas ECM N and ECM H had almost no metabolic activity.

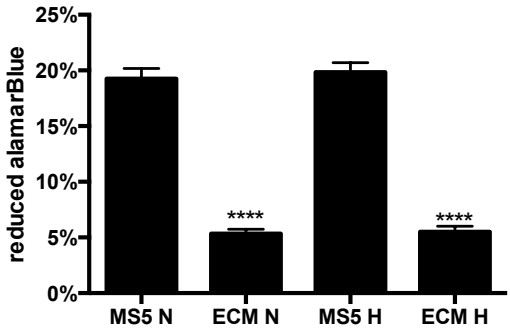

Figure 5.9 - AlamarBlue assay. Graph shows the percentage of reduced AlamarBlue of MS5 cells in normoxia and hypoxia and ECM N and ECM H (n=6). All the statistic differences are compared with control MS5 live cells. One-way-ANOVA * P<0.05, ** P<0.01, *** P<0.001 and **** P<0.0001.

5.3.2.2 ECM iDS

Following ECM iDS production, it was important to prove that all cells that produced ECM iDS were dead. Therefore, a PI/annexin V staining was performed on MS5 and MS5 iDS cells. However, during the ECM production process it was noticed that cells in the presence of ECM were taking longer to die. With the aim of understanding if ECM was delaying apoptosis, cells were cultured for 2 days or for 7 days, according to the ECM production protocol (**Figure 5.10**).

During this experiment it was also noticed that cells in hypoxia were taking longer to die. With the aim of understanding if hypoxia was delaying apoptosis, the cells cultured in the

same conditions described above were cultured for 2 or 7 days under normoxic or hypoxic conditions, and treated for different periods of time with apoptosis inducer (**Figure 5.10**).

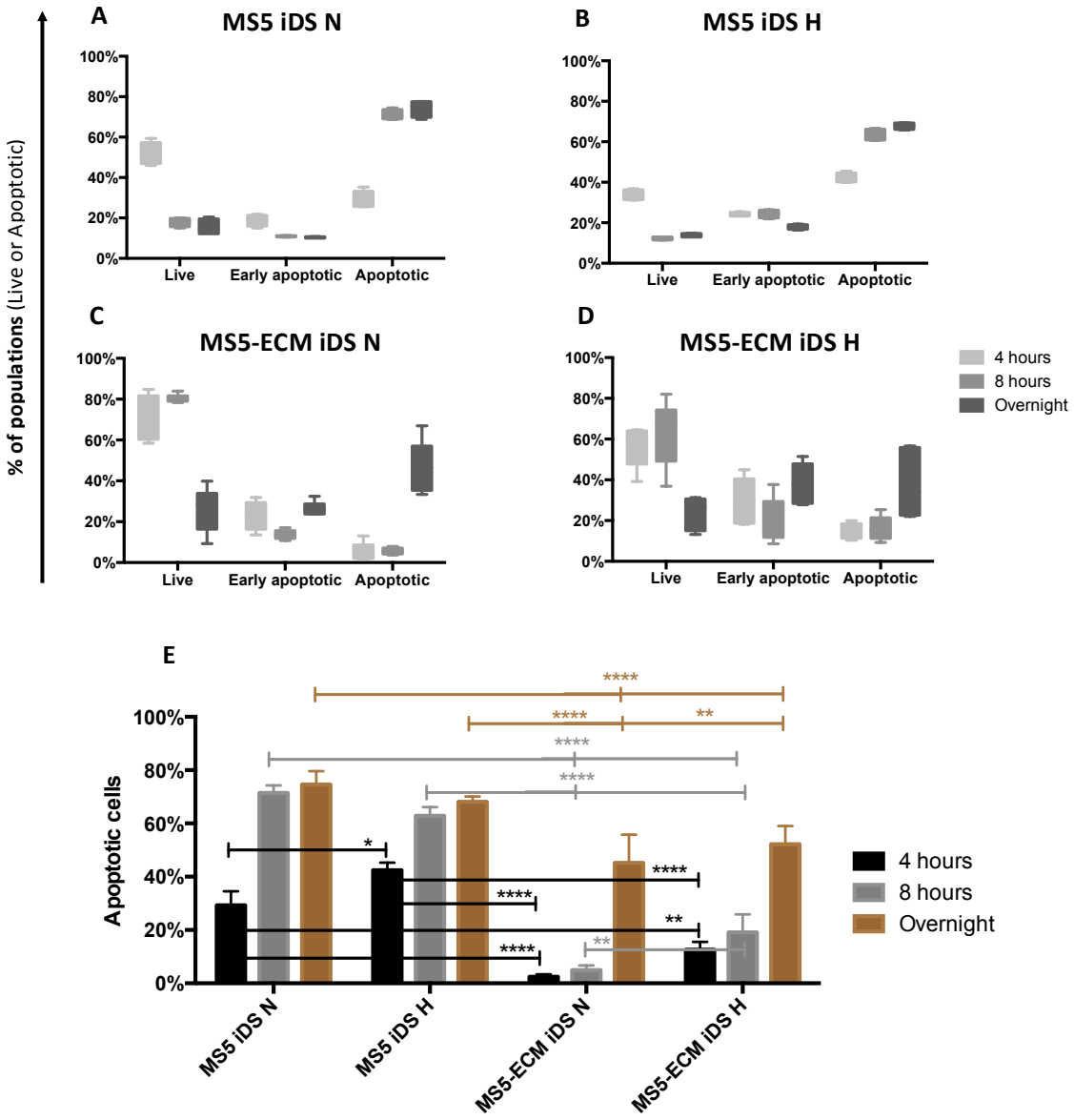

Figure 5.10 - Percentage of MS5 iDS cell in different viable stages, after 4 h, 8 h or overnight treatment with apoptosis inducible reagent. **A** and **B** shows MS5 iDS cells cultured for 2 days in normoxia and hypoxia, respectively. **C** and **D** shows MS5-ECM iDS - ECM cultured for 7 days in normoxia and hypoxia, respectively. **E** shows just apoptotic cells from four conditions. Results represent 1 experiment with triplicates.

First of all, these results show that 4 hours was not enough time to have all cells dead, in the four conditions. Second, results show that MS5 iDS cells in the presence of ECM take longer to die, as there are more live cells in the presence of ECM at 4 and 8 hours (**Figure 5.10 A-D**). Third, hypoxia seems not to interfere with the apoptotic process as there were no significant differences in presence or absence of ECM between normoxic and hypoxic conditions (**Figure 5.10 E**).

5.3.2.3 Immunocytochemistry staining

To prove that the generated matrices, using both methods, contained the common ECM proteins, immunocytochemical (ICC) staining was performed to identify collagen IV, collagen VI, thrombospondin, laminin, heparin sulphate and fibronectin (**Figure 5.11**). DAPI staining was used to detect remaining nuclei.

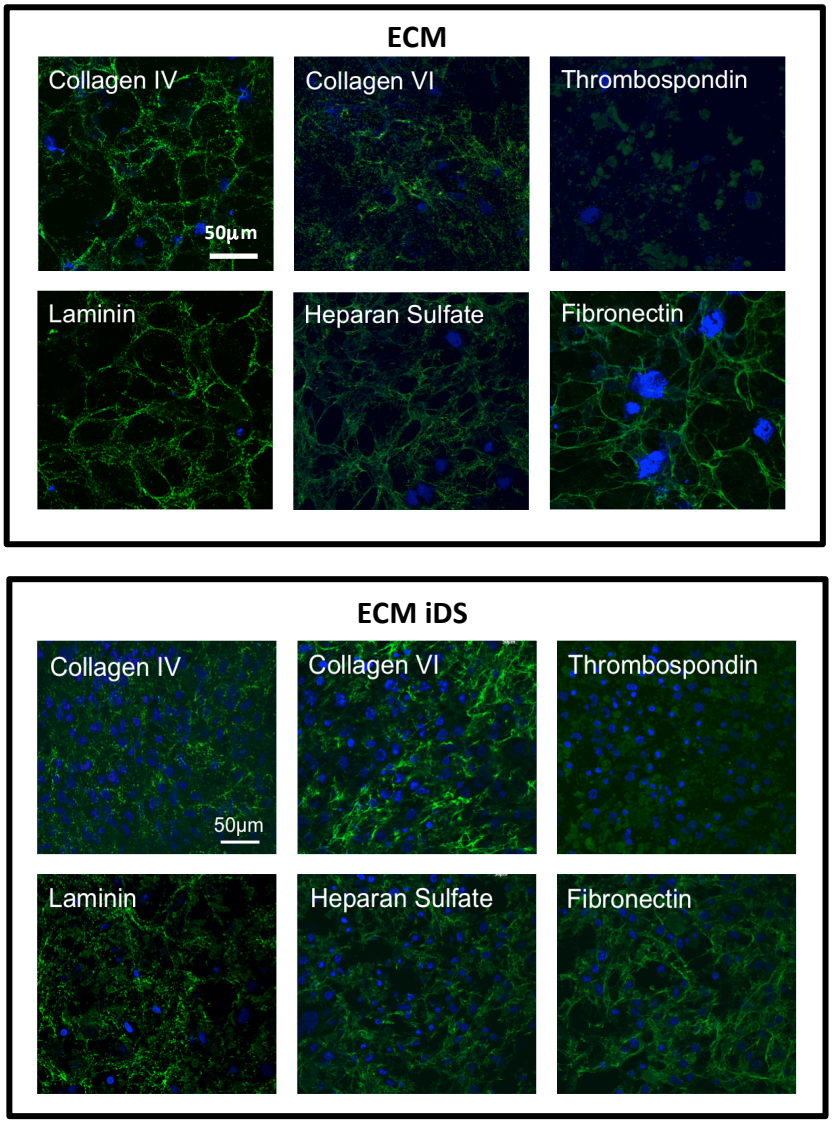

Figure 5.11 - Immunocytochemistry staining. Representative pictures of ECM H (top) and ECM iDS H (bottom) from one experiment, no differences were found in normoxia and hypoxia pictures.

As shown in **Figure 5.11**, both ECM preparations contain the common ECM proteins. However, in both methods of decellularization, nuclei or nuclear remnants (or ghosts) were found, more in ECM than ECM iDS.

Staining for other important proteins including, integrin and aggrecan, was also performed. However these antibodies did not appear to work. Since it was used the confocal

Olympus microscope to take pictures of matrices, it was possible, by always keeping the same settings, to quantify and compare protein expression between matrices. The mean grey value (obtain by the Fluoview 10ASW software) of each antibody fluorescence was used for protein quantification, using 4 different fields from each staining/protein.

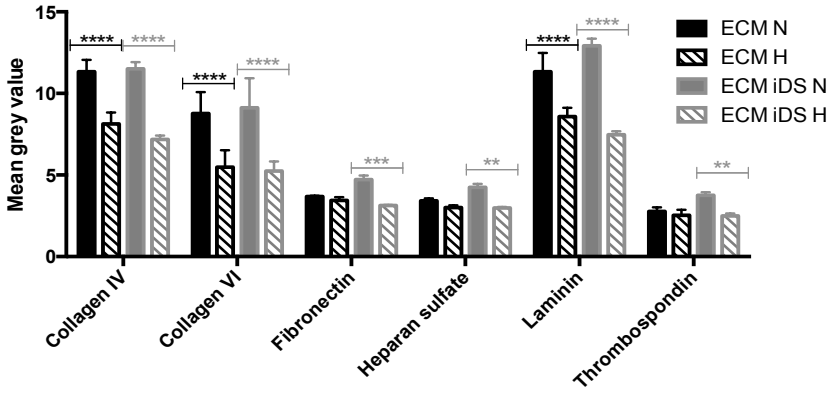

Figure 5.12 - Mean grey value of protein fluorescence of four matrices. Mean and standard deviation of 4 different fields, one experiment of two. Statistic differences are compared with hypoxic conditions. Two-way-ANOVA * P<0.05, ** P<0.01, *** P<0.001 and **** P<0.0001.

Figure 5.12 shows that collagen IV, VI and laminin were significantly highly expressed on ECM N, compared with ECM H. In contrast, there was no difference in fibronectin, heparin sulfate and thrombospondin. In the case of ECM iDS, all proteins were expressed in greater quantities in normoxia. Results also show that there are no big differences between decellularization methods. Collagen IV, VI and laminin were also the proteins with higher mean grey value when compared with other proteins. This quantification needs to be considered with care since it could depend on antibody concentration. The concentrations of antibodies used were optimized previously by titration experiments and were used at saturating concentrations, meaning that with that antibody concentration all proteins were identified optimally.

To confirm the above results, Western blots were performed using NuPAGE 3-8% tris-acetate protein gels. However, these ECM proteins are macromolecular proteins and it was not possible to compare ECM preparations by Western blot, therefore it was not possible to corroborate the results obtained by FloView software.

5.3.2.4 MS5 and MS5 iDS expression of ECM related genes

To try to correlate protein expression with transcripts encoding the corresponding proteins, expression of ECM related gene transcripts in RNA isolated from MS5 and MS5 iDS cells cultured in normoxia and hypoxia, was determined. Expression of transcripts encoding

Col4α1 (collagen IV), Col6α1 (collagen VI), fibronectin, HSPG2 (heparan sulphate) and Lamb2 (laminin) were quantified. Taking advantage of the availability of other primers, additional genes were also studied, including: integrin β1, Acan (aggrecan), Adam9 (disintegrin, metalloproteinase) and Col2 (collagen II). Regarding MS5 cells, there did not appear to be changes in gene transcripts for collagen IV, VI and laminin, between cells cultured either in normoxia or hypoxia; in both conditions the genes were expressed at very similar levels (**Figure 5.13** top). Interestingly, aggrecan and collagen II were more highly expressed in hypoxic cells.

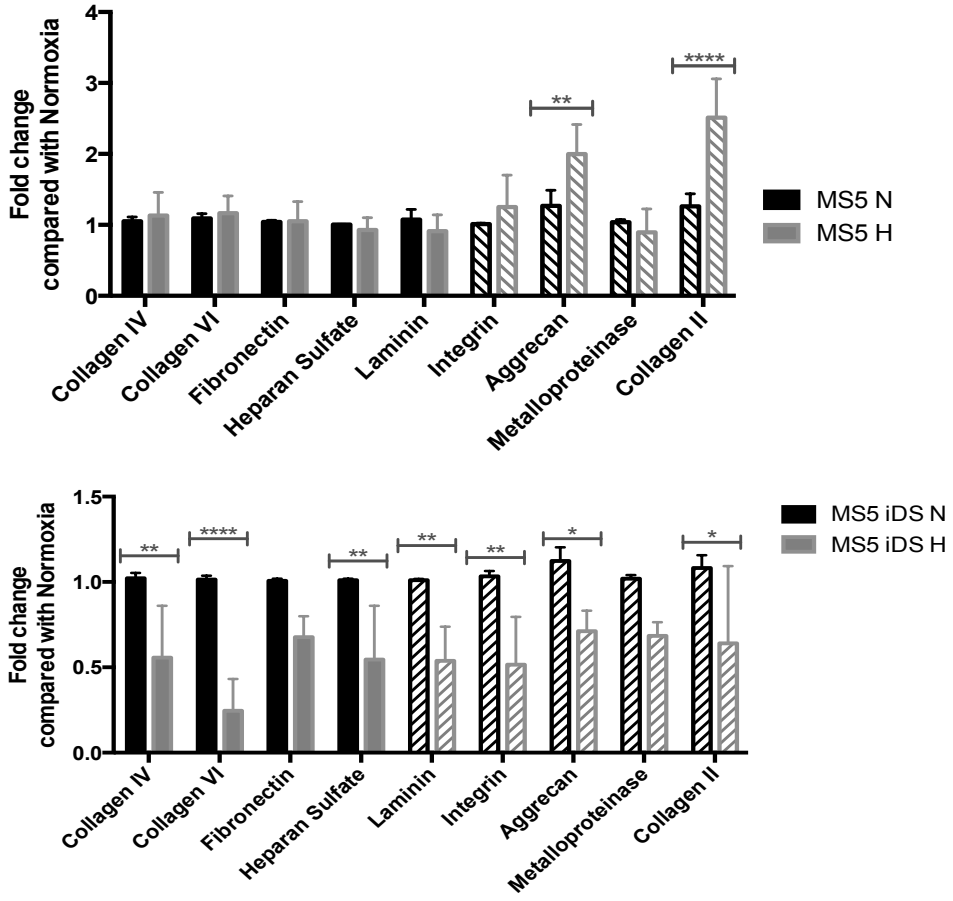

Figure 5.13 - Gene expression of ECM related genes by MS5 (top) and MS5 iDS (bottom) cells cultured in normoxia and hypoxia. Full bars are genes that could be correlated with ICC protein expression. Results represent 4 RT-PCR runs with triplicates and samples were normalized to cells cultured in normoxia. Two-way-ANOVA * P<0.05, ** P<0.01, *** P<0.001 and **** P<0.0001.

In contrast, and as shown in **Figure 5.13**, in the lower histograms, transcripts for all the genes from MS5 iDS cells cultured in hypoxia were down-regulated compared to the normoxic sample. Changes in gene expression were statistically significant for all genes measured except fibronectin and metalloproteinase.

Results of RT-PCR analysis of MS5 iDS cells seemed to correlate approximately with results from ICC analysis in that in hypoxia, there was a reduction in transcripts encoding for

ECM proteins and a corresponding reduction in protein expressed. However, this correlation was not found for control MS5 cells.

5.3.2.5 MS5 and MS5 iDS cell density

To ensure that in normoxia and hypoxia the same number of cells were producing matrix and confirming that the differences between matrices were related with hypoxia and not because of differences in cell number, MS5 (**Figure 5.14 A**) and MS5 iDS (**Figure 5.14 B**) cells were grown in normoxic and hypoxic conditions and cell counts determined.

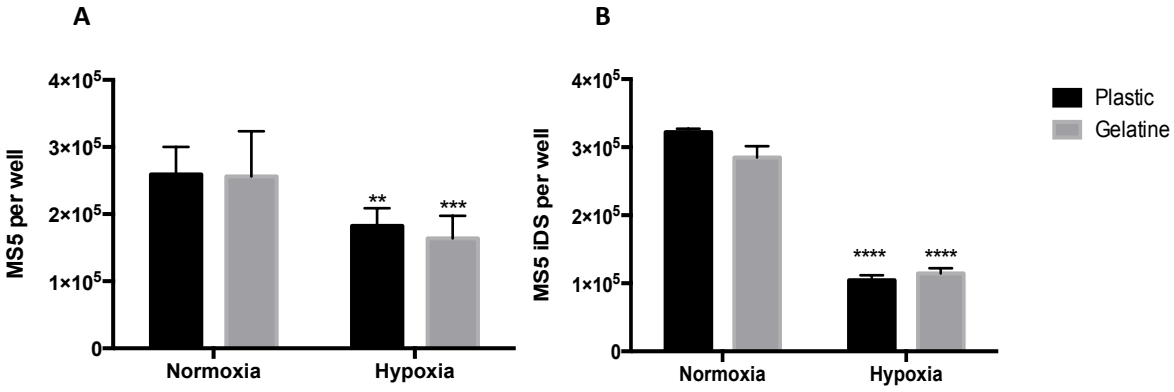

Figure 5.14 - MS5 (A) and MS5 iDS (B) proliferation. Cells cultured in normoxia and hypoxia, directly on plastic or on coated gelatine wells. Following 3 days cells were counted (n=3). Statistic differences are compared with normoxia. Two-way-ANOVA * P<0.05, ** P<0.01, *** P<0.001 and **** P<0.0001.

Initially, $3x10^4$ MS5 and MS5 iDS cells were seeded per well, the same high cell density used to prepare the matrices. After 3 days, (corresponding to the time Mitomicyn C treatment lasted), the cells were counted. Results show that when cells were grown in hypoxia, either on plastic or gelatine, there were significantly fewer cells per well. This result suggests that cells plated at high cell density did not proliferate so much in hypoxic conditions. MS5 and MS5 iDS cells in normoxia proliferated 1.5 and 3 fold respectively more than in hypoxia. However, the results also suggest that gelatine did not interfere with cell growth.

5.3.2.6 Proteomic characterization

Preliminary proteomic results had suggested that there were differences between ECM N and ECM H. For these reasons, new ECM N, ECM H, ECM iDS N and ECM iDS H preparations were sent for proteomic analyses to compare compositions.

First of all, using a mathematical model, the different samples were clustered to confirm that the duplicates were similar. **Figure 5.15** shows exactly that, ECM N1 - ECM N2 and ECM H1 - ECM H2 were clustered, as well as ECM iDS N1 - ECM iDS N2 and ECM iDS H1 - ECM iDS H2, as expected. Using a different analysis, **Figure 5.16** also shows that there are huge

differences in protein expression between matrices. This figure represents a 3D principal component analysis that emphasizes variation between samples. This technique is used to bring out strong patterns between samples. The figure, besides showing that there are big variations between matrices (the four matrices are in different axis), also shows that the duplicated samples are clustered.

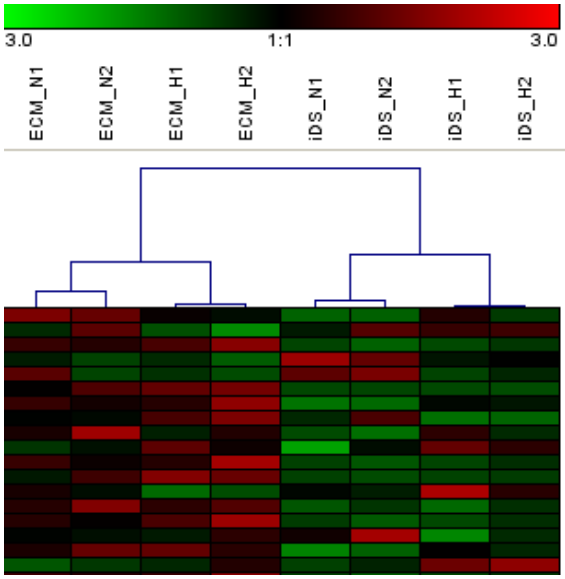

Figure 5.15 - Hierarchical Clustering.

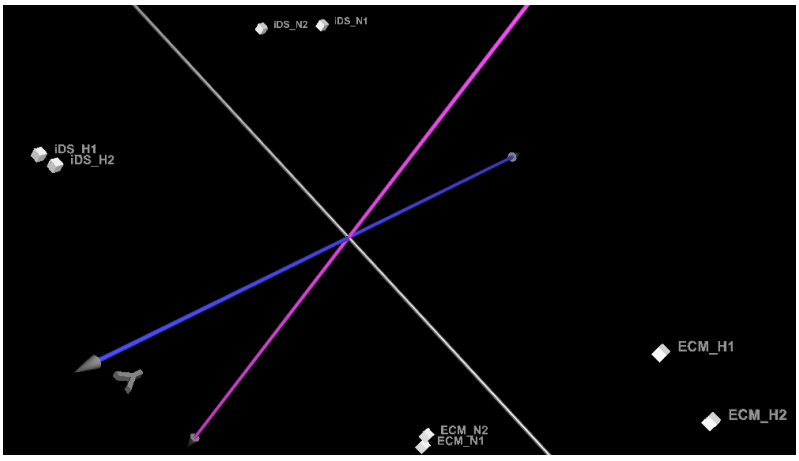

Figure 5.16 - Principal component analysis.

Concerning to the number of proteins, it was possible to observe that ECM N had more proteins (2 230) compared with ECM H (1 826), and 1 630 proteins were common (**Figure 5.17 A**). ECM iDS N and ECM iDS H had almost the same number of proteins, 3 453 and 3 350, respectively (**Figure 5.17 B**). Comparing ECM and ECM iDS, ECM iDS had more proteins in both conditions. Regarding the 4 matrices, there were 1 137 common proteins. ECM N vs ECM iDS N had more common proteins (1 475) than ECM H vs ECM iDS H (1 232), and ECM N and vs ECM iDS H (1 453) and ECM H vs ECM iDS N (1 234), had almost the same number of common proteins than ECM iDS N and ECM iDS H (**Figure 5.17 C**).

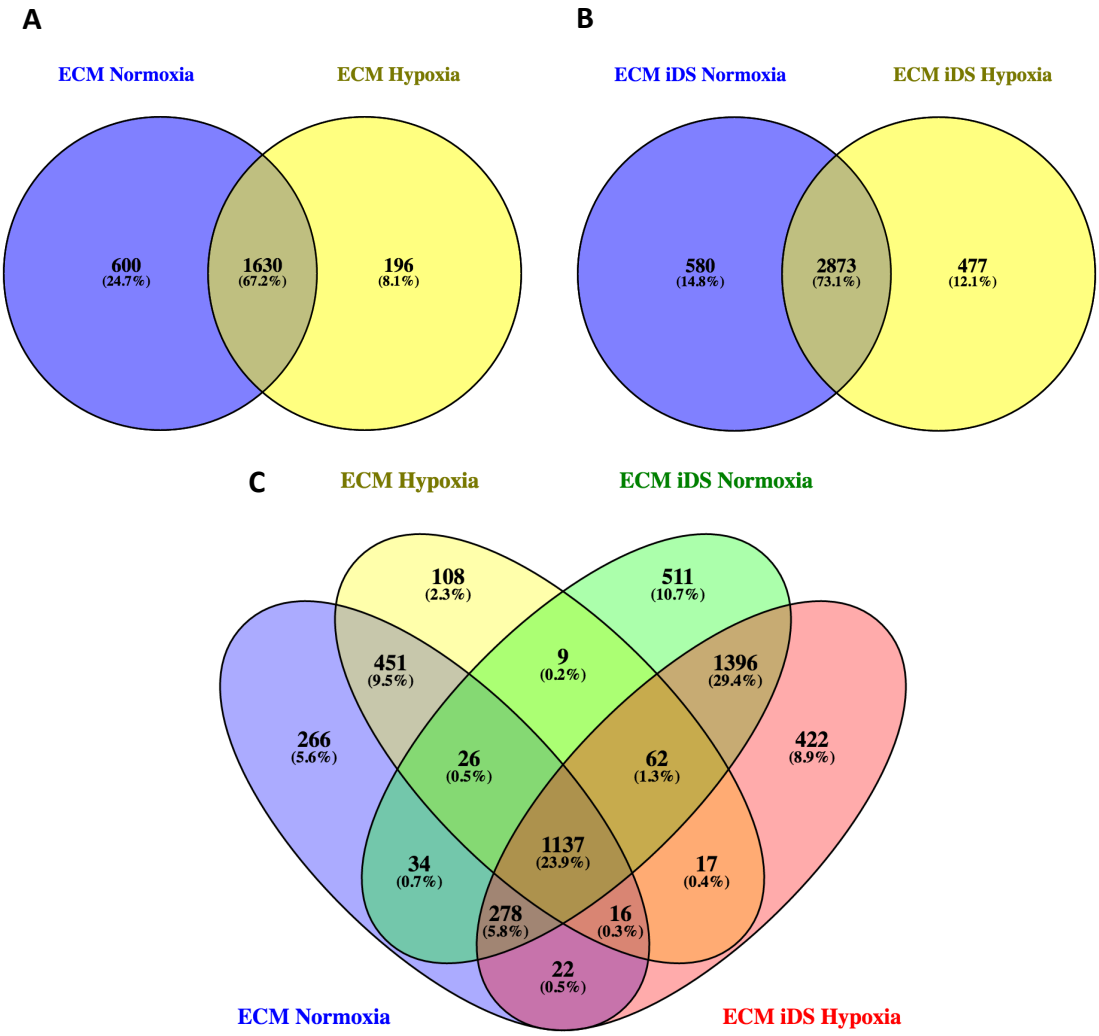

Figure 5.17 - Venn diagram. Common proteins in different conditions. **A** comparing ECM N and H, **B** comparing ECM iDS N and H and **C** comparing the 4 matrices.

Regarding the ECM related proteins, **Figure 5.18** shows that there was a higher fold change in ECM samples compared with than ECM iDS, especially with collagen VI. Thus, ECM H had more than a 4 fold increase of collagen VI, around 3 fold increase of collagen IV and integrin, and around 2 fold increase of fibronectin, heparin sulphate, laminin and thrombospondin. With ECM iDS H increases in protein expression were only about 1.5 fold, except collagen VI where there was hardly any difference between N and H. These results do not corroborate with the results obtained by ICC staining and mean grey value analysis. These results also do not correlate with gene expression of ECM related proteins, where MS5 had no difference in gene expression between N and H, whereas MS5 iDS had a significant difference between N and H.

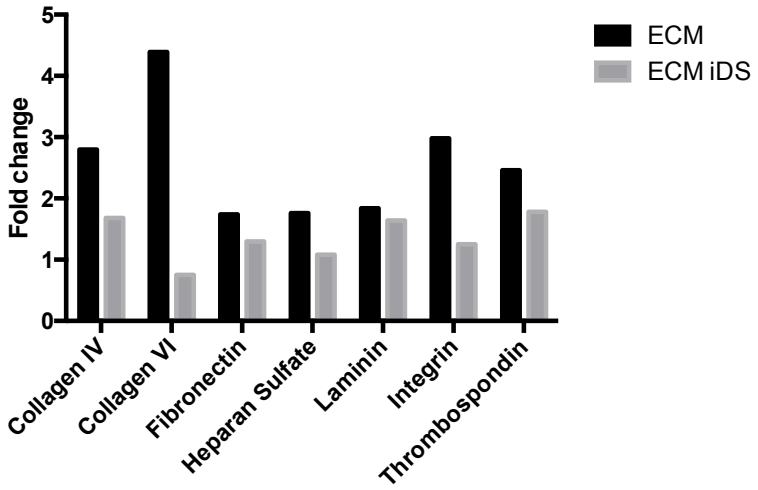

Figure 5.18 - Fold change hypoxia/normoxia of ECM proteins.

Regarding the proteomic results in general, several software packages were used and different analysis carried out. The general analysis provides results regarding: molecular function, cellular component, biological process, gene ontology, protein classes and pathways. In Annex B the complete results are presented in form of graphs, however in order to more easily understand the results, the two tables below (**Table 5.3** and **Table 5.4**) summarize these results. The first table confirms that there were more nuclei in the ECM iDS preparations than in ECM, as well as cytoplasmic proteins (blue box).

Table 5.3 - Functional categories where proteins were found in higher concentration or the most relevant to ECM study.

Functional categories:	ECM N	ECM H	ECM iDS N	ECM iDS
Acetylation	833	713	1177	1203
Phosphoprotein	942	781	1536	1563
Cytoplasm	510	403	848	874
ATP-binding	259	204	376	335
Oxidoreductase	145	126	186	180
Transport	207	167	357	344
Endoplasmic reticulum	102	88	186	161
Hydrolase	164	-	299	296
Transferases	144	-	270	241
Coiled coil	-	154	299	307
Nucleus	-	-	674	708
Glycolysis	22	24	23	23
Cell cycle	72	50	109	109
Cell division	47	35	74	71
Mitoses	35	24	50	47

Table 5.4 - Pathways where proteins were found in higher concentration or the most relevant to ECM study.

Pathways:	ECM N	ECM H	ECM iDS N	ECM iDS
Oxidative phosphorilation	53	48	72	61
Glycolysis/gluconeogenisis	29	30	32	32
Focal adhesion	56	57	66	62
Pyruvate metabolism	19	21	22	24
DNA replication	17	17	17	18
ECM-receptor interaction	-	20	-	-

Table 5.5 - Stem cell regulation and biomarkers present in ECM and ECM iDS normoxia and hypoxia overlay.

	Negative regulation stem cell differentiation:		**Biomarkers of stem cell:**	
	Proteins present in the sample	**Total proteins**	**Proteins present in the sample**	**Total proteins**
ECM	3	31	3	52
ECM iDS	-	31	-	52

It was also possible to observe from these two tables, that there were no significant differences between metabolic proteins between N and H in both matrices (orange boxes). This can be explained by the fact that ECM samples were analysed rather than cells, therefore these results mean that there was no difference in the metabolic proteins on the matrices, however this did not mean that there were no differences in the cells cultured in N and H.

Interestingly, there were more proteins involved in cell cycle and cell division on ECM iDS compared with ECM.

According to pathway analysis, several proteins in all preparations were present, while just ECM H is the only one with proteins specific for ECM-receptor interactions (green pathways) (**Table 5.4**).

When ECM N and H where compared, the results suggest that the ECM had a negative regulatory effect on stem cell differentiation, having 3 proteins of 31, and 3 of 52 biomarkers of induction of pluripotent stem cell, while these proteins were not present on ECM iDS N and H (**Table 5.5**). When ECM iDS N and H where compared, 15 of 232 proteins of apoptotic pathway were present. Regarding biomarkers, these ECM iDS had adipocyte biomarkers present.

The following figures show the proteins present in each sample according to: biological process, cellular component and class of proteins.

Figure 5.19 - Proteins involved in biological process. All graphs have the same legend except ECM iDS N that has one more process "cell killing" (red arrow). Results generated by Panther software.

Figure 5.20 - Proteins present in cellular components. All graphs have the same legend except ECM iDS N that has one more component "synapse" (red arrow). Results generated by Panther software.

ECM N

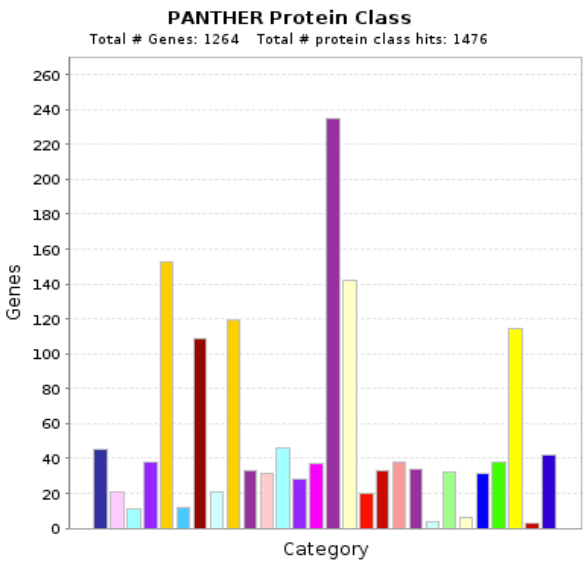

ECM H

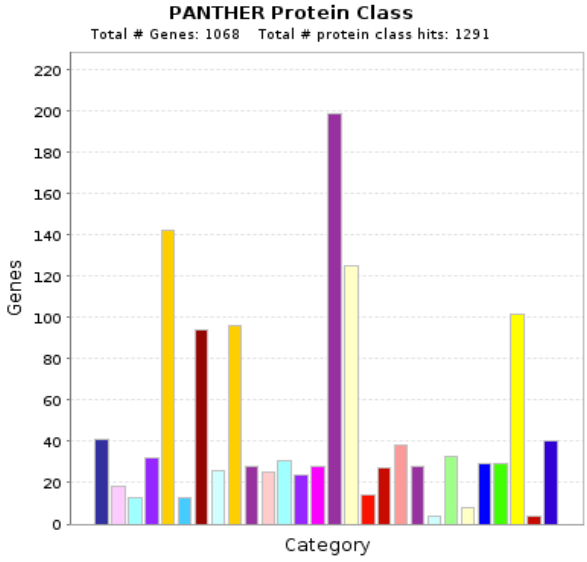

ECM iDS N

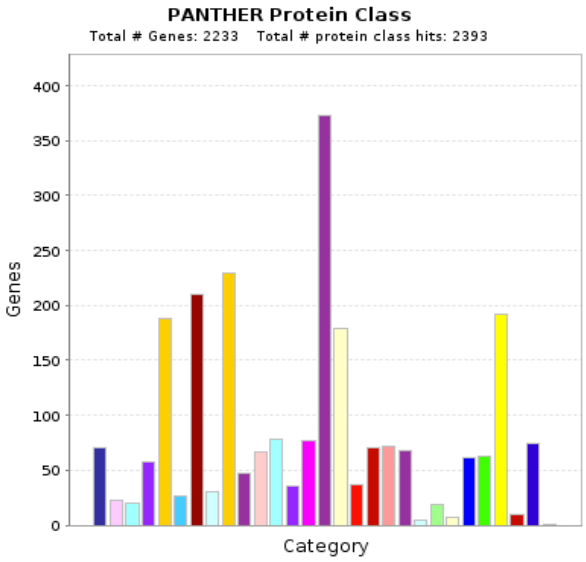

ECM iDS H

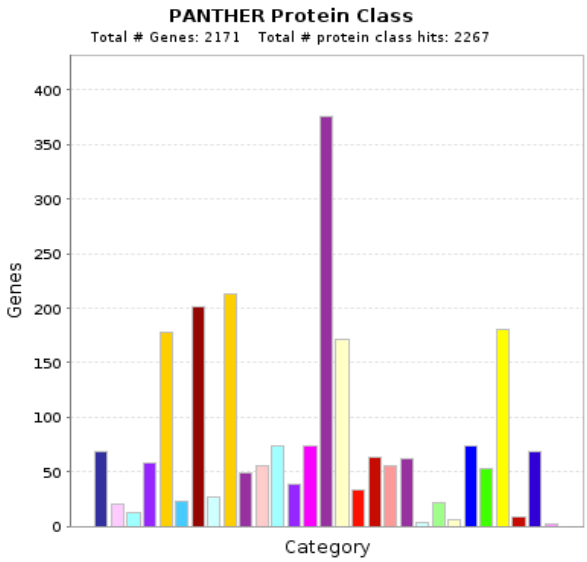

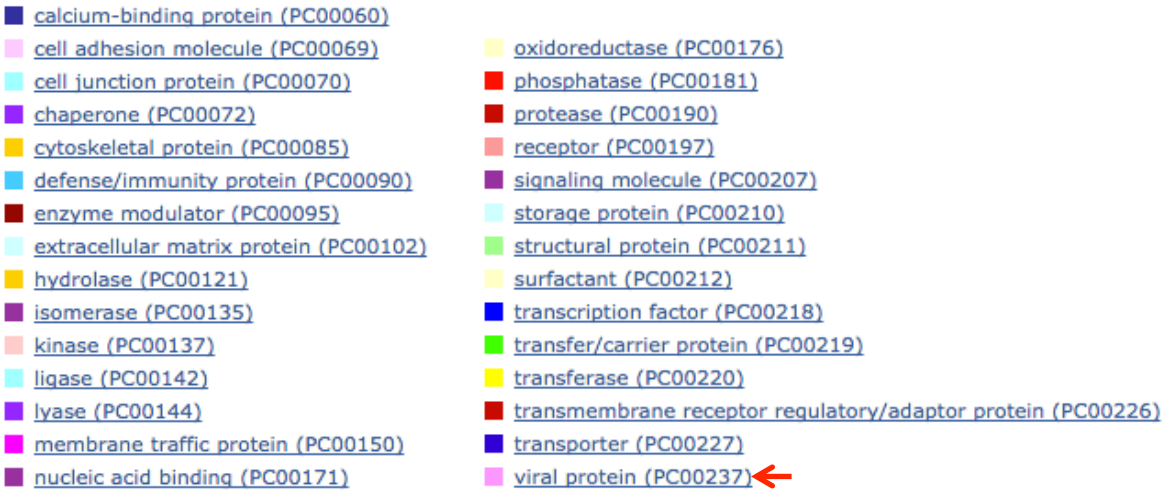

Figure 5.21 - Proteins class. All graphs have the same legend except ECM iDS N that has one more protein class “viral protein” (red arrow). Results generated by Panther software.

This analysis provides insight into the different proteins present in the samples involved in biological processes and cellular components. According to these results there are no significant differences between all matrices, except ECM iDS N that present an extra biological process, cellular component and protein class.

In general, the results show that proteins involved in cellular and metabolic processes are the most abundant in all matrices (**Figure 5.19**).

According with cellular components there were more cell parts proteins, and macromolecular complexes and organelle related proteins (**Figure 5.20**).

Regarding to protein classes: nucleic acid binding, cytoskeletal proteins, enzyme modulator, hydrolase, oxidoreductase and transferase are the most common in all matrices (**Figure 5.21**).

More results can be found in Annex B.

5.3.3 Biologic role of matrices

5.3.3.1 Release of inflammatory cytokines and DAMPs

One aspect of ECM biology includes the effect of culturing cells on dishes pre-coated with ECM. It was important to investigate if ECM prepared from MS5 or MS5 iDS cells contained substances capable of inducing inflammatory reactions or inadvertently stimulating cultured cells. Apoptosis is a stressful event leading to the release of inflammatory cytokines and DAMPs. Following apoptosis and lysis these molecules are released, even after washes, and can probably get trapped in the matrices. Also lysis by osmotic shock leads to the release of cell contents that can lead to an immunogenic effect.

To confirm if the different matrices had inflammatory cytokines and DAMPs, the supernatants of these samples were used to identify the presence of these molecules.

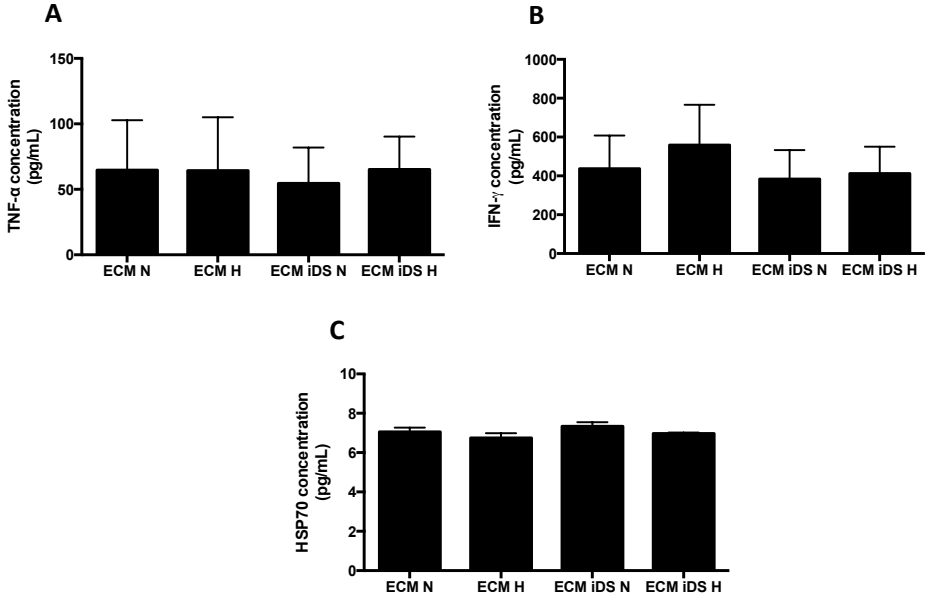

Figure 5.22 - ELISA results. **A**, **B** and **C** show TNF-α, IFN-γ and HSP70 concentrations, respectively, measured in the ECM N, ECM H, ECM iDS N and ECM iDS H supernatants (n=2, triplicated). No statistically significant differences were found.

No differences were found between ECM prepared in normoxia and hypoxia as regards TNF-α, IFN-γ and DAMP (HSP70) concentrations. The cytokine IFN-γ was found in higher concentration compared with the other cytokine TNF-α and the DAMP, HSP70.

5.3.3.2 Induction of inflammation

Following identification of the presence of inflammatory cytokines and HSP70 in the supernatants of the matrices, these results did not indicate if they could initiate an inflammatory response on cells. For this reason different cells were cultured on top of the four

ECMs. Cells were then stained for intracytoplasmic cytokines, an indirect measure of whether they had been activated.

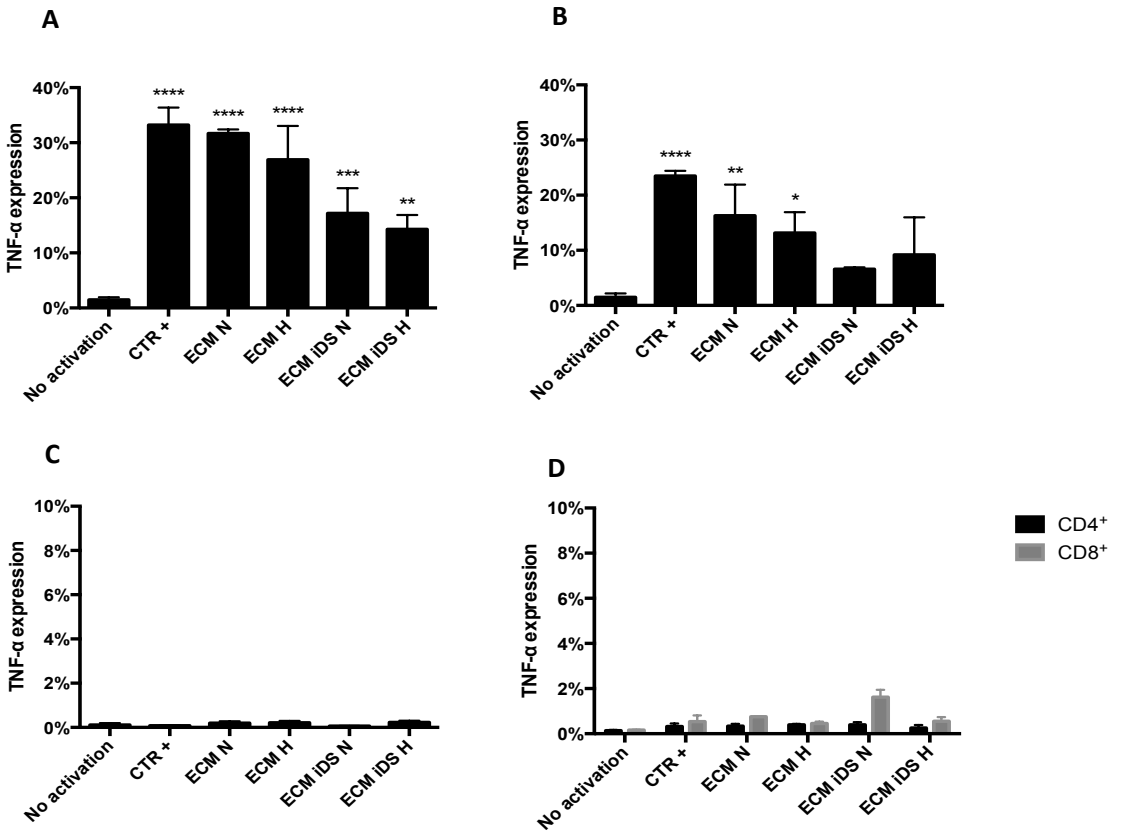

Figure 5.23 - Percentage of TNF-α expression by cell lines and primary cells after 24 h culture on top of matrices. **A** shows Raw 264.7 (P_9-P_{11}) and panel **B** J774A.1 (P_{10}-P_{11}), panel **C** Balb/c (P_7-P_{10}) and panel **D** $CD4^+$ and $CD8^+$ T cells (n=3). Statistic differences are compared with no activation. Two-way-ANOVA * P<0.05, ** P<0.01, *** P<0.001 and **** P<0.0001.

As shown in **Figure 5.23**, all matrices were capable of inducing intracytoplasmic expression of TNF-α in Raw 264.7 cell line; thus between 30 and 20% cells were expressing TNF-α. ECM prepared by lysis, was also able to stimulate J774A.1 cells, with less than 20% expressing TNF-α. However, Balb/c MSC cultured on top of the four matrices did not express any TNF-α, as was the case with primary T cells, where less than 2% expressed TNF-α.

5.3.3.3 Balb/c MSC immunophenotyping

Passage 10 Balb/c mouse MSC (P_{10}) were characterized by positive expression of CD29, CD44, CD49e, CD105 and Sca-1; and for lack of expression of MHC II, CD11b, CD34 and CD45 (**Figure 5.24**). For CD73 and CD90.2, expression levels were relatively low.

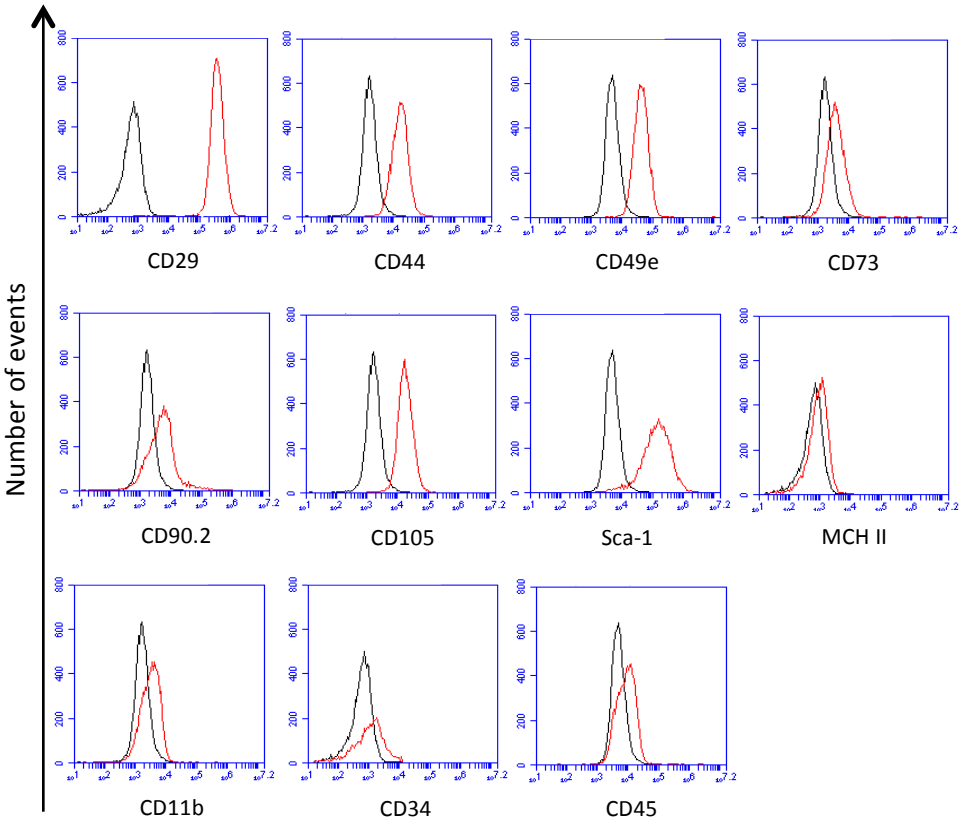

Figure 5.24 - Balb/c mouse MSC immunophenotyping. Red lines indicate the labelled antibodies and the black line the corresponding isotype control.

5.3.3.4 Mouse BM-MSC adipogenic and osteogenic differentiation on top of matrices

To better understand if ECM or hypoxia had an influence on MSC differentiation, Balb/c MSC were cultured on top of ECM N, ECM H, ECM iDS N and ECM iDS H, plastic N and plastic H, and differentiation assays were performed on these samples.

5.3.3.4.1 Lipid identification and quantification

Adipogenic differentiation assay is successful when lipid droplets can be found within differentiated cells. These stored lipids can be used for energy, steroid synthesis, or membrane formation. Oil red O staining allows the detection of these lipid droplets.

Balb/c mouse MSC were able to differentiate into adipocytes directly on plastic culture plates and on top the four matrices. **Figure 5.25** shows distinct lipid droplets on Balb/c cultured in presence of adipogenic media, when compared with control conditions (top pictures).

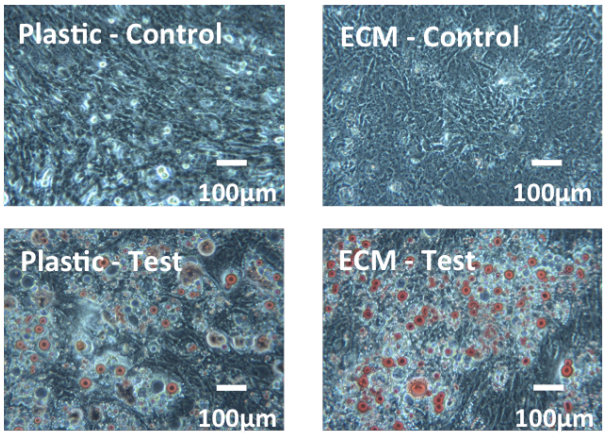

Figure 5.25 - Balb/c adipogenic differentiation, Oil red O staining. On top are control samples and on the bottom Balb/c that were culture with Adipogenic media. Left shows Balb/c cultured directly in plastic while on the right the cells were cultures on top of ECM. Representative pictures of one experiment, no differences were found between ECM iDS N and ECM iDS H conditions.

To compare the accumulation of cytoplasmic lipids in the cells differentiated under different conditions, Oil Red O was extracted using isopropanol. The absorbance of the extracted Oil Red O was spectrophotometrically determined at 520 nm to measure lipid accumulation.

First, to observe if hypoxia had an effect on Balb/c MSC adipogenic differentiation capacity, differences between several normoxia-hypoxia combinations were compared on plastic (**Figure 5.26**). **Figure 5.26** A shows just the test samples, while in B the control samples are also shown, in order to demonstrate that the cells differentiated.

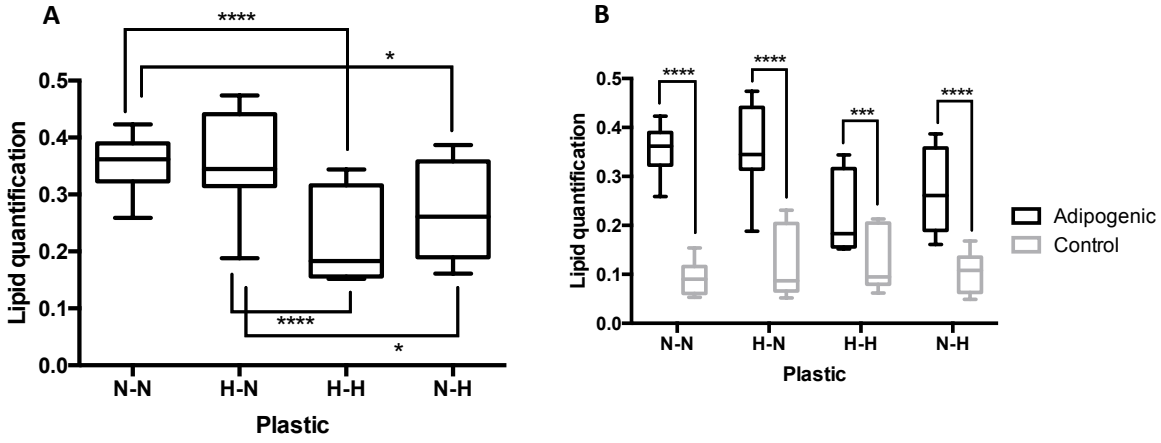

Figure 5.26 - Lipid quantification following Oil red O staining spectrophotometrically determined at 520 nm. **A** and **B** shows the lipid accumulation of Balb/c cells differentiated into adipocytes in different normoxia-hypoxia combinations in plastic tissue culture plates. In the *X* axis the first letter represents the condition that the Balb/c were before differentiation and the second letter indicates the condition that the cells were during adipogenic differentiation. The graph represent 5 experiments and triplicates, 15 wells were analysed. Control wells (in grey) had significantly lower accumulation of lipids (**B**). Two-way-ANOVA * P<0.05, ** P<0.01, *** P<0.001 and **** P<0.0001.

The results show that, when the assay was performed in plastic tissue culture plates, there were significant differences in adipogenesis in normoxia compared to hypoxia conditions. However, there were no differences when the Balb/c MSC were in normoxia and hypoxia before differentiation, and changed to hypoxia or normoxia during adipogenic differentiation. For this reason and to be easier to interpret the results, the following data were relative to Balb/c MSC that were in culture in normoxia and were differentiated in normoxia, as well as cells that were cultured in hypoxia and differentiated in hypoxia. Complete results are presented in Annex C.

When cells were differentiated under different ECM conditions, and the lipid accumulation was compared, the results showed that MSC differentiated in plastic N and ECM iDS N were the conditions with the highest lipid concentrations (**Figure 5.27**). While there were no differences between normoxia and hypoxia with ECM prepared by the lysis method.

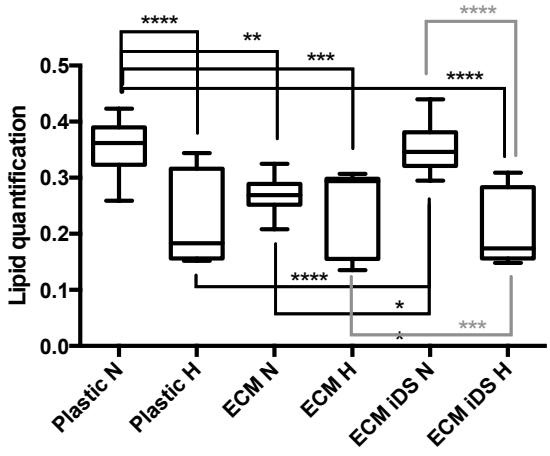

Figure 5.27 - Lipid quantification following Oil red O staining spectrophotometrically determined at 520 nm. Lipid accumulation of Balb/c differentiated into adipocytes in different conditions. The graph represent 5 experiments and triplicates, 15 wells were analysed. Control wells had significantly lower accumulation of lipids. Two-way-ANOVA * P<0.05, ** P<0.01, *** P<0.001 and **** P<0.0001.

5.3.3.4.2 Calcium identification and quantification

To study the role of oxygen and ECM during osteogenic differentiation, Balb/c MSC were differentiated in normoxic and hypoxic conditions in plastic and on top of matrices. To demonstrate the osteogenic differentiation capacity of Balb/c MSC, calcium accumulation was quantified by Alizarin red S staining (**Figure 5.28**).

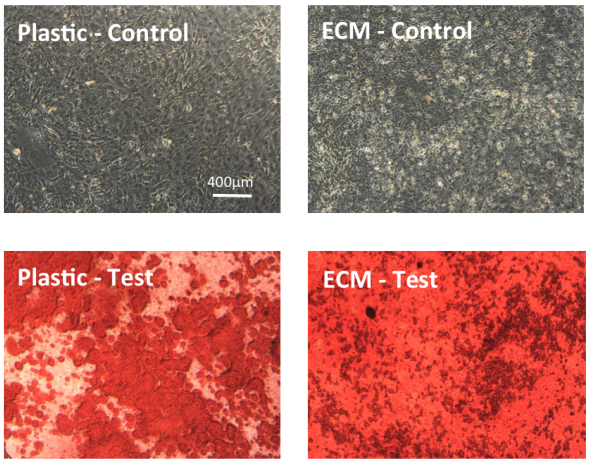

Figure 5.28 - Balb/c osteogenic differentiation, Alizarin red S staining. On top are control samples and on the bottom Balb/c MSC that were cultured with osteogenic media. Left shows Balb/c cultured directly in plastic while on the right the cells were cultured on top of ECM iDS. Representative pictures of one experiment; no differences were found between ECM N and ECM H conditions.

Balb/c MSC were able to differentiate into osteocytes in plastic culture plates and on top of matrices. The figure shows representative examples of calcium deposition in test samples compared with control conditions.

Then, to compare the calcium accumulation on differentiated cells in different conditions, a Calcium LiquiColor kit from Stanbio was used to quantify calcium, using different wells from the Alizarin red S staining.

However it was noticed that, in different experiments performed with the same cells, there were wide variations in calcium concentrations. **Figure 5.29** shows that, in Experiment 1, hypoxia was associated with a modest but significant increase in osteogenesis when cells were cultured on plastic alone. However, in Experiment 2, the levels of calcium accumulation were considerably lower and there was no significant difference between normoxia and hypoxia. So, regarding osteogenic differentiation on plastic, differences between normoxia and hypoxia were inconsistent.

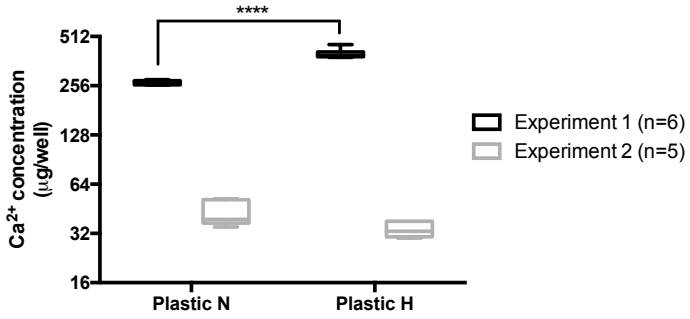

Figure 5.29 - Calcium quantification following Balb/c osteogenic differentiation in normoxic and hypoxic conditions, directly on plastic. The graph represents 2 experiments with a total of 11 wells analysed. Control wells had significantly lower calcium concentration. Two-way-ANOVA * P<0.05, ** P<0.01, *** P<0.001 and **** P<0.0001.

Despite this variability, **Figure 5.30** shows that some differences were observed between normoxia and hypoxia for some ECM conditions. Here, Balb/c MSC had highest calcium accumulation when they were cultured and differentiated on top of ECM N, compared with other conditions. It is also to be noted that comparing normoxic and hypoxic conditions, in both plastic (left two box plots) and ECM (middle two box plots) conditions, Balb/c MSC had higher calcium concentration in normoxia, whereas there was no significant difference between ECM iDS N and H (right two box plots).

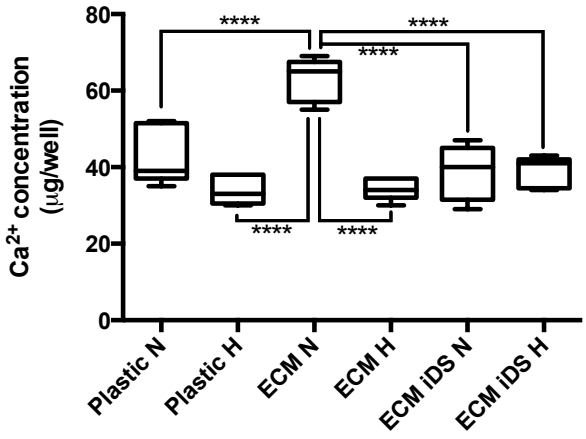

Figure 5.30 - Calcium quantification following Balb/c osteogenic differentiation under different conditions. Control wells had distinctively lower calcium concentration. This graph is a representation of 1 experiment and 5 replicates. Two-way-ANOVA * P<0.05, ** P<0.01, *** P<0.001 and **** P<0.0001.

5.3.3.5 Confirmation of MSC differentiation by RT-PCR

To prove that MSC were expressing transcripts for genes involved in their differentiation and to compare gene expression between different conditions, Balb/c MSC were subjected to differentiation assays under normoxic conditions and expression of adipogenic and osteogenic related genes was quantified (**Figure 5.31**).

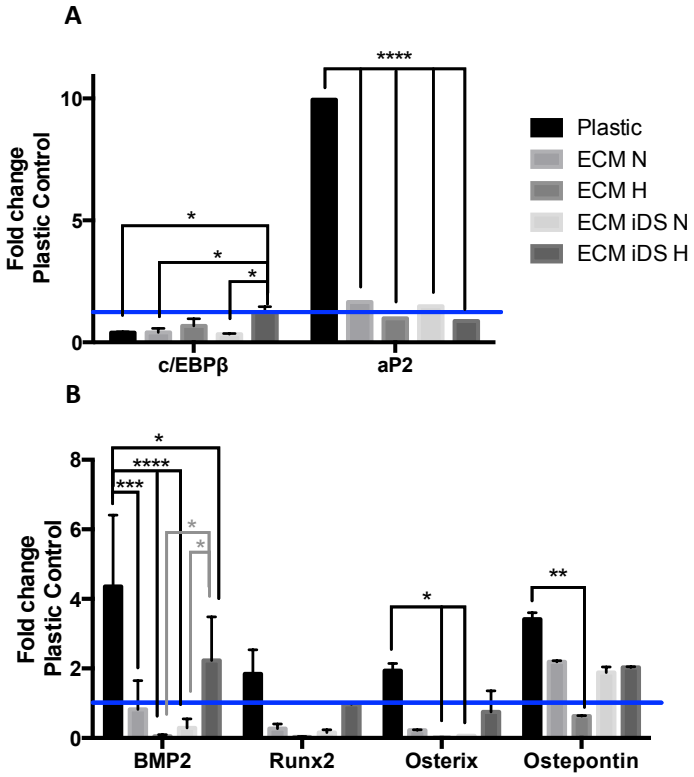

Figure 5.31 - Balb/c gene expression following adipogenic and osteogenic differentiation for one week under normoxic conditions in different conditions. **A** shows adipogenic related genes and **B** osteogenic related genes. Results represent 2 RT-PCR runs with triplicates and samples were normalized to Balb/c cultured in plastic with normal culture medium (blue line). Two-way-ANOVA * P<0.05, ** P<0.01, *** P<0.001 and **** P<0.0001.

In general, the adipogenic related genes c/EBPβ and aP2 were not up-regulated. However, the samples differentiated on top of plastic expressed 10-fold higher levels of mRNA for aP2 compared to control, c/EBPβ was only weakly expressed in all conditions (<0.5).

Regarding the osteogenic related genes BMP2, Runx2, Osterix and Osteopontin, it is evident that Balb/c MSC differentiated on plastic had the highest expression of the four genes followed by cells differentiated on top of ECM iDS H. Comparing ECM N and ECM H, the main difference was that Balb/c MSC cultured on top of ECM N up-regulated osteopontin expression. Comparing ECM iDS N and ECM iDS H, hypoxia generally led to an increased expression of osteogenic genes.

5.3.3.6 Effect of matrices and hypoxia on MSC stemness

To determine if MSC cultured on ECM upregulated expression of transcripts encoding stemness-related gene products, mRNAs for Sox2, Nanog and Oct4 were also quantified.

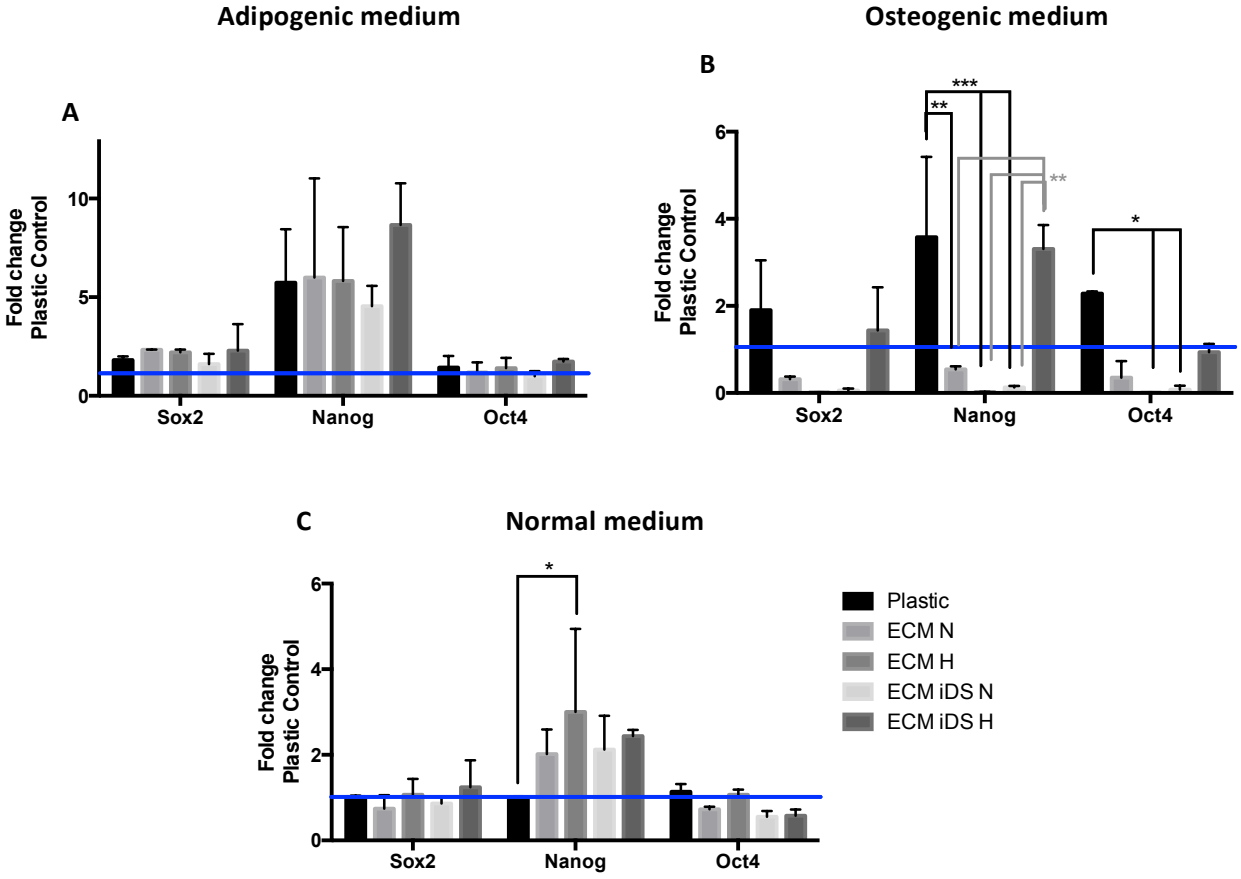

Figure 5.32 - Stem cell gene expressed by Balb/c MSC following adipogenic and osteogenic differentiation for one week under normoxic conditions in different conditions. **A** and **B** show respectively the effect of adipogenic and osteogenic medium on Sox2, Nanog and Oct 4 expression. C shows the effect of normal culture media in the same genes. Results represent 2 RT-PCR runs with triplicates and samples were normalized to Balb/c cultured in plastic with normal culture medium (blue line). Two-way-ANOVA * P<0.05, ** P<0.01, *** P<0.001 and **** P<0.0001.

Figure 5.32 shows clearly that Balb/c MSC cultured in the presence of adipogenic and normal culture media up-regulated Nanog expression in all conditions, whereas levels of Sox2 and Oct4 expression were not very different from plastic control samples. Osteogenic media had a different effect on the expression of these three genes, namely up-regulated in plastic and ECM iDS H conditions, and down-regulated in the other conditions.

To study the kinetics of these stem cell genes, MSC were cultured for 3 and 7 days on plastic and on top of different ECM, with normal culture medium in normoxic conditions (**Figure 5.33**).

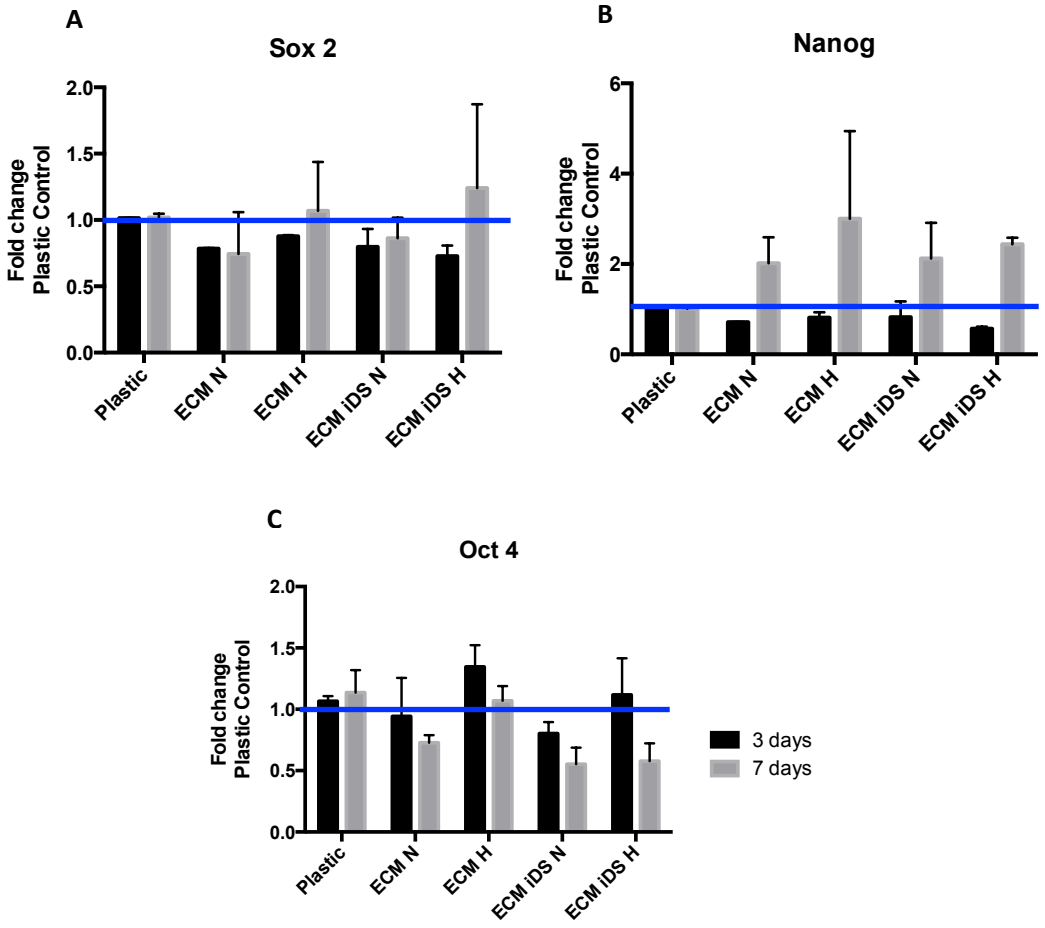

Figure 5.33 - Kinetics of stem cell gene expression. Sox2 (**A**), Nanog (**B**) and Oct4 (**C**) expressed by Balb/c when cultured for 3 and 7 days under normoxic conditions in different conditions. Results represent 2 RT-PCR runs with triplicates. Samples were normalized to Balb/c cultured in plastic (blue line). No statistically significant differences were found.

Expression of Sox2, Nanog and Oct4 at these time points was different. Thus, Sox2 expression did not change from day 3 to day 7 whereas Nanog expression was generally up-regulated at 7 days in the presence of matrices. Regarding Oct4 expression, it seems to be generally down-regulated with time when cells are cultured on ECM.

To study the effect of hypoxia and ECM on MSC stemness properties, a preliminary experiment was performed in which Balb/c MSC were cultured on plastic and on top of matrices under normoxic or hypoxic conditions for 3 days. Stem cell related genes and HIF genes were also quantified (**Figure 5.34**).

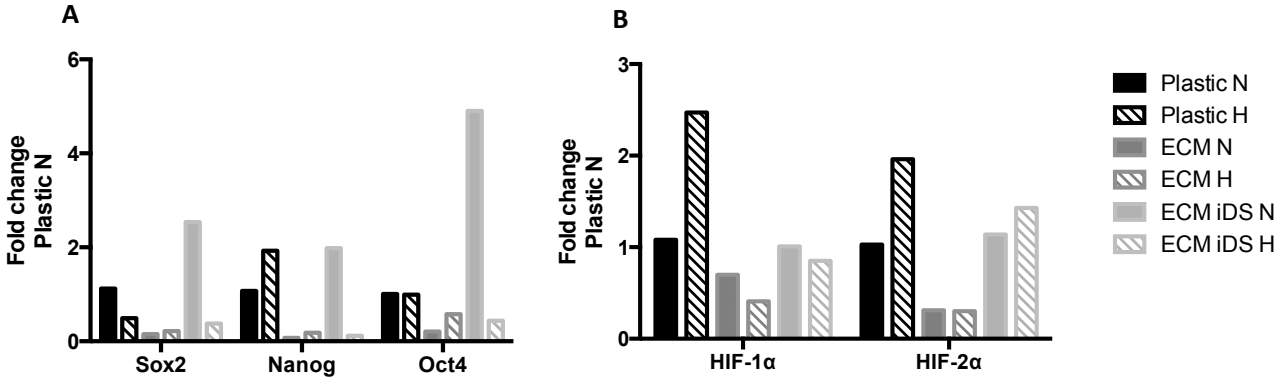

Figure 5.34 - Balb/c gene expression of stemness related genes (**A**) and HIF genes (**B**). Balb/c were cultured for 3 days on plastic or ECM, normoxic or hypoxic conditions. Preliminary results from 1 experiment and 1 RT-PCR run with triplicates. Results were normalized to plastic normoxia.

Results of this experiment, shown in **Figure 5.34**, suggest that on plastic, Balb/c MSC up-regulated Nanog expression in hypoxia, however on ECM iDS normoxia increased the expression of all three genes. With respect to HIF-1 α and HIF-2α, as expected, transcripts of these genes were up-regulated in hypoxia, especially on plastic.

5.4 Discussion

From a biological and clinical point of view, it is important to investigate ECM-cell interactions in order to recognize the role of ECM in the haematopoietic environment and to better understand the outcomes of haematological disorders. ECM is also important from a translational point of view, since ECM scaffolds have been reported to be an attractive option to support the regeneration of several tissues [40-42].

Although almost all cells can produce ECM, certain cells produce matrix in greater abundance, an certain cells produce specialised types of matrix. For example, fibroblasts secrete connective tissue ECM, osteoblasts secrete bone-forming ECM and chondroblasts secrete cartilage-forming ECM [360-362]. In this chapter, ECM produced by MSC was specifically evaluated since one of the main aims of the project was to eventually study the biological effects of ECM produced by MSC on haematopoiesis. Importantly, stromal cells are likely to be a key source of ECM in the bone marrow [363]. The characteristics of ECM produced by MSC are also important for tissue engineering applications, particularly because MSC have multi-lineage differentiation capacity [364].

The composition of ECM is complex and includes structural proteins such as collagens, laminins and fibronectin (which are predominant) as well as polysaccharides, growth factors and integrins (which are less abundant but may mediate critical functions) [11, 330]. As referred above, the composition of ECM depends on the nature of the cells contributing to its production and this characteristically leads to variability in composition and, consequently, to different biologic and mechanotransductive properties [16, 365]. Of particular relevance to haematopoiesis, ECM architecture and composition provides an environment (“niche”) that may greatly influence cell adhesion, proliferation, survival and differentiation of HSC [366].

A variety of matrices have been produced *in vitro* for different proposes. *In vitro* decellularized ECM production can be a particularly valuable approach to studying the role of ECM on cell fate decisions, as it can mimic specific niches that are normally difficult to recreate *in vitro*. Cell-derived decellularized ECM has certain advantages over tissue-derived ECM and synthetic polymers. These advantages include the ability to obtain such material from a small tissue sample and the possibility for large-scale *in vitro* analysis [11]. However, it is important to consider that there are several methods available to produce decellularized ECM and that, to date, all methods described are associated with some damage to the ECM ultrastructure and composition and may also have a subsequent immunogenic effect on cells [341, 343]. Crapo *et al*. describe in detail the disadvantages of the use of physical, chemical and biological decellularization agents [343]. Improved decellularization methods are required, therefore, in order to obtain ECM that is closer to its native state, Bourgine *et al*. suggest that

manufacturing ECM using a suicide gene may result in lower ECM immunogenicity [341]. However, these authors did not directly compare ECM prepared using the suicide gene approach with the commonly-used alternative decellularization methods. For this reason, in the experimental work presented in this chapter, the characteristics of *in vitro* cell-derived ECM prepared either by subjecting cultured stromal cells to osmotic shock or by inducing programmed cell death using a transfected suicide gene were compared.

Initially, it was possible to demonstrate that the MS5 cells were efficiently transduced with the iCasp9 suicide gene and that the induction of apoptosis worked very efficiently (**Figure 5.4** and **Figure 5.7**). Importantly, and in keeping with the report of Ramos *et al.*, MS5 iDS cells did not demonstrate other phenotypic changes or changes in differentiation capacity after transduction (**Figure 5.5**) [356].

5.4.1 Characterization and comparison of the matrices

One important factor for this project was to determine whether both methods used to produce matrices were efficiently decellularizing the ECM, such that all cells were killed and all cell debris had been removed. With regard to the first method, results showed that, following overnight incubation with a hypotonic solution, all cells that produced ECM were non-viable. Furthermore, the ECM produced under normoxic and hypoxic conditions did not present metabolic activity, indicating that the MS5 cells had been efficiently lysed. In regard to the second method, the induction of apoptosis in MS5 iDS cells was, as noted above, initially very efficient. However, it was observed that, following 7 days of ECM production, the efficiency of cell killing was reduced. When this observation was more closely investigated (**Figure 5.10**) it was found that the presence of ECM had an impact on the rate of apoptotic cell death, while hypoxia did not interfere with apoptosis progression. Of interest, it has been shown that ECM suppresses apoptosis by coordinating the expression and function of several key molecules [34]. Since these findings revealed that not all the cells were immediately killed following overnight treatment with the B/B homodimerizer, the resulting ECM preparations were not used experimentally until several days later, to ensure that there were no viable cells present at the time of the experiments.

After the culture and decellularization procedures, the matrices were characterized and compared using different approaches. Initially (**Figure 5.11**), it was found that decellularized ECM generated under both protocols contained the common ECM proteins collagen IV, collagen VI, thrombospondin, laminin, heparin sulphate and fibronectin. However, despite the efficiency of cell killing, it was also observed that there were residual nuclei present in the matrix in both methods and that such nuclear contamination was greater for the “ECM iDS” than for “ECM” method. Considering protein quantification by the mean grey value of the ICC

pictures, both preparation methods appeared to result in similar amounts of ECM protein. It was also clear that matrices prepared in normoxia had higher protein intensity than those prepared under hypoxic culture conditions. However, somewhat surprisingly, gene expression studies of MS5 cells from the iDS condition did not reflect these protein-based findings. MS5 iDS cells cultured under hypoxic conditions had all the genes down-regulated, even genes from proteins not identified by ICC. It should be noted, that the correlation between gene expression and protein abundances in the cell has been considered to be poor [367]. However, the differences between protein abundance in normoxia and hypoxia determined by the mean grey value, can be explained by the fact that the cells cultured to high confluence in hypoxic conditions did not proliferate as much as those cultured in normoxia (**Figure 5.14**). There were significantly lower numbers of MS5 and MS5 iDS in hypoxia, producing less ECM and leading to lower amounts of the most abundant ECM proteins, the collagens and laminin. These results contrast with existing reports that show that hypoxia increases cell proliferation. Indeed, from our group, Sugrue *et al.* have specifically reported MS5 as having enhanced proliferation in hypoxia [368]. However, it is important to consider that the "clonogenicity" experiments in the Sugrue *et al*. study, were performed with an initial lower number of MS5, not in high concentration as it is describe here. As it is known that hypoxia and cell-cell contact may be associated with cell cycle arrest it is hypothesise that the apparent inconsistency with Sugrue *et al.* reflects the combined effects of high cell density plating and hypoxia leading to cell cycle arrest rather than the enhanced proliferation associated with low density hypoxic seeding [334, 368, 369].

It is also important to consider that cellular levels and trends in protein and mRNA transcripts are not necessarily concordant and it is assumed that this is why the results for RT-PCR of ECM-related transcripts did not reflect those of the microscopic protein quantifications. One limitation of the study in this regard, was that it was not possible to confirm protein quantification by Western blots since collagens, fibronectin and laminin are macromolecular proteins. Nonetheless, proteomic analysis was also performed allowing a comparison of ECM preparations using a separate approach. As described in the Results section, the proteomic analysis results revealed that there were large differences in the overall protein compositions of the four matrices. In the first place, the individual matrix preparations had different total numbers of proteins detected, although all of them contained the common ECM proteins collagen IV and VI, fibronectin, laminin, heparin sulphate and thrombospondin. Furthermore, the proteomic analysis results showed that the "ECM" preparations had higher fold changes for ECM proteins than the "ECM iDS" preparations and that there were higher concentrations under hypoxic conditions for both matrices. Therefore, despite the fact that there were lower

cell numbers in hypoxia for both preparation conditions, the results of proteomic analyses indicated that these cells produced more protein than their normoxic counterparts.

Neither ECM preparation method are ideal in that neither represents pure ECM. The lysis method is relatively rapid allowing little time for cells to alter their metabolic status and protein profile. However, ECM prepared by cell lysis is clearly contaminated by both cytoplasmic and nuclear proteins. The same can be stated about ECM prepared by apoptosis (the iDS method). Here, cells take some time to die which leaves them ample time to modify their protein profile. In addition, nuclear degradation takes place contaminating the preparation with additional, apoptosis-induced, proteins. The aims of the project were i) to compare the proteomic composition of ECM prepared by the two methods ii) to determine how hypoxia may alter ECM composition iii) to determine if ECM prepared by the different methods had different biological activity on MSC but also whether ECM had pro-inflammatory activity. Clearly, these experiments had ambitious objectives which were only partially achieved in the time available.

It is important to acknowledge that proteomic analysis provides a very large amount of data and that their interpretation is a complex process, typically requiring multiple strategies and software packages. In general, the results from this study suggest (against expectations) that the “ECM” approach to decellularization represented a better option for preparation of matrix from cultured MSC when compared to the “ECM iDS” approach. These results also highlight the fact that matrix prepared by the “ECM” approach negatively regulates stem cell differentiation. Based on these results, it might be concluded that the “ECM” decellularization protocol provides matrix that better supports the stemness of MSC, while the “ECM iDS” protocol may result in a matrix preparation that is superior for adipocyte differentiation. Also of interest is the fact that the proteomic results reflect significant compositional differences between the ECM preparations generated by the two decellularization methods. For example, it was possible to observe more proteins from the nucleus and related to apoptotic signalling pathway were present in ECM prepared by triggering of a suicide gene when compared to ECM prepared by osmotic shock.

For the first time is presented a proteomic analysis of matrices prepared by different methods under both normoxic and hypoxic conditions. Previously, various approaches have been taken to determine ECM composition and its influence on cell fate and function. Of direct relevance to this work, Tiwari *et al.* performed a comparative gene expression profile of ECM produced by MS5 cells [370]. However, some limitations of this approach included the fact that it could not detect high molecular weight proteins such as GAGs as well as cytokines and growth factors that were expressed at very low levels. Flaim *et al.* used a microarray strategy

to probe ECM effects on cellular differentiation however, rather than using native ECM, these researchers utilised a combination of 5 common ECM components [371].

5.4.2 Biological role of ECM iDS

Certain ECM proteins, such as collagen I and fibronectin, are known to specifically influence MSC fate [35]. For example, Trappmann *et al.* showed that changes in collagen crosslinking modify the differentiation outcome of MSC. They also demonstrated a link between MSC adhesion and differentiation [372]. In general, ECM signalling properties that dictate its functional effects on diverse cell types depend upon its three dimensional organization [34]. However, detailed correlative analyses of ECM proteins and MSC stemness and differentiation have not been performed to date. The proteomic results provided by this study brought a broad indication of the complexity of MSC-ECM interactions but additional approaches are needed in order to better understand how ECM protein composition and three-dimensional structure regulate MSC decisions. With this in mind, experiments were also performed in which MSC were cultured on top of different matrix preparations. Before proceeding to assays of MSC differentiation however, first the "immunogenic" effect of the ECM preparations was evaluated.

The potential for *in vitro*-prepared decellularized ECM to trigger innate immune responses in cells with which they come into contact is particularly important for the application of ECM scaffolds to tissue regeneration. The initial hypothesis was that the "ECM iDS" preparation approach would be less immunogenic than the "ECM" method because, when cells die by osmotic shock, they release intracellular contents capable of stimulating pattern recognition receptors [342]. In contrast, it was expected that the suicide gene strategy should not be associated with cell rupture and release of pro-inflammatory intracellular molecules. It was also considered likely that ECM decellularization by induction of apoptosis could contribute towards a regenerative effect through the release of important paracrine signals, such as PGE2 [341, 373]. However, since there were no macrophages in the *in vitro* culture to remove the apoptotic bodies, there was also the possibility that the contents of these apoptotic bodies would be released over time and would result in immunogenic modifications to the ECM compositions. Chapter 3 describes how inflammation leads to ECM degradation *in vivo* and a similar process can occur under culture conditions in which matrix components are exposed to intracellular contents. In keeping with this concept, the ICC and proteomic results presented in the current chapter clearly show that "ECM iDS" had more nuclei present than ECM prepared by osmotic shock. Thus, the findings using a transduced suicide gene approach disproved the initial hypothesis that, following apoptosis, the resulting cyto-morphological changes led the treated cells to fully lose contact with ECM [341].

MS5 iDS cells were transduced with a retrovirus that should have minimal effects on their physiology. Nevertheless, viruses are recognized by intracellular pattern recognition receptors (PRRs) and, upon recognition of viral PAMPs, the associated intracellular signals generally trigger pro-inflammatory and antimicrobial responses including the production of cytokines, chemokines, cell adhesion molecules, and immunoreceptors [374]. Although no evidence was found for activation of such PRR-mediated responses during retroviral transduction in this study, pro-inflammatory cytokines and DAMPs, released during lysis and/or apoptosis, have been proposed to explain the potential immunogenicity of dying cells even in the absence of viral infection [375].

To determine whether this was occurring in the experimental system, the two decellularization methods were compared for their immunogenic potential when placed in contact with fresh stromal cells. ELISA results showed no differences between the four matrices in regard to the stimulation of TNF-α, IFN-γ and HSP70 secretion by MS5 cells (**Figure 5.22**). In order to compare the effects of the different matrices on "professional" immune responders with their effects on stromal cells, similar experiments were performed where monocytic cell lines, T cells or MSC cultured on their own ECM preparations. These results suggested that ECM decellularized with a lysis buffer caused a higher percentage of Raw 264.7 and J774A.1 cells to express TNF-α. The results also showed, as expected, that Raw 264.7 and J774A.1 cell lines were more responsive to innate immune stimuli than MSC. Monocytes are important cells of the innate immune system and activate rapidly during inflammation while T cells, as explained in chapter 2, require antigen-specific activation through the T cell receptor (TCR)/CD3 complex along with co-stimulatory signalling. Thus, whereas matrices alone did not activate resting T cells, it remains possible that they could serve as co-stimulators of T cells in the context of a TCR/CD3 stimulus. Indeed, Bayrak *et al.* showed that collagen I and elastin, in combination with anti-CD3 antibody, resulted in T cell release of TNF-α and IFN-γ [376]. As expected, given their predominantly immunosuppressive properties, MSC did not secrete detectable TNF-α in these assays. It was not determined, however, whether either of the ECM preparations modulated MSC secretion of anti-inflammatory mediators.

MSC respond to physical and biological properties, such as the oxygen concentration in their microenvironment [377]. Based on preliminary data and existing literature suggesting that a combination of ECM and hypoxia serves to maintain the stemness of MSC, one of the goals of the project was to study the biological role of ECM composition and hypoxia on MSC differentiation capacity and expression of stemness factors [378]. For these experiments, the ECM was produced by MS5, a well-characterised murine stromal cell line. Of note, Tiwari *et al.* had previously reported the use of ECM derived from MS5 and had shown that ECM prepared

in normoxia with osteogenic medium was superior for expanding committed HSC, while ECM prepared in hypoxia without osteogenic medium provided better support for primitive progenitors [370]. In other studies, D'Ippolito *et al*. and Grayson *et al.* also reported results indicating that hypoxic culture conditions favour stemness of MSC [334, 379]. In these studies, mouse MSC were differentiated in normoxic and hypoxic conditions on tissue plastic alone and on plastic coated with decellularized ECM prepared by the two different protocols. Although adipogenic and osteogenic differentiation does not occur within the haematopoietic niche, these experiments were viewed as an *in vitro* system in which to study MSC plasticity and stemness. Initially it was thought to perform the experiments using a cloned mouse MSC line but, as this approach did not prove successful, bulk Balb/c bone marrow-derived MSC were used.

In the first set of experiments, the role of hypoxia on MSC differentiation capacity using different combinations of normoxia-hypoxia MSC cultured on tissue culture plastic alone were considered. As depicted in **Figure 5.26** MSC differentiation was more efficient in normoxic conditions regardless of whether the cells had been previously cultured in normoxia or hypoxia. Subsequently, in experiments comparing tissue culture plastic alone with the two ECM preparations, it was again found that adipogenic differentiation of MSC was best supported in normoxic cultures. In these experiments, plastic alone and ECM iDS showed equivalent capacity to support adipogenesis. These findings regarding oxygen conditions are in keeping with Lin *et al.* who reported that hypoxia arrests differentiation and with Hung *et al.* who showed that MSC adipogenic differentiation is inhibited by hypoxia [380, 381]. These results are in keeping with the concept that hypoxia in the stem cell niche is critical for the maintenance of an undifferentiated stem or precursor cell phenotype, although the role of ECM in this process remains less clear. Of interest, it is known that adipocytes are surrounded by a thick ECM containing mainly collagen IV, and that, during the adipogenic process, the differentiating cells expend a large amount of energy on ECM production [382]. Thus, further studies of MSC-derived ECM in the setting of adipogenic differentiation or on adipocyte precursors may be of value in better understanding how adipose tissue mass is regulated.

In the case of osteogenic differentiation, the results were less consistent with one experiment indicating a modest advantage of hypoxic culture and a second experiment showing equivalence between normoxia and hypoxia (**Figure 5.29**). One general limitation of such experiments may relate to methodology for quantifying osteogenesis. Alizarin red S staining has been used for decades to evaluate calcium-rich deposits by cells in culture but the reaction is not strictly specific for calcium, and may also be influenced by concentrations of magnesium, manganese, barium, strontium, and iron. Nonetheless, the results were also

confirmed by specific measurement of calcium using a commercial kit, believed to reflect the extent of osteogenesis. Furthermore, the variability observed between the two experiments is also reflected in the literature. While D'Ippolito *et al.* demonstrated that low oxygen tension inhibited osteogenic differentiation of MSC [379]. Hung *et al.* reported that hypoxia favours osteogenic differentiation. Thus, it may be the case that osteogenic differentiation of MSC is only marginally influenced by oxygen tension or that the biological effects of hypoxia on this differentiation pathway are diverse. In regard to the effect of ECM composition on osteogenic differentiation, the results suggest that MSC undergo osteogenesis most effectively under normoxic conditions in the presence of stromal cell ECM that had been decellularized by osmotic shock. In keeping with this, studies have suggested that ECM creates a microenvironment that is conducive to osteogenic differentiation [383, 384].

Interestingly, while it has been reported that MSC lose the ability to differentiate *in vitro* after 5 to 7 passages, relatively effective differentiation into adipocytes and osteocytes of mouse MSC that had already been passaged 10 to 12 times was observed [144]. It is possible that the loss or retention of differentiation capacity by MSC is influenced by culture conditions including the presence and composition of ECM. In regard to the high degree of variability among published studies, Hoshiba *et al.* have suggested that MSC differentiation capacity is tissue and ECM specific [385]. In addition, and relevant to the experimental results, the heterogeneity of "bulk" MSC cultures expanded from bone marrow or other tissues may also play a role in the variability of results for differentiation assays. Indeed, as described in chapter 1, cloned MSC have been previously shown to have distinct expression profiles for key functional molecules [67]. In an attempt to overcome this factor, it experiments were performed in which the cell line MS5 was cultured on top of the decellularized matrices. However, it proved not to be possible to consistently differentiate these cells into adipocytes and osteocytes.

Concerning the RT-PCR results, it was found that expression levels of the transcripts for adipogenesis-related genes, c/EBPβ and aP2 were not consistently up-regulated during the differentiation protocol compared to non-differentiated conditions with the exception of aP2 in MSC differentiated on plastic alone. As it was clear from the Oil Red O assays that the MSC were capable of adipogenic differentiation, it is possible that a broader panel of gene expression analyses or analysis at additional time-points would have provided clearer understanding of differences between culture conditions. In regard to osteogenic differentiation, it was observed that the RT-PCR results did not correspond closely to those of the calcium quantification. While expression of osteogenesis-related genes showed a clear pattern of up-regulation following one week of normoxic differentiation culture on plastic

alone, several of the genes were down-regulated in cells that were pre-expanded on matrices that had been prepared under both normoxic and hypoxic conditions. One exception, perhaps, was differentiation of MSC on “hypoxic ECM iDS” in which 2 of the 4 genes measured were up-regulated. A technical issue which may have confounded the RT-PCR results was the presence of calcium accumulation at the time of analysis which may have led to reduced efficiency of amplification in the more heavily calcified samples [386]. It is also possible that gene expression patterns differed among the conditions at earlier time-points in the differentiation protocol that were not analysed in these experiments.

It is generally accepted that expression of the transcription factors Nanog, Sox2 and Oct4 is associated with pluripotency [387]. In the final experimental series of this project, it was observed that culture of MSC in control and adipogenic media under normoxic conditions was associated with up-regulation of mRNA for Nanog but not for Sox2 and Oct4 in MSC regardless of the presence or absence of the various ECM preparations (**Figure 5.32**). In contrast, osteogenic medium was associated with up-regulation of Sox2, Nanog and Oct 4 in MSC differentiated on plastic alone and in MSC differentiated on “hypoxic ECM iDS”. Overall, these results suggest that MSC expression of pluripotency-related transcription factors is influenced both by differentiation conditions and by the presence of ECM.

In order to further investigate the dynamic expression of these pluripotency-related genes, Nanog, Sox2 and Oct4 mRNA expression in MSC following 3 and 7 days of normoxic, non-differentiation culture conditions with and without the various ECM were compared. Although a trend was observed towards an increased Nanog expression at 7 days in all conditions, there was, otherwise, no evidence of changing expression of these stemness-related genes in this experiment. It is important to consider that these genes are normally expressed at low levels by MSC and that this expression is affected by passage number [387-389]. The bone marrow-derived Balb/c MSC used for these experiments were of relatively high passage number and the interpretation of these results indicate that culture of these cells on ECM, generated using the two decellularization protocols was not sufficient to restore expression of pluripotency-related transcription factors.

Hypoxia itself has been reported to exert important influences on expression of pluripotency factors in stem/progenitor cells and on differentiation pathways [378, 379]. Whether the effect of hypoxia on ECM composition can specifically regulate differentiation and retention of stemness is less well understood. In the experiments involving induction of adipogenesis and osteogenesis, the most efficient differentiation was observed in MSC cultured on top of “normoxic ECM” and “normoxic ECM iDS” respectively. This suggests that ECM produced by stromal cells experiencing a hypoxic environment may be less supportive of

differentiation than ECM generated by the same cells under normoxic conditions. Regarding the possible role of hypoxia in ECM-mediated regulation of MSC stemness, the preliminary experiments did not find evidence for such an effect despite the fact that MSC are well reported to increase HIF-1α stability along with the expression of HIF-controlled genes. The complexity of the interplay between MSC heterogeneity, hypoxia, ECM composition, time in culture and decellularization process may have confounded the ability to detect specific effects of "hypoxic" ECM on the stemness phenotype of the cells. Although the majority of the published studies have demonstrated that ECM generally preserves cell stemness [11], the specific ECM components involved in this process and the relative potency of ECM produced by different cells or prepared using different protocols requires further study.

Overall, the cell culture experiments demonstrated that it was possible, to varying degrees, to differentiate MSC into adipocytes and osteocytes in the presence of each of the four ECM preparations developed. However, no clear evidence was found that the ECM preparations, whether generated under normoxic or hypoxic conditions, served to robustly preserve MSC stemness. If these issues are to be further pursued for application to the fields of tissue engineering and regenerative medicine, it will be essential to overcome the technical limitation of incomplete clearance of cellular material/proteins from *in vitro*-generated ECM as well as the lack of mechanical tension and three dimensional architecture associated with ECM that is deposited during conventional cell culture.

5.5 Conclusion

In this project, the combined effects of two different decellularization methods and of oxygen tension on the composition of ECM laid down by the cultured murine stromal cell line MS5 was described for the first time. It was shown that these factors do indeed influence the protein constituents of *in vitro*-generated stromal cell ECM. It is reasonable to conclude that culture of MSC in the presence of a physiological matrix represents a valid approach to re-create the physiologic micro-environment of stromal cells *in vivo*. However, the ECM preparation method and the influence of ECM on the experimental or therapeutic goals for the cells must be carefully considered and evaluated in advance. For example, the differentiation assay results suggest that stromal cell ECM laid down under normoxic conditions and decellularized by activation of a suicide gene ("EMC iDS N") was optimal for osteogenesis. The results regarding the optimisation of stromal cell ECM for maintenance of MSC stemness were less informative for several reasons that are discussed above. Nevertheless, it is believed that there is great promise for future research to more precisely dissect the mechanisms whereby ECM in the bone marrow and other tissues contributes the preservation of stemness among MSC themselves as well as other stem cell populations.

Chapter 6 | Future Perspectives

6.1 Perspectives

Mesenchymal stromal cells are a promising cell source for regenerative medicine and tissue engineering because of their ability to self-renew and to divide into cells that can undergo multi- lineage differentiation. The differentiation capacity of stem cells is regulated by the combined effects of intrinsic and extrinsic factors [11, 15, 390]. Intrinsic factors include the transcription factors expressed and the epigenetic profile of the cell while extrinsic factors are potentially numerous and are often collectively referred to the "niche" in which the cells reside [15]. The contents of the stem cell niche include different cell types together with the cytokines and trophic factors they produce [11, 63, 326, 327, 391]. Of particular relevance to the project described in this thesis, is the ECM.

Research focussed on matrix biology, analysis of ECM composition and *ex vivo* generation of sheets or 3D "scaffolds" of ECM have become central to the fields of stem cell therapeutics, regenerative medicine and tissue engineering. Although the manufacture of entirely artificial ECM that is "tailor made" for specific therapeutic targets represents, perhaps, the future ideal, it is currently not possible to recreate the complexity of physiological ECM using recombinant proteins. Thus, many research and translational projects that require the presence of ECM continue to rely on decellularization of *in vitro* cultured cells or of explanted organs and tissues. Unfortunately, it remains unclear which decellularization methods are optimal for specific clinical proposes. Furthermore, available cell number is often a significant limitation for the preparation of sufficient quantities of ECM – particularly in the case of stem cells. The use of immortalised cell lines (such as human TERT or mouse MS5 cells) may represent a good strategy for overcoming this limitation and, for some applications, could have the added advantage of being more homogenous than primary stem cell cultures. On the other hand, some applications may require ECM produced by multiple cell types. For example, to fully recreate the haematopoietic stem cell niche, it may be necessary to include contributions from osteoblasts, adipocytes and vascular endothelial cells in addition to MSC. In this study, the use of the immortalised mouse marrow stromal cell line MS5 exemplifies these issues in regard to the strengths and limitations of using a homogenous cell culture to generate ECM for the purpose of enhancing MSC differentiation capacity or stemness.

Although not dealt with in this project, another important factor in regard to the production of ECM for regenerative medicine and tissue engineering purposes is biocompatibility. To better mimic the human stem cell niche, it would be necessary to replicate results observed with mouse stromal cell lines with human cells. Furthermore, if these experiments provided promising results for a specific culture and decellularization protocol, it would also be necessary to convert the protocol to an "animal-free" culture system

in order to reach the manufacturing standards required for clinical application of an ECM product.

Cell-ECM interactions are complex and several factors need to be considered. Several studies demonstrated that ECM is an important component of stem cell niches and that ECM contributes to the maintenance of their stemness [363, 392, 393]. However the results are not very satisfactory, in this project the results were heterogeneous, for this reason a different approach should be used to study cell-ECM interactions. Also, several variables need to be considered when the haematopoietic niche is being studied, namely MSC, ECM and oxygen concentration. Bulk MSC contribute to heterogeneous results, ECM prepared in different ways by different cells leads to diverse results and finally different levels of oxygen can switch on or off important stem cell genes, inconsistent changes in oxygen levels can also lead to heterogeneous results.

Stem cell-ECM-hypoxia interactions are being considered by different groups, however they are not considering the three factors together. When ECM-stem cell relations are being studied, it is important to consider that responses vary between different cells and ECM composition, stiffness and topography.

ECM has been shown to increase cell survival, adhesion, migration, proliferation and differentiation [33, 34]. These properties are especially relevant when MSC are being expanded for clinical proposes on a large scale such as in bioreactors, where keeping cells happy is extremely important [394]. ECM scaffolds in cell culture would also be beneficial to expand rare cells, especially rare cells such as HSC [395]. For example, the combination of ECM scaffolds with well-established protocols to produce HSC from iPS cells, could give more detailed information on how cells take decisions in the haematopoietic environment.

ECM scaffolds are a powerful model to study the impact of ECM on stem cell differentiation, however it is important to consider the different techniques available for ECM production. Decellularized ECM production using a suicide gene to induce apoptosis is probably the best available method, since it exploits natural cell death. Furthermore, it is important to consider that different cells produce different ECM, having different effects on cell stemness. In the end, decellularized ECM-scaffold produced by cell lines are probably the best option for tissue engineering and regenerative medicine, however for cell biology research, ECM with a more native configuration would be a better option.

In future it would also be interesting to observe the consequences of inflammation on ECM production, by exposing MSC or other stromal cells or inflammatory mediators. This would be of extremely importance in oncology filed. Abnormal ECM affects cancer progression by directly promoting cellular transformation and metastasis [396]. Understanding ECM

composition and the role of its constituents in these events could contribute to the development of newer therapeutic approaches. For example, multiple myeloma (MM) is a B-cell malignancy characterized by the slow proliferation of malignant plasma cells in the bone marrow. It is a very devastating cancer, with a high capacity to destroy bone matrix and bone trabeculae [397]. The bone marrow niche appears to play an important role in the tumour microenvironment, contributing to the regulation of cell survival, proliferation, migration, differentiation and metastasis of the malignant plasma cells [398]. It is currently unclear why some tumours have a predilection of metastasizing to bone, but may well have something to do with the microenvironment created by the ECM generated by BM stromal cells.

ECM is mostly composed of structural proteins (collagens and elastin), glycoproteins (laminin and fibronectin), GAGs and MMPs. MMPs play a critical role in bone remodelling and tumour invasion. These enzymes have been implicated in the physiologic turnover of extracellular matrix and in bone remodelling. As observed in wound healing, angiogenesis, bone reabsorption, and several pathologic processes such as rheumatoid arthritis and tumour invasion [397, 399, 400]. Collagen I is one of the main structural proteins of ECM, with its degradation being critical for the initiation of bone resorption. Moreover, MMP-2 and MMP-9 degrade collagen IV, the other main protein of ECM, and have been implicated in tumour invasion and metastasis [329, 397]. Excessive bone resorption and tumour invasion process inside and outside the bone marrow are characteristics of MM [397]. In MM, ECM components, such as integrins, fibronectin and collagens, have been shown to be critical for the pathogenesis of the disease and the development of drug resistance [401]. Drug resistance is a major obstacle to treatment failure in a number of hematopoietic cancers. This issue is important in diseases such as MM, where the neoplastic plasma cells home to and proliferate in the bone marrow microenvironment until very late stages of differentiation [329].

Other important factor in bone marrow microenvironment is the low oxygen levels. Hypoxia negatively affects the treatment outcome, causing resistance to therapy, since some drugs and radiation require oxygen to be maximally cytotoxic. Studies show that hypoxia can enhance genetic instability in tumour cells, allowing a rapid development of drug resistant cells [402]. In the tumour environment, hypoxia inhibits malignant cell proliferation and induces cell cycle arrest, conferring chemo-resistance, once anticancer drugs preferentially target rapidly proliferating cells. However, this knowledge has been largely neglected while screening for drugs *in vitro*, resulting in hypoxia-mediated failure of most newly identified substances in vivo [403]. The mechanisms that drive tumour cell responses to hypoxia have recently been better understood. A major regulator of cellular adaptation to hypoxia is the HIF family of transcription factors. HIFs are causally involved in key aspects of tumour biology such as

angiogenesis, cell survival, resistance to apoptosis, metabolic reprogramming and pH homeostasis [403].

Annex D shows exactly how ECM can interfere with different drugs to treat MM, specially how ECM prepared with different cells lead to different results.

Finally, cell biology and tissue engineering fields should work together to improve cell-ECM scaffolds, delivering safe and new therapies for regenerative medicine. In addition, increasing the knowledge of cell-ECM-hypoxia interactions will contribute to possible new approaches to treat haematological disorders. Besides the basic research, in the future this could bring new off-the-shelf products with an evident commercial benefit, and an important approach will be to investigate ECM generated by human cells because it would be more clinically relevant.

Chapter 7 | Annexes

7.1 Annex A

The following figure is a representative experiment from whole blood assay, where peripheral blood was in culture with $5x10^5$ BM-MSC for 6 hours in absence of presence of LPS, and the TNF-α expression by monocytes and MSC was measured.

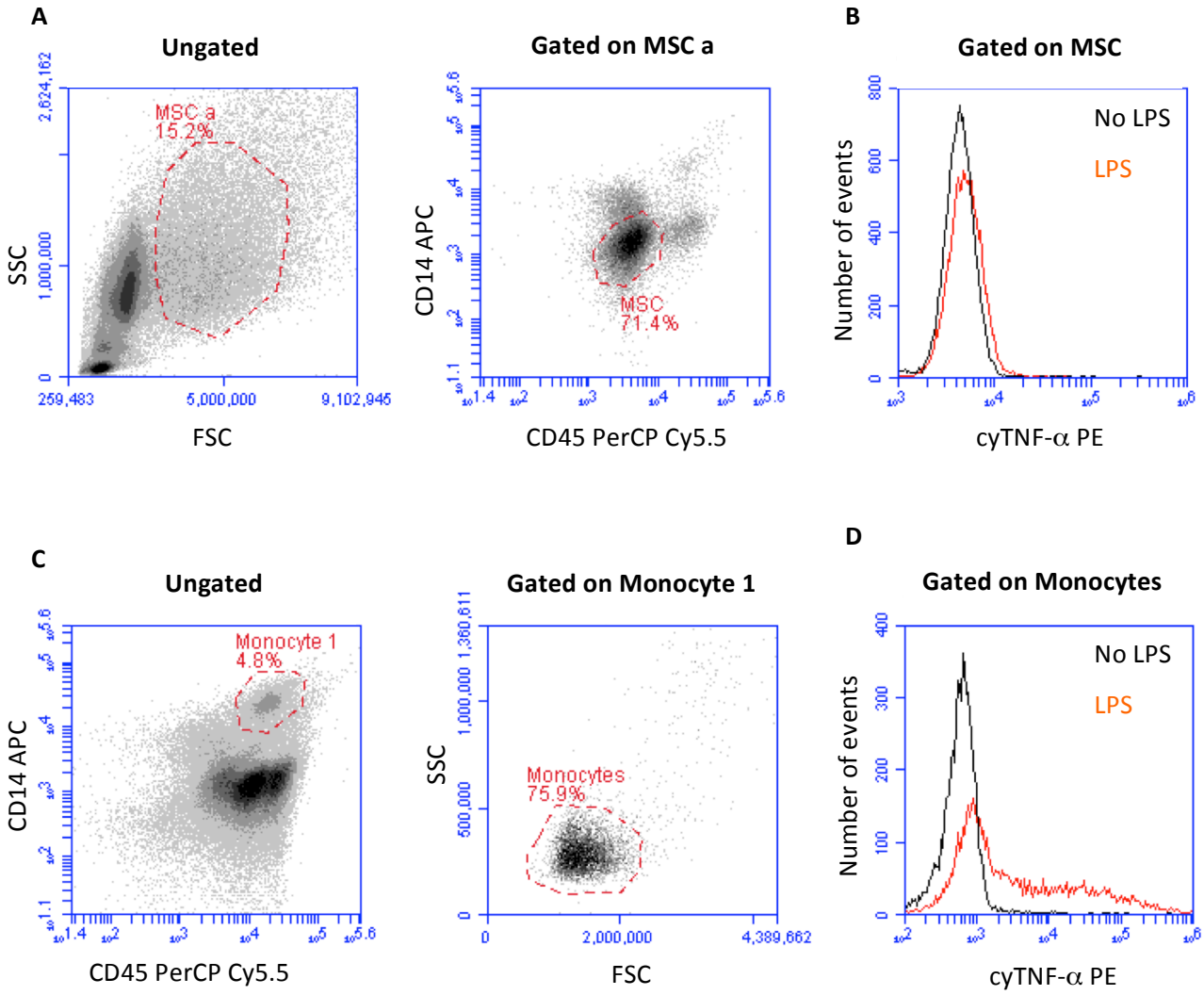

Annex A Figure 1 - MSC type 2, immunosuppressive. **A** shows the gate strategy used to identify MSC by high SSC and FSC among total cells and lacking of expression of CD14 and CD45 previously gated on MSC a. **B** shows that MSC do not express intracellular TNF-α, with or without LPS present. **C** shows monocyte identification by SSC and FSC among total cells after $CD14^+CD45^+$ gating. **D** shows come TNF-α expression by monocytes in presence of LPS and MSC.

7.2 Annex B

This annex present more details of proteomic results. Here are presented data from results analysed by Gorrilla Gene Ontology and DAVID functional annotation softwares.

ECM N

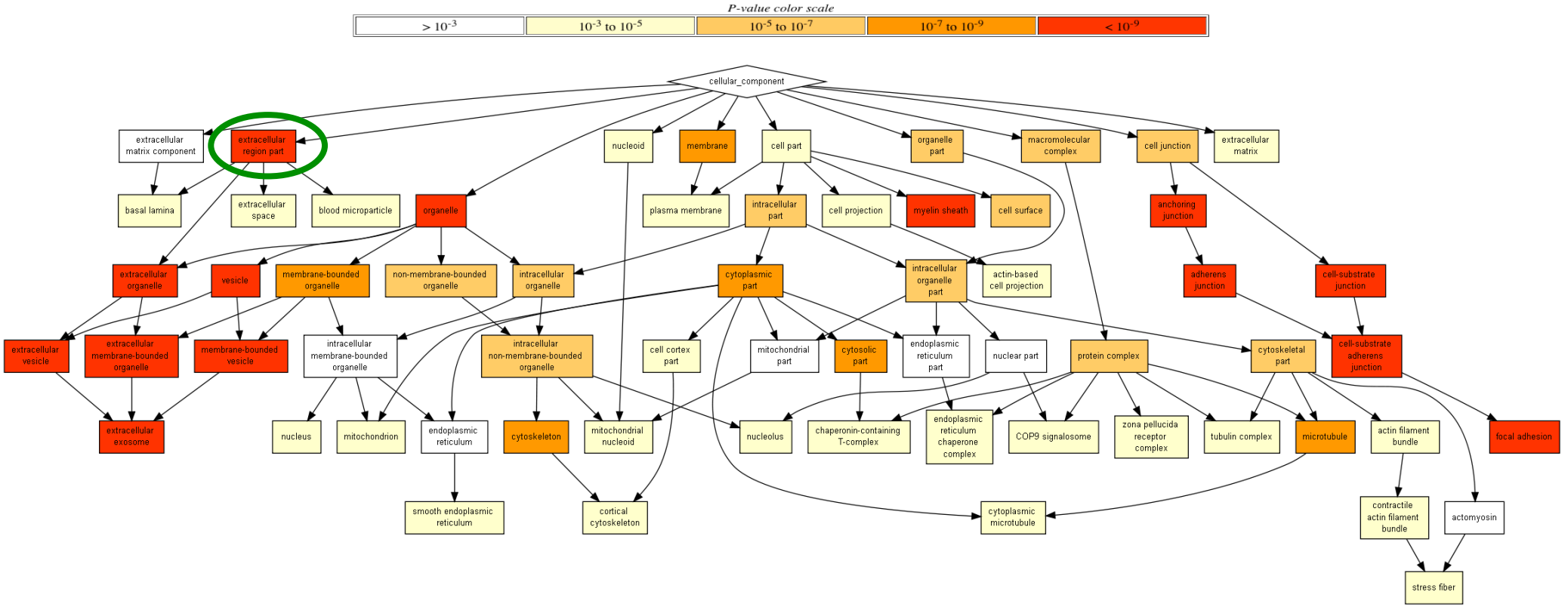
P-value color scale
> 10-3
10-3 to 10-5
10-5 to 10-7
10-7 to 10-9
< 10-9
cellular_component
extracellular matrix component
extracellular region part
nucleoid
membrane
cell part
organelle part
macromolecular complex
cell junction
extracellular matrix
basal lamina
extracellular space
blood microparticle
organelle
plasma membrane
intracellular part
cell projection
myelin sheath
cell surface
anchoring junction
extracellular organelle
vesicle
membrane-bounded organelle
non-membrane-bounded organelle
intracellular organelle
cytoplasmic part
intracellular organelle part
actin-based cell projection
adherens junction
cell-substrate junction
extracellular vesicle
extracellular membrane-bounded organelle
membrane-bounded vesicle
intracellular membrane-bounded organelle
intracellular non-membrane-bounded organelle
cell cortex part
mitochondrial part
cytosolic part
endoplasmic reticulum part
nuclear part
protein complex
cytoskeletal part
cell-substrate adherens junction
extracellular exosome
nucleus
mitochondrion
endoplasmic reticulum
cytoskeleton
mitochondrial nucleoid
nucleolus
chaperonin-containing T-complex
endoplasmic reticulum chaperone complex
COP9 signalosome
zona pellucida receptor complex
tubulin complex
microtubule
actin filament bundle
focal adhesion
smooth endoplasmic reticulum
cortical cytoskeleton
cytoplasmic microtubule
contractile actin filament bundle
actomyosin
stress fiber

ECM H

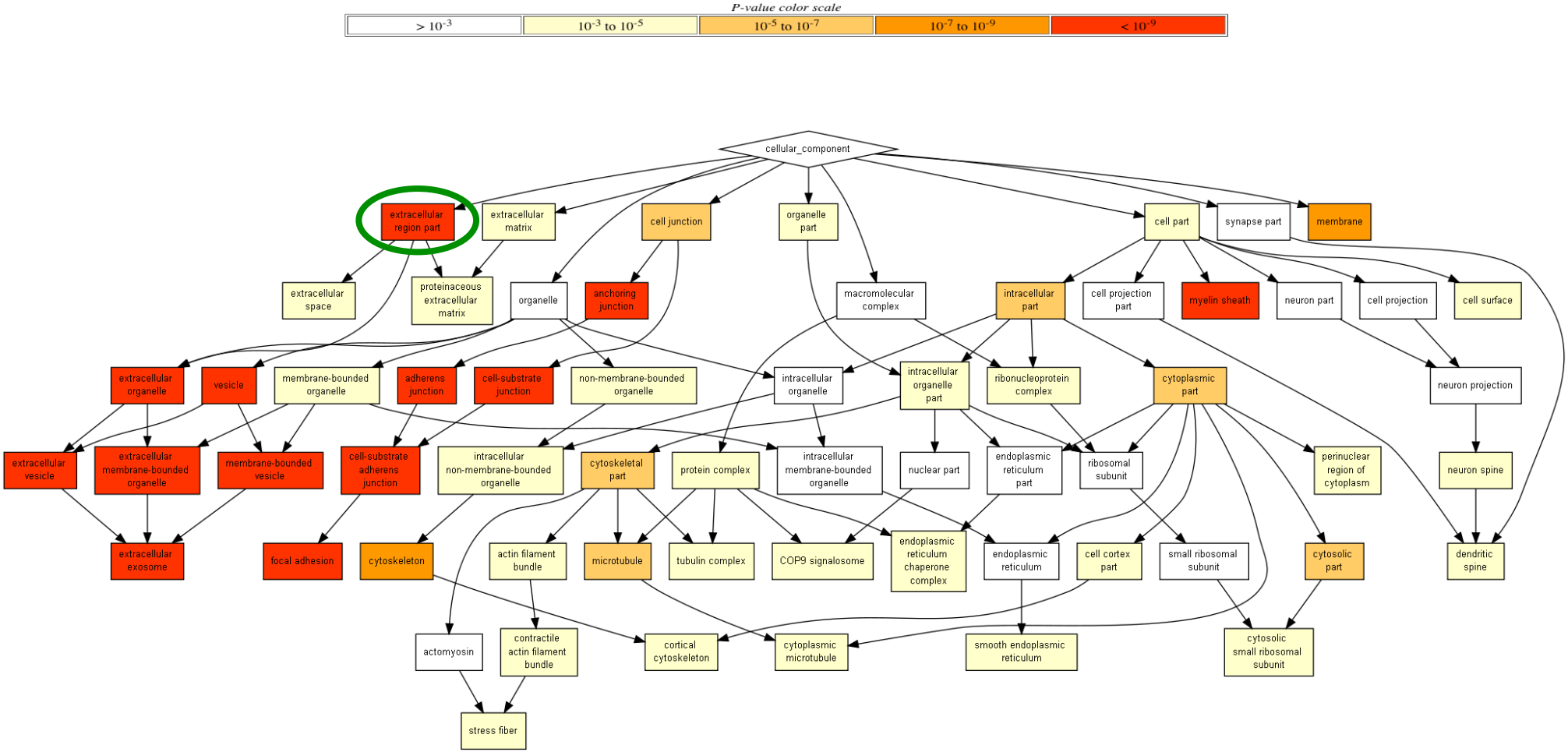
P-value color scale
> 10-3
10-3 to 10-5
10-5 to 10-7
10-7 to 10-9
< 10-9
cellular_component
extracellular region part
extracellular matrix
cell junction
organelle part
cell part
synapse part
membrane
extracellular space
proteinaceous extracellular matrix
organelle
anchoring junction
macromolecular complex
intracellular part
cell projection part
myelin sheath
neuron part
cell projection
cell surface
extracellular organelle
vesicle
membrane-bounded organelle
adherens junction
cell-substrate junction
non-membrane-bounded organelle
intracellular organelle
intracellular organelle part
ribonucleoprotein complex
cytoplasmic part
neuron projection
extracellular vesicle
extracellular membrane-bounded organelle
membrane-bounded vesicle
cell-substrate adherens junction
intracellular non-membrane-bounded organelle
cytoskeletal part
protein complex
intracellular membrane-bounded organelle
nuclear part
endoplasmic reticulum part
ribosomal subunit
perinuclear region of cytoplasm
neuron spine
extracellular exosome
focal adhesion
cytoskeleton
actin filament bundle
microtubule
tubulin complex
COP9 signalosome
endoplasmic reticulum chaperone complex
endoplasmic reticulum
cell cortex part
small ribosomal subunit
cytosolic part
dendritic spine
actomyosin
contractile actin filament bundle
cortical cytoskeleton
cytoplasmic microtubule
smooth endoplasmic reticulum
cytosolic small ribosomal subunit
stress fiber

ECM iDS N

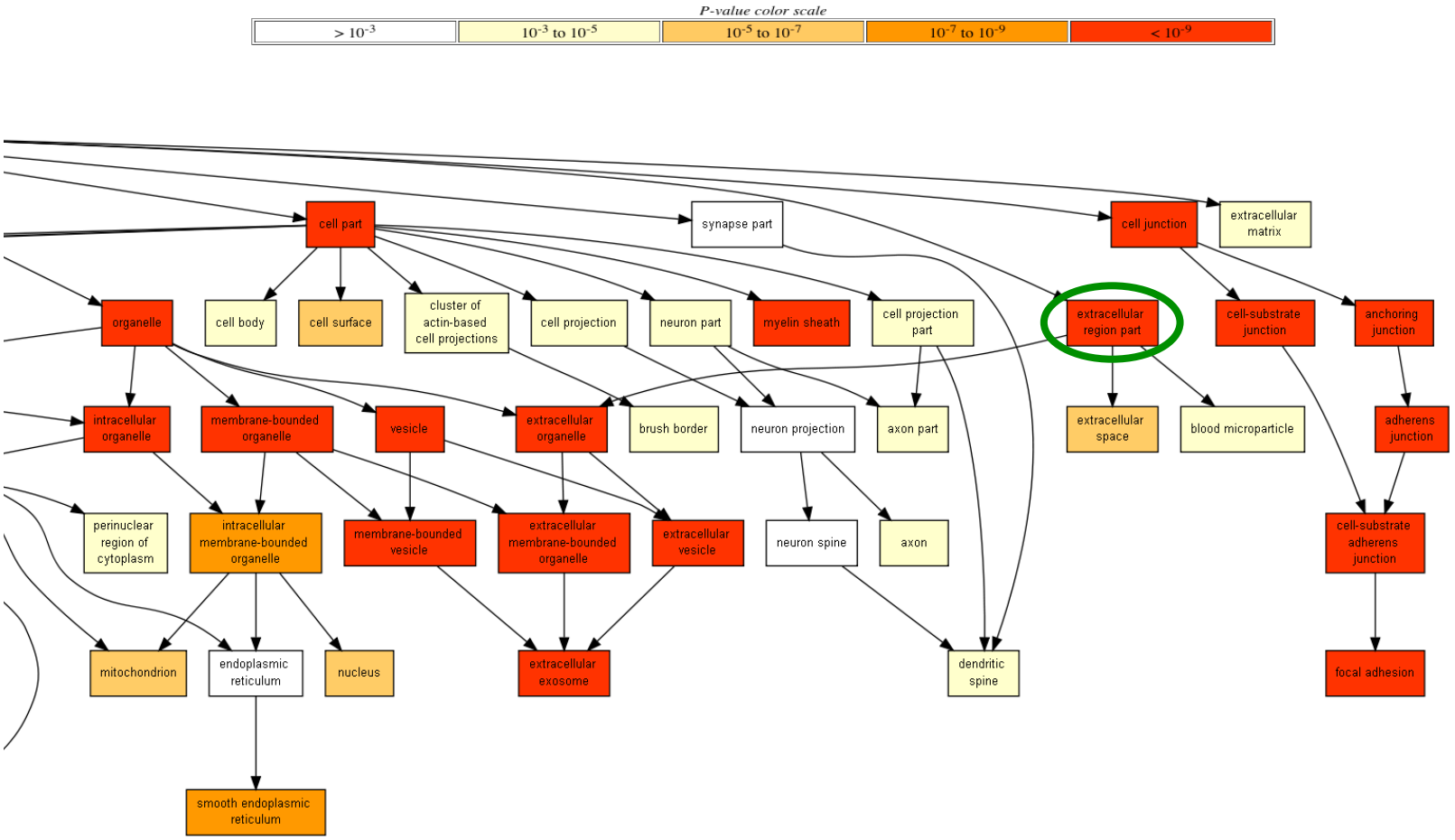
P-value color scale
> 10-3
10-3 to 10-5
10-5 to 10-7
10-7 to 10-9
< 10-9
cell part
synapse part
cell junction
extracellular matrix
organelle
cell body
cell surface
cluster of actin-based cell projections
cell projection
neuron part
myelin sheath
cell projection part
extracellular region part
cell-substrate junction
anchoring junction
intracellular organelle
membrane-bounded organelle
vesicle
extracellular organelle
brush border
neuron projection
axon part
extracellular space
blood microparticle
adherens junction
perinuclear region of cytoplasm
intracellular membrane-bounded organelle
membrane-bounded vesicle
extracellular membrane-bounded organelle
extracellular vesicle
neuron spine
axon
cell-substrate adherens junction
mitochondrion
endoplasmic reticulum
nucleus
extracellular exosome
dendritic spine
focal adhesion
smooth endoplasmic reticulum

ECM iDS H

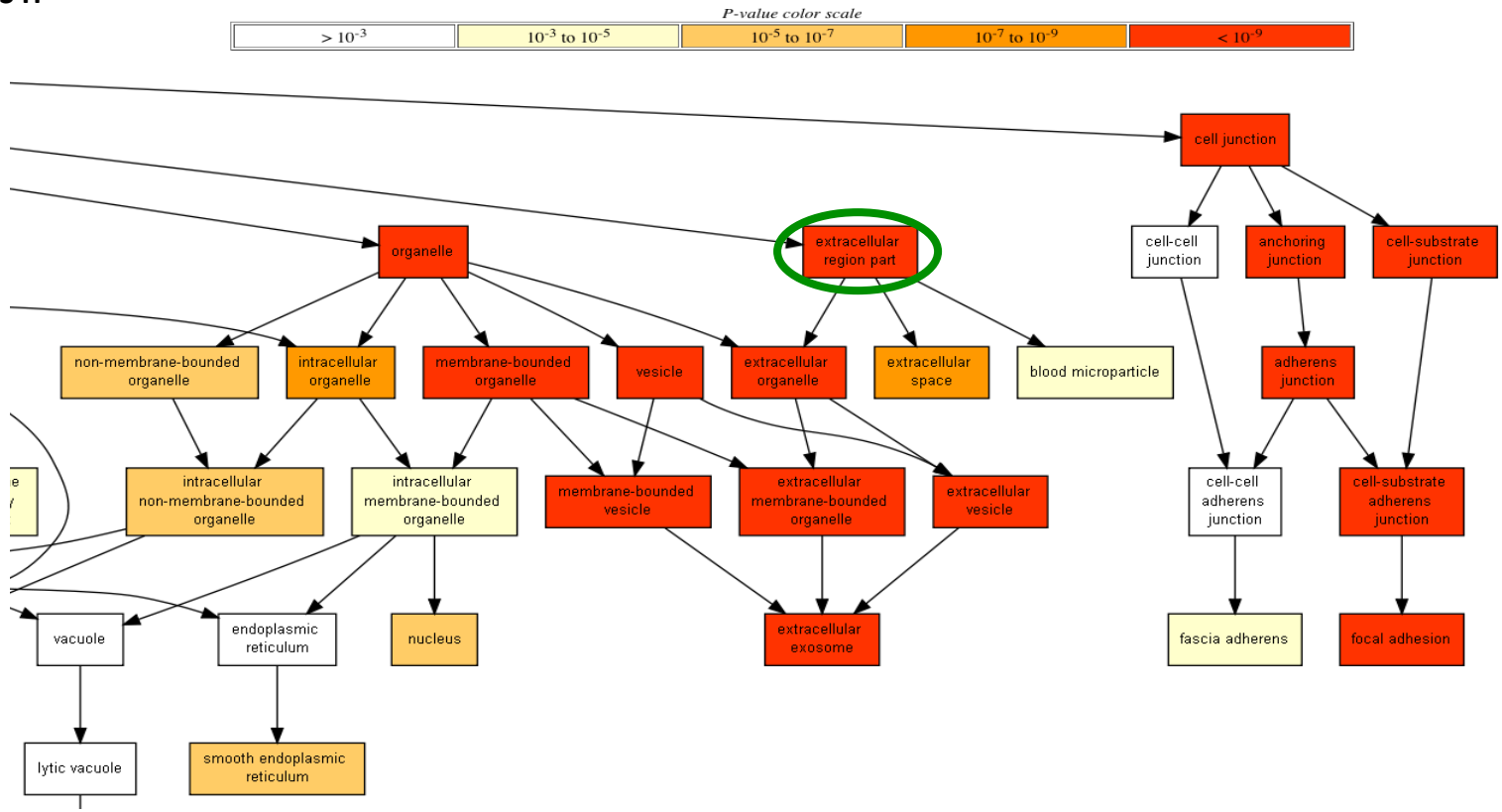

Annex B Figure 1 - Cellular component of matrices. The color-coding reflects the degree of protein enrichment, red with high enrichment and white whit low enrichment. At green is highlighted the extracellular region part, showing that this cellular component is highly enrich in all matrices. The ECM iDS N and H results is just represented part of the figure because it was to big and unnecessary to show. Results generated by Gorilla software.

According with this Gorilla gene ontology analysis, where the cellular component were analysed individually, it is possible to observe that the different matrices had different organization of cellular component, but all of them were enriched for extracellular region part.

ECM N vs H

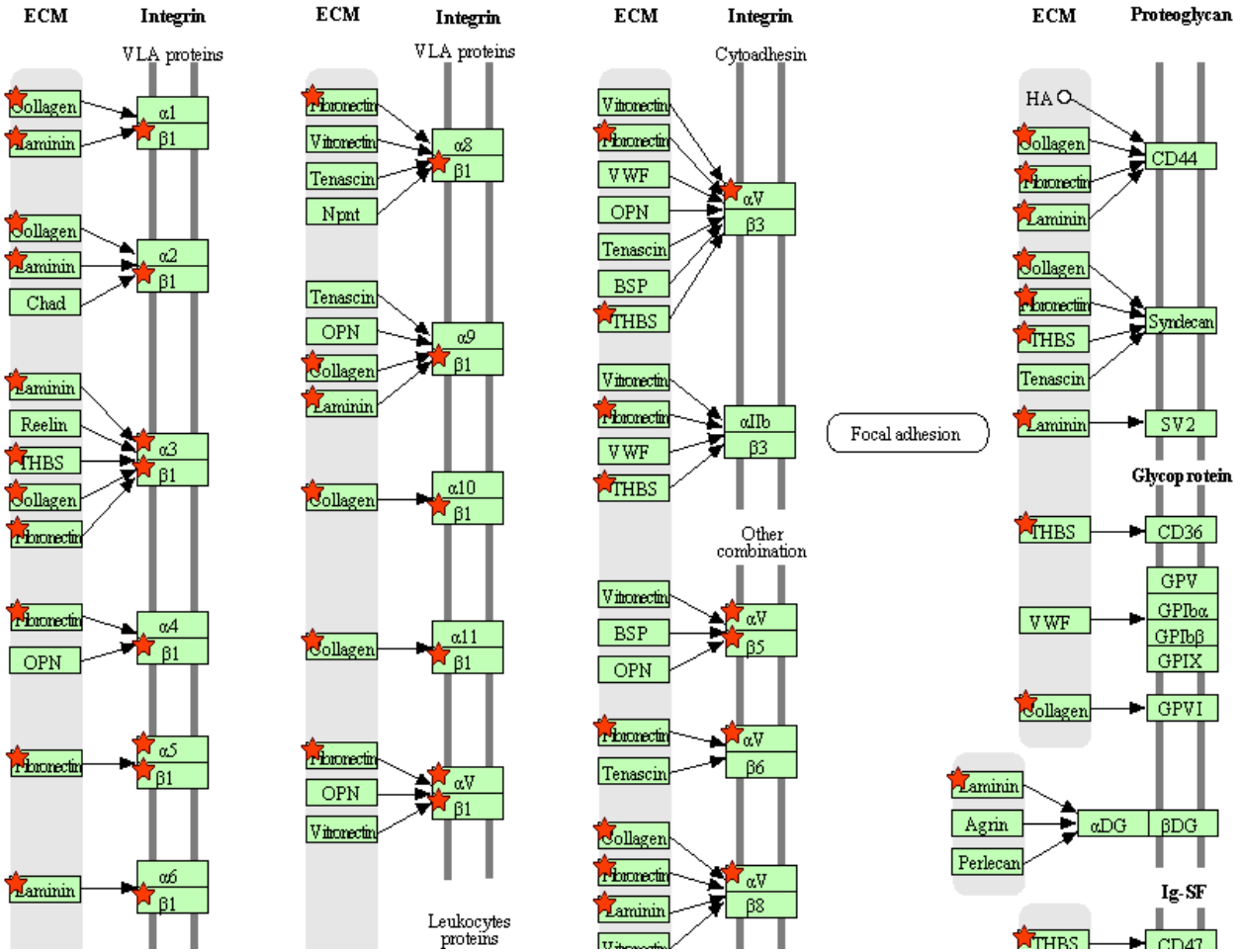

Annex B Figure 2 - ECM-receptor interaction. Overlay file of ECM N and ECM H. Red start indicate the presence of the protein in both matrixes and the arrow indicate the interactions between ECM proteins with integrins and proteoglycans. Results generated by DAVID Functional Annotation software.

ECM N vs H

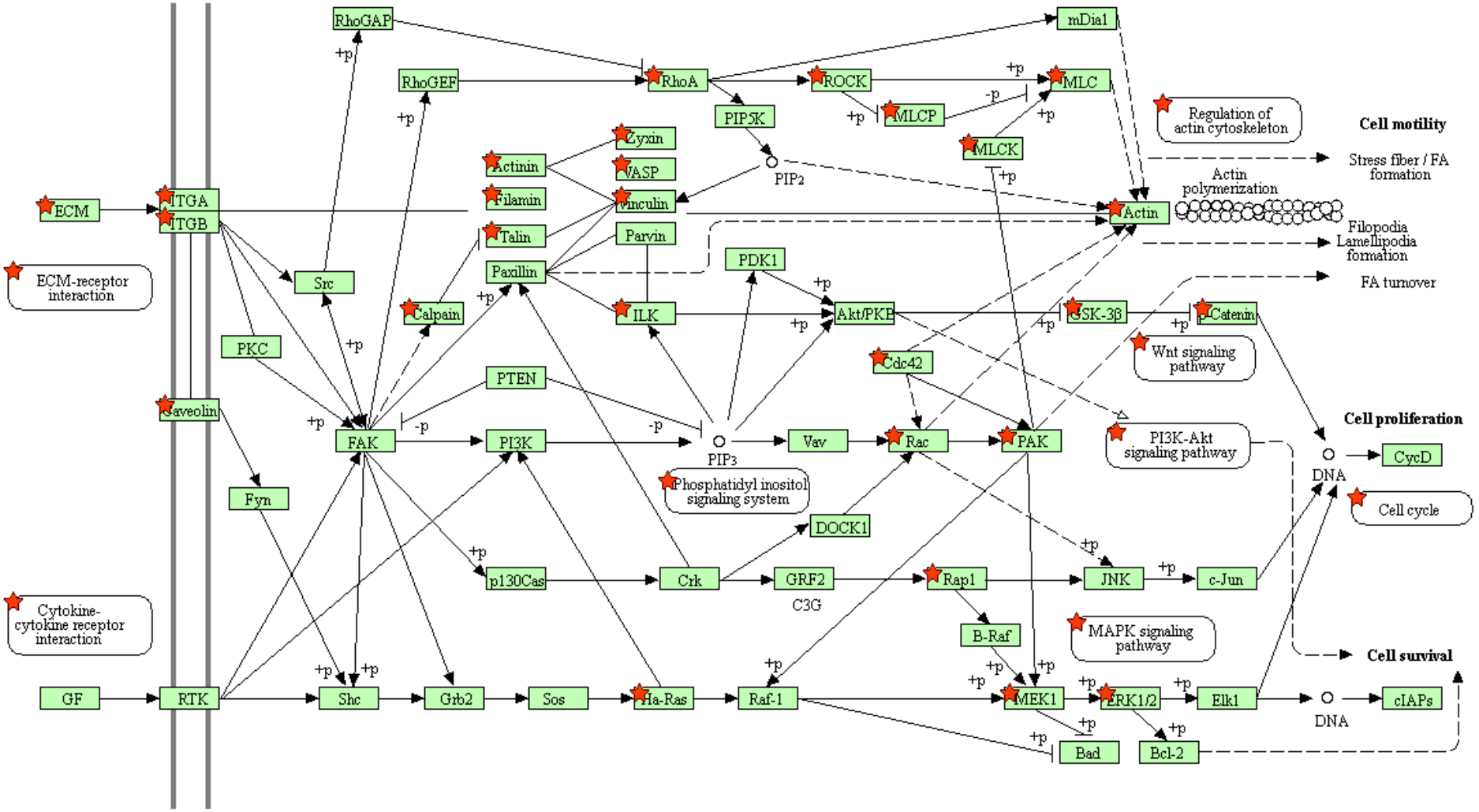
RhoGAP
RhoGEF
RhoA
mDia1
ROCK
MLC
MLCP
MLCK
PIP5K
PIP2
Regulation of actin cytoskeleton
Cell motility
Stress fiber / FA formation
Actin polymerization
Filopodia
Lamellipodia formation
FA turnover
Actin
Zyxin
VASP
Vinculin
Parvin
Actinin
Filamin
Talin
Paxillin
ILK
Calpain
Src
PDK1
Akt/PKB
GSK-3β
β-Catenin
Wnt signaling pathway
Cdc42
Rac
PAK
PI3K-Akt signaling pathway
Cell proliferation
CycD
Cell cycle
DNA
ECM
ITGA
ITGB
ECM-receptor interaction
PKC
Caveolin
Fyn
FAK
PTEN
PI3K
PIP3
Phosphatidyl inositol signaling system
Vav
DOCK1
p130Cas
Crk
GRF2
C3G
Rap1
JNK
c-Jun
B-Raf
MAPK signaling pathway
Cytokine-cytokine receptor interaction
GF
RTK
Shc
Grb2
Sos
Ha-Ras
Raf-1
MEK1
ERK1/2
Elk1
Cell survival
cIAPs
Bad
Bcl-2
+p
-p

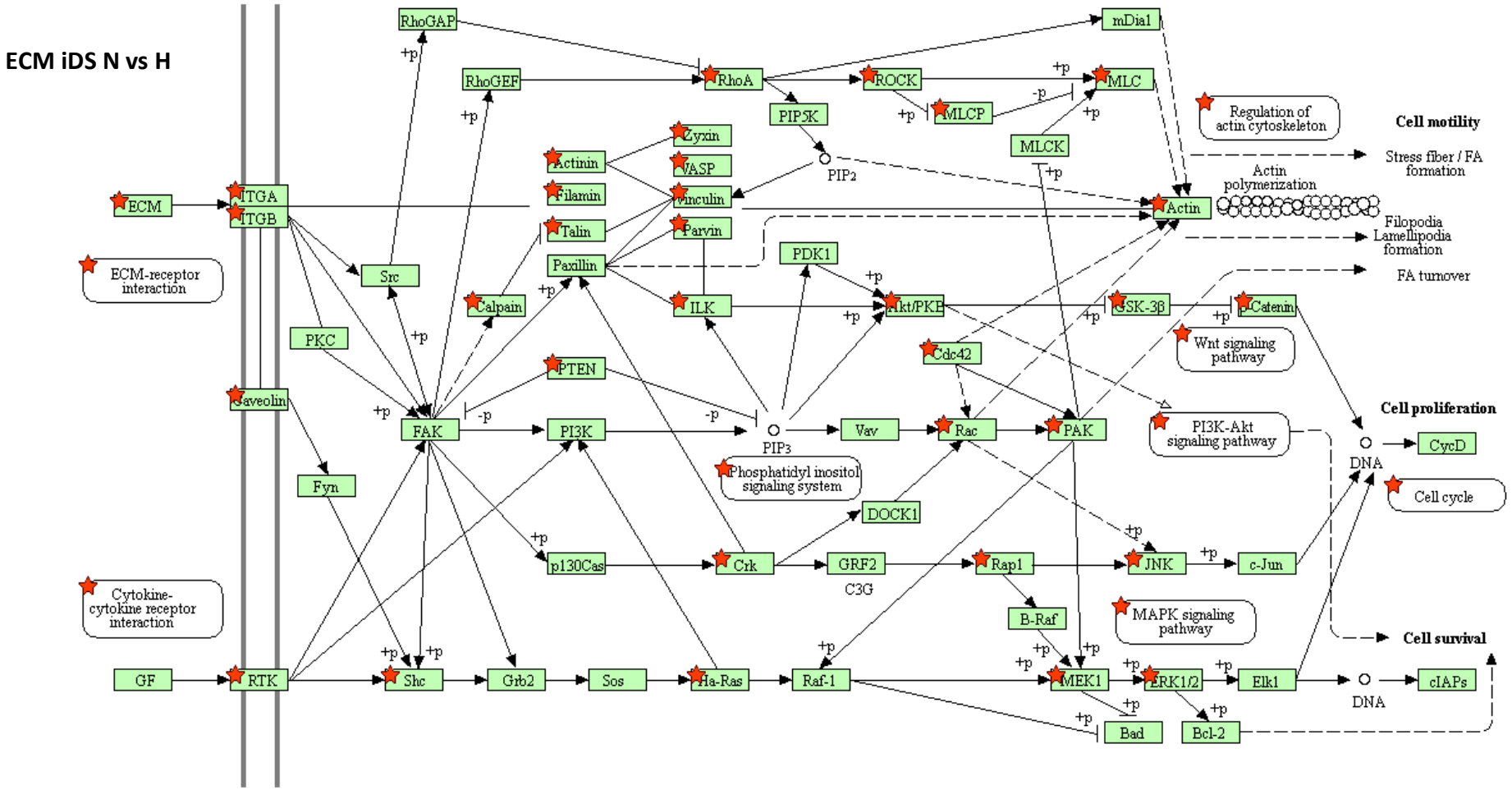

Annex B Figure 3 - Focal adhesion pathway. Overlay file of ECM N - ECM H and ECM iDS N – ECM iDS H. Red start indicate the presence of the protein in both matrixes. Full arrows indicate an interaction, while the dotted arrows indicates an indirect effect. Results generated by DAVID Functional Annotation software.

Proteins that are involved in several pathways compose matrices, however according with this DAVID functional annotation analysis, it was possible to have ECM-receptor interaction pathway only in ECM not in ECM iDS. Indicating that ECM iDS did not have proteins involved in ECM-receptor interaction. Comparing to focal adhesion pathway ECM iDS had more proteins present (41 red starts) than ECM (35 red starts).

7.3 Annex C

Balb/c mouse MSC were able to differentiate into adipocytes in different conditions. To observe if hypoxia had an effect on Balb/c differentiation capacity, it was compared the difference between performing the adipogenic assay in several normoxia-hypoxia combinations, in plastic and on top of ECM and ECM iDS.

The figures show the comparison of cytoplasmic lipids accumulation in the cells between different conditions, Oil Red O staining was extracted using isopropanol. The absorbance of the extracted Oil Red O was spectrophotometrically determined at 520 nm to measure lipid accumulation.

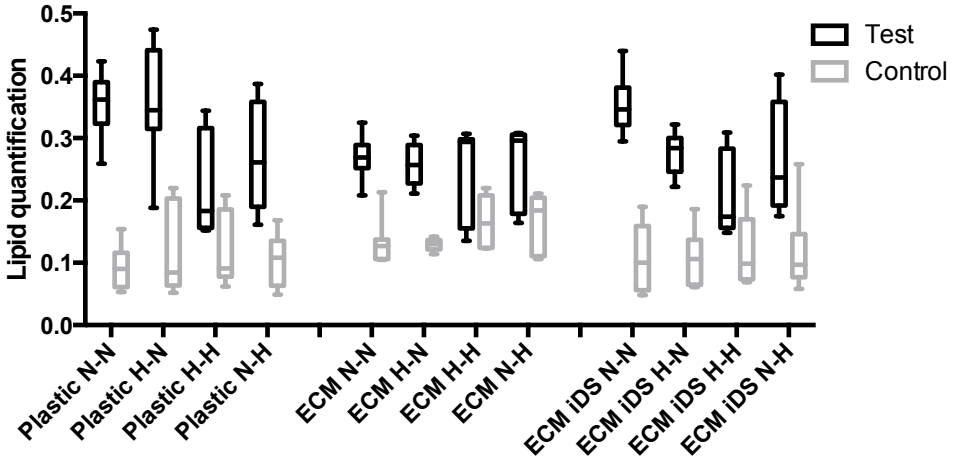

Annex C Figure 1- Comparison of lipid quantification between adipogenic differentiation under different conditions. Lipid accumulation of Balb/c cells differentiated into adipocytes in different normoxia-hypoxia combinations in plastic and on top of ECM and ECM iDS. In the X axis the first letter represents the condition that the Balb/c were before differentiation and the second letter indicates the condition that the cells were during adipogenic differentiation. The graph represent 5 experiments and triplicates, 15 wells were analysed. Control wells had significantly lower accumulation of lipids (grey).

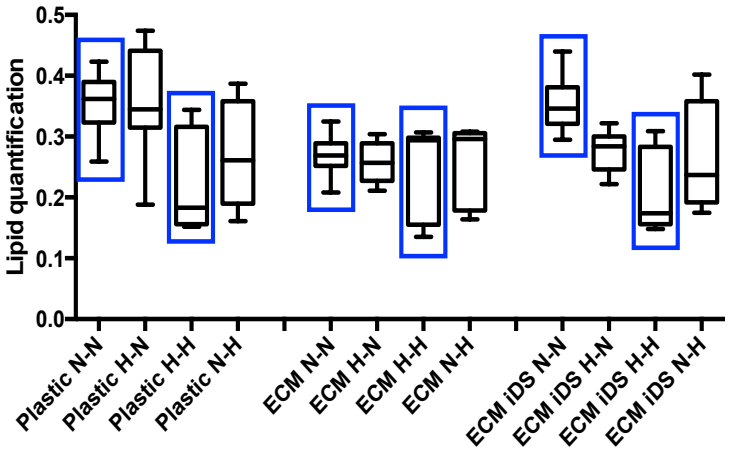

Annex C Figure 2- Comparison of lipid quantification between adipogenic differentiation under different conditions. Figure shows the same results above but just with test samples. Blue boxes indicate the results used in Chapter 5.

7.4 Annex D

In the following of Chapter 6, better screening methods for new drugs to treat MM are needed, since conventional approached do not take into consideration hypoxia and proteins present on ECM.

The hypothesis was that cells cultured on top of hypoxic ECM will mimic better the bone marrow microenvironment, thereby providing a more physiological system for drug screening.

Preliminary results show that a MM cell line (MM1S) treated with 2 drugs, Bortezomib and Melphalan, had different responses in the presence of ECM, compared with plastic. The ECM were prepared with primary fibroblasts and BM-MSC cell line (TERT cells). These drugs have distinctive mechanism of action; Bortezomib is a proteasome inhibitor and Melphalan a DNA alkylating agent. MM1S were cultured on top of four types of ECM:

* ECM from human Fibroblasts in normoxic conditions
* ECM from human Fibroblasts in hypoxic conditions
* ECM from human BM-MSC cell line in normoxic conditions
* ECM from human BM-MSC cell line in hypoxic conditions

This results show that Fibroblast ECM offers a higher protection against both drugs, than MSC ECM. Other interesting results are that Fibroblast ECM prepared in normoxia protects cells against Bortesomib, however, the opposite result is obtained with Melphalan.

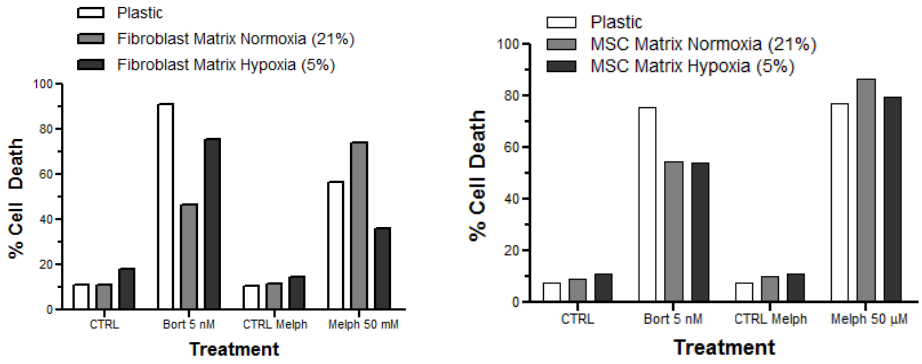

Annex D Figure 1 - MM1S cells were plated on top of ECM or plastic and incubated at 37°C in humidified incubator for 24 h, with 21% O2. Following 24 h the cells were treated with 5 nM of Bortezomib and 50 ?M of Melphalan for 24 h in the same conditions. Cell death was determined by flow cytometry using Annexin V FITC/PI staining.

This data demonstrate that some ECM-related factors can influence drug-induced cell death in multiple myeloma. For this reason and since ECM has a role on drug efficacy, the objectives of a future project would be:

* To identify the best ECM model to test drug resistance;

* To study the effect of 5% O2 on drug resistance;

* Characterization of ECM components prepared in 21% and 5% O2 by proteomics;

* Using different B cell lines, titrate different drugs to treat MM.

Stromal cells are the main cells producing ECM in the bone marrow and since this environment is hypoxic, the best ECM model to study drug efficiency on B cells should be ECM from MSC prepared in hypoxia.

From the results above, Bortezomib had an effect on MM1S cultures on top of MSC ECM, with 30% less cell death. However, in this case, the BM MSC used were a cell line. These results should be compared with those using primary MSC.

Additionally, it also should be tested ECM prepared by a mixture of cells in different proportions. Since bone marrow niche is composed of MSC, fibroblasts, osteoblasts, adipocytes, vascular endothelial cells and others.

Another factor that should be considered is hypoxia. In the preliminary results MM1S cells were cultured in normoxia. However, these cells should be cultured in hypoxia to mimic better the conditions of BM B cell differentiation. Other cells lines or even primary B cells also should be tested.

7.5 Annex E

7.5.1 Accepted publications:

"Development of a flow cytometry-based potency assay for measuring the in vitro immunomodulatory properties of Mesenchymal Stromal Cells". **Andreia Ribeiro**, Matthew Griffin, Thomas Ritter, Rhodri Ceredig. Immunology Letters, 177 (38-46); 2016.

"Immunomodulatory effects of natural polysaccharides assessed in human whole blood culture and THP-1 cells show greater sensitivity of whole blood culture". Gill SK, Islam N, Shaw I, **Ribeiro A**, Bradley B, Brien TO, Kilcoyne M, Ceredig R, Joshi L. International Immunopharmacology journal, 36 (315-323); 2016.

"Infliximab exerts selective inhibitory actions on circulating subsets of blood monocytes in Crohn's disease patients". Slevin, S. M., Dennedy, M. C., Connaughton, E. C., **Ribeiro, A**., Ceredig, R., Griffin, M. D. and Egan, L. E.. Journal of Crohn's and Colitis, 2016.

7.5.2 Patent:

PCT/EP2014/059397 or WO2014180933 A1

7.5.3 Oral communications and posters:

- Oral communication: "A rapid and quantifiable flow cytometry-based potency assay to measure the immunomodulatory properties of Mesenchymal Stromal Cells". **Andreia Ribeiro**, Aoife Dunne, Mary Murphy, Matthew Griffin, Thomas Ritter, Rhodri Ceredig. 5th European Immunology Conference. Berlin, Germany. 21-23 July 2016.
- Oral communication: "Effect of extracellular matrix and hypoxia on Mesenchymal Stromal Cell differentiation". **Andreia Ribeiro**, Lokesh Joshi, Rhodri Ceredig. 5th European Immunology Conference. Berlin, Germany. 21-23 July 2016.
- Poster: "Qualitative effects of hypoxia on the composition of Extracellular Matrix produced by a cloned mouse Mesenchymal Stromal Cell". **Andreia Ribeiro**, Satbir Gill, Abhigyan Satyam, Lokesh Joshi, Dimitrios Zeugolis, Rhodri Ceredig. Matrix Biology Ireland (MBI) – 2nd Meeting of the Irish Society for Matrix Biology. Dublin, Ireland. 2-4 December 2015.
- Oral communication: "Proteomic and glycomic analysis of extracellular matrix produced by murine stromal cells under hypoxic and normoxic conditions". Satbir Kaur Gill, **Andreia Ribeiro**, Michelle Kilcoyne, Rhodri Ceredig, Lokesh Joshi. GLYCO 23 International Symposium on Glycoconjugates. Croatia, Split. 15-20 September 2015.
- Poster: "Validation of a potency assay for the assessment of adipose-derived stromal cells in

the modulation of osteoarthritis". Aoife Dunne, **Andreia Ribeiro**, Marielle Moran, Frank Barry, Rhodri Ceredig and Mary Murphy. Irish Society for Immunology, annual meeting. Dublin, Ireland. 17-18 September 2015.

- Poster: "Effects of hypoxia on the Extracellular Matrix produced by the mouse MS-5 Mesenchymal Stromal cell line". **Andreia Ribeiro**, Satbir Gill, Abhigyan Satyam, Lokesh Joshi, Dimitrios Zeugolis, Rhodri Ceredig. Matrix Biology Ireland (MBI) – 1st Meeting of the Irish Society for Matrix Biology. Galway, Ireland. 19-21 November 2014.
- Oral communication: "Development of a flow cytometry-based potency assay for the immunomodulatory properties of mesenchymal stromal cells". **Andreia Ribeiro**, Matthew Griffin, Thomas Ritter, Rhodri Ceredig. International conference on Stem Cell Translation; Stem cell Galway 2014/8th UK Mesenchymal Stem Cell meeting. Galway, Ireland. 29-30 October 2014.
- Poster: "Development of a flow cytometry-based potency assay for the immunomodulatory properties of mesenchymal stromal cells". **Andreia Ribeiro**, Matthew Griffin, Thomas Ritter, Rhodri Ceredig. Irish Society for Immunology, annual meeting. Dublin, Ireland. 4-5 September 2014.
- Poster: "B lymphopoiesis in pregnant women". **Andreia Ribeiro,** Tiago Carvalheiro, Ana Lopes, Artur Paiva, Rhodri Ceredig. Irish Society for Immunology, annual meeting. Dublin, Ireland. 4-5 September 2014.
- Poster: "Development of a flow cytometry-based potency assay for the immunomodulatory properties of mesenchymal stromal cells". **Andreia Ribeiro**, Matthew Griffin, Thomas Ritter, Rhodri Ceredig. 9th Annual Meeting of the Irish Cytometry Society. Dublin, Ireland. 25-26 February 2014.
- Poster: "B lymphopoiesis in pregnant women". **Andreia Ribeiro**, Tiago Carvalheiro, Ana Lopes, Artur Paiva, Rhodri Ceredig. 9th Annual Meeting of the Irish Cytometry Society. Dublin, Ireland. 25-26 February 2014.
- Poster: "Monocytes and T cells in Haemochromatosis". McLoughlin P, **Ribeiro A**, Duffy L, Lee J, Hanley S, Ceredig R. 9th Annual Meeting of the Irish Cytometry Society. Dublin, Ireland. 25-26 February 2014.
- Oral communication: "Development of a flow cytometry-based potency assay for the immunomodulatory properties of mesenchymal stromal cells". **Andreia Ribeiro**, Matthew Griffin, Thomas Ritter, Rhodri Ceredig. XIII Meeting of the Iberian Cytometry Society. Aveiro, Portugal. 9-11 May 2013.

7.6 Annex F

Annex F Table 1 - List of cells used. N.A. not applicable and N.K. not known.

Cells	Supplier	Reference	Lot
Balb/c mouse MSC	REMEDI	N.A.	N.A.
BM-MSC human immortalized cells - TERT	[189]	N.A.	N.A.
BM-MSC iCasp9^{+} human immortalized cells	[346]	N.A.	N.A.
J774A.1 mouse monocytic/macrophage cell line	Sigma Aldrich	91051511	11F015
Jurkat human T cell line	ATCC	TIB-152	N.K.
Mouse T cells	REMEDI	N.A.	N.A.
MS5 mouse stromal cell line	[357]	N.A.	N.A.
Multiple Myeloma (MM) human cell line	ATCC	CRL-2975	N.K.
Neonal human foreskin Fibroblats	amsbio	GSC-3002	94300894
Raw264.7 mouse monocytic/macrophage cell line	Sigma Aldrich	91062702	12F026

Annex F Table 2 - List of medium used.

Media	Supplier	Reference
RPMI 1640	Gibco, Invitrogen	31870-025
MEM alpha medium (1X) + GlutaMax	Gibco, Invitrogen	32561-029
DMEM High Glucose (1X) + GlutaMax	Gibco, Invitrogen	31966-021
DMEM Low Glucose (1X) + GlutaMax	Gibco, Invitrogen	21885 -025

Annex F Table 3 - Cell culture medium recipes. All media were stored at 4°C.

Human BM-MSC and Fibroblasts:
MEM alpha medium GlutaMax
10% HyClone FBS
1% P/S

Human ASC:
MEM alpha medium GlutaMax
5% Pooled human platelet lysate
1% P/S

Human Jurkat, MM and PBMC:
RPMI 1640
10% FBS
1% P/S

Mouse Balb/c (following harvest):
MEM alpha medium GlutaMax
10% FBS
10% Equine serum
1% P/S

Mouse Balb/c:
MEM alpha medium GlutaMax
10% FBS
1% P/S

Mouse MS5:
DMEM Low Glucose GlutaMax
10% FBS
1% P/S

Mouse Raw264.7 and J774A.1:
DMEM High Glucose GlutaMax
10% FBS
1% P/S

Adipogenic Induction medium:
DMEM High Glucose GlutaMax
1 µM Dexamethasone
10 µg/mL Insuline
200 µM Indomethacin
500 µM MIX
1% P/S
10% FBS
Filtered (0.2 µm)

Adipogenic Maintenance medium:
DMEM High Glucose GlutaMax
10 µg/mL Insuline
1% P/S
10% FBS
Filtered (0.2 µm)

Osteogenic medium:
DMEM Low Glucose GlutaMax
100 nM Dexamethasone
50 µM Ascorbic acid 2-P
20 mM β-glycerophosphate
50 ng/mL L-thyroxine
2 mM L-glutaminne
1% P/S
9% Equine serum
9% FBS
Filtered (0.2 µm)

Freezing media for hMSC:
HyClone Fetal Bovine Serum
10% DMSO

Freezing media:
FBS
10% DMSO

Annex F Table 4 - Recipes of solutions.

PBS 1X:

1 L dH_2O
10 tables
Filtered (0.2 µm) and stored at 4°C

FACS Buffer:

PBS 1X
2% FBS
0.05% Sodium azide (NaN_3)
Filtered (0.2 µm) and stored at 4°C

0.1% Gelatine:

1 L dH_2O
1 g Gelatine from bovine skin
Autoclaved and filtered (0.2 µm)
Stored at room temperature

Tris/EDTA lysis buffer:

dH_2O
10 mM Tris
1 mM EDTA
Correct pH to 7.4
Autoclaved and filtered (0.2 µm)

DTT and guanidine solution:

dH_2O
10 mM DTT
5 M guanidine hydrochloride
Add NaOH to achieve pH 7
Filtered (0.2 µm) and stored at room temperature

Blocking buffer:

PBS 1X
4% FBS

AlamarBlue solution:

PBS 1X
10% AlamarBlue® dye

Oil Red O solution:

100 mL Isopropanol (99%)
0.3 g Oil Red O
Stored at room temperature

Before use:

6 parts of Oil Red O soluition
4 parts dH_2O
Filtered with Whatman paper

2% Alizarin Red solution:

100 mL dH_2O
2 g Alizarin Red S
Add NH_4OH to achieve pH 4.2
Stored at room temperature
Filteedr with Whatman paper before use

60% Isopropanol:

60 mL Isopropanol (99%)
40 mL dH_2O
Stored at room temperature

Annex F Table 5 - List of reagents used.

Reagent	Supplier	Reference
0.25% Trypsin-EDTA (1X)	Gibco, Invitrogen	25200-056
10% Neutral buffered formalin	Sigma Aldrich	HT501128
Absolot ethanol	Fisher Scientific	E/0600DF/17
AlamarBlue® dye	Invitrogen	DAL1100
Alizarin Red S	Sigma Aldrich	A5533
Ascorbic acid 2-Phosphate	Sigma Aldrich	A8960
B/B homodimerizer - AP20187	ApexBio	B1274
BD FACS Lysin solution	Becton Dickinson	349202
Biotinamidocaproate N-Hydroxysuccinimide Ester	Sigma Aldrich	B2643
Brefeldin A Solution (1000X – 3mg/mL)	eBioscience	00-4506-51
Calcein AM	Life technologies	C3100MP
Calcium liquicolor kit	StanBio	150
Chloroform	Sigma Aldrich	496189
Collagenase	Sigma Aldrich	C9891
Dexamethasone	Sigma Aldrich	D4302
DharmaFECT Transfection reagent	GE Healthcare – Dharmacon	T-2001-S29124097
Distilled H_2O	BRB building	N.A.
Dithiothreitol	Sigma Aldrich	43815-1G
DMSO	Sigma Aldrich	D2650
DPBS 1X 500mL	Gibco, Invitrogen	14190-094
Dynabeads® Human T-Activator CD3/CD28	Gibco, Life Technologies	11131D
Dynabeads® Mouse T-Activator CD3/CD28	Gibco, Life Technologies	11452D
EDTA	Fisher Scientific	B120-1
EGTA	Sigma Aldrich	E3889
Fetal Bovine Serum	Sigma Aldrich	F7524
Ficoll-Paque	GE Healthcare	17-1440-03
Gelatine from bovine skin	Sigma Aldrich	G9382
Guanidine hydrochloride	Sigma Aldrich	G4630
HCl	Sigma Aldrich	H1758
High Capacity cDNA Reverse Transcription kit	Applied Biosystems	4368815
High Pure RNA Isolation kit	Roche	11828665001
Human/Mouse/Rat Total HSP70 DuoSet IC ELISA	R&D Systems	DYC1663-2
Hyclone equine serum	Sigma Aldrich	H1270
HyClone Fetal Bovine Serum	Thermo scientific	SV30160.03
IBMX	Sigma Aldrich	I7018
IMS	Lennox	SI-033-0716
Indomethacin	Sigma Aldrich	I7378
Insulin	Roche	11376497001
IntraPrep Kit (reagent 1 and 2)	Beckman Coulter	A07803
Ionomycin calcium salt	Sigma Aldrich	I0634-1mg
Isopropanol	Fisher Chemical	P/7490/PB17
L-Glutamine	Gibco, Invitrogen	25030-024
L-Thyroxine	Sigma Aldrich	*T1775*
LightCycler 480 SYBRE Green I Master	Roche	4707516001
LPS-EB Ultrapure	InvivoGen	tlrl-3pelps
MDP	InvivoGen	53678-77-6

Methanol	Sigma Aldrich	494437
Mitomycin C	Acros Organics	10286710
Mouse IFN gamma ELISA Ready-Set-Go	eBioscience	88-7314
Mouse TNF alpha ELISA Ready-Set-Go	eBioscience	88-7324
NH_4OH	Sigma Aldrich	338818
Nuclease-Free Water	Life technologies	AM9937
Oil Red O	Sigma Aldrich	O-0625
Pam3CSK4	InvivoGen	tlrl-pms
PBS tablets	Fisher Chemical	1282-1680
Penecillin/Streptomycin	Gibco, Invitrogen	15140-122
PFA	ChemCruz	sc-281692
PHA-L	Vector Laboratories	L-1110
PMA	Sigma Aldrich	P8139
Polybrene	N.K.	N.K.
PolyIC	Sigma Aldrich	P9582
Pooled human platelet lysate	Stem Cell	6960
Saponin	Sigma Aldrich	47036
siGLO Red Transfection Indicator	GE Healthcare – Dharmacon	D-001630-02-05
Sodim azide (NaN_3)	Sigma Aldrich	A2152
Tris (Trimethylol Aminomethane) base, DNase RNase protease free	Fisher Scientific	BP152-1
Trypan blue	Sigma Aldrich	T8154
β-glygerophosphate	Sigma Aldrich	G6251

7.7 Annex G

Annex G Table 1 - List of human and mouse antibodies used for flow cytometry and ICC.

Flow cytometry antibodies			
Human antibodies	**Supplier**	**Clone**	**Catalogue number**
Anti-Human CCL2 (MCP-1) PE	eBioscience	2H5	12-7096
Anti-Human CD14 APC	Becton Dickinson	MϕP9	340684
Anti-Human CD14 APC	Miltenyi Biotec	TÜK4	130-091-243
Anti-Human CD16 FITC	eBioscience	eBioCB16 (CB16)	11-0168
Anti-Human CD25 PerCP Cy 5.5	eBioscience	BC96	45-0259
Anti-Human CD3 FITC	eBioscience	SK7	11-0036
Anti-Human CD33 PerCP Cy5.5	Becton Dickinson	P67.6	333146
Anti-Human CD4 APC	BD Pharmingen	RPA-T4	561841
Anti-Human CD45 PerCP Cy 5.5	eBioscience	2D1	45-9459
Anti-Human CD45 V500-C	Becton Dickinson	2D1	655873
Anti-Human CD69 PeCy7	eBioscience	FN50	25-0699
Anti-Human CD8 V500	BD Horizon	SK1	561617
Anti-Human CD86 FITC	Immunotools	BU63	21480863
Anti-Human CD8α PE-Cy7	eBioscience	SK1	25-0087
Anti-Human IFN gamma PE	eBioscience	4S.B3	12-7319
Anti-Human IL-10 PE	eBioscience	JES3-9D7	12-7108
Anti-Human IL-12/IL-23 p40 PE	eBioscience	C8.6	12-7129
Anti-Human IL-17A PeCy7	eBioscience	eBio64DEC17	25-7179
Anti-Human TNF alpha PE	eBioscience	MAb11	12-7349
Anti-HumanCD8 APC	ImmunoTools	UCHT-4	21620086
Mouse Anti-Human CD19 APC	Becton Dickinson	HIB19	555415
Mouse Anti-Human IL-6 FITC	BD FastImmune	AS12	340526
Mouse Anti-Human TNF-α PE	BD FastImmune	6401.1111	340512
Prodpidium Iodite (PI)	Sigma Aldrich	N.A.	P4170
Streptavidin PE	eBioscience	N.A.	12-4317
IMMUNOPHENOTYPING			
Human antibodies	**Supplier**	**Clone**	**Catalogue number**
Anti-Human CD73 PE	BD Pharmingen	AD2	550257
Anti-Human CD105 PE	Invitrogen	SN6	MHCD10504
Anti-Human CD14 PE	AbD Serotec	MEM-18	SFL2185
Anti-Human CD19 PE	Becton Dickinson	4G7	345777
Anti-Human CD3 PE	Becton Dickinson	SK7	345765
Anti-Human CD34 PE	BD Pharmingen	581	555822
Anti-Human CD45	BD Pharmingen	HI30	555483
Anti-Human CD90 PE	BD Pharmingen	5E10	555596
Anti-Human HLA-DR PE	Invitrogen	TU36	MHLDR04
Anti-Human MSC Analysis Kit	BD Stemflow	N.A.	562245
Mouse IgG1 K, Isotype Control PE	Becton Dickinson	MOPC-21	554680
Mouse IgG2b, Isotype Control PE	Invitrogen	N.A.	MG2b04

Mouse antibodies	Supplier	Clone	Catalogue number
Anti-Mouse CD105 PE	eBioscience	MJ7/18	12-1051
Anti-Mouse CD11b PE	eBioscience	M1/70	11-0112
Anti-Mouse CD29 APC	eBioscience	HMb1-1	N.K.
Anti-Mouse CD31 PE	eBioscience	390	12-0311
Anti-Mouse CD34 eFluor 660	eBioscience	N.K.	N.K.
Anti-Mouse CD44 PE	eBioscience	IM7	12-0441
Anti-Mouse CD45 FITC	eBioscience	30-F11	11-0451
Anti-Mouse CD49e FITC	eBioscience	HMa5-1	N.K.
Anti-Mouse CD73 PE	eBioscience	TY/11.8	N.K.
Anti-Mouse CD90.2 PE	BD Pharmingen	53-2.1	553006
Anti-Mouse Ly-6A/E (Sca1) FITC	eBioscience	D7	11-5981
Anti-Mouse MHC II APC eFluor 780	eBioscience	M5/114.15.2	47-5321
Rat IgG2a K, Isotype Control PE	eBioscience	N.K.	N.K.
Rat IgG2b K, Isotype Control APC	eBioscience	N.K.	N.K.
Rat IgG2b K, Isotype Control FITC	eBioscience	N.K.	N.K.

ICC antibodies			
Mouse antibodies	**Clone**	**Supplier**	**Catalogue number**
Anti-Mouse Collagen IV	Rabbit polyclonal	Abcam	ab6586
Anti-Mouse Collagen VI	Rabbit polyclonal	Abcam	ab6588
Anti-Mouse Fibronectin	Rabbit polyclonal	Abcam	ab2413
Anti-Mouse Laminin	Rabbit polyclonal	Sigma Aldrich	L9393
Anti-Mouse Integrin B1	Rabbit polyclonal	Sigma Aldrich	AB4300655
Anti-Mouse Aggrecan	Rabbit polyclonal	Santa Cruz Biotechnology	c-25674
Anti-Mouse Heparan Sulfate - PGBM (Proteoglycan)	Rat polyclonal	Abcam	ab2501
Anti-Mouse Thrombospondin 1	Goat polyclonal	Santa Cruz Biotechnology	sc-12312
Anti-Rabbit Alexa Fluor 488	Goat polyclonal	LifeTechnologies	A21441
Anti-Rat Alexa Fluor 488	Goat polyclonal	LifeTechnologies	A11006
Anti-Goat Alexa Fluor 488	Donkey	LifeTechnologies	A11055
DAPI	N.A.	N.K.	N.K.

7.8 Annex H

Annex H Table 1 - Sequences of mouse primers used. Final concentration of all primers was 0.5 μM.

	Mouse genes	Sequences (5'-3')	
HIFs	HIF 1 alpha (HIF-1α)	Forward:	TCAAGTCAGCAACGTGGAAG
		Reverse:	TATCGAGGCTGTGTCGACTG
	HIF 2 alpha (HIF-2α)	Forward:	CTAAGTGGCCTGTGGGTGAT
		Reverse:	GTGTCTTGGAAGGCTTGCTC
Stem cell	Sox2	Forward:	AAGGGTTCTTGCTGGGTTTT
		Reverse:	AGACCACGAAAACGGTCTTG
	Oct4	Forward:	CACGAGTGGAAAGCAACTCA
		Reverse:	AGATGGTGGTCTGGCTGAAC
	Nanog	Forward:	CACCCACCCATGCTAGTCTT
		Reverse:	ACCCTCAAACTCCTGGTCCT
Osteogenic	BMP2	Forward:	CCCCAAGACACAGTTCCCTA
		Reverse:	GAGACCGCAGTCCGTCTAAG
	RUNX2	Forward:	CCCAGCCACCTTTACCTACA
		Reverse:	TATGGAGTGCTGCTGGTCTG
	Osterix	Forward:	ACTCATCCCTATGGCTCGTG
		Reverse:	GGTAGGGAGCTGGGTTAAGG
	Osteopontin	Forward:	TGCACCCAGATCCTATAGCC
		Reverse:	CTCCATCGTCATCATCATCG
Adipogenic	c/EBPß	Forward:	GTTTCGGGACTTGATGCAAT
		Reverse:	CGAAACGGAAAAGGTTCTCA
	aP2	Forward:	TCACCTGGAAGACAGCTCCT
		Reverse:	AATCCCCATTTACGCTGATG
Chondrogenic	Collagen II (Col2)*	Forward:	GCCAAGACCTGAAACTCTGC
		Reverse:	GCCATAGCTGAAGTGGAAGC
	Aggrecan (Acan)*	Forward:	TGGCTTCTGGAGACAGGACT
		Reverse:	TTCTGCTGTCTGGGTCTCCT
	Sox9	Forward:	AGCTCACCAGACCCTGAGAA
		Reverse:	TCCCAGCAATCGTTACCTTC
ECM	Collagen IV (Col4α1)	Forward:	GCTCTGGCTGTGGAAAATGT
		Reverse:	CTTGCATCCCGGGAAATC
	Fibronectin	Forward:	CCCTATCTCTGATACCGTTGTCC
		Reverse:	TGCCGCAACTACTGTGATTCGG
	Heparan sulfate proteoglycan (Hspg2)	Forward:	CATTCAGGTGGTCGTCCTCTCA
		Reverse:	AGGTCAAGCGTCTGTCCTTCAG
	Thrombospondin-1 (TSP1)	Forward:	GGTAGCTGGAAATGTGGTGCGT
		Reverse:	GCACCGATGTTCTCCGTTGTGA
	Integrin β1	Forward:	CTCCAGAAGGTGGCTTTGATGC
		Reverse:	GTGAAACCCAGCATCCGTGGAA
	Collagen VI (Col6α1)	Forward:	GACACCTCTCAGTGTGCTCTGT
		Reverse:	GCGATAAGCCTTGGCAGGAAATG
	Laminin (Lamb2)	Forward:	GGAGGACTTGTTCTGAGTGCCA

		Reverse:	CTGTGGAACGATGACACTGAGG
	Metalloproteinase (Adam9)	Forward:	GAAGGCACCAAATGTGATGCTGG
		Reverse:	CCAGCCGTCTTCACAGTGACAA
House keeping	β-2 microglobulin (B2M)	Forward:	ATGGGAAGCCGAACATACTG
		Reverse:	CAGTCTCAGTGGGGGTGAAT
	Glyceraldehyde-3-phosphate dehydrogenase (GAPDH)	Forward:	CGACTTCAACAGCAACTCCCACTCTTCC
		Reverse:	TGGGTGGTCCAGGGTTTCTTACTCCTT

7.9 Annex I

Annex I Table 1 - List of material used.

Material	Supplier	Catalogue number
15/50ml Centrifuge tubes	Sarstedt	62.554.502 / 62.547.254
250/500ml Vacuum filtration units 0.2 µm	Sarstedt	83.1822.001 / 83.1823.001
96 Deep well plate with round bottom (sterile)	VWR	736-0339
Alcohol Prep (tissue with 70% isopropyl alcohol)	Romed	PREP-2000
BD Vacutainer Eclipse blood collection needle	BD Vacutainer	368609
BD Vacutainer Holder	BD Vacutainer	364815
BD Vacutainer® Plastic K_2EDTA tube with Lavender BD Hemogard™ Closure; 6mL	BD Vacutainer	367873
BD Vacutainer® Plastic Sodium Heparin tube with Green BD Hemogard™ Closure, 6mL	BD Vacutainer	367876
BD Vacutainer® Plus Citrate tube with Light Blue BD Hemogard™ Closure; 2.7mL	BD Vacutainer	363095
BioWed	Zeus	N.K.
Blood collection torniquete	N.A.	N.A.
Cell culture insert for 24 well plates with translucent membrane (PET), 0.4 µm	Greiner bio-one	662640
Cytometer tubes, 5mL	Sarstedt	55.1578
Dialysis tubing 8 kDa MWCO	Fisher Scientific	12737486
Disposable steril cell scraper 25 / 39 cm	Sarstedt	83.183 / 83.1831
Eppendorfs (sterile) - 0.2 / 1.5mL	Sarstedt	72.737.002 / 72.690.001
ePTFE (expanded ploytetrafluoroethlyene)	Proxy Biomedical	N.A.
Filtropur S 0.2µm	Sarstedt	83.1826.001
ibiTreat 8 wells chamber	ibidi GmbH	80826
LightCycler480 Multiwell plate 384 wells	Roche	4729749001
LightCycler480 Multiwell plate 96 wells	Roche	4729692001
LightCycler480 sealing foil	Roche	4729757001
Nitrile Gloves	Fisher Scientific	10226293
Nunc cell culture treated multidishes 6 / 12 / 24 / 48 wells	Thermo Scientific	140675 / 150628 / 142475 / 150687
Nunc EasYFlask 25 / 75 / 175 cm^2, filter cap	Thermo Scientific	156367 / 156499 / 159910
Nunc Sterile 1.8 ml cryovials	Thermo Scientific	363401
Parafilm; PM-992	Fisher Scientific	12378039
PCL	NFB; NUIGalway	N.A.
Plaster (sterile/hypoallergenic)	HypaPlast	D9010
Plate 96 wells, flat bottom	Sarstedt	82.1581
Plate sealers	R&D Systems	DY992
PP (polypropylene)	Ethicon	N.K.
Silicon O-ring	N.K.	N.K.
Sterile aspiration pipette 2mL	Sarstedt	86.1252.011
Sterile pipette filter tips P10 / P20 / P200 / P1000	StarLab	S1121-3810 / S1120-1810 / S1120-8810 / S1122-1830

Sterile pipette tips P10 / P200 / P1250	StarLab	S1110-3700 / S1111-1706 / S1112-1720
Sterile serological pipettes 5 / 10 / 25 mL	Sarstedt	86.1253.001 / 86.1254.001 / 86.1685.001
Sterile transfer-pipette	Sarstedt	86.1171.001
Syringe 10mL	BD Plastipak	302188
Tissue culture plate 96 wells, flat bottom	Sarstedt	83.3924.300
Tissue culture plate 96 wells, round bottom	Sarstedt	183.1837
Tissue paper	Fisher Scientific	12784326
Whatman no.1 paper filter (90 mm)	Fisherbrand	1156-6873

7.10 Annex J

Annex J Table 1 - List of equipment used.

Equipment
BD Accuri C6 4 colour flow cytometer (Becton Dickinson)
BD Canto II
Biological Safety Cabinet (hood)
Calculator
Centrifuge (Eppendorf)
Fume hood
Gilson Pipettes (P10, P20, P100, P1000)
Ice box
Incubator at 37°C with 5% and 21% CO_2
Incubator at 37°C with 5% and 5% CO_2
LightCycler 480 II Real Time PCR System (Roche)
NanoDrop 2000 (Thermo Scientific)
Neubauer chamber
Olympus IX71 inverted fluorescent microscope
Olympus IX81 inverted confocal microscope
Orbital shaker
Small centrifugue - Heraeus Fresco 17 (Thermo Scientific)
Timer
Ultracentrifuge - Sorvall Discovery 100SE (Hitachi)
Varioskan Flash microplate reader (Thermo Scientific)
Veriti Gradient Thermal Cycler (Applied Biosystems)
37°C water bath
4°C Refrigerator
-20°C Freezer
-80°C Freezer

Annex J Table 2 - List of softwares used.

Software
BD Csample Analysis software (Becton Dickinson)
FlowJo, version 10 (Tree star)
Infinicyt, version 1.7 (Cytognos)
DIVA Diva version 6.1.3 (Becton Dickinson)
GraphPad Prism software, version 6
CellSens (Olympus Life Science)
Fluoview 10 ASW (Olympus Life Science)
Gorilla gene ontology (online)
DAVID functional annotation (online)
Panther gene ontology (online)

7.11 Annex K

7.11.1 Cytometers configuration:

BD Accuri C6 - 2 lasers, 4 fluorescences

Lasers:

Blue 488 nm

Red 640 nm

Emission detection:

Blue: FL1 533/30 nm; FL2 585/40; FL3 > 670 nm

Red: FL4 675/25

BD FACS Canto II - 3 lasers, 8 fluorescences

Lasers:

Violet 405 nm

Blue 488 nm

Red 633 nm

Fluorescence detectors:

8 PMTs in 4-2-2 configuration

Detector bands:

Violet: 450/50; 502 to 525 nm

Blue: 530/30; 585/42; >670; 780/60 nm

Red: 660/20; 780/60 nm

Chapter 8 | Bibliography

1. Wagers, A.J. and I.L. Weissman, *Plasticity of adult stem cells.* Cell, 2004. **116**(5): p. 639-48.

2. Cvejic, A., *Mechanisms of fate decision and lineage commitment during haematopoiesis.* Immunol Cell Biol, 2016. **94**(3): p. 230-5.

3. Morrison, S.J. and A.C. Spradling, *Stem cells and niches: mechanisms that promote stem cell maintenance throughout life.* Cell, 2008. **132**(4): p. 598-611.

4. Kiel, M.J. and S.J. Morrison, *Uncertainty in the niches that maintain haematopoietic stem cells.* Nat Rev Immunol, 2008. **8**(4): p. 290-301.

5. Ceredig, R., A.G. Rolink, and G. Brown, *Models of haematopoiesis: seeing the wood for the trees.* Nat Rev Immunol, 2009. **9**(4): p. 293-300.

6. Simsek, T., et al., *The distinct metabolic profile of hematopoietic stem cells reflects their location in a hypoxic niche.* Cell Stem Cell, 2010. **7**(3): p. 380-90.

7. Mohyeldin, A., T. Garzon-Muvdi, and A. Quinones-Hinojosa, *Oxygen in stem cell biology: a critical component of the stem cell niche.* Cell Stem Cell, 2010. **7**(2): p. 150-61.

8. Jones, D.L. and A.J. Wagers, *No place like home: anatomy and function of the stem cell niche.* Nat Rev Mol Cell Biol, 2008. **9**(1): p. 11-21.

9. Orkin, S.H. and L.I. Zon, *Hematopoiesis: an evolving paradigm for stem cell biology.* Cell, 2008. **132**(4): p. 631-44.

10. Wilson, A. and A. Trumpp, *Bone-marrow haematopoietic-stem-cell niches.* Nat Rev Immunol, 2006. **6**(2): p. 93-106.

11. Hoshiba, T., et al., *Decellularized Extracellular Matrix as an In Vitro Model to Study the Comprehensive Roles of the ECM in Stem Cell Differentiation.* Stem Cells Int, 2016. **2016**: p. 6397820.

12. Wang, L.D. and A.J. Wagers, *Dynamic niches in the origination and differentiation of haematopoietic stem cells.* Nat Rev Mol Cell Biol, 2011. **12**(10): p. 643-55.

13. Larsson, J. and S. Karlsson, *The role of Smad signaling in hematopoiesis.* Oncogene, 2005. **24**(37): p. 5676-92.

14. Gordon, M.Y., *Extracellular matrix of the marrow microenvironment.* Br J Haematol, 1988. **70**(1): p. 1-4.

15. Watt, F.M. and W.T. Huck, *Role of the extracellular matrix in regulating stem cell fate.* Nat Rev Mol Cell Biol, 2013. **14**(8): p. 467-73.

16. Hynes, R.O., *The extracellular matrix: not just pretty fibrils.* Science, 2009. **326**(5957): p. 1216-9.

17. Klein, G., *The extracellular matrix of the hematopoietic microenvironment.* Experientia, 1995. **51**(9-10): p. 914-26.

18. Saller, M.M., et al., *Increased stemness and migration of human mesenchymal stem cells in hypoxia is associated with altered integrin expression.* Biochem Biophys Res Commun, 2012. **423**(2): p. 379-85.

19. Ramakrishnan, M.K., et al., *Untold story of collagen dressings.* Indian Journal of Burns, 2014. **22**(1): p. 33-36.

20. Sherman, V.R., W. Yang, and M.A. Meyers, *The materials science of collagen.* J Mech Behav Biomed Mater, 2015. **52**: p. 22-50.

21. nptel.ac.in/courses/102103012/8.

22. Halper, J. and M. Kjaer, *Basic Components of Connective Tissues and Extracellular Matrix: Elastin, Fibrillin, Fibulins, Fibrinogen, Fibronectin, Laminin, Tenascins and Thrombospondins*, in *Progress in Heritable Soft Connective Tissue Diseases*, J. Halper, Editor. 2014, Springer Netherlands: Dordrecht. p. 31-47.

23. Bosman, F.T. and I. Stamenkovic, *Functional structure and composition of the extracellular matrix.* J Pathol, 2003. **200**(4): p. 423-8.

24. Drivalos, A., et al., *The role of the cell adhesion molecules (integrins/cadherins) in prostate cancer.* Int Braz J Urol, 2011. **37**(3): p. 302-6.

25. De Arcangelis, A. and E. Georges-Labouesse, *Integrin and ECM functions: roles in vertebrate development.* Trends Genet, 2000. **16**(9): p. 389-95.

26. Alberts, B., et al., *Integrins*, in *Molecular Biology of the Cell*, G. Science, Editor. 2002: New York.

27. Seguin, L., et al., *Integrins and cancer: regulators of cancer stemness, metastasis, and drug resistance.* Trends Cell Biol, 2015. **25**(4): p. 234-40.

28. Yanagishita, M., *[Function of proteoglycans in the extracellular matrix].* Kokubyo Gakkai Zasshi, 1997. **64**(2): p. 193-204.

29. Mott, J.D. and Z. Werb, *Regulation of matrix biology by matrix metalloproteinases.* Curr Opin Cell Biol, 2004. **16**(5): p. 558-64.

30. Sternlicht, M.D. and Z. Werb, *How matrix metalloproteinases regulate cell behavior.* Annu Rev Cell Dev Biol, 2001. **17**: p. 463-516.

31. Visse, R. and H. Nagase, *Matrix metalloproteinases and tissue inhibitors of metalloproteinases: structure, function, and biochemistry.* Circ Res, 2003. **92**(8): p. 827-39.

32. Dempke, W., et al., *Human hematopoietic growth factors: old lessons and new perspectives.* Anticancer Res, 2000. **20**(6D): p. 5155-64.

33. Rakian, R., et al., *Native extracellular matrix preserves mesenchymal stem cell "stemness" and differentiation potential under serum-free culture conditions.* Stem Cell Res Ther, 2015. **6**: p. 235.

34. Lukashev, M.E. and Z. Werb, *ECM signalling: orchestrating cell behaviour and misbehaviour.* Trends Cell Biol, 1998. **8**(11): p. 437-41.

35. Lin, H., et al., *Influence of decellularized matrix derived from human mesenchymal stem cells on their proliferation, migration and multi-lineage differentiation potential.* Biomaterials, 2012. **33**(18): p. 4480-9.

36. Escobedo-Lucea, C., et al., *Development of a human extracellular matrix for applications related with stem cells and tissue engineering.* Stem Cell Rev, 2012. **8**(1): p. 170-83.

37. Kuhn, N.Z. and R.S. Tuan, *Regulation of stemness and stem cell niche of mesenchymal stem cells: implications in tumorigenesis and metastasis.* J Cell Physiol, 2010. **222**(2): p. 268-77.

38. Santiago-Medina, M., et al., *Regulation of ECM degradation and axon guidance by growth cone invadosomes.* Development, 2015. **142**(3): p. 486-96.

39. Maldonado, M. and J. Nam, *The role of changes in extracellular matrix of cartilage in the presence of inflammation on the pathology of osteoarthritis.* Biomed Res Int, 2013. **2013**: p. 284873.

40. Akhyari, P., et al., *The quest for an optimized protocol for whole-heart decellularization: a comparison of three popular and a novel decellularization technique and their diverse*

effects on crucial extracellular matrix qualities. Tissue Eng Part C Methods, 2011. **17**(9): p. 915-26.

41. Badylak, S.F., D.O. Freytes, and T.W. Gilbert, *Extracellular matrix as a biological scaffold material: Structure and function.* Acta Biomater, 2009. **5**(1): p. 1-13.
42. Jin, C.Z., et al., *Cartilage engineering using cell-derived extracellular matrix scaffold in vitro.* J Biomed Mater Res A, 2010. **92**(4): p. 1567-77.
43. Parmar, K., et al., *Distribution of hematopoietic stem cells in the bone marrow according to regional hypoxia.* Proc Natl Acad Sci U S A, 2007. **104**(13): p. 5431-6.
44. Doan, P.L. and J.P. Chute, *The vascular niche: home for normal and malignant hematopoietic stem cells.* Leukemia, 2012. **26**(1): p. 54-62.
45. Tiwari, A., et al., *Ex vivo expansion of haematopoietic stem/progenitor cells from human umbilical cord blood on acellular scaffolds prepared from MS-5 stromal cell line.* J Tissue Eng Regen Med, 2013. **7**(11): p. 871-83.
46. Keith, B. and M.C. Simon, *Hypoxia-inducible factors, stem cells, and cancer.* Cell, 2007. **129**(3): p. 465-72.
47. Abdollahi, H., et al., *The role of hypoxia in stem cell differentiation and therapeutics.* J Surg Res, 2011. **165**(1): p. 112-7.
48. Scholz, C.C. and C.T. Taylor, *Targeting the HIF pathway in inflammation and immunity.* Curr Opin Pharmacol, 2013. **13**(4): p. 646-53.
49. Takubo, K., et al., *Regulation of the HIF-1alpha level is essential for hematopoietic stem cells.* Cell Stem Cell, 2010. **7**(3): p. 391-402.
50. Li, Z., et al., *Hypoxia-inducible factors regulate tumorigenic capacity of glioma stem cells.* Cancer Cell, 2009. **15**(6): p. 501-13.
51. Seifter, J., D. Sloane, and A. Ratner, *Concepts in Medical Physiology*. 2005: Lippincott Williams & Wilkins. 669.
52. Covello, K.L. and M.C. Simon, *HIFs, hypoxia, and vascular development.* Curr Top Dev Biol, 2004. **62**: p. 37-54.
53. Wang, Y.H., et al., *Cell-state-specific metabolic dependency in hematopoiesis and leukemogenesis.* Cell, 2014. **158**(6): p. 1309-23.
54. Zheng, J., *Energy metabolism of cancer: Glycolysis versus oxidative phosphorylation (Review).* Oncol Lett, 2012. **4**(6): p. 1151-1157.
55. Lunt, S.Y. and M.G. Vander Heiden, *Aerobic glycolysis: meeting the metabolic requirements of cell proliferation.* Annu Rev Cell Dev Biol, 2011. **27**: p. 441-64.
56. Semenza, G.L., *Hypoxia-inducible factors in physiology and medicine.* Cell, 2012. **148**(3): p. 399-408.
57. Distler, J.H., et al., *Hypoxia-induced increase in the production of extracellular matrix proteins in systemic sclerosis.* Arthritis Rheum, 2007. **56**(12): p. 4203-15.
58. Uccelli, A., L. Moretta, and V. Pistoia, *Mesenchymal stem cells in health and disease.* Nat Rev Immunol, 2008. **8**(9): p. 726-36.
59. Frenette, P.S., et al., *Mesenchymal stem cell: keystone of the hematopoietic stem cell niche and a stepping-stone for regenerative medicine.* Annu Rev Immunol, 2013. **31**: p. 285-316.
60. Dazzi, F., et al., *The role of mesenchymal stem cells in haemopoiesis.* Blood Rev, 2006. **20**(3): p. 161-71.

61. Corselli, M., et al., *Perivascular support of human hematopoietic stem/progenitor cells.* Blood, 2013. **121**(15): p. 2891-901.

62. Pittenger, M.F., et al., *Multilineage potential of adult human mesenchymal stem cells.* Science, 1999. **284**(5411): p. 143-7.

63. Bosnakovski, D., et al., *Chondrogenic differentiation of bovine bone marrow mesenchymal stem cells (MSCs) in different hydrogels: influence of collagen type II extracellular matrix on MSC chondrogenesis.* Biotechnol Bioeng, 2006. **93**(6): p. 1152-63.

64. Dominici, M., et al., *Minimal criteria for defining multipotent mesenchymal stromal cells. The International Society for Cellular Therapy position statement.* Cytotherapy, 2006. **8**(4): p. 315-7.

65. Laranjeira, P., et al., *Immunophenotypic Characterization of Normal Bone Marrow Stem Cells*, in *Flow Cytometry - Recent Perspectives*, S. I, Editor. 2012, InTech: Rijeka, Croatia. p. 457-478.

66. Siegel, G., et al., *Phenotype, donor age and gender affect function of human bone marrow-derived mesenchymal stromal cells.* BMC Med, 2013. **11**: p. 146.

67. Russell, K.C., et al., *In vitro high-capacity assay to quantify the clonal heterogeneity in trilineage potential of mesenchymal stem cells reveals a complex hierarchy of lineage commitment.* Stem Cells, 2010. **28**(4): p. 788-98.

68. Haddad, R. and F. Saldanha-Araujo, *Mechanisms of T-cell immunosuppression by mesenchymal stromal cells: what do we know so far?* Biomed Res Int, 2014. **2014**: p. 216806.

69. Ren, G., et al., *Inflammatory cytokine-induced intercellular adhesion molecule-1 and vascular cell adhesion molecule-1 in mesenchymal stem cells are critical for immunosuppression.* J Immunol, 2010. **184**(5): p. 2321-8.

70. Chamberlain, G., et al., *Concise review: mesenchymal stem cells: their phenotype, differentiation capacity, immunological features, and potential for homing.* Stem Cells, 2007. **25**(11): p. 2739-49.

71. Baustian, C., S. Hanley, and R. Ceredig, *Isolation, selection and culture methods to enhance clonogenicity of mouse bone marrow derived mesenchymal stromal cell precursors.* Stem Cell Res Ther, 2015. **6**: p. 151.

72. Stagg, J., *Immune regulation by mesenchymal stem cells: two sides to the coin.* Tissue Antigens, 2007. **69**(1): p. 1-9.

73. Kolf, C.M., E. Cho, and R.S. Tuan, *Mesenchymal stromal cells. Biology of adult mesenchymal stem cells: regulation of niche, self-renewal and differentiation.* Arthritis Res Ther, 2007. **9**(1): p. 204.

74. Gu, J., et al., *Importance of N-glycosylation on alpha5beta1 integrin for its biological functions.* Biol Pharm Bull, 2009. **32**(5): p. 780-5.

75. Bardin, N., et al., *Identification of CD146 as a component of the endothelial junction involved in the control of cell-cell cohesion.* Blood, 2001. **98**(13): p. 3677-84.

76. Zeng, G.F., S.X. Cai, and G.J. Wu, *Up-regulation of METCAM/MUC18 promotes motility, invasion, and tumorigenesis of human breast cancer cells.* BMC Cancer, 2011. **11**: p. 113.

77. Jurisic, G., et al., *Thymus cell antigen 1 (Thy1, CD90) is expressed by lymphatic vessels and mediates cell adhesion to lymphatic endothelium.* Exp Cell Res, 2010. **316**(17): p. 2982-92.

78. Rege, T.A. and J.S. Hagood, *Thy-1 as a regulator of cell-cell and cell-matrix interactions in axon regeneration, apoptosis, adhesion, migration, cancer, and fibrosis.* FASEB J, 2006. **20**(8): p. 1045-54.

79. Rogers, M.L., et al., *ProNGF mediates death of Natural Killer cells through activation of the p75NTR-sortilin complex.* J Neuroimmunol, 2010. **226**(1-2): p. 93-103.

80. Micera, A., et al., *Nerve growth factor and tissue repair remodeling: trkA(NGFR) and p75(NTR), two receptors one fate.* Cytokine Growth Factor Rev, 2007. **18**(3-4): p. 245-56.

81. Kyurkchiev, D., et al., *Secretion of immunoregulatory cytokines by mesenchymal stem cells.* World J Stem Cells, 2014. **6**(5): p. 552-70.

82. Keating, A., *Mesenchymal stromal cells: new directions.* Cell Stem Cell, 2012. **10**(6): p. 709-16.

83. Bara, J.J., et al., *Concise review: Bone marrow-derived mesenchymal stem cells change phenotype following in vitro culture: implications for basic research and the clinic.* Stem Cells, 2014. **32**(7): p. 1713-23.

84. Halfon, S., et al., *Markers distinguishing mesenchymal stem cells from fibroblasts are downregulated with passaging.* Stem Cells Dev, 2011. **20**(1): p. 53-66.

85. Honczarenko, M., et al., *Human bone marrow stromal cells express a distinct set of biologically functional chemokine receptors.* Stem Cells, 2006. **24**(4): p. 1030-41.

86. Lee, M.W., et al., *Effect of ex vivo culture conditions on immunosuppression by human mesenchymal stem cells.* Biomed Res Int, 2013. **2013**: p. 154919.

87. Caplan, A.I., *Adult mesenchymal stem cells for tissue engineering versus regenerative medicine.* J Cell Physiol, 2007. **213**(2): p. 341-7.

88. Ribeiro, A., et al., *Mesenchymal stem cells from umbilical cord matrix, adipose tissue and bone marrow exhibit different capability to suppress peripheral blood B, natural killer and T cells.* Stem Cell Res Ther, 2013. **4**(5): p. 125.

89. Secco, M., et al., *Gene expression profile of mesenchymal stem cells from paired umbilical cord units: cord is different from blood.* Stem Cell Rev, 2009. **5**(4): p. 387-401.

90. Vasandan, A.B., et al., *Functional differences in mesenchymal stromal cells from human dental pulp and periodontal ligament.* J Cell Mol Med, 2014. **18**(2): p. 344-54.

91. Giuliani, M., et al., *Long-lasting inhibitory effects of fetal liver mesenchymal stem cells on T-lymphocyte proliferation.* PLoS One, 2011. **6**(5): p. e19988.

92. Ivanova-Todorova, E., et al., *Adipose tissue-derived mesenchymal stem cells are more potent suppressors of dendritic cells differentiation compared to bone marrow-derived mesenchymal stem cells.* Immunol Lett, 2009. **126**(1-2): p. 37-42.

93. Roemeling-van Rhijn, M., et al., *Human Allogeneic Bone Marrow and Adipose Tissue Derived Mesenchymal Stromal Cells Induce CD8+ Cytotoxic T Cell Reactivity.* J Stem Cell Res Ther, 2013. **3**(Suppl 6): p. 004.

94. DelaRosa, O., et al., *Human adipose-derived stem cells impair natural killer cell function and exhibit low susceptibility to natural killer-mediated lysis.* Stem Cells Dev, 2012. **21**(8): p. 1333-43.

95. Barcia, R.N., et al., *What Makes Umbilical Cord Tissue-Derived Mesenchymal Stromal Cells Superior Immunomodulators When Compared to Bone Marrow Derived Mesenchymal Stromal Cells?* Stem Cells Int, 2015. **2015**: p. 583984.

96. Najar, M., et al., *Adipose-tissue-derived and Wharton's jelly-derived mesenchymal stromal cells suppress lymphocyte responses by secreting leukemia inhibitory factor.* Tissue Eng Part A, 2010. **16**(11): p. 3537-46.

97. Najar, M., et al., *Mesenchymal stromal cells use PGE2 to modulate activation and proliferation of lymphocyte subsets: Combined comparison of adipose tissue, Wharton's Jelly and bone marrow sources.* Cell Immunol, 2010. **264**(2): p. 171-9.

98. Diekman, B.O., et al., *Chondrogenesis of adult stem cells from adipose tissue and bone marrow: induction by growth factors and cartilage-derived matrix.* Tissue Eng Part A, 2010. **16**(2): p. 523-33.

99. Juge-Aubry, C.E., E. Henrichot, and C.A. Meier, *Adipose tissue: a regulator of inflammation.* Best Pract Res Clin Endocrinol Metab, 2005. **19**(4): p. 547-66.

100. Eljaafari, A., et al., *Adipose Tissue-Derived Stem Cells From Obese Subjects Contribute to Inflammation and Reduced Insulin Response in Adipocytes Through Differential Regulation of the Th1/Th17 Balance and Monocyte Activation.* Diabetes, 2015. **64**(7): p. 2477-88.

101. Zhu, X., et al., *Tumor Necrosis Factor-alpha Enhances Adipogenesis of Adipose Tissue-derived Mesenchymal Stem Cells during Evolution of Obesity.* Oral Abstract Presentations; Session Title: Concurrent Session IV A: Diabetes, Obesity and Metabolic Disorders - Arteriosclerosis, Thrombocis, and Vascular Biology, 2015.

102. Bernardo, M.E., D. Pagliara, and F. Locatelli, *Mesenchymal stromal cell therapy: a revolution in Regenerative Medicine?* Bone Marrow Transplant, 2012. **47**(2): p. 164-71.

103. Ennis, W.J., A. Sui, and A. Bartholomew, *Stem Cells and Healing: Impact on Inflammation.* Adv Wound Care (New Rochelle), 2013. **2**(7): p. 369-378.

104. Sutton, M.T. and T.L. Bonfield, *Stem cells: innovations in clinical applications.* Stem Cells Int, 2014. **2014**: p. 516278.

105. Ankrum, J.A., J.F. Ong, and J.M. Karp, *Mesenchymal stem cells: immune evasive, not immune privileged.* Nat Biotechnol, 2014. **32**(3): p. 252-60.

106. Droujinine, I.A., M.A. Eckert, and W. Zhao, *To grab the stroma by the horns: from biology to cancer therapy with mesenchymal stem cells.* Oncotarget, 2013. **4**(5): p. 651-64.

107. Djouad, F., et al., *Immunosuppressive effect of mesenchymal stem cells favors tumor growth in allogeneic animals.* Blood, 2003. **102**(10): p. 3837-44.

108. Karnoub, A.E., et al., *Mesenchymal stem cells within tumour stroma promote breast cancer metastasis.* Nature, 2007. **449**(7162): p. 557-63.

109. Psaltis, P.J., et al., *Concise review: mesenchymal stromal cells: potential for cardiovascular repair.* Stem Cells, 2008. **26**(9): p. 2201-10.

110. Lucchini, G., et al., *Platelet-lysate-expanded mesenchymal stromal cells as a salvage therapy for severe resistant graft-versus-host disease in a pediatric population.* Biol Blood Marrow Transplant, 2010. **16**(9): p. 1293-301.

111. Athersys, *Results From Phase 2 Study of MultiStem Cell Therapy for Treatment of Ischemic Stroke*. 2015.

112. Griffin, M.D., et al., *Concise review: adult mesenchymal stromal cell therapy for inflammatory diseases: how well are we joining the dots?* Stem Cells, 2013. **31**(10): p. 2033-41.

113. Griffin, M.D., et al., *Anti-donor immune responses elicited by allogeneic mesenchymal stem cells: what have we learned so far?* Immunol Cell Biol, 2013. **91**(1): p. 40-51.

114. Herrmann, R.P. and M.J. Sturm, *Adult human mesenchymal stromal cells and the treatment of graft versus host disease.* Stem Cells Cloning, 2014. **7**: p. 45-52.

115. Lopez-Villar, O., et al., *Both expanded and uncultured mesenchymal stem cells from MDS patients are genomically abnormal, showing a specific genetic profile for the 5q- syndrome.* Leukemia, 2009. **23**(4): p. 664-72.

116. Jorgensen, C., *MSC signature associated with therapeutical effect in osteoarticular diseases.* Symposia / Transfusion Clinique et Biologique 22, 2015: p. 191.

117. English, K., *Mechanisms of mesenchymal stromal cell immunomodulation.* Immunol Cell Biol, 2013. **91**(1): p. 19-26.

118. Le Blanc, K. and L.C. Davies, *Mesenchymal stromal cells and the innate immune response.* Immunol Lett, 2015. **168**(2): p. 140-6.

119. Willms, E., et al., *Cells release subpopulations of exosomes with distinct molecular and biological properties.* Sci Rep, 2016. **6**: p. 22519.

120. Xin, H., Y. Li, and M. Chopp, *Exosomes/miRNAs as mediating cell-based therapy of stroke.* Front Cell Neurosci, 2014. **8**: p. 377.

121. Xin, H., et al., *MiR-133b promotes neural plasticity and functional recovery after treatment of stroke with multipotent mesenchymal stromal cells in rats via transfer of exosome-enriched extracellular particles.* Stem Cells, 2013. **31**(12): p. 2737-46.

122. Liu, X., et al., *Cell based therapies for ischemic stroke: from basic science to bedside.* Prog Neurobiol, 2014. **115**: p. 92-115.

123. Taylor, D.D. and C. Gercel-Taylor, *Exosomes/microvesicles: mediators of cancer-associated immunosuppressive microenvironments.* Semin Immunopathol, 2011. **33**(5): p. 441-54.

124. Bobrie, A., et al., *Exosome secretion: molecular mechanisms and roles in immune responses.* Traffic, 2011. **12**(12): p. 1659-68.

125. Gyorgy, B., et al., *Membrane vesicles, current state-of-the-art: emerging role of extracellular vesicles.* Cell Mol Life Sci, 2011. **68**(16): p. 2667-88.

126. Chaput, N. and C. Thery, *Exosomes: immune properties and potential clinical implementations.* Semin Immunopathol, 2011. **33**(5): p. 419-40.

127. Zhang, B., et al., *Mesenchymal stem cells secrete immunologically active exosomes.* Stem Cells Dev, 2014. **23**(11): p. 1233-44.

128. Lai, R.C., R.W. Yeo, and S.K. Lim, *Mesenchymal stem cell exosomes.* Semin Cell Dev Biol, 2015. **40**: p. 82-8.

129. Yeo, R.W., et al., *Mesenchymal stem cell: an efficient mass producer of exosomes for drug delivery.* Adv Drug Deliv Rev, 2013. **65**(3): p. 336-41.

130. Li, Y., et al., *The role of astrocytes in mediating exogenous cell-based restorative therapy for stroke.* Glia, 2014. **62**(1): p. 1-16.

131. Okoye, I.S., et al., *MicroRNA-containing T-regulatory-cell-derived exosomes suppress pathogenic T helper 1 cells.* Immunity, 2014. **41**(1): p. 89-103.

132. Yona, S., et al., *Fate mapping reveals origins and dynamics of monocytes and tissue macrophages under homeostasis.* Immunity, 2013. **38**(1): p. 79-91.

133. Geissmann, F., et al., *Development of monocytes, macrophages, and dendritic cells.* Science, 2010. **327**(5966): p. 656-61.

134. Guilliams, M., et al., *Dendritic cells, monocytes and macrophages: a unified nomenclature based on ontogeny.* Nat Rev Immunol, 2014. **14**(8): p. 571-8.

135. De, B., *Macrophage progenitor cells in mouse bone marrow.* 1997.

136. Ginhoux, F., et al., *Langerhans cells arise from monocytes in vivo.* Nat Immunol, 2006. **7**(3): p. 265-73.

137. Davies, L.C. and P.R. Taylor, *Tissue-resident macrophages: then and now.* Immunology, 2015. **144**(4): p. 541-8.

138. Martinez, F.O., et al., *Transcriptional profiling of the human monocyte-to-macrophage differentiation and polarization: new molecules and patterns of gene expression.* J Immunol, 2006. **177**(10): p. 7303-11.

139. Shi, C. and E.G. Pamer, *Monocyte recruitment during infection and inflammation.* Nat Rev Immunol, 2011. **11**(11): p. 762-74.

140. Peranzoni, E., et al., *Myeloid-derived suppressor cell heterogeneity and subset definition.* Curr Opin Immunol, 2010. **22**(2): p. 238-44.

141. Iijima, N., L.M. Mattei, and A. Iwasaki, *Recruited inflammatory monocytes stimulate antiviral Th1 immunity in infected tissue.* Proc Natl Acad Sci U S A, 2011. **108**(1): p. 284-9.

142. Tacke, F. and G.J. Randolph, *Migratory fate and differentiation of blood monocyte subsets.* Immunobiology, 2006. **211**(6-8): p. 609-18.

143. Belge, K.U., et al., *The Proinflammatory CD14+CD16+DR++ Monocytes Are a Major Source of TNF.* The Journal of Immunology, 2002. **168**(7): p. 3536-3542.

144. Armaka, M., et al., *Mesenchymal cell targeting by TNF as a common pathogenic principle in chronic inflammatory joint and intestinal diseases.* J Exp Med, 2008. **205**(2): p. 331-7.

145. Aggarwal, S. and M.F. Pittenger, *Human mesenchymal stem cells modulate allogeneic immune cell responses.* Blood, 2005. **105**(4): p. 1815-22.

146. Bates, R.C. and A.M. Mercurio, *Tumor necrosis factor-alpha stimulates the epithelial-to-mesenchymal transition of human colonic organoids.* Mol Biol Cell, 2003. **14**(5): p. 1790-800.

147. Duijvestein, M., et al., *Autologous bone marrow-derived mesenchymal stromal cell treatment for refractory luminal Crohn's disease: results of a phase I study.* Gut, 2010. **59**(12): p. 1662-9.

148. Ziegler-Heitbrock, L., et al., *Nomenclature of monocytes and dendritic cells in blood.* Blood, 2010. **116**(16): p. e74-80.

149. Wong, K.L., et al., *The three human monocyte subsets: implications for health and disease.* Immunol Res, 2012. **53**(1-3): p. 41-57.

150. Almeida, J., et al., *Comparative analysis of the morphological, cytochemical, immunophenotypical, and functional characteristics of normal human peripheral blood lineage(-)/CD16(+)/HLA-DR(+)/CD14(-/lo) cells, CD14(+) monocytes, and CD16(-) dendritic cells.* Clin Immunol, 2001. **100**(3): p. 325-38.

151. Zhao, C., et al., *Identification of novel functional differences in monocyte subsets using proteomic and transcriptomic methods.* J Proteome Res, 2009. **8**(8): p. 4028-38.

152. Zawada, A.M., et al., *SuperSAGE evidence for CD14++CD16+ monocytes as a third monocyte subset.* Blood, 2011. **118**(12): p. e50-61.

153. Ancuta, P., et al., *Transcriptional profiling reveals developmental relationship and distinct biological functions of CD16+ and CD16- monocyte subsets.* BMC Genomics, 2009. **10**: p. 403.

154. Randolph, G.J., C. Jakubzick, and C. Qu, *Antigen presentation by monocytes and monocyte-derived cells.* Curr Opin Immunol, 2008. **20**(1): p. 52-60.

155. Zhu, J. and W.E. Paul, *CD4 T cells: fates, functions, and faults.* Blood, 2008. **112**(5): p. 1557-1569.

156. Jenkins, M.R. and G.M. Griffiths, *The synapse and cytolytic machinery of cytotoxic T cells.* Curr Opin Immunol, 2010. **22**(3): p. 308-13.

157. Thompson, C. and F. Powrie, *Regulatory T cells.* Curr Opin Pharmacol, 2004. **4**(4): p. 408-14.

158. Sakaguchi, S., et al., *Regulatory T cells and immune tolerance.* Cell, 2008. **133**(5): p. 775-87.

159. Owen, J.A., et al., *Kuby Immunology*. 7th ed. ed. 2013, New York: W.H. Freeman and Company.

160. Chiossone, L., et al., *Mesenchymal stromal cells induce peculiar alternatively activated macrophages capable of dampening both innate and adaptive immune responses.* Stem Cells, 2016.

161. Nauta, A.J., et al., *Mesenchymal stem cells inhibit generation and function of both CD34+-derived and monocyte-derived dendritic cells.* J Immunol, 2006. **177**(4): p. 2080-7.

162. Djouad, F., et al., *Mesenchymal stem cells inhibit the differentiation of dendritic cells through an interleukin-6-dependent mechanism.* Stem Cells, 2007. **25**(8): p. 2025-32.

163. Bernardo, M.E. and W.E. Fibbe, *Mesenchymal stromal cells: sensors and switchers of inflammation.* Cell Stem Cell, 2013. **13**(4): p. 392-402.

164. Needham, B.D. and M.S. Trent, *Fortifying the barrier: the impact of lipid A remodelling on bacterial pathogenesis.* Nat Rev Microbiol, 2013. **11**(7): p. 467-81.

165. Kawai, T. and S. Akira, *The role of pattern-recognition receptors in innate immunity: update on Toll-like receptors.* Nat Immunol, 2010. **11**(5): p. 373-384.

166. Dziarski, R. and D. Gupta, *Peptidoglycan recognition in innate immunity.* J Endotoxin Res, 2005. **11**(5): p. 304-10.

167. Girardin, S.E., et al., *Nod2 is a general sensor of peptidoglycan through muramyl dipeptide (MDP) detection.* J Biol Chem, 2003. **278**(11): p. 8869-72.

168. Schultz, H., K. Engel, and M. Gaestel, *PMA-induced activation of the p42/44ERK- and p38RK-MAP kinase cascades in HL-60 cells is PKC dependent but not essential for differentiation to the macrophage-like phenotype.* J Cell Physiol, 1997. **173**(3): p. 310-8.

169. Chopra, R.K., et al., *Phorbol myristate acetate and calcium ionophore A23187-stimulated human T cells do not express high-affinity IL-2 receptors.* Immunology, 1989. **66**(1): p. 54-60.

170. Chilson, O.P., A.W. Boylston, and M.J. Crumpton, *Phaseolus vulgaris phytohaemagglutinin (PHA) binds to the human T lymphocyte antigen receptor.* EMBO J, 1984. **3**(13): p. 3239-45.

171. Bortolotti, F., et al., *In vivo therapeutic potential of mesenchymal stromal cells depends on the source and the isolation procedure.* Stem Cell Reports, 2015. **4**(3): p. 332-9.

172. Nauta, A.J. and W.E. Fibbe, *Immunomodulatory properties of mesenchymal stromal cells.* Blood, 2007. **110**(10): p. 3499-506.

173. Trounson, A., et al., *Clinical trials for stem cell therapies.* BMC Med, 2011. **9**: p. 52.

174. Caplan, A.I., *Why are MSCs therapeutic? New data: new insight.* J Pathol, 2009. **217**(2): p. 318-24.

175. Jiang, X.X., et al., *Human mesenchymal stem cells inhibit differentiation and function of monocyte-derived dendritic cells.* Blood, 2005. **105**(10): p. 4120-6.

176. Ren, G., et al., *Mesenchymal stem cell-mediated immunosuppression occurs via concerted action of chemokines and nitric oxide.* Cell Stem Cell, 2008. **2**(2): p. 141-50.

177. Spaggiari, G.M., et al., *MSCs inhibit monocyte-derived DC maturation and function by selectively interfering with the generation of immature DCs: central role of MSC-derived prostaglandin E2.* Blood, 2009. **113**(26): p. 6576-83.

178. Bloom, D.D., et al., *A reproducible immunopotency assay to measure mesenchymal stromal cell-mediated T-cell suppression.* Cytotherapy, 2015. **17**(2): p. 140-51.

179. Jaklenec, A., et al., *Progress in the tissue engineering and stem cell industry "are we there yet?".* Tissue Eng Part B Rev, 2012. **18**(3): p. 155-66.

180. Vemuri, M.C., L.G. Chase, and M.S. Rao, *Mesenchymal stem cell assays and applications.* Methods Mol Biol, 2011. **698**: p. 3-8.

181. Jiao, J., et al., *A mesenchymal stem cell potency assay.* Methods Mol Biol, 2011. **677**: p. 221-31.

182. McKernan, R., J. McNeish, and D. Smith, *Pharma's developing interest in stem cells.* Cell Stem Cell, 2010. **6**(6): p. 517-20.

183. Ketterl, N., et al., *A robust potency assay highlights significant donor variation of human mesenchymal stem/progenitor cell immune modulatory capacity and extended radio-resistance.* Stem Cell Res Ther, 2015. **6**: p. 236.

184. Davie, E.W., K. Fujikawa, and W. Kisiel, *The coagulation cascade: initiation, maintenance, and regulation.* Biochemistry, 1991. **30**(43): p. 10363-70.

185. Gulati, G.L., et al., *Changes in automated complete blood cell count and differential leukocyte count results induced by storage of blood at room temperature.* Arch Pathol Lab Med, 2002. **126**(3): p. 336-42.

186. de Baca, M.E., et al., *Effects of Storage of Blood at Room Temperature on Hematologic Parameters Measured on Sysmex XE-2100.* Laboratory Medicine, 2006. **37**(1): p. 28-36.

187. Reardon, D.M., B. Warner, and E.A. Trowbridge, *EDTA, the traditional anticoagulant of haematology: with increased automation is it time for a review?* Med Lab Sci, 1991. **48**(1): p. 72-5.

188. Brunialti, M.K., et al., *Influence of EDTA and heparin on lipopolysaccharide binding and cell activation, evaluated at single-cell level in whole blood.* Cytometry, 2002. **50**(1): p. 14-8.

189. Simonsen, J.L., et al., *Telomerase expression extends the proliferative life-span and maintains the osteogenic potential of human bone marrow stromal cells.* Nat Biotechnol, 2002. **20**(6): p. 592-6.

190. Picozza, M., L. Battistini, and G. Borsellino, *Mononuclear phagocytes and marker modulation: when CD16 disappears, CD38 takes the stage.* Blood, 2013. **122**(3): p. 456-7.

191. DeForge, L.E. and D.G. Remick, *Kinetics of TNF, IL-6, and IL-8 gene expression in LPS-stimulated human whole blood.* Biochemical and Biophysical Research Communications, 1991. **174**(1): p. 18-24.

192. de Waal Malefyt, R., et al., *Interleukin 10(IL-10) inhibits cytokine synthesis by human monocytes: an autoregulatory role of IL-10 produced by monocytes.* The Journal of Experimental Medicine, 1991. **174**(5): p. 1209-1220.

193. Shin, D.I., et al., *Interleukin 10 inhibits TNF-alpha production in human monocytes independently of interleukin 12 and interleukin 1 beta.* Immunol Invest, 1999. **28**(2-3): p. 165-75.

194. Gupta, M., R. Chaturvedi, and A. Jain, *Role of monocyte chemoattractant protein-1 (MCP-1) as an immune-diagnostic biomarker in the pathogenesis of chronic periodontal disease.* Cytokine, 2013. **61**(3): p. 892-7.

195. Panee, J., *Monocyte Chemoattractant Protein 1 (MCP-1) in obesity and diabetes.* Cytokine, 2012. **60**(1): p. 1-12.

196. Gremmels, H., et al., *Neovascularization capacity of mesenchymal stromal cells from critical limb ischemia patients is equivalent to healthy controls.* Mol Ther, 2014. **22**(11): p. 1960-70.

197. Abdi, K., et al., *Free IL-12p40 monomer is a polyfunctional adaptor for generating novel IL-12-like heterodimers extracellularly.* J Immunol, 2014. **192**(12): p. 6028-36.

198. Krishnan, V.V., et al., *Multiplexed measurements of immunomodulator levels in peripheral blood of healthy subjects: Effects of analytical variables based on anticoagulants, age, and gender.* Cytometry B Clin Cytom, 2014. **86**(6): p. 426-35.

199. Duffy, M.M., et al., *Mesenchymal stem cell effects on T-cell effector pathways.* Stem Cell Res Ther, 2011. **2**(4): p. 34.

200. Bournazos, S., et al., *Choice of anticoagulant critically affects measurement of circulating platelet-leukocyte complexes.* Arterioscler Thromb Vasc Biol, 2008. **28**(1): p. e2-3.

201. Visintin, A., et al., *Regulation of Toll-Like Receptors in Human Monocytes and Dendritic Cells.* The Journal of Immunology, 2001. **166**(1): p. 249-255.

202. Dasu, M.R., et al., *Increased toll-like receptor (TLR) activation and TLR ligands in recently diagnosed type 2 diabetic subjects.* Diabetes Care, 2010. **33**(4): p. 861-8.

203. Tadema, H., et al., *Increased expression of Toll-like receptors by monocytes and natural killer cells in ANCA-associated vasculitis.* PLoS One, 2011. **6**(9): p. e24315.

204. Sabroe, I., et al., *Selective Roles for Toll-Like Receptor (TLR)2 and TLR4 in the Regulation of Neutrophil Activation and Life Span.* The Journal of Immunology, 2003. **170**(10): p. 5268-5275.

205. Goriely, S., et al., *Interferon regulatory factor 3 is involved in Toll-like receptor 4 (TLR4)- and TLR3-induced IL-12p35 gene activation.* Blood, 2006. **107**(3): p. 1078-84.

206. Rossol, M., et al., *Extracellular Ca2+ is a danger signal activating the NLRP3 inflammasome through G protein-coupled calcium sensing receptors.* Nat Commun, 2012. **3**: p. 1329.

207. Melief, S.M., et al., *Multipotent stromal cells induce human regulatory T cells through a novel pathway involving skewing of monocytes toward anti-inflammatory macrophages.* Stem Cells, 2013. **31**(9): p. 1980-91.

208. Luk, F., et al., *Inactivated Mesenchymal Stem Cells Maintain Immunomodulatory Capacity.* Stem Cells Dev, 2016.

209. Chen, H.W., et al., *Mesenchymal stem cells tune the development of monocyte-derived dendritic cells toward a myeloid-derived suppressive phenotype through growth-regulated oncogene chemokines.* J Immunol, 2013. **190**(10): p. 5065-77.

210. Valadi, H., et al., *Exosome-mediated transfer of mRNAs and microRNAs is a novel mechanism of genetic exchange between cells.* Nat Cell Biol, 2007. **9**(6): p. 654-9.

211. Lai, R.C., et al., *Proteolytic Potential of the MSC Exosome Proteome: Implications for an Exosome-Mediated Delivery of Therapeutic Proteasome.* Int J Proteomics, 2012. **2012**: p. 971907.

212. Rasmusson, I., et al., *Mesenchymal stem cells fail to trigger effector functions of cytotoxic T lymphocytes.* J Leukoc Biol, 2007. **82**(4): p. 887-93.

213. Chen, P.M., et al., *Immunomodulatory properties of human adult and fetal multipotent mesenchymal stem cells.* J Biomed Sci, 2011. **18**: p. 49.

214. Griffin, M.D., T. Ritter, and B.P. Mahon, *Immunological aspects of allogeneic mesenchymal stem cell therapies.* Hum Gene Ther, 2010. **21**(12): p. 1641-55.

215. English, K. and B.P. Mahon, *Allogeneic mesenchymal stem cells: agents of immune modulation.* J Cell Biochem, 2011. **112**(8): p. 1963-8.

216. Stolzing, A., et al., *Age-related changes in human bone marrow-derived mesenchymal stem cells: consequences for cell therapies.* Mech Ageing Dev, 2008. **129**(3): p. 163-73.

217. Centers for Disease, C. and Prevention, *Prevalence of doctor-diagnosed arthritis and arthritis-attributable activity limitation--United States, 2010-2012.* MMWR Morb Mortal Wkly Rep, 2013. **62**(44): p. 869-73.

218. Hench, P.S., *Arthritis.* J Am Med Assoc, 1946. **132**(16): p. 974-9.

219. Buckwalter, J.A., H.J. Mankin, and A.J. Grodzinsky, *Articular cartilage and osteoarthritis.* Instr Course Lect, 2005. **54**: p. 465-80.

220. Decker, R.S., E. Koyama, and M. Pacifici, *Genesis and morphogenesis of limb synovial joints and articular cartilage.* Matrix Biol, 2014. **39**: p. 5-10.

221. Berenbaum, F., *Osteoarthritis as an inflammatory disease (osteoarthritis is not osteoarthrosis!).* Osteoarthritis Cartilage, 2013. **21**(1): p. 16-21.

222. Bijlsma, J.W.J., F. Berenbaum, and F.P.J.G. Lafeber, *Osteoarthritis: an update with relevance for clinical practice.* The Lancet, 2011. **377**(9783): p. 2115-2126.

223. http://www.medicinenet.com/rheumatoid_arthritis/article.htm.

224. Houard, X., M.B. Goldring, and F. Berenbaum, *Homeostatic mechanisms in articular cartilage and role of inflammation in osteoarthritis.* Curr Rheumatol Rep, 2013. **15**(11): p. 375.

225. Bank, R.A., et al., *The increased swelling and instantaneous deformation of osteoarthritic cartilage is highly correlated with collagen degradation.* Arthritis Rheum, 2000. **43**(10): p. 2202-10.

226. Martin, J.A. and J.A. Buckwalter, *The role of chondrocyte-matrix interactions in maintaining and repairing articular cartilage.* Biorheology, 2000. **37**(1-2): p. 129-40.

227. de Sousa, E.B., et al., *Synovial fluid and synovial membrane mesenchymal stem cells: latest discoveries and therapeutic perspectives.* Stem Cell Res Ther, 2014. **5**(5): p. 112.

228. Firestein, G.S., *Invasive fibroblast-like synoviocytes in rheumatoid arthritis. Passive responders or transformed aggressors?* Arthritis Rheum, 1996. **39**(11): p. 1781-90.

229. Uth, K. and D. Trifonov, *Stem cell application for osteoarthritis in the knee joint: A minireview.* World J Stem Cells, 2014. **6**(5): p. 629-36.

230. Nelson, A.E., et al., *A systematic review of recommendations and guidelines for the management of osteoarthritis: The chronic osteoarthritis management initiative of the U.S. bone and joint initiative.* Semin Arthritis Rheum, 2014. **43**(6): p. 701-12.

231. Woolf, A.D. and B. Pfleger, *Burden of major musculoskeletal conditions.* Bull World Health Organ, 2003. **81**(9): p. 646-56.

232. Spector, T.D., et al., *Genetic influences on osteoarthritis in women: a twin study.* Bmj, 1996. **312**(7036): p. 940-943.

233. Blagojevic, M., et al., *Risk factors for onset of osteoarthritis of the knee in older adults: a systematic review and meta-analysis.* Osteoarthritis Cartilage, 2010. **18**(1): p. 24-33.

234. Bliddal, H., A.R. Leeds, and R. Christensen, *Osteoarthritis, obesity and weight loss: evidence, hypotheses and horizons - a scoping review.* Obes Rev, 2014. **15**(7): p. 578-86.

235. Barr, A.J., et al., *A systematic review of the relationship between subchondral bone features, pain and structural pathology in peripheral joint osteoarthritis.* Arthritis Res Ther, 2015. **17**: p. 228.

236. Martin, J.A. and J.A. Buckwalter, *Aging, articular cartilage chondrocyte senescence and osteoarthritis.* Biogerontology, 2002. **3**(5): p. 257-64.

237. Link, T.M., et al., *Osteoarthritis: MR imaging findings in different stages of disease and correlation with clinical findings.* Radiology, 2003. **226**(2): p. 373-81.

238. Buckwalter, J.A. and H.J. Mankin, *Articular cartilage: degeneration and osteoarthritis, repair, regeneration, and transplantation.* Instr Course Lect, 1998. **47**: p. 487-504.

239. Pearle, A.D., et al., *Elevated high-sensitivity C-reactive protein levels are associated with local inflammatory findings in patients with osteoarthritis.* Osteoarthritis Cartilage, 2007. **15**(5): p. 516-23.

240. Benito, M.J., et al., *Synovial tissue inflammation in early and late osteoarthritis.* Ann Rheum Dis, 2005. **64**(9): p. 1263-7.

241. Scanzello, C.R., et al., *Synovial inflammation in patients undergoing arthroscopic meniscectomy: molecular characterization and relationship to symptoms.* Arthritis Rheum, 2011. **63**(2): p. 391-400.

242. Wieland, H.A., et al., *Osteoarthritis - an untreatable disease?* Nat Rev Drug Discov, 2005. **4**(4): p. 331-44.

243. Geven, E., et al., *Locally induced experimental osteoarthritis results in a system bone marrow shift towards a pro-inflammatory monocyte subpopulation.* Annals of the Rheumatic Diseases, 2015. **74**(Suppl 1): p. A13-A13.

244. Blom, A.B., et al., *Synovial lining macrophages mediate osteophyte formation during experimental osteoarthritis.* Osteoarthritis Cartilage, 2004. **12**(8): p. 627-35.

245. Gallagher, B., et al., *Chondroprotection and the prevention of osteoarthritis progression of the knee: a systematic review of treatment agents.* Am J Sports Med, 2015. **43**(3): p. 734-44.

246. Meeus, M., et al., *Central sensitization in patients with rheumatoid arthritis: a systematic literature review.* Semin Arthritis Rheum, 2012. **41**(4): p. 556-67.

247. Brooks, P.M., *The burden of musculoskeletal disease--a global perspective.* Clin Rheumatol, 2006. **25**(6): p. 778-81.

248. Alamanos, Y. and A.A. Drosos, *Epidemiology of adult rheumatoid arthritis.* Autoimmun Rev, 2005. **4**(3): p. 130-6.

249. Kurko, J., et al., *Genetics of rheumatoid arthritis - a comprehensive review.* Clin Rev Allergy Immunol, 2013. **45**(2): p. 170-9.

250. Gonzalez-Rey, E., et al., *Human adipose-derived mesenchymal stem cells reduce inflammatory and T cell responses and induce regulatory T cells in vitro in rheumatoid arthritis.* Ann Rheum Dis, 2010. **69**(1): p. 241-8.

251. De Bari, C., *Are mesenchymal stem cells in rheumatoid arthritis the good or bad guys?* Arthritis Res Ther, 2015. **17**: p. 113.

252. Strand, V., R. Kimberly, and J.D. Isaacs, *Biologic therapies in rheumatology: lessons learned, future directions.* Nat Rev Drug Discov, 2007. **6**(1): p. 75-92.

253. Ma, X. and S. Xu, *TNF inhibitor therapy for rheumatoid arthritis.* Biomed Rep, 2013. **1**(2): p. 177-184.

254. Gaujoux-Viala, C., et al., *Efficacy of conventional synthetic disease-modifying antirheumatic drugs, glucocorticoids and tofacitinib: a systematic literature review informing the 2013 update of the EULAR recommendations for management of rheumatoid arthritis.* Ann Rheum Dis, 2014. **73**(3): p. 510-5.

255. Singh, J.A., et al., *2012 update of the 2008 American College of Rheumatology recommendations for the use of disease-modifying antirheumatic drugs and biologic agents in the treatment of rheumatoid arthritis.* Arthritis Care Res (Hoboken), 2012. **64**(5): p. 625-39.

256. Matcham, F., et al., *The prevalence of depression in rheumatoid arthritis: a systematic review and meta-analysis.* Rheumatology (Oxford), 2013. **52**(12): p. 2136-48.

257. Smolen, J.S., et al., *EULAR recommendations for the management of rheumatoid arthritis with synthetic and biological disease-modifying antirheumatic drugs.* Ann Rheum Dis, 2010. **69**(6): p. 964-75.

258. Murphy, J.M., et al., *Reduced chondrogenic and adipogenic activity of mesenchymal stem cells from patients with advanced osteoarthritis.* Arthritis Rheum, 2002. **46**(3): p. 704-13.

259. Gillogly, S.D., M. Voight, and T. Blackburn, *Treatment of articular cartilage defects of the knee with autologous chondrocyte implantation.* J Orthop Sports Phys Ther, 1998. **28**(4): p. 241-51.

260. Noth, U., A.F. Steinert, and R.S. Tuan, *Technology insight: adult mesenchymal stem cells for osteoarthritis therapy.* Nat Clin Pract Rheumatol, 2008. **4**(7): p. 371-80.

261. Orozco, L., et al., *Treatment of knee osteoarthritis with autologous mesenchymal stem cells: a pilot study.* Transplantation, 2013. **95**(12): p. 1535-41.

262. Desando, G., et al., *Intra-articular delivery of adipose derived stromal cells attenuates osteoarthritis progression in an experimental rabbit model.* Arthritis Res Ther, 2013. **15**(1): p. R22.

263. Jo, C.H., et al., *Intra-articular injection of mesenchymal stem cells for the treatment of osteoarthritis of the knee: a proof-of-concept clinical trial.* Stem Cells, 2014. **32**(5): p. 1254-66.

264. Vega, A., et al., *Treatment of Knee Osteoarthritis With Allogeneic Bone Marrow Mesenchymal Stem Cells: A Randomized Controlled Trial.* Transplantation, 2015. **99**(8): p. 1681-90.

265. Santos, J.M., et al., *The role of human umbilical cord tissue-derived mesenchymal stromal cells (UCX(R)) in the treatment of inflammatory arthritis.* J Transl Med, 2013. **11**: p. 18.

266. Papadopoulou, A., et al., *Mesenchymal stem cells are conditionally therapeutic in preclinical models of rheumatoid arthritis.* Ann Rheum Dis, 2012. **71**(10): p. 1733-40.

267. Al-Nbaheen, M., et al., *Human stromal (mesenchymal) stem cells from bone marrow, adipose tissue and skin exhibit differences in molecular phenotype and differentiation potential.* Stem Cell Rev, 2013. **9**(1): p. 32-43.

268. Strioga, M., et al., *Same or not the same? Comparison of adipose tissue-derived versus bone marrow-derived mesenchymal stem and stromal cells.* Stem Cells Dev, 2012. **21**(14): p. 2724-52.

269. Elman, J.S., et al., *A comparison of adipose and bone marrow-derived mesenchymal stromal cell secreted factors in the treatment of systemic inflammation.* J Inflamm (Lond), 2014. **11**(1): p. 1.

270. Yanez, R., et al., *Adipose tissue-derived mesenchymal stem cells have in vivo immunosuppressive properties applicable for the control of the graft-versus-host disease.* Stem Cells, 2006. **24**(11): p. 2582-91.

271. Reinders, M.E., et al., *Autologous bone marrow-derived mesenchymal stromal cells for the treatment of allograft rejection after renal transplantation: results of a phase I study.* Stem Cells Transl Med, 2013. **2**(2): p. 107-11.

272. Francois, M., et al., *Human MSC suppression correlates with cytokine induction of indoleamine 2,3-dioxygenase and bystander M2 macrophage differentiation.* Mol Ther, 2012. **20**(1): p. 187-95.

273. Neuhuber, B., et al., *Axon growth and recovery of function supported by human bone marrow stromal cells in the injured spinal cord exhibit donor variations.* Brain Res, 2005. **1035**(1): p. 73-85.

274. Kretlow, J.D., et al., *Donor age and cell passage affects differentiation potential of murine bone marrow-derived stem cells.* BMC Cell Biol, 2008. **9**: p. 60.

275. von Bahr, L., et al., *Long-term complications, immunologic effects, and role of passage for outcome in mesenchymal stromal cell therapy.* Biol Blood Marrow Transplant, 2012. **18**(4): p. 557-64.

276. Furth, M.E., A. Atala, and M.E. Van Dyke, *Smart biomaterials design for tissue engineering and regenerative medicine.* Biomaterials, 2007. **28**(34): p. 5068-73.

277. Chan, B.P. and K.W. Leong, *Scaffolding in tissue engineering: general approaches and tissue-specific considerations.* Eur Spine J, 2008. **17 Suppl 4**: p. 467-79.

278. Rosso, F., et al., *Smart materials as scaffolds for tissue engineering.* J Cell Physiol, 2005. **203**(3): p. 465-70.

279. Bhattacharjee, P., et al., *Non-mulberry silk fibroin grafted PCL nanofibrous scaffold: Promising ECM for bone tissue engineering.* European Polymer Journal, 2015. **71**: p. 490-509.

280. Rezwan, K., et al., *Biodegradable and bioactive porous polymer/inorganic composite scaffolds for bone tissue engineering.* Biomaterials, 2006. **27**(18): p. 3413-31.

281. Zhang, H. and S. Hollister, *Comparison of bone marrow stromal cell behaviors on poly(caprolactone) with or without surface modification: studies on cell adhesion, survival and proliferation.* J Biomater Sci Polym Ed, 2009. **20**(14): p. 1975-93.

282. Anderson, J.M., *Biological resposes to materials.* Annual Review of materials Research, 2001. **31**: p. 81-110.

283. Zadpoor, A.A., *Relationship between in vitro apatite-forming ability measured using simulated body fluid and in vivo bioactivity of biomaterials.* Mater Sci Eng C Mater Biol Appl, 2014. **35**: p. 134-43.

284. Anderson, J.M., A. Rodriguez, and D.T. Chang, *Foreign body reaction to biomaterials.* Semin Immunol, 2008. **20**(2): p. 86-100.

285. Tang, L., T.A. Jennings, and J.W. Eaton, *Mast cells mediate acute inflammatory responses to implanted biomaterials.* Proc Natl Acad Sci U S A, 1998. **95**(15): p. 8841-6.

286. Ginhoux, F. and S. Jung, *Monocytes and macrophages: developmental pathways and tissue homeostasis.* Nat Rev Immunol, 2014. **14**(6): p. 392-404.

287. Tang, L. and J.W. Eaton, *Fibrin(ogen) mediates acute inflammatory responses to biomaterials.* J Exp Med, 1993. **178**(6): p. 2147-56.

288. Yuan, S.Y. and R.R. Rigor, *Chapter 2, Structure and Function of Exchange Microvessels*, in *Regulation of Endothelial Barrier Function.* 2010, Morgan & Claypool Life Sciences: San Rafael (CA).

289. Flannagan, R.S., V. Jaumouille, and S. Grinstein, *The cell biology of phagocytosis.* Annu Rev Pathol, 2012. **7**: p. 61-98.

290. Stuart, L.M. and R.A. Ezekowitz, *Phagocytosis and comparative innate immunity: learning on the fly.* Nat Rev Immunol, 2008. **8**(2): p. 131-41.

291. Henson, P.M., *Mechanisms of exocytosis in phagocytic inflammatory cells. Parke-Davis Award Lecture.* Am J Pathol, 1980. **101**(3): p. 494-511.

292. DeFife, K.M., et al., *Interleukin-13 induces human monocyte/macrophage fusion and macrophage mannose receptor expression.* J Immunol, 1997. **158**(7): p. 3385-90.

293. Doktorovova, S., E.B. Souto, and A.M. Silva, *Nanotoxicology applied to solid lipid nanoparticles and nanostructured lipid carriers - a systematic review of in vitro data.* Eur J Pharm Biopharm, 2014. **87**(1): p. 1-18.

294. Pagliari, S., et al., *Adult stem cells and biocompatible scaffolds as smart drug delivery tools for cardiac tissue repair.* Curr Med Chem, 2013. **20**(28): p. 3429-47.

295. Mouritsen, O., *The Science of Seaweeds - Marine macroalgae benefit people culturally, industrially, nutritionally, and ecologically.* American Scientist, 2013. **101**(6): p. 458.

296. http://www.seaweed.ie.

297. Wijesinghe, W.A.J.P. and Y.-J. Jeon, *Biological activities and potential industrial applications of fucose rich sulfated polysaccharides and fucoidans isolated from brown seaweeds: A review.* Carbohydrate Polymers, 2012. **88**(1): p. 13-20.

298. Khan, S.I. and S.B. Satam, *Seaweed Mariculture: Scope and potential in India.* Aquaculture Asia, 2003. **VIII**.

299. Zemke-White, W.L. and M. Ohno, *World seaweed utilisation: An end-of-century summary.* Journal of Applied Phycology, 1999. **11**: p. 369-376.

300. FAO, *FishStat data set on Aquaculture Production (Quantities and values) 1950-2010.* Food and Agriculture Organization of the United Nations - Fisheries and Aquaculture Department 2012.

301. Myers, S.P., et al., *A combined Phase I and II open-label study on the immunomodulatory effects of seaweed extract nutrient complex.* Biologics, 2011. **5**: p. 45-60.

302. Chojnacka, K., et al., *Biologically Active Compounds in Seaweed Extracts - the Prospects for the Application.* The Open Conference Proceedings Journal, 2012. **3**: p. 20-28.

303. Teruya, T., et al., *Anti-proliferative activity of oversulfated fucoidan from commercially cultured Cladosiphon okamuranus TOKIDA in U937 cells.* Int J Biol Macromol, 2007. **41**(3): p. 221-6.

304. Haneji, K., et al., *Fucoidan extracted from Cladosiphon okamuranus Tokida induces apoptosis of human T-cell leukemia virus type 1-infected T-cell lines and primary adult T-cell leukemia cells.* Nutr Cancer, 2005. **52**(2): p. 189-201.

305. Athukorala, Y., et al., *Anticoagulant activity of marine green and brown algae collected from Jeju Island in Korea.* Bioresour Technol, 2007. **98**(9): p. 1711-6.

306. Yuan, H., et al., *Enhanced immunostimulatory and antitumor activity of different derivatives of κ-carrageenan oligosaccharides from Kappaphycus striatum.* Journal of Applied Phycology, 2010. **23**(1): p. 59-65.

307. Kim, M.H. and H.G. Joo, *Immunostimulatory effects of fucoidan on bone marrow-derived dendritic cells.* Immunol Lett, 2008. **115**(2): p. 138-43.

308. Kang, S.-M., et al., *Anti-inflammatory activity of polysaccharide purified from AMG-assistant extract of Ecklonia cava in LPS-stimulated RAW 264.7 macrophages.* Carbohydrate Polymers, 2011. **85**(1): p. 80-85.

309. Nguemfo, E.L., et al., *Anti-inflammatory and anti-nociceptive activities of the stem bark extracts from Allanblackia monticola STANER L.C. (Guttiferae).* J Ethnopharmacol, 2007. **114**(3): p. 417-24.

310. Barker, J.P., R.A. Cattolico, and G. E., *Multiparametric Analysis of Microalgae for Biofuels Using Flow Cytometry.* BD Bioscience, 2012.

311. Faulk, D.M., et al., *ECM hydrogel coating mitigates the chronic inflammatory response to polypropylene mesh.* Biomaterials, 2014. **35**(30): p. 8585-95.

312. Gill, S.K., et al., *Immunomodulatory effects of natural polysaccharides assessed in human whole blood culture and THP-1 cells show greater sensitivity of whole blood culture.* Int Immunopharmacol, 2016. **36**: p. 315-23.

313. Cardinal, K.O., et al., *Tissue-engineered vascular grafts as in vitro blood vessel mimics for the evaluation of endothelialization of intravascular devices.* Tissue Eng, 2006. **12**(12): p. 3431-8.

314. Robinson, K.A., et al., *Extracellular matrix scaffold for cardiac repair.* Circulation, 2005. **112**(9 Suppl): p. I135-43.

315. Costello, C.R., et al., *Materials characterization of explanted polypropylene hernia meshes.* J Biomed Mater Res B Appl Biomater, 2007. **83**(1): p. 44-9.

316. Communication, F.s., *Update on serious complications associated with transvaginal placement of surgical mesh for pelvic organ prolapse.* U.S. Department of Health and Human Services, 2011.

317. Jones, J.A., et al., *Proteomic analysis and quantification of cytokines and chemokines from biomaterial surface-adherent macrophages and foreign body giant cells.* J Biomed Mater Res A, 2007. **83**(3): p. 585-96.

318. Kang, J.Y., et al., *Antipyretic, analgesic, and anti-inflammatory activities of the seaweed Sargassum fulvellum and Sargassum thunbergii in mice.* J Ethnopharmacol, 2008. **116**(1): p. 187-90.

319. Holdt, S.L. and S. Kraan, *Bioactive compounds in seaweed: functional food applications and legislation.* Journal of Applied Phycology, 2011. **23**(3): p. 543-597.

320. Bravery, C.A., et al., *Potency assay development for cellular therapy products: an ISCT review of the requirements and experiences in the industry.* Cytotherapy, 2013. **15**(1): p. 9-19.

321. Salmikangas, P., et al., *Manufacturing, characterization and control of cell-based medicinal products: challenging paradigms toward commercial use.* Regen Med, 2015. **10**(1): p. 65-78.

322. Galipeau, J., et al., *International Society for Cellular Therapy perspective on immune functional assays for mesenchymal stromal cells as potency release criterion for advanced phase clinical trials.* Cytotherapy, 2016. **18**(2): p. 151-9.

323. Viswanathan, S., et al., *Soliciting strategies for developing cell-based reference materials to advance mesenchymal stromal cell research and clinical translation.* Stem Cells Dev, 2014. **23**(11): p. 1157-67.

324. Ten Brinke, A., et al., *Redefining Strategies to Introduce Tolerance-Inducing Cellular Therapy in Human beings to Combat Autoimmunity and Transplantation Reactions.* Front Immunol, 2014. **5**: p. 392.

325. Vaes, B., et al., *Application of MultiStem((R)) Allogeneic Cells for Immunomodulatory Therapy: Clinical Progress and Pre-Clinical Challenges in Prophylaxis for Graft Versus Host Disease.* Front Immunol, 2012. **3**: p. 345.

326. Park, D., D.B. Sykes, and D.T. Scadden, *The hematopoietic stem cell niche.* Front Biosci (Landmark Ed), 2012. **17**: p. 30-9.

327. Wasnik, S., et al., *Osteohematopoietic stem cell niches in bone marrow.* Int Rev Cell Mol Biol, 2012. **298**: p. 95-133.

328. Morrison, S.J. and D.T. Scadden, *The bone marrow niche for haematopoietic stem cells.* Nature, 2014. **505**(7483): p. 327-34.

329. Damiano, J.S. and W.S. Dalton, *Integrin-mediated drug resistance in multiple myeloma.* Leuk Lymphoma, 2000. **38**(1-2): p. 71-81.

330. Discher, D.E., D.J. Mooney, and P.W. Zandstra, *Growth factors, matrices, and forces combine and control stem cells.* Science, 2009. **324**(5935): p. 1673-7.

331. Gjorevski, N. and C.M. Nelson, *Bidirectional extracellular matrix signaling during tissue morphogenesis.* Cytokine Growth Factor Rev, 2009. **20**(5-6): p. 459-65.

332. Chastain, S.R., et al., *Adhesion of mesenchymal stem cells to polymer scaffolds occurs via distinct ECM ligands and controls their osteogenic differentiation.* J Biomed Mater Res A, 2006. **78**(1): p. 73-85.

333. Khokha, R., A. Murthy, and A. Weiss, *Metalloproteinases and their natural inhibitors in inflammation and immunity.* Nat Rev Immunol, 2013. **13**(9): p. 649-65.

334. Grayson, W.L., et al., *Effects of hypoxia on human mesenchymal stem cell expansion and plasticity in 3D constructs.* J Cell Physiol, 2006. **207**(2): p. 331-9.

335. Bose, S., M. Roy, and A. Bandyopadhyay, *Recent advances in bone tissue engineering scaffolds.* Trends Biotechnol, 2012. **30**(10): p. 546-54.

336. Lee, S.J. and A. Atala, *Scaffold technologies for controlling cell behavior in tissue engineering.* Biomed Mater, 2013. **8**(1): p. 010201.

337. Martin, I., *Engineered tissues as customized organ germs.* Tissue Eng Part A, 2014. **20**(7-8): p. 1132-3.

338. Datta, N., et al., *In vitro generated extracellular matrix and fluid shear stress synergistically enhance 3D osteoblastic differentiation.* Proc Natl Acad Sci U S A, 2006. **103**(8): p. 2488-93.

339. Herklotz, M., et al., *Availability of extracellular matrix biopolymers and differentiation state of human mesenchymal stem cells determine tissue-like growth in vitro.* Biomaterials, 2015. **60**: p. 121-9.

340. Huang, G.S., et al., *Spheroid formation of mesenchymal stem cells on chitosan and chitosan-hyaluronan membranes.* Biomaterials, 2011. **32**(29): p. 6929-45.

341. Bourgine, P.E., et al., *Tissue decellularization by activation of programmed cell death.* Biomaterials, 2013. **34**(26): p. 6099-108.

342. Boer, U., et al., *The effect of detergent-based decellularization procedures on cellular proteins and immunogenicity in equine carotid artery grafts.* Biomaterials, 2011. **32**(36): p. 9730-7.

343. Crapo, P.M., T.W. Gilbert, and S.F. Badylak, *An overview of tissue and whole organ decellularization processes.* Biomaterials, 2011. **32**(12): p. 3233-43.

344. Wainwright, J.M., et al., *Preparation of cardiac extracellular matrix from an intact porcine heart.* Tissue Eng Part C Methods, 2010. **16**(3): p. 525-32.

345. Ouyang, L., et al., *Programmed cell death pathways in cancer: a review of apoptosis, autophagy and programmed necrosis.* Cell Prolif, 2012. **45**(6): p. 487-98.

346. Gargett, T. and M.P. Brown, *The inducible caspase-9 suicide gene system as a "safety switch" to limit on-target, off-tumor toxicities of chimeric antigen receptor T cells.* Front Pharmacol, 2014. **5**: p. 235.

347. Ziegler, U. and P. Groscurth, *Morphological features of cell death.* News Physiol Sci, 2004. **19**: p. 124-8.

348. Vanden Berghe, T., et al., *Regulated necrosis: the expanding network of non-apoptotic cell death pathways.* Nat Rev Mol Cell Biol, 2014. **15**(2): p. 135-47.

349. Elmore, S., *Apoptosis: a review of programmed cell death.* Toxicol Pathol, 2007. **35**(4): p. 495-516.

350. Fulda, S. and K.M. Debatin, *Extrinsic versus intrinsic apoptosis pathways in anticancer chemotherapy.* Oncogene, 2006. **25**(34): p. 4798-811.

351. Degterev, A., M. Boyce, and J. Yuan, *A decade of caspases.* Oncogene, 2003. **22**(53): p. 8543-67.

352. Erwig, L.P. and P.M. Henson, *Clearance of apoptotic cells by phagocytes.* Cell Death Differ, 2008. **15**(2): p. 243-50.

353. Chan, C.W. and F. Housseau, *The 'kiss of death' by dendritic cells to cancer cells.* Cell Death Differ, 2008. **15**(1): p. 58-69.

354. Renatus, M., et al., *Dimer formation drives the activation of the cell death protease caspase 9.* Proc Natl Acad Sci U S A, 2001. **98**(25): p. 14250-5.

355. Pop, C., et al., *The apoptosome activates caspase-9 by dimerization.* Mol Cell, 2006. **22**(2): p. 269-75.

356. Ramos, C.A., et al., *An inducible caspase 9 suicide gene to improve the safety of mesenchymal stromal cell therapies.* Stem Cells, 2010. **28**(6): p. 1107-15.

357. Lenfant, M., et al., *Enhancement of the adherence of hematopoietic stem cells to mouse bone marrow-derived stromal cell line MS-1-T by a tetrapeptide acetyl-N-Ser-Asp-Lys-Pro.* Exp Hematol, 1989. **17**(8): p. 898-902.

358. Tiwari, A., et al., *Expansion of human hematopoietic stem/progenitor cells on decellularized matrix scaffolds.* Curr Protoc Stem Cell Biol, 2014. **28**: p. Unit 1C 15.

359. Bourgine, P., et al., *Combination of immortalization and inducible death strategies to generate a human mesenchymal stromal cell line with controlled survival.* Stem Cell Res, 2014. **12**(2): p. 584-98.

360. Chang, H.Y., et al., *Diversity, topographic differentiation, and positional memory in human fibroblasts.* Proc Natl Acad Sci U S A, 2002. **99**(20): p. 12877-82.

361. Glass, D.A., 2nd, et al., *Canonical Wnt signaling in differentiated osteoblasts controls osteoclast differentiation.* Dev Cell, 2005. **8**(5): p. 751-64.

362. Fang, J. and B.K. Hall, *Chondrogenic cell differentiation from membrane bone periostea.* Anat Embryol (Berl), 1997. **196**(5): p. 349-62.

363. Chen, X.D., et al., *Extracellular matrix made by bone marrow cells facilitates expansion of marrow-derived mesenchymal progenitor cells and prevents their differentiation into osteoblasts.* J Bone Miner Res, 2007. **22**(12): p. 1943-56.

364. Davies, O.G., et al., *Isolation of adipose and bone marrow mesenchymal stem cells using CD29 and CD90 modifies their capacity for osteogenic and adipogenic differentiation.* J Tissue Eng, 2015. **6**: p. 2041731415592356.

365. Baker, B.M. and C.S. Chen, *Deconstructing the third dimension: how 3D culture microenvironments alter cellular cues.* J Cell Sci, 2012. **125**(Pt 13): p. 3015-24.

366. Rao Pattabhi, S., J.S. Martinez, and T.C. Keller, 3rd, *Decellularized ECM effects on human mesenchymal stem cell stemness and differentiation.* Differentiation, 2014. **88**(4-5): p. 131-43.

367. Maier, T., M. Guell, and L. Serrano, *Correlation of mRNA and protein in complex biological samples.* FEBS Lett, 2009. **583**(24): p. 3966-73.

368. Sugrue, T., N.F. Lowndes, and R. Ceredig, *Hypoxia enhances the radioresistance of mouse mesenchymal stromal cells.* Stem Cells, 2014. **32**(8): p. 2188-200.

369. Leontieva, O.V., Z.N. Demidenko, and M.V. Blagosklonny, *Contact inhibition and high cell density deactivate the mammalian target of rapamycin pathway, thus suppressing the senescence program.* Proc Natl Acad Sci U S A, 2014. **111**(24): p. 8832-7.

370. Christophe Lefevre, A.T., *Comparative Gene Expression Profiling of Stromal Cell Matrices that Support Expansion of Hematopoietic Stem/Progenitor Cells.* Journal of Stem Cell Research & Therapy, 2013. **03**(04).

371. Flaim, C.J., S. Chien, and S.N. Bhatia, *An extracellular matrix microarray for probing cellular differentiation.* Nat Methods, 2005. **2**(2): p. 119-25.

372. Trappmann, B., et al., *Extracellular-matrix tethering regulates stem-cell fate.* Nat Mater, 2012. **11**(7): p. 642-9.

373. Li, F., et al., *Apoptotic cells activate the "phoenix rising" pathway to promote wound healing and tissue regeneration.* Sci Signal, 2010. **3**(110): p. ra13.

374. Mogensen, T.H., *Pathogen recognition and inflammatory signaling in innate immune defenses.* Clin Microbiol Rev, 2009. **22**(2): p. 240-73, Table of Contents.

375. Green, D.R., et al., *Immunogenic and tolerogenic cell death.* Nat Rev Immunol, 2009. **9**(5): p. 353-63.

376. Bayrak, A., et al., *Human immune responses to porcine xenogeneic matrices and their extracellular matrix constituents in vitro.* Biomaterials, 2010. **31**(14): p. 3793-803.

377. Lakatos, K., et al., *Mesenchymal Stem Cells Respond to Hypoxia by Increasing Diacylglycerols.* J Cell Biochem, 2016. **117**(2): p. 300-7.

378. Fotia, C., et al., *Hypoxia enhances proliferation and stemness of human adipose-derived mesenchymal stem cells.* Cytotechnology, 2015. **67**(6): p. 1073-84.

379. D'Ippolito, G., et al., *Low oxygen tension inhibits osteogenic differentiation and enhances stemness of human MIAMI cells.* Bone, 2006. **39**(3): p. 513-22.

380. Lin, Q., Y.J. Lee, and Z. Yun, *Differentiation arrest by hypoxia.* J Biol Chem, 2006. **281**(41): p. 30678-83.

381. Hung, S.P., et al., *Hypoxia promotes proliferation and osteogenic differentiation potentials of human mesenchymal stem cells.* J Orthop Res, 2012. **30**(2): p. 260-6.

382. Pierleoni, C., et al., *Fibronectins and basal lamina molecules expression in human subcutaneous white adipose tissue.* Eur J Histochem, 1998. **42**(3): p. 183-8.

383. Stiehler, M., et al., *Effect of dynamic 3-D culture on proliferation, distribution, and osteogenic differentiation of human mesenchymal stem cells.* J Biomed Mater Res A, 2009. **89**(1): p. 96-107.

384. Kang, Y., et al., *The osteogenic differentiation of human bone marrow MSCs on HUVEC-derived ECM and beta-TCP scaffold.* Biomaterials, 2012. **33**(29): p. 6998-7007.

385. Hoshiba, T., N. Kawazoe, and G. Chen, *The balance of osteogenic and adipogenic differentiation in human mesenchymal stem cells by matrices that mimic stepwise tissue development.* Biomaterials, 2012. **33**(7): p. 2025-31.

386. Opel, K.L., D. Chung, and B.R. McCord, *A study of PCR inhibition mechanisms using real time PCR.* J Forensic Sci, 2010. **55**(1): p. 25-33.

387. Rodda, D.J., et al., *Transcriptional regulation of nanog by OCT4 and SOX2.* J Biol Chem, 2005. **280**(26): p. 24731-7.

388. Pierantozzi, E., et al., *Pluripotency regulators in human mesenchymal stem cells: expression of NANOG but not of OCT-4 and SOX-2.* Stem Cells Dev, 2011. **20**(5): p. 915-23.

389. Han, S.M., et al., *Enhanced proliferation and differentiation of Oct4- and Sox2-overexpressing human adipose tissue mesenchymal stem cells.* Exp Mol Med, 2014. **46**: p. e101.

390. Watt, F.M. and R.R. Driskell, *The therapeutic potential of stem cells.* Philos Trans R Soc Lond B Biol Sci, 2010. **365**(1537): p. 155-63.

391. Hall, P.A. and F.M. Watt, *Stem cells: the generation and maintenance of cellular diversity.* Development, 1989. **106**(4): p. 619-33.

392. Bi, Y., et al., *Identification of tendon stem/progenitor cells and the role of the extracellular matrix in their niche.* Nat Med, 2007. **13**(10): p. 1219-27.

393. Watt, F.M. and B.L. Hogan, *Out of Eden: stem cells and their niches.* Science, 2000. **287**(5457): p. 1427-30.

394. Liao, J., et al., *Bioactive polymer/extracellular matrix scaffolds fabricated with a flow perfusion bioreactor for cartilage tissue engineering.* Biomaterials, 2010. **31**(34): p. 8911-20.

395. Gattazzo, F., A. Urciuolo, and P. Bonaldo, *Extracellular matrix: a dynamic microenvironment for stem cell niche.* Biochim Biophys Acta, 2014. **1840**(8): p. 2506-19.

396. Lu, P., V.M. Weaver, and Z. Werb, *The extracellular matrix: a dynamic niche in cancer progression.* J Cell Biol, 2012. **196**(4): p. 395-406.

397. Barille, S., et al., *Metalloproteinases in multiple myeloma: production of matrix metalloproteinase-9 (MMP-9), activation of proMMP-2, and induction of MMP-1 by myeloma cells.* Blood, 1997. **90**(4): p. 1649-55.

398. Manier, S., et al., *Bone marrow microenvironment in multiple myeloma progression.* J Biomed Biotechnol, 2012. **2012**: p. 157496.

399. Arendt, B.K., et al., *Increased expression of extracellular matrix metalloproteinase inducer (CD147) in multiple myeloma: role in regulation of myeloma cell proliferation.* Leukemia, 2012. **26**(10): p. 2286-96.

400. Teoh, G. and K.C. Anderson, *Interaction of tumor and host cells with adhesion and extracellular matrix molecules in the development of multiple myeloma.* Hematol Oncol Clin North Am, 1997. **11**(1): p. 27-42.

401. Glavey, S.V., et al., *Proteomic characterization of the extracellular matrix in multiple myeloma.* Cancer Research, AACR Annual Meeting, 2014.

402. Teicher, B.A., *Hypoxia and drug resistance.* Cancer Metastasis Rev, 1994. **13**(2): p. 139-68.

403. Rohwer, N. and T. Cramer, *Hypoxia-mediated drug resistance: novel insights on the functional interaction of HIFs and cell death pathways.* Drug Resist Updat, 2011. **14**(3): p. 191-201.